Origins of Microorganisms in Deep Subsurface Shales and Sandstones at Cerro Negro, NM

By

Catherine S. Dickey

Submitted in Partial Fulfillment of the Requirement for the
Master of Science Degree in Hydrology

New Mexico Institute of Mining and Technology
Socorro, New Mexico

January, 1996

ABSTRACT

Sixty-five subsurface cores were collected from three boreholes at a site in north-central New Mexico. The boreholes ranged from 402 m (670 ft) to 297 m (974 ft) deep. The site was 80 km (50 mi) west of Albuquerque, NM, on the Seboyeta Land Grant. The 18 shale and 47 sandstone samples cores were from both the saturated (60 samples) and unsaturated (5 samples) zones. The site was at Cerro Negro, an elongate volcanic neck that intruded through interbedded Cretaceous Mancos Shale and Dakota Sandstone 3.39 million years ago. At the time of intrusion, rock immediately adjacent to the neck was heated, presumably to temperatures sufficient for sterilization, and created a paleo-thermal aureole around the intrusion. One of the boreholes was drilled at an angle, through the horizontally-bedded shale and sandstone, sampling rock that had been increasingly heated as the borehole approached the volcanic plug. The two vertical boreholes were 1.2 km from the intrusion; most likely the rock from the vertical boreholes had not been heated by the intrusion. The purpose of the angled drilling was to test the hypothesis that microbes in subsurface strata are the original residents (or their progeny) of that strata. Less (or no) activity, as compared to analogous rock from the vertical boreholes, in samples closest to the intrusion would suggest that no new microbes have been transported to these rocks via groundwater flow since the intrusion. The other hypothesis tested was that microbial activity increases at shale-sandstone interfaces, compared to activity in rock above or below the interface.

To assure that the samples were representative of the subsurface an elaborate system of non-reactive tracers in both the core barrel and drilling fluids, and a subcoring procedure were used to minimize and quantify

contamination. The samples were subcored and prepared in an on-site lab for over-night shipping to collaborating investigators. Upon arrival at New Mexico Institute of Mining and Technology each sample was analyzed for moisture content, total microorganisms were quantified by direct microscopic counts, and culturable aerobic heterotrophs were enumerated by plate counts. Evidence of microbial activity was measured by ^{14}C-mineralization and by CO_2-production and O_2-uptake.

Plate counts and direct counts were low. Plate counts ranged from below detection (<30) to 2.43×10^3 colony-forming units g^{-1} (dry weight) of crushed rock; direct counts ranged from below detection ($<3.00 \times 10^4$) to 5.13×10^6 cells g^{-1} (dry weight) of crushed rock. Most samples mineralized less than 5% of the added glucose; two samples mineralized more than 20%. O_2-uptake and CO_2-production were highly influenced by abiotic reactions. Microbial activity did not uniformly decrease in the deeper, heated samples from the angled borehole. However, at this writing, there is considerable debate regarding the maximum temperature in the vicinity of the intrusion; the rocks in all three boreholes may have been heat sterilized. Indirect evidence suggests that some of the present-day microbes could be remnants of the depositional microbial communities: 1) the average porethroat sizes in many of the samples are too small for microbes to be transported through, and 2) marine microorganisms were found in many of the samples. There was increased microbial activity at one shale-sandstone interface, suggesting that electron donors from the organic-rich shale, and electron acceptors from the sandstone make a favorable environment for microbes at such interfaces. Sandstones, which are more permeable, generally had more activity than the less permeable shale.

TABLE OF CONTENTS

LIST OF FIGURES

LIST OF TABLES

Acknowledgments

The research presented in this thesis is a small portion of a large collaborative project. It was funded by the United States Department of Energy, as part of the Subsurface Science Program managed by Dr. Frank Wobber.

I was privileged to meet many of the investigators that participated in the project. I greatly appreciate their providing me with the data and information I needed to complete this thesis. I especially want to thank Dr. Tom Kieft, the head microbiologist for the project, and also my research advisor. Others that made a special effort to help me include Dr. Phil Long, Dr. Bruce Bjornstad, Dr. Jim McKinley, and Dr. Cheryl Gullett, all of Pacific Northwest Laboratory, and Dr. T.C. Onstott of Princeton University.

My deepest debt of gratitude goes to Dr. Jim Fredrickson of Pacific Northwest Laboratory. Jim encouraged me to apply for a graduate research fellowship jointly funded by the Department of Energy and Associated Western Universities. When Jim learned that I was not awarded the fellowship due to lack of funds, he allocated part of his research budget to fund the fellowship for me. I am very appreciative of Dr. Fredrickson's generous support of my graduate career.

In addition to Dr. Tom Kieft, Drs. Fred Phillips and Robert Bowman, both of New Mexico Institute of Mining and Technology's Hydrology Department were members of my thesis committee. Dr. Mark Person of University of Minnesota was also a valuable source of information.

Page Pegram, a fellow graduate student, did considerable work on the hydrologic characterization of the field site as her masters thesis project. I used Page's results extensively (not to mention several of her computer-generated figures) in my interpretation of the hydrologic influence on the sites' microbiology.

This project generated a huge volume of lab work. I am indebted to those who helped me process it all: Kristina O'Connor, our research technician, Bill Kovacik and Ellen Wilch, fellow graduate students, and Nolan Bennett, Kayvan Ellini, and Russell Higgens, all undergraduate research technicians.

1.0 Introduction

Bacterial activity associated with oil-bearing formations was reported decades ago (33, 56), but early reports of microbial populations in deep soils suggested sparse activity (56, 75). As recently as 1977, Alexander (1) reported that microbial activity was confined to the uppermost 1 -2 cm in cropped soil, and to the upper 1.5 - 2.0 m in organic-rich soils. Reports of significant microbial populations in deep subsurface environments began appearing only in the early 1980's (6, 18, 79).

1.1 Significance of Deep-Subsurface Microbes

Recent research has indicated that deep subsurface organisms have an important, often overlooked, impact on their environment. Microorganisms have been shown to exist in all manner of subsurface environments and may have significant effects on hydrologic and geochemical processes (4, 12, 17, 31, 34, 47, 49, 51, 72, 73). Deep subsurface organisms may also affect groundwater contamination in both desirable (i.e. contaminant degradation) and undesirable (i.e. colloid transport) ways. Further study of these organisms may reveal useful properties other than contaminant degradation, such as the production of antibiotic compounds.

1.1.1 Microbial Effects on Hydrological and Geochemical Processes

Bacteria, and their associated metabolic processes, can reduce the effective porosity of porous media, a property that is exploited in the petroleum industry in microbially enhanced oil recovery (MEOR). To enhance oil recovery, large quantities of bacterial cells are cultured, then starved to produce "ultramicrobacteria". These cells are introduced to the oil-

bearing formation, where their small size allows them to move into the pores. A substrate is then added to resuscitate the cells. The revived cells and the extracellular polymers they produce improve reservoir seep efficiency, and bacterially produced gasses and biosurfactants increase the oil mobility in the reservoir (17, 34).

Extracellular polymers excreted by bacteria have been also shown to decrease the hydraulic conductivity in natural porous media. Polysaccharidic in nature, these exopolymers occur in two basic forms. Exopolymers in the form of a capsule are intimately associated with the cell surface and may be covalently bound; in the form of a slime layer, exopolymers are only loosely associated with the cell surface (9). Several researchers have shown that exopolymer-producing bacteria, particularly slime producers, can clog porous media (4, 49, 73). Precipitates of the byproducts of bacterial metabolism, such as iron sulfide or iron hydroxides may also be responsible for plugging porous media (72, 73). These biological process can have adverse effects in the disposal of wastewater, artificial recharge, and *in situ* bioremediation of aquifers (73).

Examples of microbial activity enhancing porosity also exist. In studies with shallow subsurface sediments contaminated with petroleum hydrocarbons, high concentrations of organic acids, formed by bacteria during metabolism of hydrocarbon, selectively mobilized silica and aluminum from mineral surfaces. It is possible that similar processes may be important in deep subsurface environments as well, particularly in organic-rich or hydrocarbon-bearing horizons (31).

Microbes have significant effects on the geochemistry of the subsurface. Elevated concentrations of dissolved ferrous iron, hydrogen sulfide, and methane in aquifers can result from microbially mediated iron reduction,

sulfate reduction, and methanogenesis, respectively (Eq. 1-4). Furthermore, the degradation products (such as CO_2 and organic acids) of these and other microbial processes react with aquifer sediments to cause elevated concentration of dissolved inorganic carbon, sodium and silica in groundwater (12, 47, 51). These microbial sources and sinks must be understood and accounted for when attempting geochemical modeling of an aquifer system.

Bacteria can not only change the chemical signature of groundwater, they can alter its isotopic signature as well. Bacteria preferentially incorporate as cell mass the compounds containing the lighter isotope (50, 51) . In the case of carbon, ^{12}C is used preferentially over ^{13}C. The impact of this preference on the isotopic signature of the dissolved inorganic carbon (DIC) differs for various microbial processes common in groundwater. Due to slightly different diffusion rates of $^{12}CO_2$ and $^{13}CO_2$, when CH_4 is produced by the reduction of CO_2 (Eq 1), the remaining DIC is enriched for ^{13}C, and becomes isotopically heavy.

$$CO_2 + 4H_2 \rightarrow CH_4 + 2H_2O \qquad (1)$$

Methanogenesis can also occur through the reduction of organics such as acetate:

$$CH_3COO^- + H_2O \rightarrow CH_4 + HCO_3^- \qquad (2)$$

The preference for ^{12}C in this case would lead to lighter $\delta^{13}C$ values in the DIC pool (45, 51). Acetate can also be the substrate for sulfate (Eq 3) and iron (Eq 4) reduction:

$$CH_3COO^- + SO_4^{2-} \rightarrow HS^- + 2HCO_3^- \quad (3)$$

$$CH_3COO^- + 8Fe^{3+} + 3H_2O \rightarrow 8Fe^{2+} + HCO_3^- + CO_2 + 8H^+ \quad (4)$$

These reactions would also lead to lighter $\delta^{13}C$ values in the DIC pool. In the case of sulfate reduction, the lighter sulfur isotope, ^{32}S, is also used preferentially (51).

In some subsurface environments, sulfate and iron-reduction or methanogenesis may lead to ^{13}C-enriched DIC. Blair *et al.* (8) suggested that substantial isotope fractionation could occur during the cycling of acetate in anaerobic environments. Blair found that the mean $\delta^{13}C$ value for acetate (-14.3‰) was heavier than the mean $\delta^{13}C$ value of the sedimentary carbon (-19.0‰), and that the carboxyl group in the acetate was greatly enriched in ^{13}C compared to the methyl group (-6.0 versus -26.4‰ respectively). If microbes selectively remove organic structures that are rich in carboxyl groups (such as acetate), then their metabolic products could be ^{13}C-enriched. Other researchers have reported such ^{13}C-enrichments as a product of microbial activity. Chapelle (13) reported bacterially produced CO_2 that was much heavier isotopically ($\delta^{13}C \sim$ -10‰ to -15‰) than associated sedimentary organic material ($\delta^{13}C \sim$ -21‰), in the apparent absence of methanogenesis. McMahon *et al.* (48) reported that microbially produced CO_2 from downdip sediments was ^{13}C-enriched, compared to CO_2 from updip sediments.

1.1.2 Microbial Effects on Groundwater Pollution

The ability of microbes to degrade certain environmental contaminants is well known and widely utilized in bioremediation efforts. These efforts are usually confined to the vadose zone and to relatively shallow saturated

bioremediation. Recent work at DOE's Savannah River Site has shown that bacteria in the deep subsurface carry a number of plasmids that code for a variety of characteristics, such as antibiotic resistance, metal resistance, and hydrocarbon degradation (23). Isolates from the Savannah River Site have been shown to degrade quinoline, toluene, naphthalene, and other aromatic compounds (10, 22).

While the degradation of a contaminant is a desirable consequence of microbes present in the subsurface, microbes can also have the undesirable effect of increasing contaminant transport. Microbes can change the speciation of a contaminant, thereby (in some cases) increasing its solubility, and therefore its mobility (77). Microbially mediated metal and metalloid reductions include: U^{6+} to U^{4+}, Se^{4+} to Se^{0}, Cr^{6+} to Cr^{3+}, Mo^{6+} to Mo^{5+} and Au^{3+} to Au^{0} (45). Microbes can also act as colloids to which contaminants, such as radionuclides, can attach, increasing their mobility (21, 32). Tsezos (69, 70) reported that bacteria can sorb thorium, radium and uranium. Khovrychev (36) found considerable sorption of strontium, cesium and plutonium, even at concentrations in the 10^{-4} to 10^{-8} g L^{-1} range. These properties have been found to be particularly important in the transport of contaminants from buried nuclear waste (77).

Bacteria themselves, of course, can be groundwater pollutants. Of all groundwater contaminants, bacteria and viruses affect more of the world's population than any other contaminant. The most common disease-causing bacterial species found in groundwater are *Shigella* spp., *Salmonella* spp. and *Vibrio* spp. Regional surveys of drinking-water wells in the United States have found that 25 to 75% of the wells were positive for fecal coliforms (26).

1.1.3 Microbial Transport in Porous Media

The parameters controlling transport of bacteria through porous media are poorly understood. In many unconsolidated aquifers, adsorption appears to be the dominant factor controlling microbial transport (21, 25, 62). Scholl *et al.* (62) reported that reversible sorption seems to occur because the bacteria/surface association is governed by electrostatic, rather than hydrophobic, interaction. These electrostatic attractions or repulsions are effected by the ionic strength, pH, and presence of divalent cations and anions. Grain size, organism, and the ionic strength of the water have also been shown to be important (32). Fontes *et al.* (21) found that, of the three, grain size was the most influential factor in microbial transport, and that ionic strength and cell size were influential, but less so. Gannon *et al.* (25) confirmed that smaller cells are transported more quickly through a saturated soil column; they also found no correlation between speed of transport and either hydophobicity, degree of negative surface charge, presence of extracellular capsules, or motility. However, Jenneman *et al.* (34) , Reynolds *et al.* (60) and Sharma *et al.* (64) all report that motile strains penetrated porous media 3 to 8 times faster than non-motile strains. Jenneman *et al.* (34) also found that the depth of penetration into a sandstone core was independent of permeability when permeability was >100 millidarcies (mD), but decreased rapidly with permeabilities <100 mD. In the higher permeability cores, organisms moved through the core in a front, but not in lower permeability cores. In unsaturated conditions, Wan *et al.* (76) found that, due to preferential sorption of bacteria onto the gas-water interface over the solid-water interface, the retention rate of bacteria is proportional to the gas saturation in the porous media. Whether or not an organism will be

growth. There is evidence that microbial growth is inhibited by small pore spaces, even when nutrient limitation is not a factor (63).

1.2 Microbes in Unconsolidated Strata

Public concern over the contamination of aquifers has been a significant motivating force to examine these sediments for the occurrence of microorganisms. Hence, the bulk of research on microorganisms in the deep subsurface has been on sandy aquifers (12, 14, 65). Substantial numbers of viable bacteria (10^5 - 10^8 gdw^{-1} by acridine orange direct counts [AODC]) have been reported in the transmissive, aquifer sediments, with fewer bacteria ($<10^3$ gdw^{-1}, AODC method) in clayey confining layers (5, 12, 40, 65). Green algae, phytoflagellates, diatoms, and a few cyanobacteria have been reported at low population densities in aquifer sediments (65). Bacteria have been reported in unconsolidated vadose sediments in population densities slightly less (10^5 gdw^{-1}, AODC method) than for saturated sediments (15, 38, 39).

1.3 Microbes in Consolidated Strata

Microorganisms have also been reported in consolidated strata. Population densities of 10^5 cells mL^{-1} (AODC method) were reported in the formation water of a deep granitic aquifer in Sweden (54). Acridine orange direct counts on waters from a dolomitic limestone aquifer in Montana revealed 1000 to 1300 cells mL^{-1} (53). Endolithic bacteria have been reported in volcanic tuff from the unsaturated zone in numbers ranging from 10^5 to 10^7 gdw^{-1} (4'-6-diamidino-2-phenylindole [DAPI] direct counts) (3, 28).

1.4 Types of Bacteria Found in the Deep Subsurface

Bacteria from virtually all metabolic functional groups have been isolated from deep subsurface sediments. Aerobic hetero- and chemoheterotrophs were reported in numbers ranging from 10^5 to 10^8 CFU gdw^{-1} in sediments from an aquifer in South Carolina (5, 65). Aerobic hetero- and chemoheterotrophs have also been shown in unsaturated subsurface soil (15). Anaerobic microbes predominate (though in low numbers) in clayey layers, but were also common in the more oxic sandy layers (35, 63). Nitrate reduction, sulfate reduction and methanogenesis were all demonstrated. Most of the bacteria isolated have been mesophilic, relatively few psychrophiles or thermophiles have been detected. Thermophiles are more common in very deep environments (5).

Early attempts to identify deep subsurface isolates were hampered by the lack of an identification system appropriate for environmental isolates. API-NFT (Analytab Products, Plainview, NY) and BIOLOG (Biolog, Hayward, CA) systems are designed to identify clinically important bacteria and thus have a limited ability to identify environmental organisms (28) . A newer system, MIDI, (Microbial Identification System, Microbial ID, Inc., Newark, DE) has been more successful. MIDI provides identification of environmental isolates by comparing methyl ester fatty acid profiles of unknown organisms to profiles of known organisms contained in a data base (3). Most of the isolates from unsaturated volcanic tuff have been of the genera *Pseudomonas, Arthrobacter, Gordona* and *Acinetobacter* (3, 28).

Another method that is proving useful for identifying deep subsurface microbes is ribosomal RNA (rRNA) analysis. This method utilizes computer analysis of rRNA sequences to identify signature sequences. or short oligonucleotides unique to a certain group or groups of organisms. Originally

used to place organisms into the 3 currently recognized domains of Bacteria, Archaea (both prokaryotic) and Eukarya, signature information has been expanded to include the construction of genus- and species-specific nucleic acid probes which can be used to identify unknown organisms (9).

1.5 Purpose and Hypotheses

The U.S. Department of Energy (DOE) has funded research to address the question of the origins of microbes present in the deep subsurface strata in its Subsurface Microbial Origins Research program. The project on which this thesis is based is designated the Cerro Negro project, and is one of many conducted under the Subsurface Microbial Origins Research program. The Cerro Negro project, like other DOE Deep Microbiology projects, is a collaboration among many scientists from many disciplines at several institutions. The data presented in this thesis were collected primarily at New Mexico Institute of Mining and Technology (NMIMT), but necessarily includes data collected by other researchers. The purpose of the Cerro Negro project was to test the following hypotheses:

1.5.1 Original Inhabitants Hypothesis:

The microbes found in present day subsurface strata are the original residents (or their progeny) of that strata. That is, these organisms have survived since deposition; survived consolidation, burial, and other geologic processes.

A unique approach was taken to test this hypothesis. A rock type (shale) with a potentially favorable microbial environment, but with very small pores, thereby preventing transport by groundwater, was chosen. Additionally, by selecting a site with a post-depositional igneous intrusion and employing angled drilling techniques, a paleo-thermal gradient could be

sampled. Those rocks nearest the intrusion would have been sterilized at the time of intrusion; i.e., in the absense of transport, rock nearest the intrusion should be devoid of microbial activity. Rock outside the thermal aureole should support microorganisms that are phylogenetically related and functionally similar to those present in modern near-shore marine sediments.

1.5.2 Transport by Groundwater Hypothesis:

The microbes found in present day subsurface strata are surface organisms (or their progeny) that have been transported via groundwater to their present location.

Sandstones interbedded with the shales were subjected to the same thermal history, but more generous pore sizes (and/or fractures) allow the possibility of microbial transport by groundwater. Therefore, if microbes are found in the portion of sandstone previously sterilized by igneous intrusive activity, they have been transported there via groundwater flow in more recent times.

1.5.3 Sandstone-Shale Interface Hypothesis:

There is an increase in microbial activity in rock at shale-sandstone interfaces, compared to rock above or below the interface.

McMahon (47), Chapelle (12) and others (39, 45) , have suggested that fine grained, low permeability strata, even those with abundant electron donors (i.e., high in total organic carbon, such as lacustrine sediments or shales), may have low respiratory activity due to limited electron acceptors. In these strata, rates of microbial fermentation outpace rates of respiration, the result being an accumulation of simple organic acids (47). Adjacent coarse

grained, higher permeability strata, such as fluvial sediments or sandstones, are electron donor limited, but are rich in electron acceptors such as SO_4^{2-} and Fe^{3+}. Interfaces between coarse and fine grained strata may present a more favorable microbial environment. If electron donors, in the form of organic acids, diffuse from the shales and electron-acceptors such as O_2 and SO_4^{2-} diffuse from the sandstones, increased microbial activity should be observed at the sandstone-shale interfaces.

2.0 Materials and Methods

2.1 Site Selection

Site selection was crucial to testing the hypotheses put forth in this project. Initially, 33 sites nation-wide were identified as satisfying the requirements to test at least one hypothesis. After extensive evaluation, the Cerro Negro site was selected (42). Cerro Negro is an elongate dike-like volcanic neck located about 50 miles west of Albuquerque, NM (Figure 1). In addition to satisfying the requirements for testing all hypotheses at one site, Cerro Negro is located relatively near (177 km) NMIMT, one of the collaborating institutions, and was very near (~4 km) the Jackpile Mine, a decommissioned, open-pit uranium mine. The mine provided the opportunity to inexpensively sample some of the strata in question prior to the initiation of drilling operations. Cerro Negro is located relatively near (177 km) NMIMT, one of the collaborating institutions, and is very near (~4 km) the Jackpile Mine, a decommissioned, open-pit uranium mine. The mine provided the opportunity to sample inexpensively the strata in question prior to the initiation of drilling operations.

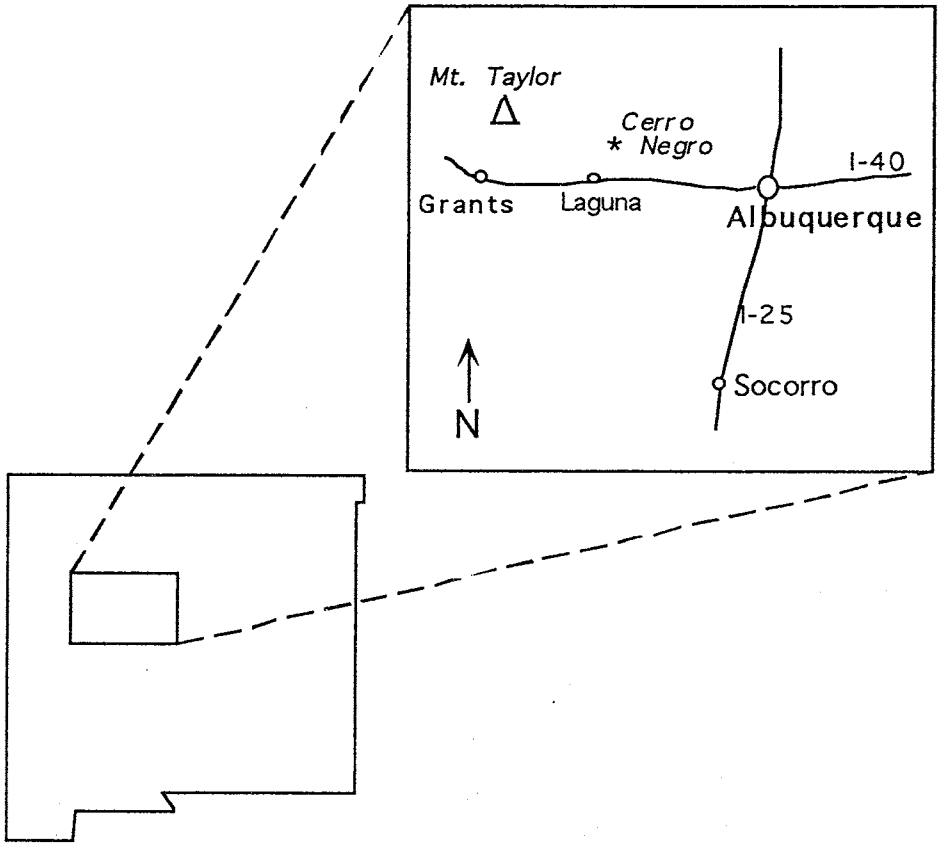

Figure 1: Location of Cerro Negro

2.2 Geology of Cerro Negro

Cerro Negro is located in the southeast corner of the San Juan Basin. The basin, a structural depression, covers approximately 77,000 km^2 of southwest Colorado and northwest New Mexico (68). The basin lies within the Colorado Plateau. Cerro Negro (Figure 2) is one of the late Cenozoic age volcanic necks that make up the Mount Taylor volcanic field. The volcanic field lies in a transition zone that separates the Rio Grande Rift and the Colorado Plateau. The Cerro Negro magmas erupted ~3.39 million yrs ago, through a Mesozoic sedimentary sequence of marine shales and sandstones which dip slightly to the northwest. Of interest to this study are the Late Cretaceous strata, the Mancos Shale and intertonguing Dakota Sandstone

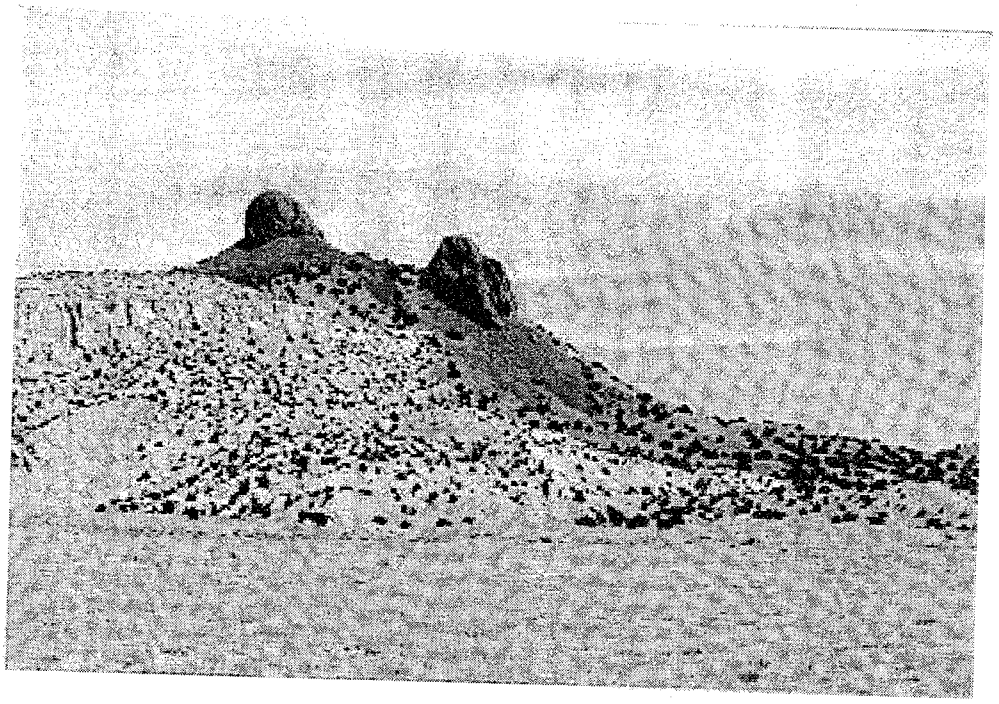

Figure 2: The west flank of the Cerro Negro volcanic neck.

which are 88 to 95 million yrs old. These formations were deposited in marine and nonmarine environments when the site was located near the western shore of the Western Interior Seaway, the result of several transgressions (Mancos) and regressions (Dakota) (29). After deposition, burial to a maximum depth of 1.75 km occurred over approximately 40 million years. Uplift during the Laramide Orogeny (35 my), Tertiary folding, fracturing and uplift, and erosion over the next 55 my brought the Mancos Shale and Dakota Sandstone to their modern elevations (43).

The Mancos Shale and Dakota Sandstone unconformably overlie the Jurassic age Jackpile Sandstone at the top of the Morrison Formation (Figure 3). The Dakota Sandstone consists of 4 members, the Oak Canyon, the Cubero, the Paguate and the Two Wells. All are fine-to-medium grained, well sorted, predominantly quartz sandstones. In the Mancos Shale, the main

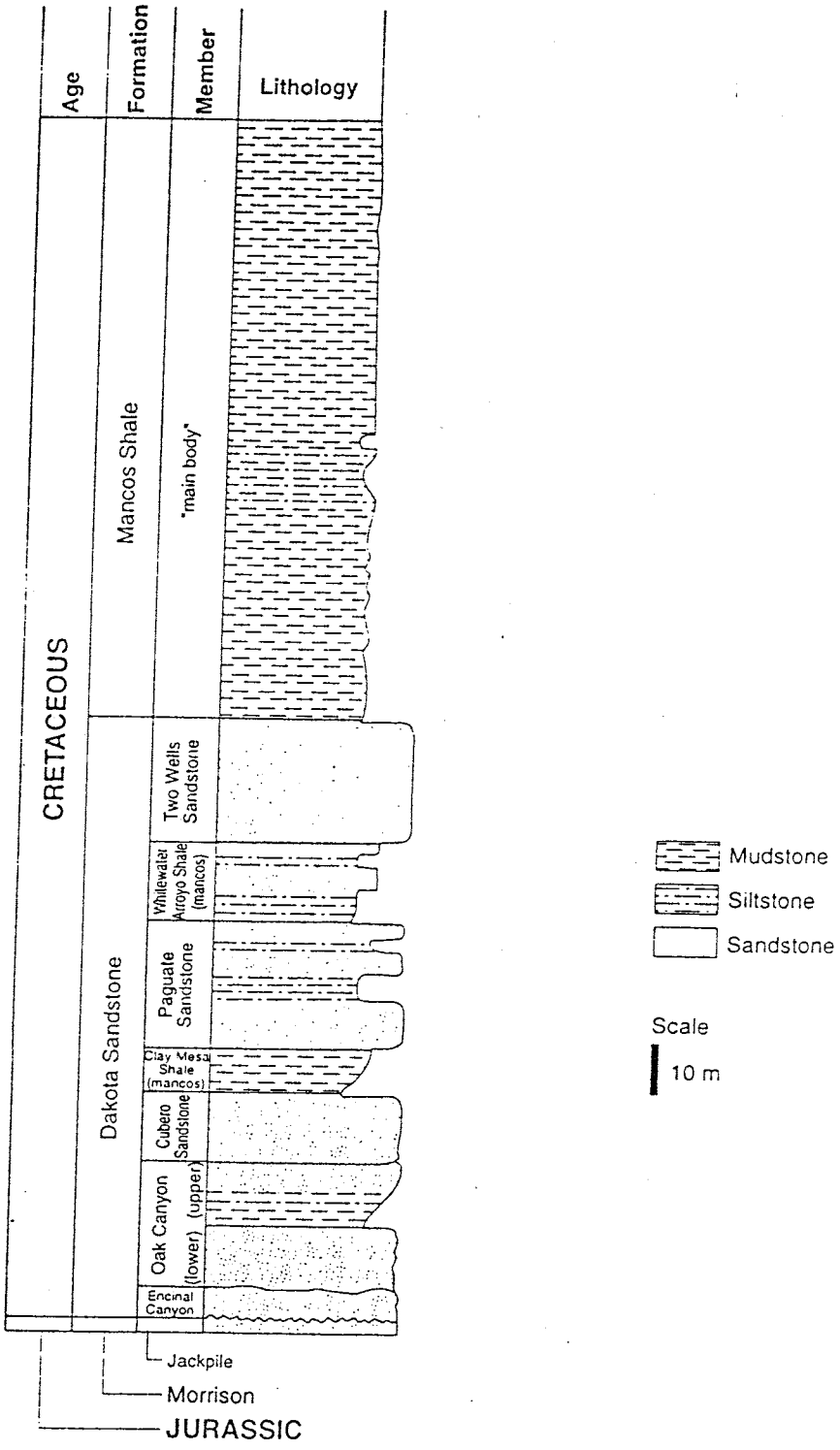

Figure 3: Stratigraphy sampled by drilling operations at Cerro Negro. Stratigraphic column courtesy of Golder Associates.

body is the thickest and stratigraphically lies above the 4 sandstone units. The other Mancos shale members, the White Water and the Clay Mesa, are thinner and are interbedded with thin beds of siltstone and limestone (29).

2.3 Regional Hydrology

The mountains which surround the San Juan Basin, the San Juan Mountains to the north and the Zuni, the Chuska, and Cebolleta Mountains the south and west, are the primary recharge areas for the basin. From these recharge areas, groundwater moves towards the center of the basin. The basin discharges in the northwest via the San Juan River, and via the Rio Salado, Rio Puerco and Rio San Jose to the southeast (68). The main aquifers are the overlying alluvium (29) and the various sandstones (68).

In the vicinity of Cerro Negro, groundwater flow is from the northwest, and is topographically, not stratigraphically controlled, as water flows to the southeast, or up-dip (55) (Figure 4). Water was collected from domestic, irrigation, and monitor wells (and from one of the study boreholes) in the vicinity of Cerro Negro (Figure 5) for geochemical and stable isotope analysis. Results of these analyses indicate that recharge in the Cerro Negro area is predominately from the Mount Taylor area (55). Some vertical recharge in the immediate vicinity of the site, through the Mancos shale, was indicated by isotopically "young" water in one of the study boreholes. Relatively large vertical permeabilities were indicated by salt contamination from a nearby mine tailings pond present in monitor wells (55). From ^{14}C dating, groundwater travel time from the main recharge area on Mount Taylor 10 km to the west is ~30,000 yrs. Flow velocities in the Two Wells, Paguate and Cubero/Morrison Sandstones in the Cerro Negro area are 0.15 to 0.18 m yr^{-1} (55).

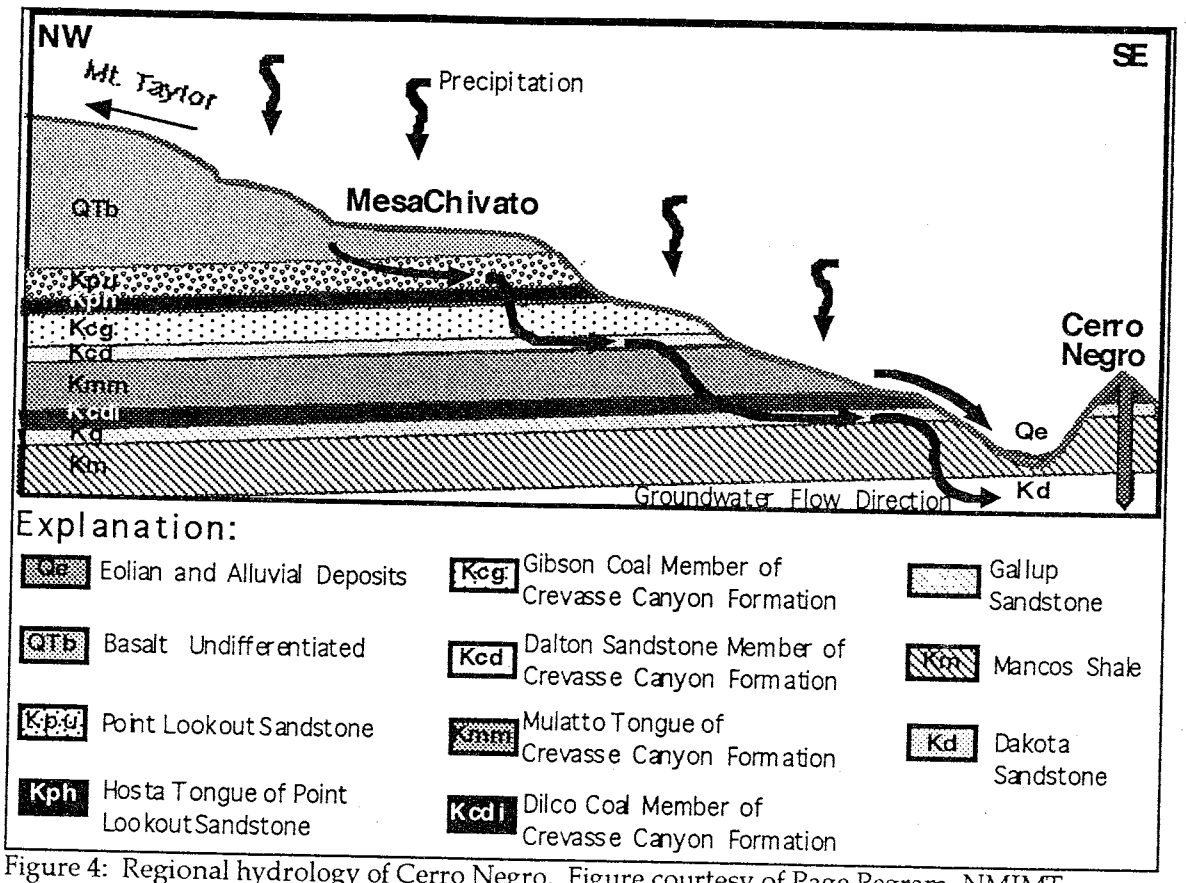

Figure 4: Regional hydrology of Cerro Negro. Figure courtesy of Page Pegram, NMIMT.

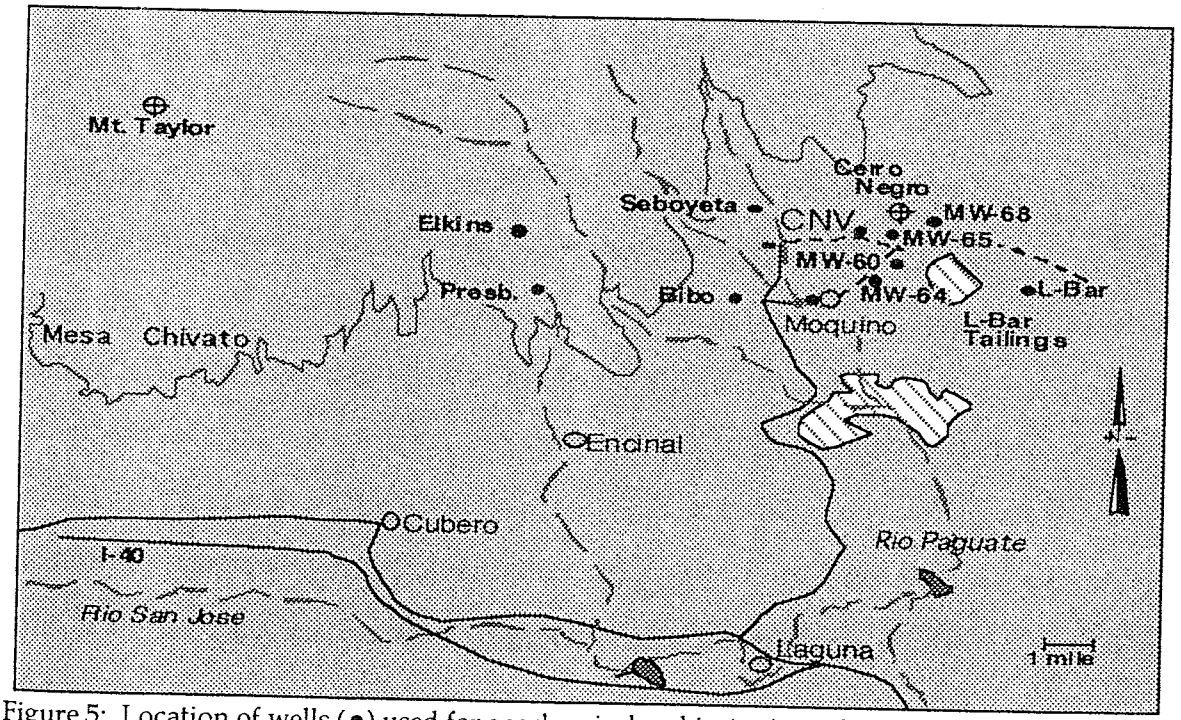

Figure 5: Location of wells (●) used for geochemical and isotopic analyses. Figure courtesy of Page Pegram, NMIMT.

2.4 Sample Collection

The boreholes from which samples were taken were drilled close to the base of the Cerro Negro neck. The first borehole, drilled vertically, was approximately 1200 m southwest of the neck (Figures 6 and 7). The distance was to assure that cores taken from this borehole had not been thermally altered by the intrusion, although the sediments did experience some heating accompanying basin sedimentation and burial. The maximum temperature that the sediments were subjected to (T_{max}) was estimated to be between 70 and 230°C (43). Microbial activity in these rocks represented a baseline to which activity in thermally altered rocks could be compared. The second borehole was drilled from a location on the shoulder of Cerro Negro, approximately 450 m southwest of the actual neck, and proceeded at an approximately 30° angle from horizontal toward the intrusive body itself (Figures 6 and 7).

Drilling services were provided by Tonto Drilling Inc. (Salt Lake City, UT). A total of 65 shale and sandstone samples were obtained from three mud and air rotary cored boreholes. Drilling muds (Desert Drilling Fluids, Albuquerque, NM) were bentonite with synthetic additives incorporated as drilling conditions dictated. The Cerro Negro vertical borehole was designated CNV, the angled borehole was designated CNAR. The "R" stands for "redrill"; the first attempt did not meet specifications and was abandoned before any samples were taken. A second vertical borehole (CNVR) was drilled when it was determined that the first one was not deep enough. Individual samples were designated according to which borehole it was taken from, followed by the distance in meters from the surface, along the borehole length, to the top of the sample interval (e.g. CNV-60.5). The CNV and

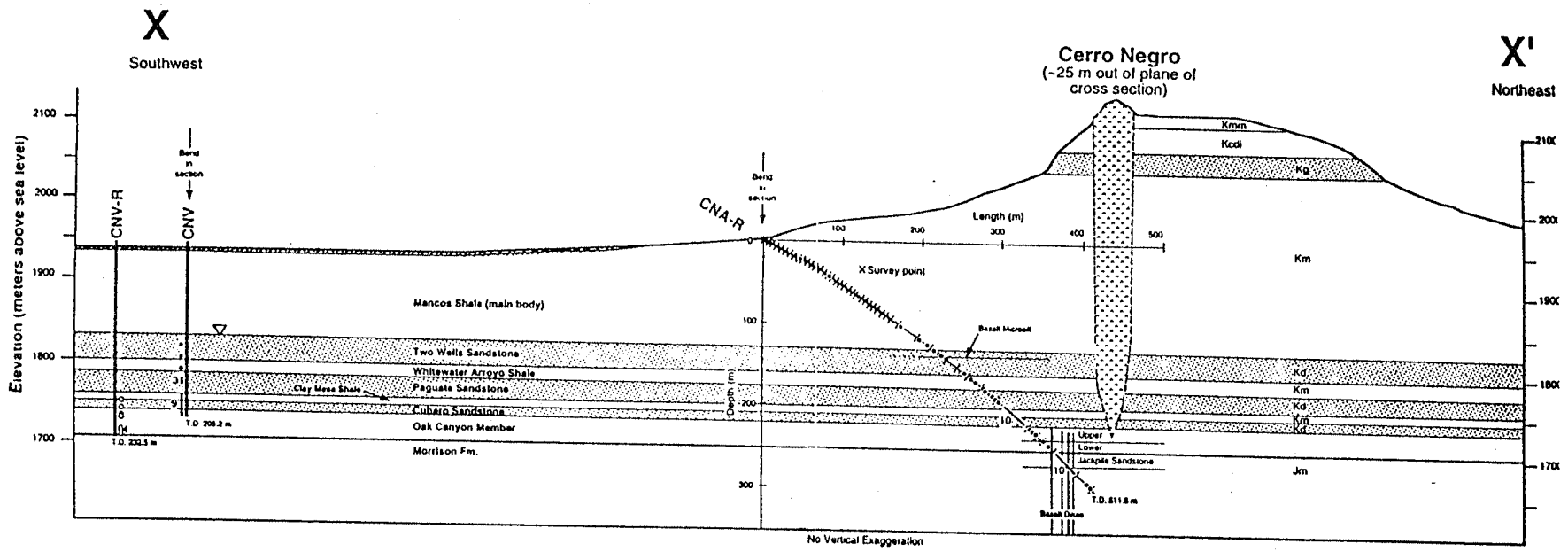

Figure 6: Geologic cross section in the vicinity of Cerro Negro, including locations of boreholes. Figure courtesy of Golder Associates.

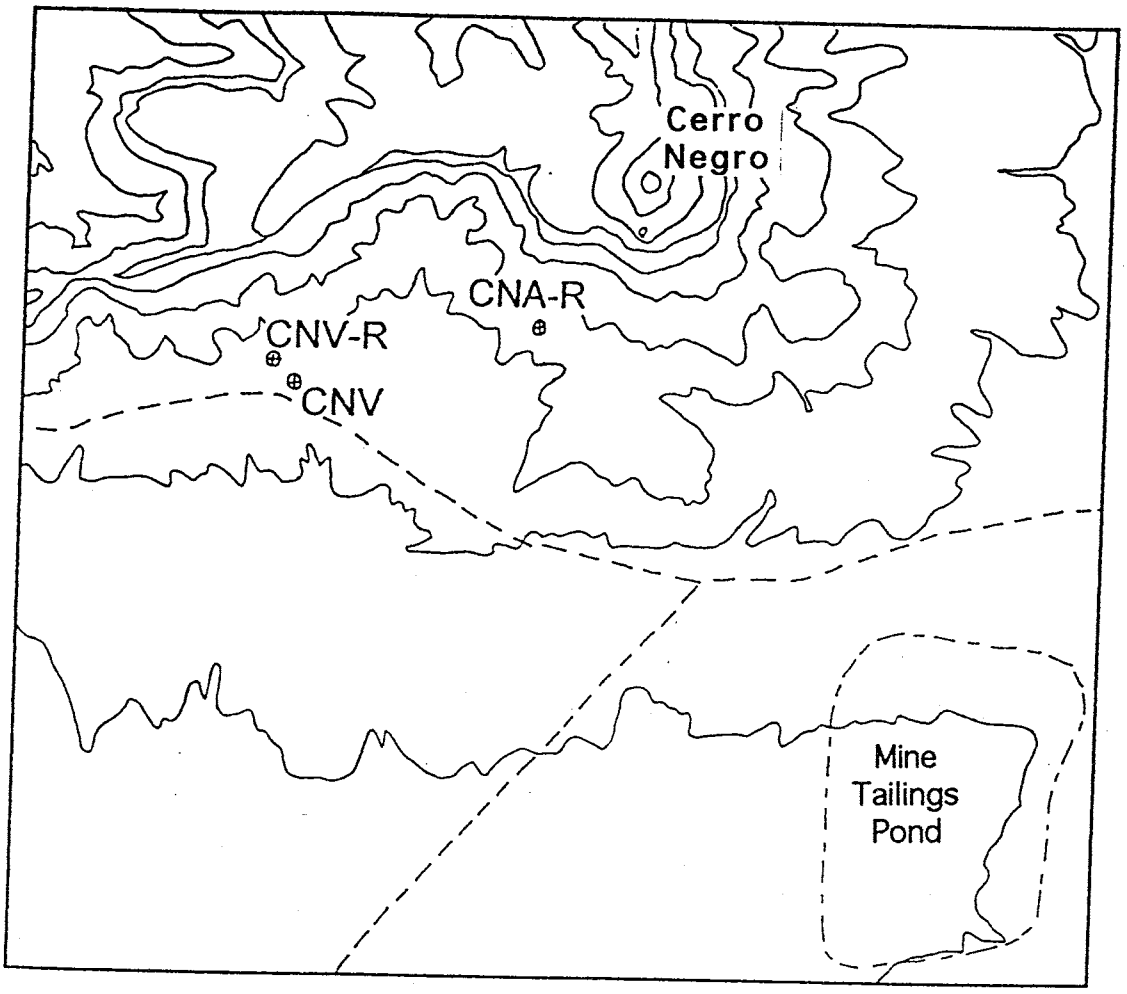

Figure 7: Location of boreholes in relation to Cerro Negro. CNV also appears on Figure 5, which depicts a larger area. Figure courtesy of Page Pegram, NMIMT.

CNVR cores were approximately 10.2 cm in diameter, CNAR cores were approximately 6.6 cm. All but one of the samples from CNV were obtained using filtered air as the drilling fluid. The remaining sample (CNV-200.3) was drilled using nitrogen gas. In the CNAR borehole, 9 cores were collected using air as the drilling fluid (CNAR-200.0, -227.6, -239.9, -251.6, -260.5, -375.3, -378.4, -390.0, and -397.1) and 2 (CNAR-381.8 and -386.5) were collected using nitrogen gas as the drilling fluid. All other sample cores (25 total) from

CNAR were collected using drilling muds. All samples from the CNVR borehole were obtained using drilling muds. Nitrogen was used to preserve any strict anaerobic organisms that other investigators were characterizing. Most of the cores used in this study were taken from the saturated zone; one sample from the CNV borehole (CNV-60.5) and four from CNAR borehole (CNAR-91.8, -200.0, -227.6 and -239.9) were from the unsaturated zone. In addition to the subsurface cores, two surface soil samples were collected near the CNV and CNAR boreholes, from areas not impacted by the drilling operations.

2.4.1 Drilling and coring operations

A sampling plan detailing the stratigraphic features and interfaces to be sampled was agreed upon by the collaborating investigators before drilling began. An on-site geologist logged the borehole and determined when sampling intervals had been reached. The CNV borehole was sampled beginning at 60.5 m; the last sample was taken at 204.0 m. CNAR borehole was sampled from 91.8 to 507.3 m (measured along the borehole) and CNVR was sampled from 189.2 to 227.8 m. Cores for microbiological analysis were obtained using procedures that varied slightly from methods described by Phelps *et al.* (56) , Kieft *et al.* (38, 39) and Colwell *et al.* (16). A 3.05 m (10 ft) long core barrel with a sterilized Lexan liner placed inside was used; however many of the cores used for microbiological analysis were not fully 3.05 m long. Several tracers were used to evaluate whether drilling fluid contamination was sufficiently minimal to allow the core to be used for microbiological analysis.

2.4.2 Tracers - PFT's, LiBr, Microspheres

Perfluoromethylcyclohexane was used as a perfluorocarbon tracer (PFT) to trace penetration of the mud or air into the core. The compound was injected into the drilling fluid at the rate of 1 - 3 mL min^{-1} via a capillary tube inserted into the uptake line from the mud tank to the drill rig. When air or N_2 was used as the drilling fluid, the PFT's were injected upstream of the air filter. The outer core mud, core parings, and homogenized subcore samples (see section 2.1.4 below) were analyzed for PFT's using gas chromatography (GC, detection limit = 1×10^{-5} $\mu g\ kg^{-1}$). Contamination of pore water was checked by adding LiBr (target concentration 100 mg L^{-1}) to the borehole fluids. This was accomplished by putting the LiBr solution in the core barrel (sealing the ends with plastic film) before it was lowered into the borehole, or by adding it to the mud tank when drilling mud was used. The homogenized samples were analyzed for Br using ion-exchange chromatography (detection limit = 10 $\mu g\ kg^{-1}$). A suspension of 1 μm fluorescent latex microspheres was placed in a Whirl-pak bag and attached to the bottom of the core barrel, inside the shoe. When the core barrel encountered the bottom of the borehole, the bag broke, coating the outside of the core with tracer. Using epifluorescent microscopy, fluorescent microspheres were quantified in the core ends and homogenized samples (limit of detection - approximately 10^3 microspheres g^{-1} of sediment). Based on the results of the 3 tracer tests, each sample was given a grade of 1, 2 or 3. In grade 1 samples, all 3 tracers were in low concentration, with 2 or more tracers below detection. In samples that received a grade 2, 2 of the 3 tracers were present in some detectable quantity but were at least 1000-fold lower than in the core ends. Grade 3 samples had high levels of at least one of the 3 tracers; data from grade 3 samples were

deleted from the final data analysis. Only 3 samples received a grade of 3; 24 received a grade of 2, the remainder (38) received a grade of 1.

2.4.3 Field-processing of samples

The Lexan liner containing the core was removed from the core barrel on the drill pad and taken immediately to an on-site laboratory. Inside an argon-filled glove bag, the Lexan liner was split using a hand-held battery-powered circular saw. The core was split into ~1 cm long sections using a hydraulic core splitter that was sterilized by wiping with a 200 mg L^{-1} sodium hypochlorite (household bleach) solution. The outside of each section was pared away using a flame sterilized hammer and chisel; the parings were used for tracer analysis. The remaining pieces of inner core from the entire length were crushed to achieve maximum particle size of approximately 3 cm^3 and pooled to produce a homogeneous sample. Portions of the homogeneous sample were double-bagged in Whirl-pak bags and placed in quart canning jars. The canning jars were then removed from the glove bag and shipped on "blue ice" to investigators via next-day shipping. Due to its close proximity to the field site, some samples were hand-carried to NMIMT in a cooler, on "blue ice".

2.4.4 Sample Quality Control

Three different quality control samples were submitted as blind controls to all appropriate investigators.

A sterile control, labeled CNV-202.5, was field-sterilized in a pressure cooker 3 times for 2 hrs each time, then field processed (see 2.1.4 below) and sent to investigators.

Sample CNVR-189.2 was a process control to validate field procedures. It was an intact core, combusted at 550°C for 24 hr, then inserted into a core barrel and dipped in drilling mud at the site. It was then field processed as usual.

Sample CNVR-93.5 was a positive control. It was Mancos shale, collected from the Jackpile Mine. One to 2 cm^3 pieces were combusted at 550°C for 24 hrs. A suspension of laboratory-grown *Arthrobacter globiformis* (Subsurface Microbial Culture Collection isolate B776) was mixed with the combusted rock. The *A. globiformis* was grown in 100% PTYG broth (see section 2.3.4) at 16°C for 36 hrs. The cells were washed twice in sterile reverse osmosis (RO) water prior to resuspension. The suspension of cells was added aseptically to the crushed rock, which was then taken to the field site where it was sent to investigators. This sample was processed outside the glove bag, to avoid introducing contamination.

2.5 Processing Core Samples at NMIMT

Upon arrival at NMIMT, samples were inspected for damage, then refrigerated at 20°C until processed. "Processing" entailed crushing the rocks and setting up all of the assays described below. Every attempt was made to completely process the samples within 24 hrs. of receipt at NMIMT, though this was not always possible. The minimum time lapse between coring a sample and processing it at NMIMT was 2 days, the maximum was 35 days.

Using aseptic technique inside a transfer hood under a flow of HEPA-filtered air, the rocks were crushed as described below. The Whirl-pak bag was emptied into a thrice flame-sterilized, cast-iron frying pan. Using a similarly sterilized hammer and chisel, the rock pieces were broken into approximately 0.5 cm^3 pieces. The rock pieces were transferred to a flame-

sterilized (3 times) cast iron mortar and pestle a few at a time. The pieces were crushed as finely and uniformly as possible, then transferred to an autoclaved, 1 pint (0.55 L) canning jar. When the entire sample had been crushed, the contents of the canning jar was mixed, then refrigerated until all the samples to be processed that day had been similarly crushed. For sandstone samples, the final product was wet sand; for shales, the end result was a fine, dry, gray powder. Even those shale samples that were taken from below the water table appeared dry, probably because the porosity of the shales is so low, there is not much interstitial water.

2.6 Analyses conducted at NMIMT

The analyses performed at NMIMT included: moisture content, ^{14}C-glucose mineralization, O_2-uptake and CO_2-production, plate counts for culturable aerobic heterotrophs, and direct counts for total and viable organisms. A variety of other microbiological, chemical, hydrological and geophysical analyses were performed by other investigators at other institutions.

2.6.1 Moisture Content

A small amount (1 - 10 g, depending on availability) of crushed sample was transferred into a pre-weighed, non-sterile, steel film can. The weight of the can plus the wet sample was recorded. The can was placed in a 105°C oven for 24 hrs. then reweighed. The percent moisture in the original sample was then calculated.

2.6.2 ^{14}C-Glucose Mineralization

Radiolabeled (universal label) glucose was obtained from Sigma Chemical Company, St. Louis, Mo. For samples CNV-60.5 through CNAR-425.0, lot no. 050H9237, specific activity 3.22 x 10^8 Bq/mmol (8.7 mCi/mmol), concentration 3.7 x 10^6 Bq/mL (0.1 mCi/mL) in aqueous solution, was used. Samples CNAR-426.5 through CNVR-227.8 used lot no. 089F9251, specific activity 2.37 x 10^8 Bq/mmol (6.4 mCi/mmol), concentration 3.7 x 10^6 Bq/mL (0.1 mCi/mL) in aqueous solution. The radiopurity for both lot numbers was >98% (specified by Sigma). The stock solution of ^{14}C-glucose was aseptically diluted 1:100 with sterile RO water immediately prior to use. The final concentration of glucose in lot no. 050H9237 was 0.011 mmol/mL; in lot no. 089F9251, the final glucose concentration was 0.016 mmol/mL.

Ten g of crushed sample was aseptically weighed and transferred to a 70 mL serum vial. Sterile RO water (usually 2 - 3 mL) was added until the sample was moistened to approximately field capacity. The vial was sealed with a sterile rubber septum. One hundred μl of the diluted ^{14}C-glucose solution was aseptically injected through the septum, and the vial was vortexed at least 3 min., until thoroughly mixed. Each sample was done in triplicate, using the same volume of RO water each time. Six of the rock samples (CNV-187.1, -204.0, -206.7, -221.7, CNAR-475.3 and -507.3) and one surface soil sample (CNV-surf) were set up as poisoned controls. These were identical to the samples, except 3.7% formaldehyde was used in place of RO water. The vials were incubated at 22°C for 1 wk.

After incubation, any CO_2 absorbed by the alkaline sample was released by injecting 1 mL of 3N HCl into the vial and vortexing. The headspace gases of each vial were bubbled through 1 mL of Carbo-sorb® (Packard Instrument Co., Meriden, CT), a CO_2-scavenging organic amine, for 1 min. (Figure 8).

Nine mL of Permafluor ® (Packard Instrument Co., Meriden, CT), a toluene-based scintillation cocktail, was added to the Carbo-sorb ® and the scintillation vials were counted for 10 min. on a Packard model 460 CD scintillation

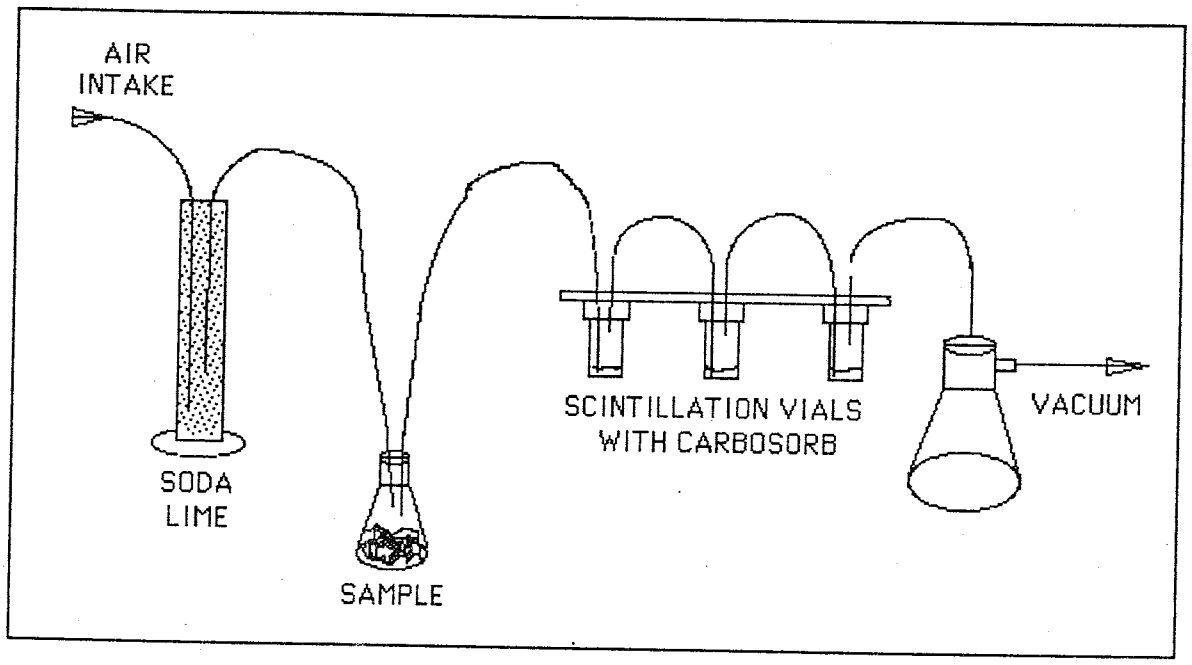

Figure 8: CO_2 collection system

counter (Packard Instrument Co., Meriden, CT). Data are reported as % glucose mineralized, with average mineralization by sterile controls subtracted.

2.6.3 O_2-Uptake/CO_2-Production

As with the ^{14}C-glucose mineralization assay, 10 g of crushed sample was aseptically weighed and transferred to a 70 mL serum vial. Enough sterile RO water (usually 2 - 3 mL) was added to moisten the sample to approximately field capacity, and the vial was sealed with a sterile rubber septum. Vials were set up in triplicate for each sample. Poisoned controls for each sample were set up in triplicate, initially using 500 μg/mL $HgCl_2$ instead

of RO water. After lush bacterial growth was discovered in a "poisoned" surface soil sample plated on 1% PTYG agar (see section 2.3.5), the concentration of $HgCl_2$ was increased to 1 mg/mL for all CNAR and CNVR samples. Twenty-four hrs. after set up, the CO_2 and O_2 concentrations in the headspace were measured using a Hach Carle ® (Loveland, CO) AGC Series 100 gas chromatograph equipped with a thermal conductivity detector. The vials were incubated at 22°C and the headspace CO_2 and O_2 concentrations were measured again. The CNV samples were incubated for 1 wk; the incubation period was increased to 2 wks for CNAR and CNVR samples. The vials were vortex mixed for 5 sec. immediately prior to sampling for GC analysis. Oxygen-uptake results are reported as the net decrease in % O_2; the CO_2-production results are reported as the net increase in % CO_2, both without subtraction of poisoned controls.

2.6.4 Aerobic Heterotrophic Plate Counts

One g of crushed sample was aseptically added to 9 mL of 0.1 M $Na_4P_2O_7$ (pH 7.0) and vortexed for 10 sec. Ten-fold serial dilutions were made in phosphate-buffered saline (Table 1):

Table 1: Phosphate buffered saline

Na_2HPO_4	1.18 g
$NaHPO_4 \cdot H_2O$	0.223 g
NaCl	8.5 g
RO water	1 L

Dilutions of 10^{-2} to 10^{-7} were spread plated in triplicate on 1% PTYG agar plates (Table 2):

Table 2: 1% PTYG agar

glucose	0.1 g
yeast extract	0.1 g
peptone	0.05 g
tryptone	0.05 g
$MgSO_4 \cdot 7H_2O$	0.6 g
$CaCl_2 \cdot H_2O$	0.07 g
agar	15 g
RO water	1 L

Plates were incubated at 22°C for 8 wks.; colony counts were performed at 48 hrs., 1 wk., 4 wks., and 8 wks. The minimum level of detection was 30 CFU g^{-1} wet weight. Results were reported in CFU g^{-1} (dry weight) of crushed rock.

2.6.5 Direct Counts for Total and Viable Organisms

Direct counts for total and viable organisms were performed using Live/Dead ® BacLight™ (Molecular Probes, Inc. Eugene, OR) viability kit (product no. L-7007, lot no. 5041-3). The kit contains a proprietary mixture of nucleic acid stains which differ both in the spectral characteristics and in their ability to penetrate healthy bacterial cell membranes. The stain allows easy distinction between live (green stained) and dead (red stained) bacteria. The manufacturer's procedure was modified as follows: 2.5 g of crushed sample and 22.5 mL of 0.1 M $Na_4P_2O_7$ were incubated for 1 hr. on a shaker incubator at room temperature. After settling for 2 min., a 900 µl aliquot of sample and 3 µl of stain mixture were incubated in the dark for 15 min. The sample/stain mixture was warmed to 50°C for 3 - 4 min. and 100 µl of 50°C Noble agar was added. Slides were then prepared and counted as for acridine orange staining procedures (65), except slides were viewed at 1000X and 220 fields were counted on each of 4 slides for each sample. Sterile control slides (no sample

aliquot) were prepared and counted as above. All glassware was combusted at 550°C for 2 hr; all fluids, including the Nobel agar were autoclaved and filter sterilized with a 0.2 μm filter. The limit of detection was 3.00×10^4 cells g^{-1} wet weight.

2.6.6 Statistical Analysis

All data expressed as a percentage (^{14}C-glucose mineralization, moisture content, porosity and total organic carbon content) were arcsin transformed (66) to make variances independent of means prior to statistical analysis. Pearson product-moment correlations and one- and two-way analysis of variance (ANOVA) analyses were performed using Student Systat®, version 1.0 (Course Technology Inc., Cambridge, MA) software.

One-way ANOVA compares several groups corresponding to a single categorical variable, called a factor. The analysis is a comparison of two variances, the between-group variance versus the within-group variance. A null hypothesis that the groups have equal means is assumed. If the between-group variance is found to be greater than the within-group variance, then the groups are said to be significantly different and the null hypothesis is rejected. A P-value is given, and represents the probability that the null hypothesis is in fact, correct. The smaller the P-value is, the less likely it is that the groups being compared have equal means. When an ANOVA analysis is run, Student Systat® also provides a matrix of pairwise comparison probabilities. The matrix of pairwise comparison probabilities is a set of significance probabilities based on Tukey's HSD (Honest Significant Difference) multiple comparison procedure. The Tukey procedure produces fewer false positives than *t* -tests do (7). The matrix lists the probability that the between-group variance is greater than the within-group variance for all

possible pair combinations. This information is useful, as even if the means are different when considering all groups together, not all pairs will be significantly different, and vice versa.

Two-way ANOVA analysis is used to learn about the effects of two factors (or effects) on the variable of interest. The test determines if there is interaction between the two factors; absence of interaction means the two factors are independent of each other. The significance of interaction is determined by the P-value. If interaction is found, an interaction plot is useful to visualize at which point or points interaction takes place. The interaction plot is a line graph of the adjusted least-squares means for each factor versus the groups. Lines that diverge widely, or cross with very different slopes indicate interaction. If no interaction is found, that is, the P-value is not significant, then the factors or main effects are checked. If only one of the factors has a significant P-value, then that factor is responsible for the effect.

A Pearson product-moment correlation matrix establishes correlations between parameters. The result of the test is a correlation coefficient and its associated P-value. Both positive and negative correlations are detected. The closer the correlation coefficient is to 1, the higher the correlation is, and the lower the P-value will be; the P-values indicate how significant the correlation is.

3.0 Results

3.1 Percent Moisture

The moisture content of the core samples ranged from 0.0 to 10.4% (Figure 9). The moisture content of the surface soil samples was 7.8 and 4.8

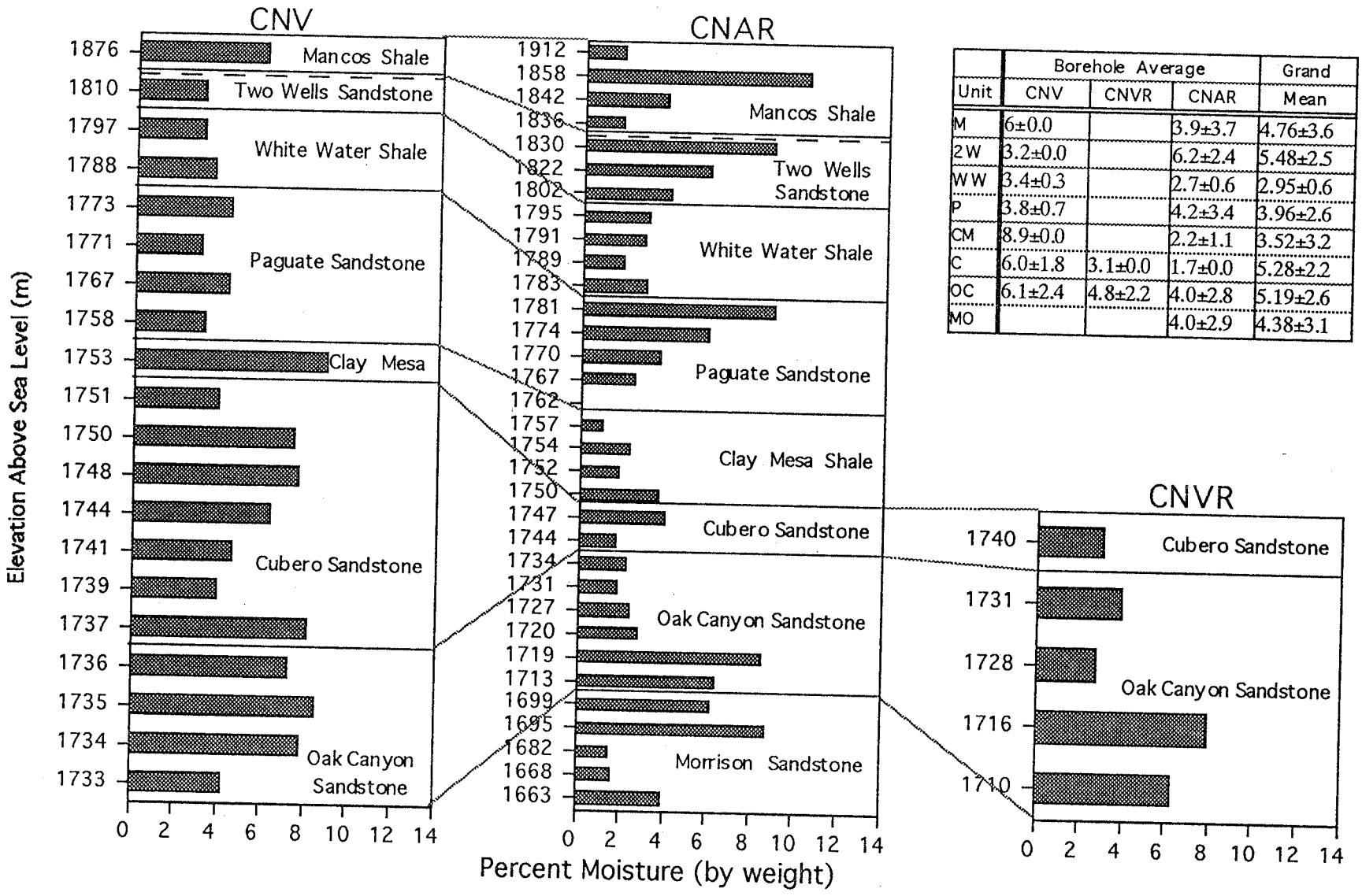

Unit	Borehole Average CNV	CNVR	CNAR	Grand Mean
M	6±0.0		3.9±3.7	4.76±3.6
2W	3.2±0.0		6.2±2.4	5.48±2.5
WW	3.4±0.3		2.7±0.6	2.95±0.6
P	3.8±0.7		4.2±3.4	3.96±2.6
CM	8.9±0.0		2.2±1.1	3.52±3.2
C	6.0±1.8	3.1±0.0	1.7±0.0	5.28±2.2
OC	6.1±2.4	4.8±2.2	4.0±2.8	5.19±2.6
MO			4.0±2.9	4.38±3.1

Figure 9: Moisture content by stratigraphic unit in all 3 boreholes. Dashed line represents the water table. Moisture contents of surface soil samples are not included.

for CNV and CNAR, respectively. There were no obvious trends in moisture content as depth increased. The reported moisture contents were lower than *in situ* values due to evaporation during the crushing process.

3.2 ^{14}C-glucose Mineralization

^{14}C-glucose mineralization over 1 week ranged from 0.0 to 31.1%. The CNV surface soil sample mineralized 15.7% of the added glucose, the CNAR surface soil mineralized 21.5%. The sterile control (CNV-202.4) mineralized 1.3% of the added glucose, the *A. globiformis*-spiked positive control (CNAR-93.5), 22.6%, and the process control (CNVR-189.2) mineralized 2.9%. Figure 10 shows the variation of glucose mineralization with depth. There was considerable ^{14}C-glucose mineralization at the Clay Mesa Shale/Cubero Sandstone interface. The type of rock, rather then depth, had the greater influence on glucose utilization. The second most active sample (CNAR-482.9) occurred in the angled borehole, 278.0 m below ground surface in the Morrison Sandstone. The Morrison and Cubero sandstones had the highest average glucose mineralization, 7.7 and 5.5% respectively. The Oak Canyon sandstone had the least average activity of the sandstones at 0.86%. The Mancos shale utilized twice as much glucose (1.2%) as the Clay Mesa (0.6%) shales. On November 23, 1994, the prescribed procedure for collection of $^{14}CO_2$ was not followed, leading to poor replication of data. The affected samples (CNAR-426.5, -436.7, -457.3 and -464.2) were removed from the data set. CNAR-451.2 was also affected, but was removed for having received a sample grade of 3.

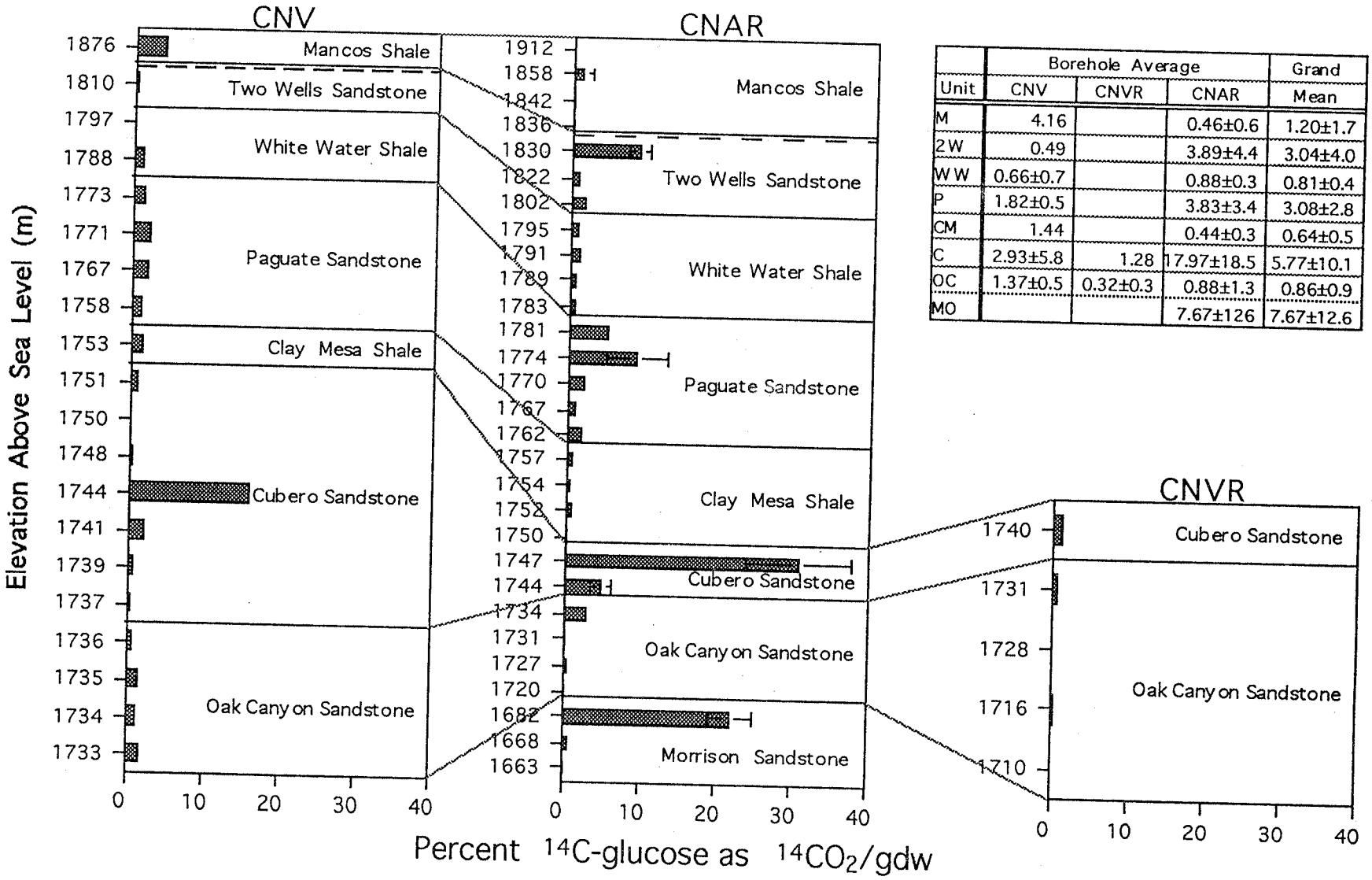

	Borehole Average			Grand
Unit	CNV	CNVR	CNAR	Mean
M	4.16		0.46±0.6	1.20±1.7
2W	0.49		3.89±4.4	3.04±4.0
WW	0.66±0.7		0.88±0.3	0.81±0.4
P	1.82±0.5		3.83±3.4	3.08±2.8
CM	1.44		0.44±0.3	0.64±0.5
C	2.93±5.8	1.28	17.97±18.5	5.77±10.1
OC	1.37±0.5	0.32±0.3	0.88±1.3	0.86±0.9
MO			7.67±126	7.67±12.6

Figure 10: Glucose mineralization by stratigraphic unit in all 3 boreholes. Dashed line represents the water table. Error bars represent 1 standard deviation. No error bar means very small or no error. Surface soil samples are not included.

3.3 O_2-Uptake and CO_2-Production

The O_2-uptake and CO_2-production results from each borehole are in Figures 11 and 12. There was considerable variation in O_2-uptake and CO_2-production among stratigraphic units. Units with the highest average CO_2-production did not have the highest average O_2-uptake (Table 3). The ratio of O_2-uptake to CO_2-production was strongly correlated to the average pH for that unit (correlation coefficient = 0.84) and to the average percent of carbon as carbonate (correlation coefficient = 0.71).

As was stated previously, the 500 μg mL^{-1} $HgCl_2$ used to poison control vials in the CNV samples was not sufficient to prevent microbial activity. Figures 7 and 8 show very clearly that for all of the CNV samples, the activity in the poisoned vials nearly equaled that of the non-poisoned counterparts. Even after the $HgCl_2$ concentration was increased to 1 mg mL^{-1}, some of the shale samples, particularly the White Water Shale, continued to have considerable activity in the poisoned control.

Table 3: Average (3 boreholes combined, ± standard deviation) O_2-uptake and CO_2-production by lithology and stratigraphic unit. Activity from poisoned controls is not subtracted. Ratio is the ratio of O_2-uptake to CO_2-production. Carbonate and pH analyses by J. McKinley at Pacific Northwest Laboratory. Values for pH and carbonate are averages for that stratigraphic unit.

Lithology	Stratigraphy	O_2-Uptake	CO_2-Production	Ratio	pH	Carbonate (%)
Shales	Mancos	5.05±1.8	0.21±0.24	24.1	8.55	2.77
	White Water	3.46±1.0	0.24±0.19	14.4	8.37	1.64
	Clay Mesa	2.42±0.7	0.21±0.19	11.5	8.29	1.20
Sandstones	Two Wells	2.51±1.3	0.94±0.36	2.7	8.26	1.19
	Paguate	2.47±0.8	0.55±0.38	4.5	8.18	1.02
	Cubero	1.94±0.5	0.56±0.29	3.5	7.94	0.34
	Oak Canyon	2.51±0.7	0.20±0.15	12.6	8.26	0.50
	Morrison	0.81±0.1	0.07±0.16	11.6	8.30	0.45

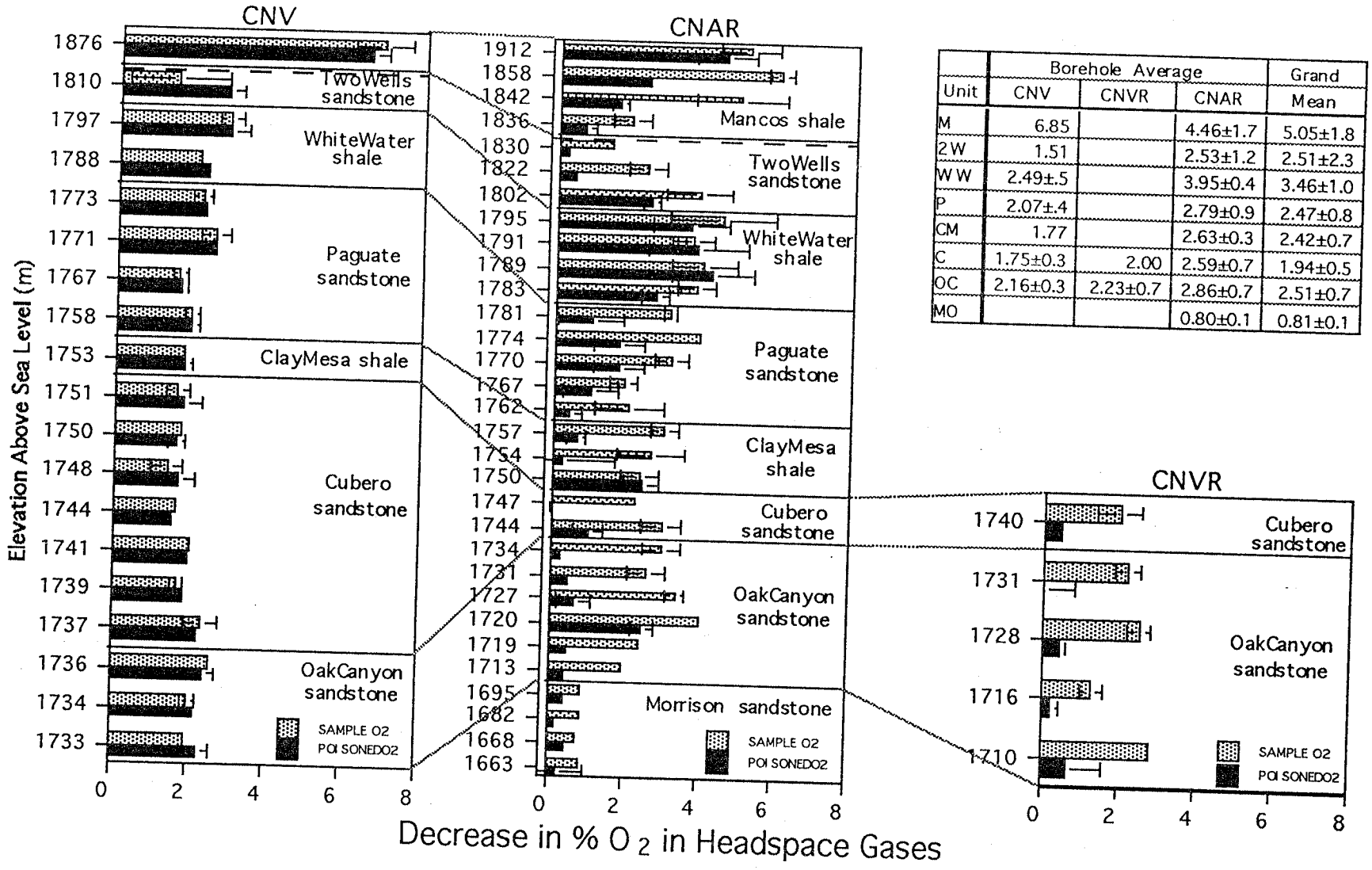

Unit	Borehole Average CNV	CNVR	CNAR	Grand Mean
M	6.85		4.46±1.7	5.05±1.8
2W	1.51		2.53±1.2	2.51±2.3
WW	2.49±.5		3.95±0.4	3.46±1.0
P	2.07±.4		2.79±0.9	2.47±0.8
CM	1.77		2.63±0.3	2.42±0.7
C	1.75±0.3	2.00	2.59±0.7	1.94±0.5
OC	2.16±0.3	2.23±0.7	2.86±0.7	2.51±0.7
MO			0.80±0.1	0.81±0.1

Figure 11: O_2-uptake in all 3 boreholes. Bar reperesents the difference (decrease) in the percentage of O_2 in headspace gases, as measured at beginning and end of incubation period. Error bars represent one standard deviation. Dashed line represents the water table. Surface soil samples are not included.

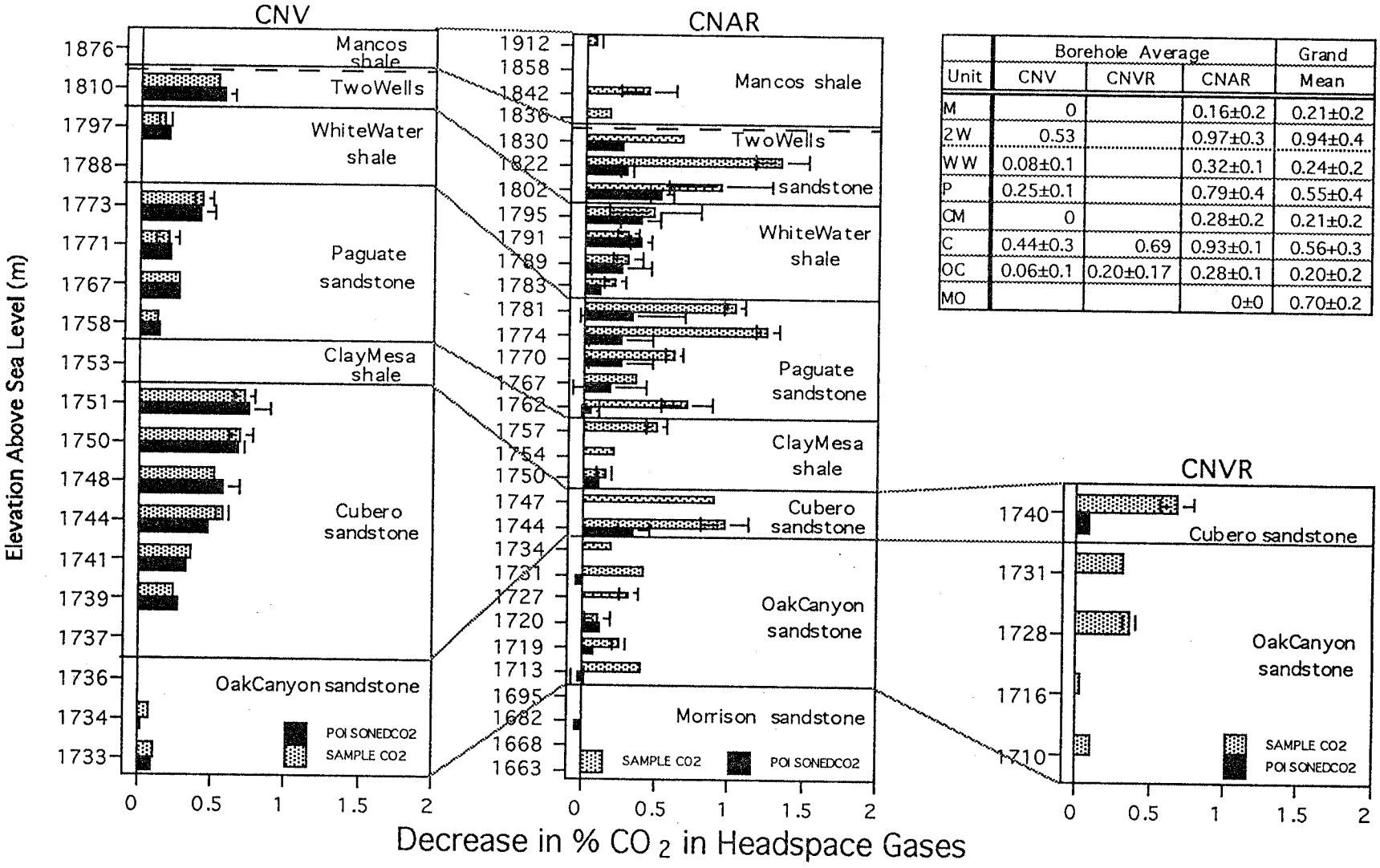

Unit	Borehole Average CNV	CNVR	CNAR	Grand Mean
M	0		0.16±0.2	0.21±0.2
2W	0.53		0.97±0.3	0.94±0.4
WW	0.08±0.1		0.32±0.1	0.24±0.2
P	0.25±0.1		0.79±0.4	0.55±0.4
CM	0		0.28±0.2	0.21±0.2
C	0.44±0.3	0.69	0.93±0.1	0.56+0.3
OC	0.06±0.1	0.20±0.17	0.28±0.1	0.20±0.2
MO			0±0	0.70±0.2

Figure 12: CO_2-production in all 3 boreholes. Bar reperesents the difference (increase) in the percentage of CO_2 in headspace gases, as measured at beginning and end of incubation period. Error bars represent one standard deviation. Dashed line represents the water table.Surface soil samples are not included.

3.4 Plate Counts

Plate counts varied from below detection (< 30) to 7.31×10^3 CFU g^{-1} (dry weight) crushed rock in the core samples (Figure 13). The CNAR surface soil had 2.24×10^8 CFU g^{-1} (dry weight) crushed rock, CNV surface soil had 1.48×10^7 CFU g^{-1} (dry weight) crushed rock. The *A. globiformis* -spiked positive control sample, CNAR-93.5, had 6.17×10^5 CFU g^{-1} (dry weight) crushed rock. Plate counts in the sterile control (CNV-202.5) and the process control (CNVR-189.2) were both below detection. The Morrison Sandstone had the highest average plate counts, 2.51×10^2 CFU g^{-1} (dry weight) of crushed rock. The sandstone with the fewest culturable cells was the Oak Canyon with 42 CFU g^{-1} (dry weight) crushed rock. In the shales, the White Water had the most culturable microbes, 87 CFU g^{-1} (dry weight) crushed rock, and the Clay Mesa had the least, 37 CFU g^{-1} (dry weight) crushed rock. The average plate counts in sandstones were quite similar to shales, 81 versus 62 CFU g^{-1} (dry weight) of crushed rock respectively. Plate counts were below detection for many samples. Ten of 16 shales samples (63%) and 23 of 42 (55%) sandstone samples were below detection. As with glucose mineralization, there was considerable activity at the Clay Mesa Shale/Cubero Sandstone interface.

3.5 BacLight® Direct Counts

In the core samples, direct counts ranged from below detection (< 3.00×10^4 for both total and viable cells) to 5.13×10^6 total and 4.68×10^6 viable cells g^{-1} (dry weight) crushed rock. Viability ranged from 50.0 to 92.7%. Only one sample, CNAR-426.5, an Oak Canyon Sandstone, was below detection for both total and viable cells. CNAR-464.2, a Morrison Sandstone, was below

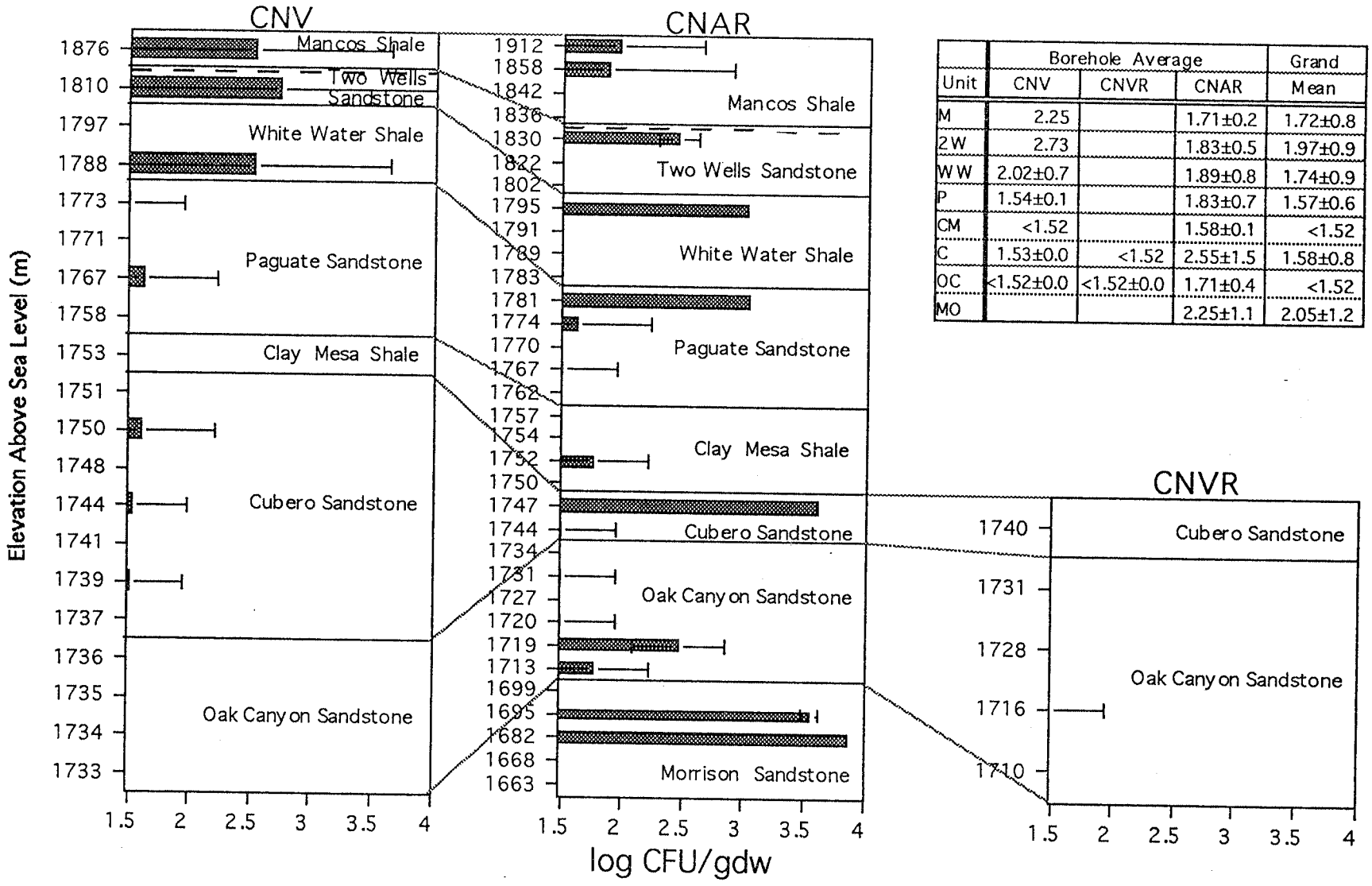

Unit	Borehole Average CNV	CNVR	CNAR	Grand Mean
M	2.25		1.71±0.2	1.72±0.8
2W	2.73		1.83±0.5	1.97±0.9
WW	2.02±0.7		1.89±0.8	1.74±0.9
P	1.54±0.1		1.83±0.7	1.57±0.6
CM	<1.52		1.58±0.1	<1.52
C	1.53±0.0	<1.52	2.55±1.5	1.58±0.8
OC	<1.52±0.0	<1.52±0.0	1.71±0.4	<1.52
MO			2.25±1.1	2.05±1.2

Figure 13: Log culturable, heterotrophic bacteria with depth by stratigraphic unit in all 3 boreholes. Dashed line represents the water table. Error bars represent 1 standard deviation. Surface soil samples are not included.

detection for viable cells only. The CNAR surface soil had a total of 6.03×10^6 cells g^{-1} (dry weight) crushed rock, with 93.8% viable. CNV surface soil had 3.39×10^6, with 87.4% viable. The *A. globiformis* -spiked control had 3.39×10^6 cells g^{-1} (dry weight) of crushed rock, 86.0% viable. The sterile control had just over the detection limit, 3.09×10^4 cells g^{-1} (dry weight) of crushed rock. The process control had 5.89×10^4 cells g^{-1} (dry weight) of crushed rock, 90.0% viable. Unlike other parameters, direct counts for both total and viable cells did not show distinct trends (Figure 14). By stratigraphic unit, average cell counts ranged from 2.09×10^5 in the Morrison Sandstone to 5.01×10^5 cells g^{-1} (dry weight) of crushed rock in the White Water Shale. By lithology, sandstone had an average of 2.88×10^5 and shale had 3.99×10^5 cells g^{-1} (dry weight) of crushed rock.

3.6 Results of Statistical Analysis

Only the CNAR borehole sampled all 8 stratigraphic units; CNV did not sample the Morrison Sandstone, and CNVR sampled only the Cubero and Oak Canyon Sandstones. Therefore, 2-way ANOVA analyses could only be performed using data from CNV and CNAR (omitting Morrison Sandstone data), or using only the Cubero and Oak Canyon Sandstone data from all 3 boreholes. All data were used in one-way ANOVA analyses. No attempt was made to separate values from those samples which may have been heat sterilized by the igneous intrusion. At this writing it is not known which samples were heated sufficiently to have sterilized them, due to incongruencies in paleo-temperature data. See section 4.1 for further discussion of the paleo-temperature data.

One-way ANOVA was used to determine if there were significant differences among boreholes, among stratigraphic units, or among lithologies

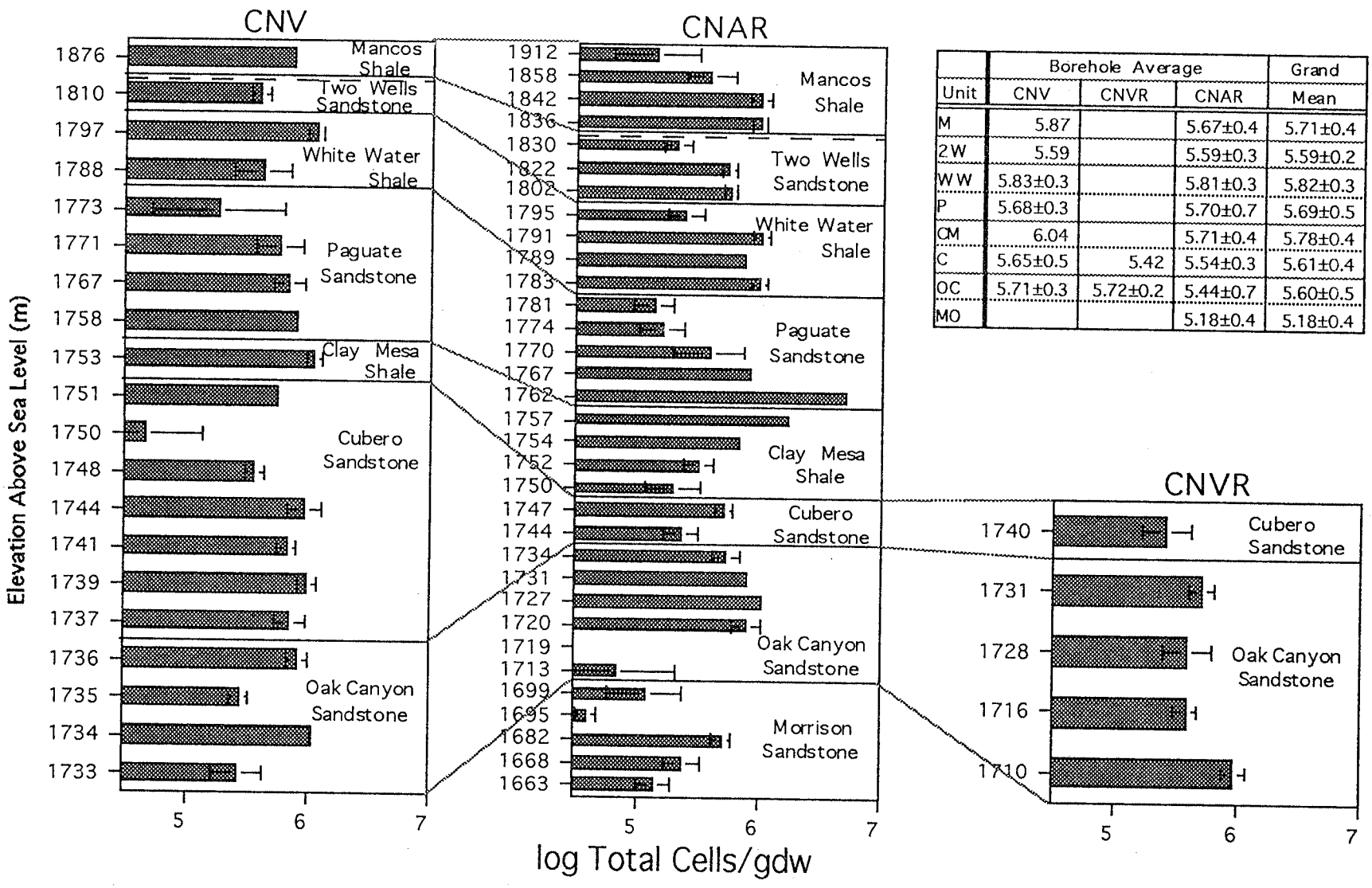

Unit	Borehole Average CNV	CNVR	CNAR	Grand Mean
M	5.87		5.67±0.4	5.71±0.4
2W	5.59		5.59±0.3	5.59±0.2
WW	5.83±0.3		5.81±0.3	5.82±0.3
P	5.68±0.3		5.70±0.7	5.69±0.5
CM	6.04		5.71±0.4	5.78±0.4
C	5.65±0.5	5.42	5.54±0.3	5.61±0.4
OC	5.71±0.3	5.72±0.2	5.44±0.7	5.60±0.5
MO			5.18±0.4	5.18±0.4

Figure 14: Log total cells by BacLight® stain method with depth by stratigraphic unit in all 3 boreholes. Dashed line represents the water table. Error bars represent 1 standard deviation. Surface soil samples are not included.

with each of the various parameters. Two-way ANOVA was used to determine if results were significantly influenced by interaction between the borehole from which the samples were collected and the stratigraphic unit from which the samples were collected (i.e. which had the greater influence on the parameter being measured, the borehole from which the sample came, or the stratigraphic unit from which the sample came?). Pearson product-moment correlation matrices were used to determine correlations between the various parameters. Because of the large number of individual observations for most parameters, P-values ≤ 0.001 (0.1%) were considered significant; all P-values are given. Refer to section 2.5.6 for a brief explanation of the statistical tests used.

3.6.1 Differences Between Lithologies

To test the hypothesis that microbial activity might be different in sandstones than in shales, the results were compared by lithology using one-way ANOVA. At this writing, it is not known which samples were heated sufficiently to have been sterilized (see Section 4.1); therefore, results from all samples were included, even from those samples near the intrusion that may have been inside the paleo-thermal aureole. Sandstone and shale had significantly different results for O_2-uptake, CO_2-production, glucose mineralization and moisture content; the average activity in sandstones was higher than in shales for all four of these analyses. There were no significant differences between lithologies for direct counts or for plate counts. Figure 15 shows the differences between lithologies in box and whisker plots, with the respective probabilities of significance (i.e., probability that the mean value of the data for that parameter is the same for sandstones and shales). To further test that microbial activity might be different in sandstones than in shales, the

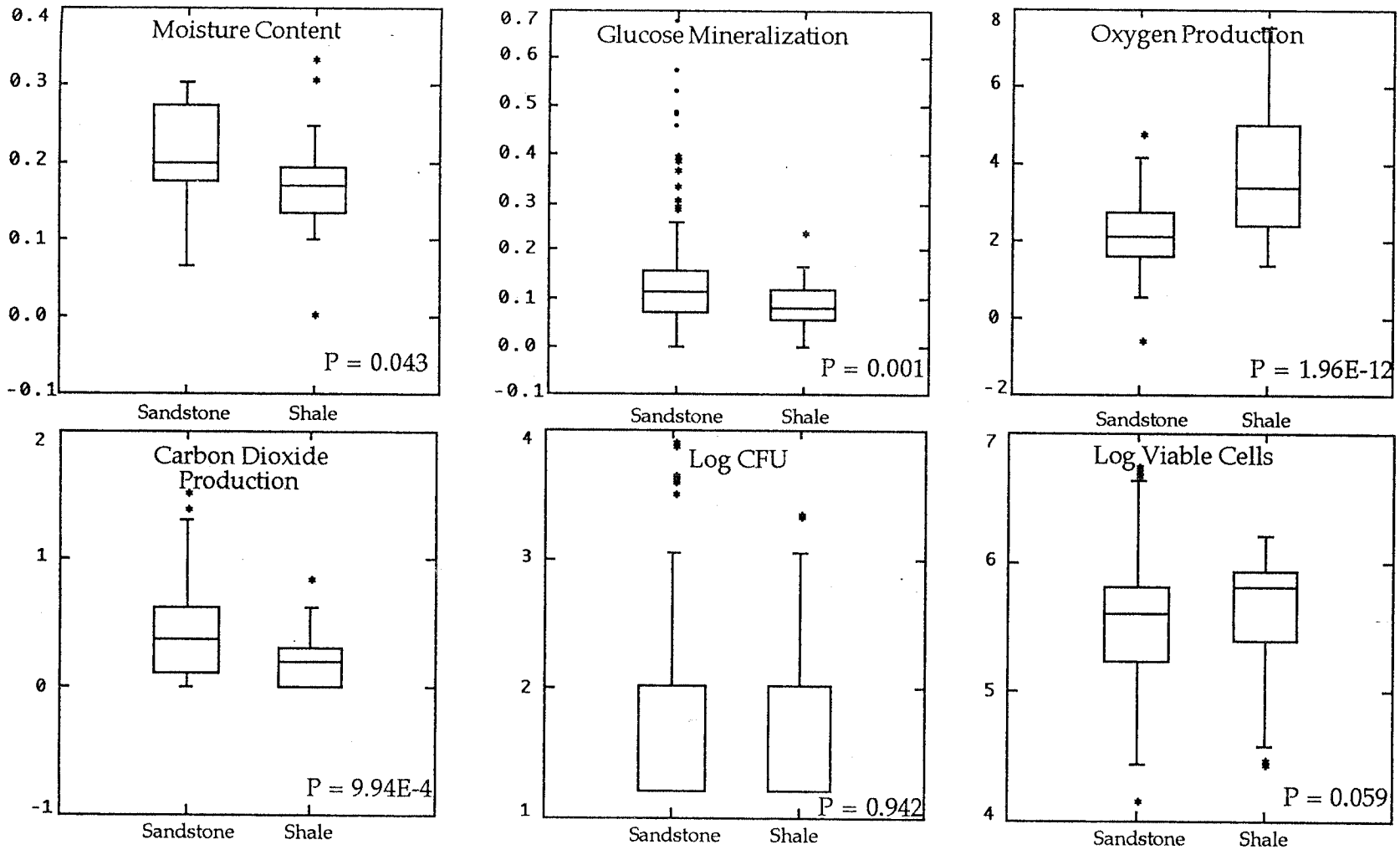

Figure 15: Differences between lithologies for 6 parameters. The box plot for total cells is quite similar to viable cells, and is not shown. The P-value is the probability that the mean for that parameter is the same for both lithologies. Center Bar of box represents median of data set. See Appendix 6 for complete explanation of box and whisker plots.

permeability, density porosity and glucose mineralization were averaged for all sandstones and all shales, and checked for correlation with lithology using a Pearson product-moment correlation matrix (Table 4). See Appendix 3 for permeability and density porosity values, and a description of how these values are arrived at. The Morrison Sandsonte was not included, as it was not logged. Glucose mineralization was chosen because it is the most accurate and most sensitive measurement of microbial activity; permeability and density porosity were chosen because they are usually very different for sandstones and shales. There were strong positive correlations between the glucose mineralization and both the permeability and the density porosity.

Table 4: Pearson product-moment correlations for average glucose mineralization, average permeability and average density porosity in sandstones and shales. Number of observations = 7, degrees of freedom = 6.

	Lithology	Gluc	Avg. k
Gluc	0.37		
Avg. k *a*	0.918**	0.621	
Avg. n *a*	0.622	0.576	0.608

** $P \leq 0.01$
k - permeability
n - density porosity
a - Data from geophysical borehole log (Schlumberger Well Services, Farmington, NM) on the CNVR borehole.

3.6.2 Differences Between Stratigraphic Units

Using one-way ANOVA, differences in microbial activity among the different stratigraphic units was analyzed. Values for O_2-uptake, CO_2-production and ^{14}C-glucose mineralization were significantly different among the various stratigraphic units. Direct counts, plate counts and moisture content were not significantly different (Figure 16). Table 5 gives the probability that the mean value of the data for that parameter is the same for the two stratigraphies being compared, for pairwise comparisons between stratigraphic units.

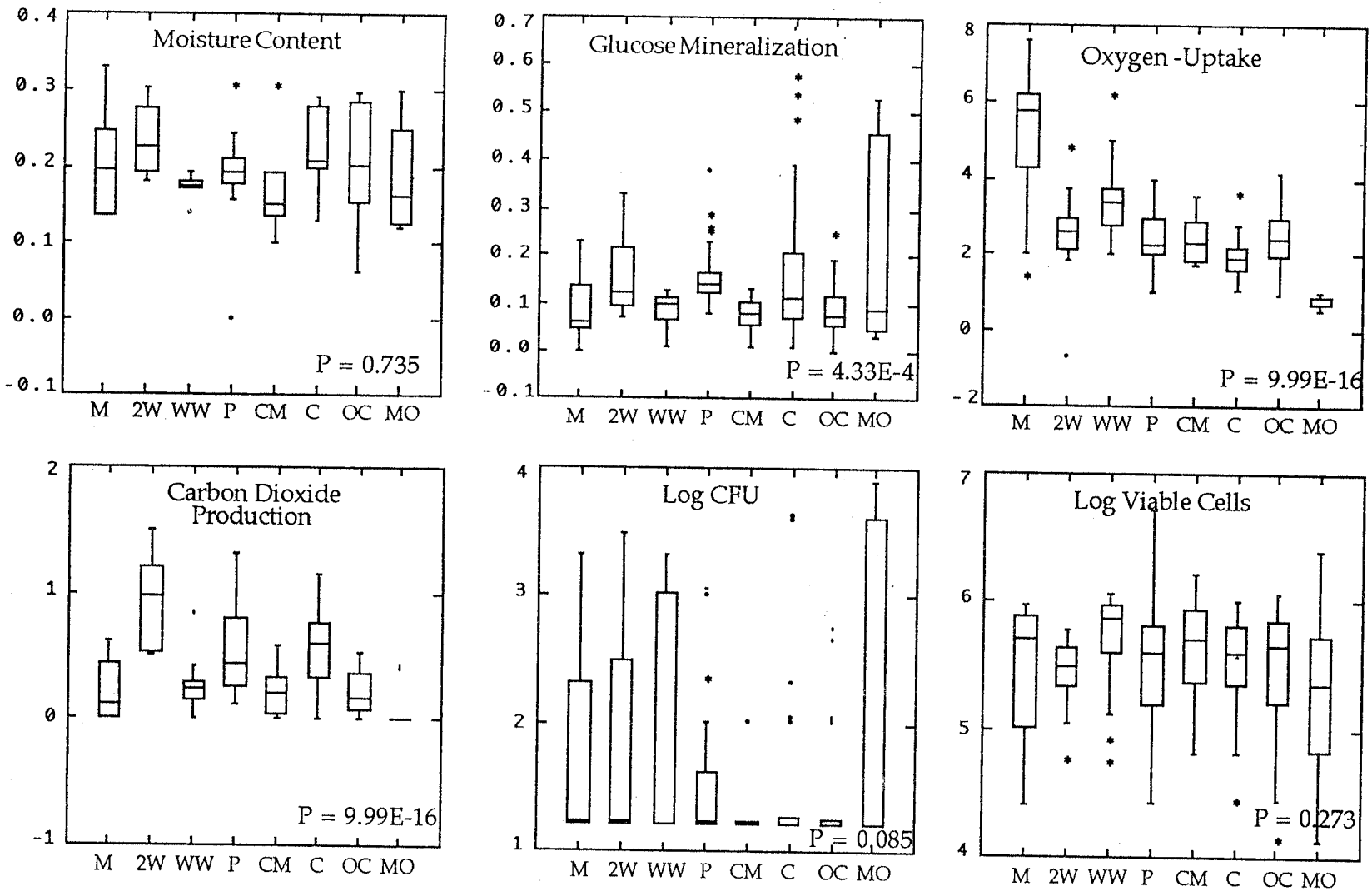

Figure 16: Differences between stratigraphic units for 6 parameters. The P-value is the probability that the mean for that parameter is the same for all units. The box plot for total cells is quite similar to viable cells, and is not shown. M = Mancos Shale, 2W = Two Wells Sandstone, WW = White Water Shale, P = Paguate Sandstone, CM = Clay Mesa Shale, C = Cubero Sandstone, OC = Oak Canyon Sandstone, MO = Morrison Sandstone.

Table 5: Probabilities (i.e. probability that the mean value of the data for that parameter is the same for the 2 stratigraphic units being compared) for pairwise comparisons between stratigraphic units for each parameter

Moisture content

	CM	C	M	MO	OC	P	2W
C	0.920						
M	0.995	1.000					
MO	1.000	0.989	1.000				
OC	0.981	1.000	1.000	0.999			
P	1.000	0.945	0.999	1.000	0.993		
2W	0.924	1.000	1.000	0.983	0.999	0.953	
WW	1.000	0.841	0.987	1.000	0.947	1.000	0.870

Glucose mineralization

	CM	C	M	MO	OC	P	2W
C	0.043*						
M	1.000	0.102					
MO	0.079	0.999	0.143				
OC	1.000	0.010**	1.000	0.059			
P	0.223	0.997	0.394	0.956	0.129		
2W	0.503	0.999	0.674	0.981	0.499	1.000	
WW	1.000	0.068	1.000	0.119	1.000	0.327	0.639

Oxygen-uptake

	CM	C	M	MO	OC	P	2W
C	0.798						
M	3.21E-6***	3.21E-5***					
MO	4.80E-4***	0.007**	3.21E-5***				
OC	1.000	0.172	3.21E-5***	3.26E-5***			
P	1.000	0.359	3.21E-5***	3.60E-5***	1.000		
2W	1.000	0.648	3.21E-5***	2.58E-4***	1.000	1.000	
WW	0.045*	3.27E-5***	5.08E-5	3.21E-5***	0.007**	0.009**	0.116

Carbon dioxide-production

	CM	C	M	MO	OC	P	2W
C	0.002**						
M	1.000	2.38E-4					
MO	0.836	3.21E-5	0.811				
OC	1.000	3.24E-5	1.000	0.655			
P	0.004**	1.000	6.63E-4***	3.22E-5***	3.44E-5***		
2W	3.21E-5***	9.92E-4	3.21E-5***	3.21E-5***	3.21E-5***	7.04E-4***	
WW	1.000	7.62E-4	1.000	0.527	1.000	0.002	3.21E-5***

table continued on next page

Table 5 (continued)

Plate Counts

	CM	C	M	MO	OC	P	2W
C	0.987						
M	0.904	0.999					
MO	0.188	0.399	0.899				
OC	1.000	0.996	0.928	0.089			
P	0.991	1.000	0.998	0.391	0.998		
2W	0.504	0.826	0.991	1.000	0.468	0.813	
WW	0.866	0.997	1.000	0.91	0.881	0.996	0.993

BacLight direct counts (viable cells)

	CM	C	M	MO	OC	P	2W
C	0.982						
M	0.910	1.000					
MO	0.467	0.858	0.995				
OC	0.783	0.997	1.000	0.986			
P	0.975	1.000	1.000	0.905	0.999		
2W	0.929	1.000	1.000	0.997	1.000	1.000	
WW	1.000	0.897	0.737	0.238	0.472	0.861	0.788

* $P \leq 0.05$; ** $P \leq 0.01$; *** $P \leq 0.001$.
CM = Clay Mesa Shale, C = Cubero Sandstone, M = Mancos Shale, MO = Morrison Sandstone, P = Paguate Sandstone, 2W = Two Wells Sandstone, WW = White Water Shale.

3.6.3 Differences Among Boreholes

There was concern that the cores from the CNAR borehole would suffer greater contamination by drilling muds because the CNAR cores were smaller in diameter than the CNV and CNVR cores, 6.6 cm versus 10.2 cm. As described in sections 3.6.1 and 3.6.2, lithology and stratigraphy both influenced microbial activity. Therefore, it was difficult to separate the effect of the borehole from which the sample was taken from the effects of both lithology and stratigraphy. One-way ANOVA was used in one attempt to determine if the core diameter had an effect on microbial activity. For each of six parameters, the results, grouped by lithology, were compared by borehole (i.e. all sandstones from CNV were compared to all sandstones from CNAR

and from CNVR). No shale samples were taken from CNVR; therefore, shales were compared between CNV and CNAR only. Due to the limited samples taken from each stratigraphic unit, results from each unit could not be compared by borehole.

CO_2-production in shale samples was significantly higher in the CNAR borehole than in the CNV borehole ($P = 1.91 \times 10^{-2}$). No shale samples were taken from the CNVR borehole. None of the other parameters in the shale samples were significantly different between CNAR and CNV (Figure 17). In sandstone samples, the number of CFU g^{-1} dry weight was the only parameter that was significantly different ($P = 3.93 \times 10^{-3}$) among boreholes (Figure 18). Based on pairwise comparisons (Table 6), this parameter is significantly different between the CNAR borehole and the CNV borehole only. In the sandstone samples, no other parameters were significantly different between pairs of boreholes.

Table 6: Probabilities of significance (i.e. probability that the mean value of the data for that parameter is the same for the two boreholes being compared) for pairwise comparisons between boreholes, sandstone samples only.

Parameter	Borehole Pairs CNAR/CNV	CNAR/CNVR	CNV/CNVR
Moisture Content	0.297	0.659	0.169
Glucose Mineralization	0.028*	0.006**	0.376
O2-uptake	0.008**	0.644	0.509
CO2-production	0.006**	0.256	0.977
Plate Counts	8.83×10^{-3}***	0.002**	0.935
Direct Counts (viable)	0.331	0.734	0.979

* $P \leq 0.05$
** $P \leq 0.01$
*** $P \leq 0.001$

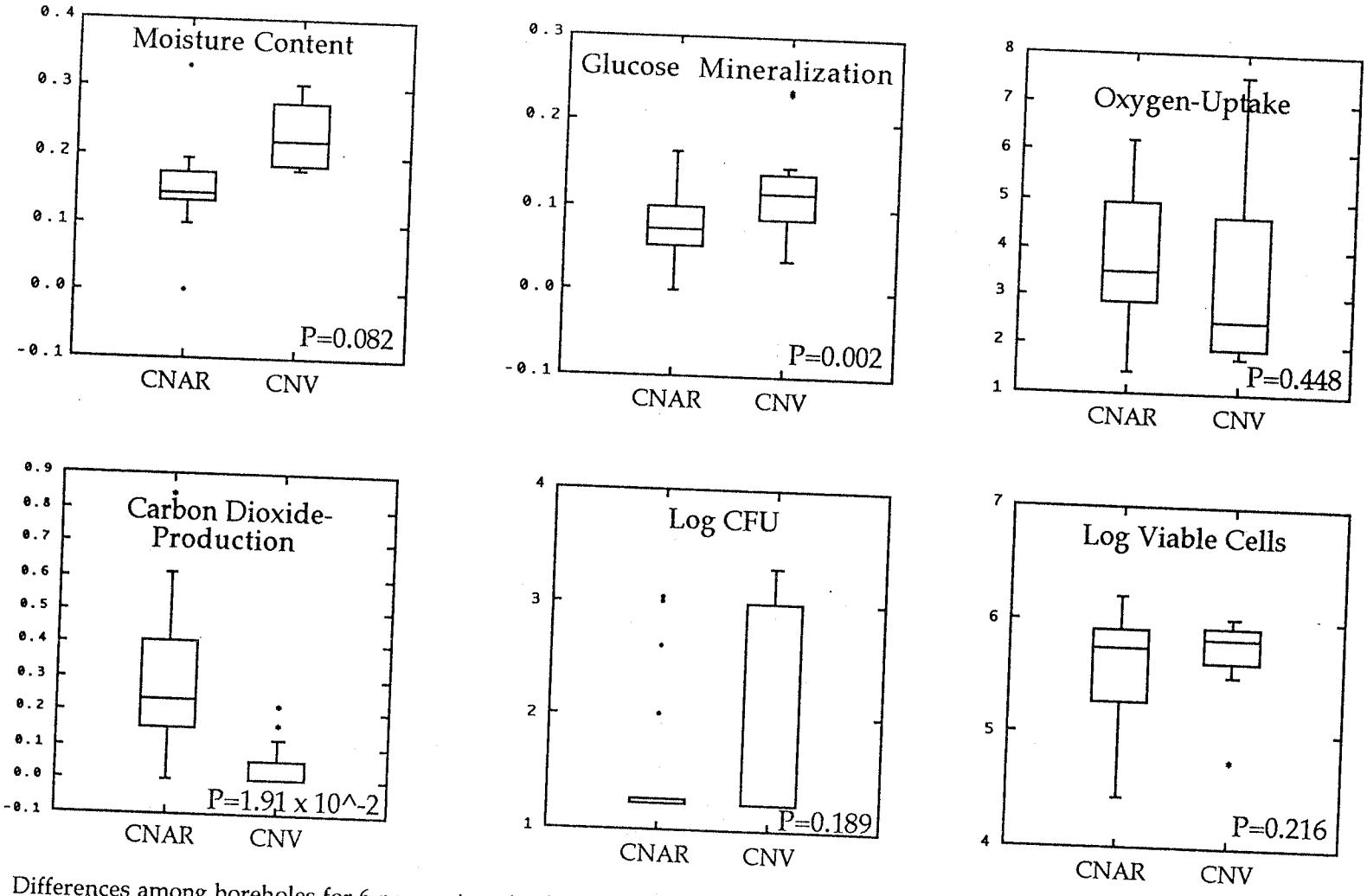

Figure 17: Differences among boreholes for 6 parameters, in shale samples only. The P-value is the probability that the mean for that parameter is the same for all three boreholes. The box plot for total cells is quite similar to viable cells, and is not shown.

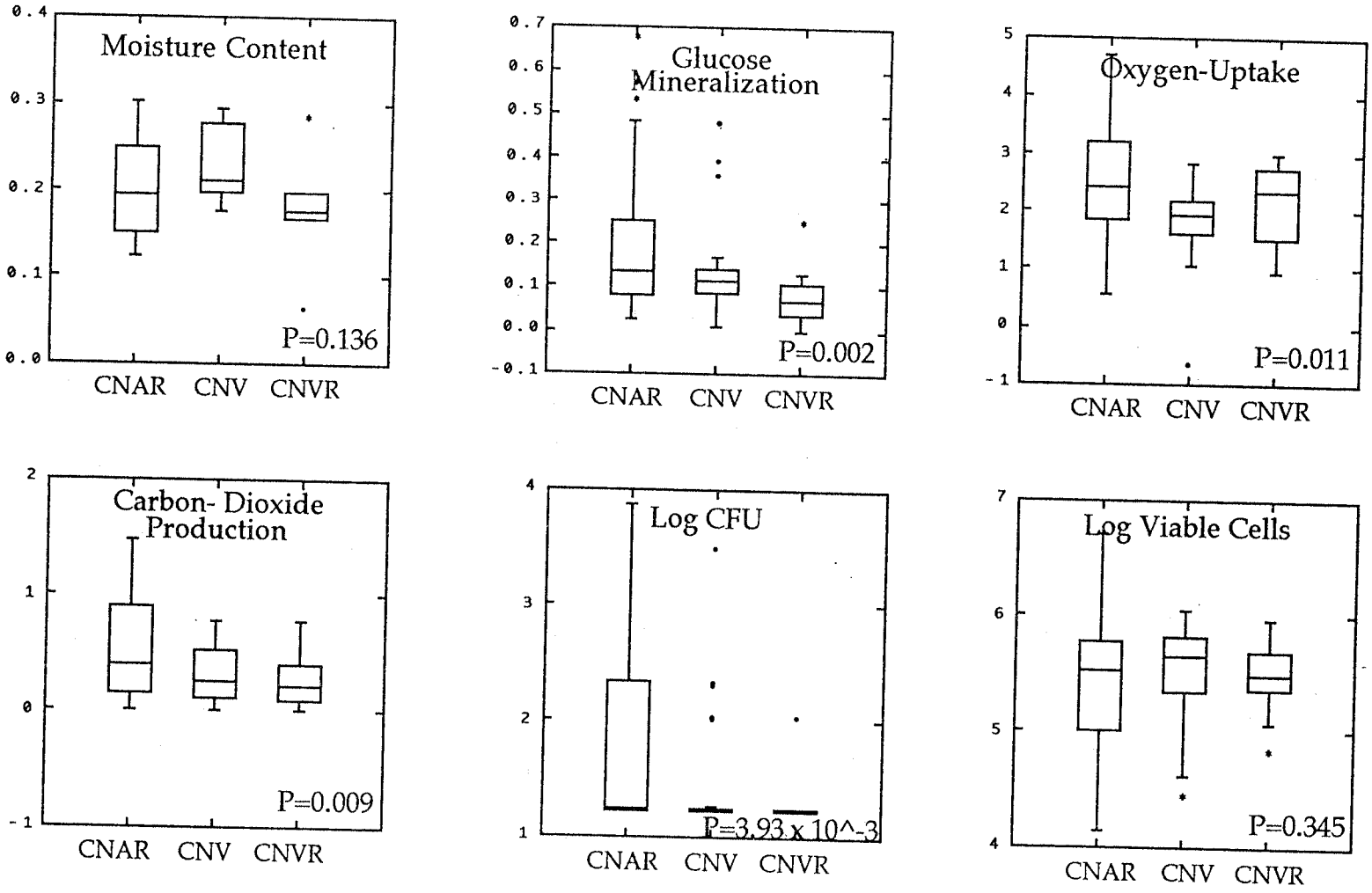

Figure 18: Differences among boreholes for 6 parameters, in sandstone samples only. The P-value is the probability that the mean for that parameter is the same for all three boreholes. The box plot for total cells is quite similar to viable cells, and is not shown.

3.6.4 Two-Way ANOVA Analyses

Two-way ANOVA analysis was used in a further attempt to determine whether the stratigraphic interval or the borehole from which the samples were collected had the stronger influence on results, and to determine if there was interaction between the two (that is, whether the effects of stratigraphy and borehole were actually independent of each other). Using data from CNAR (excluding Morrison Sandstone data) and CNV boreholes, two-way ANOVA indicated there was substantial interaction between the stratigraphic unit and boreholes for O_2-uptake ($P = 1.30 \times 10^{-5}$), ^{14}C-glucose mineralization ($P = 2.92 \times 10^{-9}$), and plate counts (1.06×10^{-3}). Interaction was not significant ($P = 0.910$) for direct counts; neither factor (stratigraphy or borehole) was significant. There was also no interaction for moisture content ($P = 0.343$); the borehole from which the sample came from had a slightly stronger influence on the moisture content ($P = 0.038$). There was no interaction at the 1% level ($P = 0.047$) between the stratigraphic unit and the borehole for CO_2-production, both factors were significant (stratigraphic unit $P = 0.99 \times 10^{-14}$, borehole $P = 0.19 \times 10^{-12}$). Figure 19 is a graphical presentation of the interactions seen for each parameter. Neither borehole and none of the stratigraphic units consistently caused interaction.

3.6.5 Pearson Product-moment Correlations

A Pearson product-moment correlation matrix (Table 7) was used to establish possible correlations among depth, moisture content, ^{14}C-glucose mineralization, plate counts, total and viable cells, O_2-uptake, CO_2-production, total organic carbon (TOC), porosity, permeability, NO_3^-, PO_4^{3+}, SO_4^{2-}, Fe^{3+} and Fe^{2+}. Data from all three boreholes were included. Notable correlations were found between depth and O_2-uptake, PO_4 and Fe^{3+}. Glucose

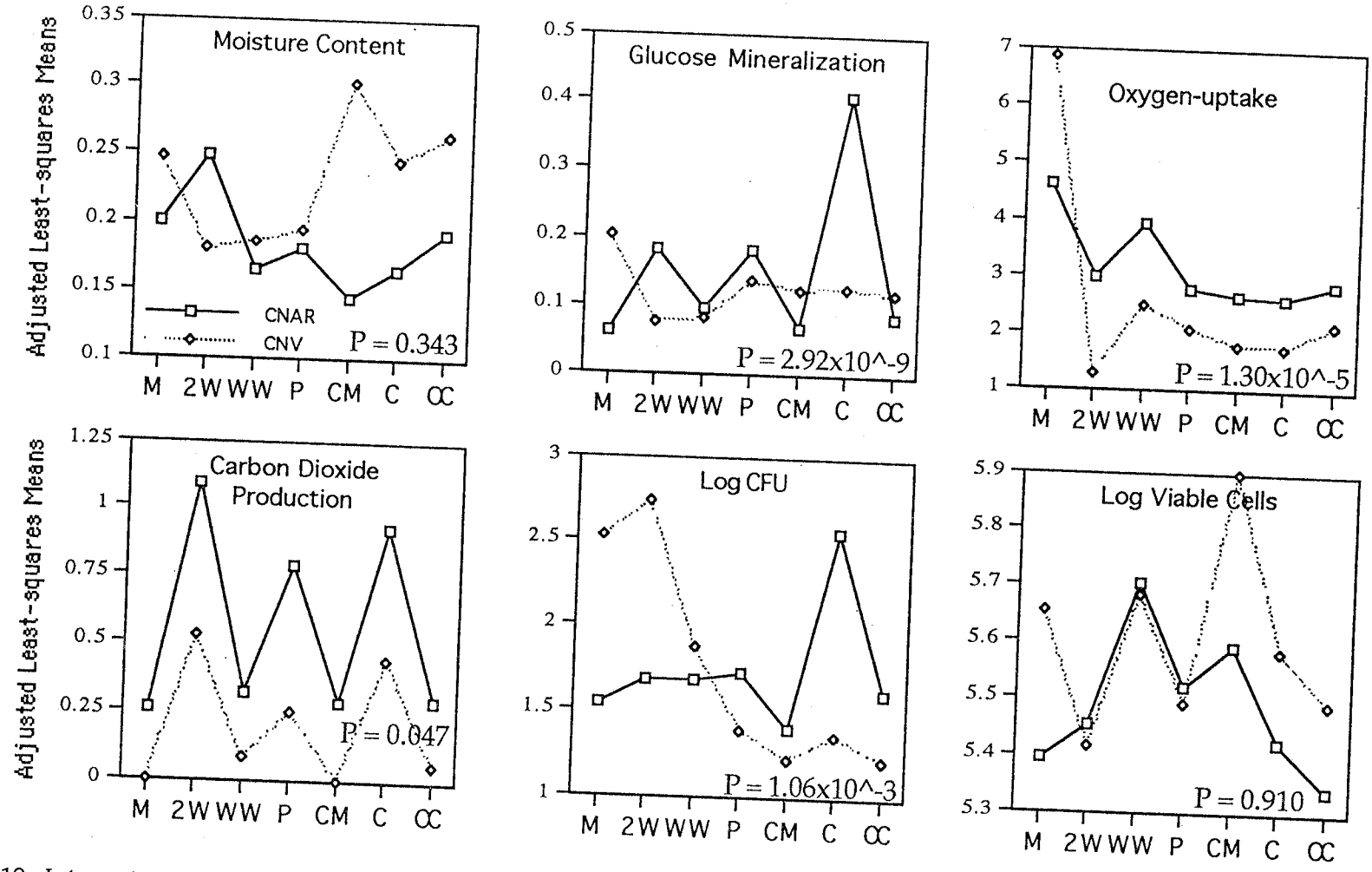

Figure 19: Interaction between borehole and stratigraphy. Lines crossing with very different slopes or widely diverging lines indicate interaction between borehole and stratigraphy. Vertical axes are adjusted least-squares means (mean predicted for unit when values for that borehole are averaged). M = Mancos Shale, 2W = Two Wells Sandstone, WW = White Water Shale, P = Paguate Sandstone, CM = Clay Mesa Shale, C = Cubero Sandstone, OC = Oak Canyon Sandstone.

Table 7: Pearson product-moment correlations between parameters.

	Depth	Moist	Gluc	CFU	Total	Viable	O2-uptake	CO2-prod.
Moist	0.012							
Gluc	-0.026	0.195						
CFU	0.314*	0.236	0.453***					
Total	1.83E-04	-0.294*	0.114	-0.243				
Viable	-0.052	-0.326*	0.108	-0.292	0.994***			
O2-uptake	0.625***	-0.023	-0.040	0.159	0.085	0.039		
CO2-prod.	-0.064	-0.066	0.505***	0.263	-0.235	-0.223	-0.095	
TOC	0.264	-0.234	-0.192	-0.127	0.225	0.227	0.253	-0.137
Porosity	0.220	0.259	0.260	0.289	-0.178	-0.183	0.123	0.084
Perm.	-0.291*	0.129	-0.118	-0.047	-0.010	-0.020	-0.222	-0.086
NO_3	0.174	0.011	-0.188	0.051	0.029	0.011	0.256	-0.106
PO_4	0.675***	0.069	-0.116	0.255	-0.060	-0.132	0.585***	-0.269
SO^4	-0.096	0.230	0.135	-0.083	0.081	0.078	-0.106	0.069
Fe^{3+}	0.593***	0.170	0.131	0.380	-0.098	-0.159	0.573***	-0.027
Fe^{2+}	0.389**	0.252	0.013	0.220	-0.063	-0.117	0.467***	-0.276

	TOC *a*	Porosity *b*	Perm. *b*	NO_3 *a*	PO_4 *a*	SO_4 *a*	Fe^{3+} *a*
Porosity	-0.300*						
Perm.	0.014	-0.409**					
NO_3	-0.276	0.274	-0.282				
PO_4	0.073	0.283	-0.070	0.342*			
SO_4	-0.210	0.302	-0.196	0.132	-0.061		
Fe^{3+}	-0.069	0.276	-0.264	0.462***	0.682***	0.069	
Fe^{2+} *a*	-0.033	0.217	-0.156	0.490***	0.618***	0.125	0.874***

* $P \leq 0.05$; ** $P \leq 0.01$; *** $P \leq 0.001$. *a* -Analyses performed by J. McKinley at Pacific Northwest Laboratories. *b* -Data from geophysical borehole log perfomed by Schlumberger Well Services on the CNVR borehole. Borehole logged to 225 m, Morrison Sandstone not logged.

mineralization was strongly correlated with CFU gdw^{-1} and with CO_2-production.

4.0 Discussion

Using both direct and indirect detection methods, microbial activity was found in all of the shale and sandstone cores. The elaborate scheme of ionic, gaseous, and particulate tracers (discussed in section 2.3.2, data from tracer analyses can be found in the Master Log in Appendix 2) used in the drilling and coring operations was essential in determining which samples had been microbiologically compromised. Thus, the microbes detected were most likely endogenous, endolithic microorganisms.

Measures of microbial activity were from samples that were greatly disturbed by the coring and crushing process. Hence, the activity measured does not reflect *in situ* microbial activity, but a *potential* activity (57).

Measures of CO_2-production and O_2-uptake could not be corrected for abiotic production of these gases because a non-reactive, reliable microbial poison could not be found. Methods development experiments to determine the most suitable poison were conducted prior to the initiation of drilling operations (see Appendix 4 for results of these experiments). These experiments, conducted using Mancos Shale, indicated that $HgCl_2$ was the most suitable growth deterrent of the methods tried. Formaldehyde caused considerable chemical evolution of the gases in question; sterilization by autoclaving for 1 hr on 3 consecutive days was deemed unreliable and too time consuming. Subsequent trials with formaldehyde confirmed the findings of increased evolution of O_2 and CO_2. The original concentration of $HgCl_2$ (500 μg mL^{-1} $HgCl_2$ or 369.4 mg L^{-1} Hg) was far greater than the 50 to 92

mg L^{-1} recommended by other researchers for poisoning sediments (71). As shown in the results section, even when the concentration of Hg was doubled, microbial activity may not have been reliably halted. The Hg was apparently being consumed by other chemical reactions, making it unavailable for uptake by microorganisms. Possible culprits are reaction of Hg with sulfur or sulfate, and sorption of Hg by cation exchange onto clay particles (74).

In aerobic microbial respiration, the ratio of oxygen used to carbon dioxide produced is 1:1. In the Cerro Negro samples, this ratio ranged from 2.7 to 24.1 (Table 3), suggesting that an abiotic process is either producing O_2 or consuming CO_2. The latter, abiotic consumption of CO_2, is the most likely. The pH of the Cerro Negro samples ranged from 7.94 to 8.44 (Table 3), meaning that microbially-produced CO_2 would react with the water used to moisten the crushed rock, forming HCO_3^-, rather than evolving into the headspace gases.

4.1. Original Inhabitants Hypotheses

The data do not directly support the hypothesis that microorganisms found in the deep subsurface today are the original inhabitants (or their progeny) of that strata, and have been there since the time of deposition. The rock in the vertical borehole should not have been thermally impacted by the volcanic intrusion. As the angled borehole approached the intrusion, it sampled rock that was increasingly heated, and therefore sterilized, at the time of intrusion. If no new bacteria have been transported to these rocks since the time of deposition, then microbial activity, as compared to comparable rock from the vertical borehole, should be quite low in the rocks nearest the intrusion (i.e. deepest in the angled borehole). Activity should

increase outward from the intrusion (upward along the angled borehole). None of the measurements of activity show this pattern (Figures 8, 9, 12, and 13).

It was intended that the angled borehole would sample all of the layers of sandstone and shale and terminate in the basalt intrusion, assuring that the entire thermal aureole had been sampled. Attempts to determine the exact location of the igneous intrusion using geophysical subsurface mapping techniques was not entirely successful. Therefore, it was not certain at the initiation of the angled drilling that the location and angle selected would guarantee "hitting" the intrusion. Once drilling started, it was also extremely difficult to maintain the borehole at the desired angle and azimuth. In addition to these technical problems, time and budgetary concerns forced the angled drilling operation to end before the basalt intrusion was encountered. However, four basalt "stringers" encountered near the end of the borehole suggest that the main body of the intrusion was nearby.

At this writing, there are only incomplete data on the thermal history of the aureole surrounding the intrusion. Several methods were used to determine the maximum temperature (T_{max}) to which the strata in the CNV and CNAR boreholes were subjected. Illite-smectite transition, illite crystallinity, smectite/chlorite transition, sterane ratios, and oxygen isotope ratios in cements all indicate that T_{max} for CNV was between 70 - 90°C at the bottom of the borehole (43). This assumes that burial was the only factor; the thermal gradient from top to bottom would be slight. Vitrinite reflectance analyses on the kerogen of the shales and sands, however, indicate that temperatures in CNV may have reached 210 - 230°C at the time of intrusion. If these higher temperatures are accurate, then the rocks in CNV, as well as CNAR, were sterilized by heat from the intrusion (43). The CNV borehole is

1.2 km from the Cerro Negro neck; other necks in the area are even farther away. Heat conduction from the intrusive is not believed to be a likely mechanism for producing 220°C temperatures; neither is burial at depths currently being proposed (T.C. Onstott, Princeton University, personal communication). In addition, neither the clay mineralogy nor the carbonates show evidence of temperatures having reached 210 - 230°C. It is possible that both clays and carbonates have totally recrystallized sometime post-intrusion, and would therefore not show evidence of heating. Evidence of such an overprinting is being sought using $^{39}Ar/^{40}Ar$ dating. One plausible mechanism for achieving the higher temperatures is heat convection by groundwater. Groundwater heated by the intrusive would rise up, then outward, in a mushroom shape. At 1.2 km way, the CNV strata could have been affected by the upper part of hot "mushroom" of water. This mechanism has been proposed, and successfully modeled, to explain the "mushroom" shape of dolomitization seen in contact-metamorphosed limestones in Italy (Mark Person, University of Minnesota, personal communication). The same model will be applied to Cerro Negro as part of the groundwater modeling efforts.

At this writing, there is also considerable question as to T_{max} in and the temperature gradient along the CNAR borehole. In the lower part of CNAR, temperatures ranged from 221 - 310°C, or from 277 - 400°C, depending on the estimation method (43). The most conservative estimate from a strictly conductive model is that within 100 m of the intrusion, T_{max} was at least 100°C (T.C. Onstott, Princeton University, personal communication). Thermophilic bacteria and spores would have survived temperatures of 100 - 120°C. If this is the correct thermal scenario, and no other bacteria have been transported to the low permeability shale, then modern microbes in this

region may be remnants of the colonies present at deposition, and should be predominately thermophiles. Outside of this high temperature zone, fewer thermophiles would be expected. At this writing, data on thermophilic organisms are not available. If T_{max} in fact reached the higher estimates of 221 - 310°C or 277 - 400°C, then sterilization certainly occurred. If this is the case, the low permeability shales near the intrusion have been recolonized post-intrusion. Early in the recolonization effort, thermophiles would be selected for, but as the rock cooled, mesophiles would also be successful. Modern communities shouldn't show any preference for thermophiles.

Temperatures in the upper sections of CNAR are thought to have ranged between 70 and 277°C (43). The same discussion applies. If T_{max} was <120°C, then modern microbes in the shales may be original residents, or they may have been transported. If T_{max} was >120°C, then any microbes present today arrived there, post-intrusion, via groundwater. Geologists participating in the study are conducting more analyses in an effort to resolve the discrepancies in the temperature data.

The present day Mancos Shale is unsaturated. The high vertical conductivity of the Mancos is presumed to be from fracture flow (55). In the matrix, water is probably under a unit gradient, and exists only as isolated "bridges" across pores (and as a wetting film over matrix surfaces). Transport of microbes in the unsaturated zone is not well studied. Studies with viruses showed that viral particles apparently have a greater degree of attachment under unsaturated than saturated conditions (41, 59). Wan *et al.* (76) showed that bacteria tend to adhere to the gas-water interface in unsaturated conditions. The Mancos shale samples from both the CNV and CNAR boreholes were probably not heated sufficiently for sterilization. The presence of fracture flow, and its closer proximity to the surface, mean the Mancos has

greater opportunity for the introduction of surface microbes, and that bacteria there are more likely to be modern. However, microbes found distant to fractures are less likely to be modern, due to the reduced possibility for transport.

Twenty-eight of the Cerro Negro samples were analyzed for average porethroat sizes (Table 8). Porethroat size was not measured on any samples from the Clay Mesa Shale. There was only a small range in average porethroat sizes (0.01-0.07 μm) in the nine samples from the upper three units, the Mancos and White Water Shales, and the Two Wells Sandstone. Conversely, there was considerable range in the size of porethroats in the 20 samples from the lower units, the Paguate, Cubero, Oak Canyon, and Morrison Sandstones. Some samples from the lower units had porethroat sizes similar to the upper units (0.02-0.06 μm), but some samples from the lower units had quite large porethroats, up to 31.65 μm. In all, 16 of the 28 samples, or 57%, had porethroats <0.1 μm; 13 of those were in the 0.01-0.08 μm range. Typical rod shaped bacterial cells are 1-3 μm in length and 0.25-1 μm in breadth. A typical cocci is 0.5-0.8 μm in diameter (9). Even so-called "dwarf" cells, which dominate in nutrient-poor environments like the deep subsurface, are 0.2 - 0.3 μm (37). Since it would be difficult for a bacterial cell to be transported through a medium whose pores are smaller than the cell, it seems likely that at least some of the cells (or their progeny) found in the non-sterilized strata have been there since deposition. There is good correlation ($r = 0.52$) between the porethroat size and glucose mineralization, and shales tended to have lower glucose mineralization than sandstones (Figure 10); both facts suggest that large porethroats are required for microbial activity to occur.

Table 8: Average porethroat sizes. Analyses by Cheryl Gullett, Pacific Northwest Laboratory. Performed using mercury injection method. No porethroat analyses were performed on any Clay Mesa Shale samples.

Stratigraphic Unit	Porethroat sizes (μm) Range	Average †	No. of Samples
Mancos Shale	0.02-0.03	0.027	3
Two Wells Sandstone	0.01-0.07	0.046	3
White Water Shale	0.03-0.04	0.033	3
Paguate Sandstone	0.03-0.2	0.103	3
Cubero Sandstone	0.06-5.05	2.132	9
Oak Canyon Sandstone	0.03-2.06	0.535	6
Morrison Sandstone	0.02-31.65	15.83	2

† Samples with mixed shale-sandstone lithology will have a greater range of porethroat sizes than samples with a more unimodal grain size. See geological log in appendix 3 for grain-size descriptions.

The presence of marine microorganisms in some samples (27) (also data from J. Fredrickson, Pacific Northwest Laboratory, Appendix 2) is further indirect evidence that at least some of the present day organisms are remnants of the depositional microbial population. It seems unlikely that a marine organism would survive being transported from a marine environment to what is now north-central New Mexico (the geography of the earth at the time such an organism would have entered the hydrologic system was not much different than it is now). Conversely, a microbe trapped in the Cerro Negro rocks since deposition probably has not had the opportunity to be transported away from its now non-marine environment, for the same reasons described above.

4.2 Transport by Groundwater Hypothesis

The hypothesis that subsurface microorganisms have been transported to their present location via groundwater flow is strongly supported. From Table 7, there is a strong positive correlation between glucose mineralization and both average permeability and average density porosity. The sandstones,

whose average permeability is 10 times greater than the shales, had an average of 2 times more glucose mineralization. This suggests that more microorganisms have been carried into the more transmissive sandstones via groundwater flow. Groundwater flow through fractures would increase the number of organisms, and reduce the time required for microbes to be transported to their present location. There is strong evidence that fracture flow exists in this system, at least in the Mancos Shale (55). This probably accounts for the higher glucose mineralization seen in the Mancos, in spite of its having the lowest average permeability. Carbon-14 and tritium data indicate that in the vicinity of the Cerro Negro intrusion modern water, but no "post-bomb" tritiated water, is present in the Two Wells Sandstone, just below the Mancos shale (55). Any microbes in the Mancos Shale then, have been there for at least 50 yrs.

There is a wide range of possible time frames for microbial colonization in the Cerro Negro rocks. As just stated, the youngest microbes, those in the fractures in the Mancos Shale, took least 50 yrs to travel from the surface to their present day location. If it is assumed that the microbial colonies are the same age as the groundwater that likely carried them there (excluding fracture flow), then it would take approximately 30,000 yrs for a bacterial cell (or its progeny) to travel from the ground surface at the aquifer recharge area on the flanks of Mt. Taylor, to the rocks around Cerro Negro. The slowest flow rate calculated from the hydrologic portion of this study was $3.5 \times 10\text{-}9$ m s^{-1} or 0.11 m yr^{-1} in the Paguate Sandstone (55). If a bacterial cell entered the flow system in the recharge area, and flowed at this rate to Cerro Negro, it (or its descendants) would arrive in approximately 91,000 yrs. The estimates for Cerro Negro are considerably longer than the 3000 to 4000 yr estimated travel time (61) and 11,500 yr approximate groundwater age for the

Middendorf Aquifer on the Atlantic coastal plain (52). Murphy *et al.* (51) estimated the maximum age of the waters, and hence possibly the microbes, of the Milk River Aquifer in Alberta, Canada to be 20,000 yrs. As discussed in section 1.1.3, bacterial transport in porous media is not well understood. It is known, however, that in unconsolidated media, adsorption of bacterial cells to the matrix is significant. If similar forces operate in consolidated media, then calculating the potential age of bacterial colonization based on groundwater travel times is probably a serious underestimate.

4.3 Sandstone-Shale Interface Hypothesis

The hypothesis that there would be an increase in microbial activity at sandstone-shale interfaces was supported by the data from one such interface. The contact between the Clay Mesa Shale and the Cubero Sandstone was quite distinct in appearance, making it easy to be certain a sample was collected from the desired interval in both the CNV and CNAR boreholes. There was a dramatic increase in glucose mineralization at the Clay Mesa-Cubero interface in both boreholes (Figure 8). A spike was also seen in the plate count values. Data comparing aerobic and anaerobic acetate mineralization (J. Fredrickson, Pacific Northwest Laboratory, see master data table in Appendix 2) showed ten times more anaerobic than aerobic mineralization in the Clay Mesa sequence just above the contact. At the actual contact and in the Cubero Sandstone just below it, aerobic acetate mineralization increased 250-fold, and anaerobic acetate mineralization increased 50-fold. These observations are consistent with the idea that small organic acids, the result of anaerobic fermentation in the shale, are diffusing into the more electron-acceptor rich sandstone.

The Clay Mesa-Cubero interface was the only shale-sandstone interface that showed an increase in microbial activity. This interface was easily identified and extensively sampled above and below it in both the CNV and CNAR boreholes. The contacts for the other shale-sandstone interfaces were not as easily located. Of the other interfaces, some were not sampled at all; for those that were, the samples were not frequent enough to see distinct trends in the data.

Currently, it is presumed that molecular diffusion is the mechanism for bringing electron donors from organic-rich strata into contact with electron acceptors (12, 14, 45). In fact, the concentration of a solute in groundwater is the result of several processes that can be described by the advection-dispersion equation (for two-dimensional flow in a homogeneous, isotropic medium (20)):

$$\frac{\partial C}{\partial t} = D_L \frac{\partial^2 C}{\partial x^2} + D_T \frac{\partial^2 C}{\partial y^2} - v_x \frac{\partial C}{\partial x} \tag{5}$$

where:

C = solute concentration
D_L = the longitudinal hydrodynamic dispersion
D_T = the transverse hydrodynamic dispersion
v_x = average linear velocity

The two hydrodynamic dispersion coefficients, D_L and D_T, are further defined as follows (20):

$$D_L = \alpha_L v_i + D^* \tag{6a}$$

$$D_T = \alpha_T v_i + D^* \tag{6b}$$

where:

D^* = effective diffusion coefficient
α_L = longitudinal dynamic dispersivity
α_T = transverse dynamic dispersivity
v_i = average linear velocity in the i direction

The first terms on the right-hand sides of these equations refer to mechanical dispersion. Mechanical dispersion is the term for the collective effects on solute concentration of these phenomenon: 1) as fluid moves through the pores of a medium, it will move faster in the center of the pores than along the edges, 2) some pores of the medium are larger than others, which allows the fluid flowing through these pores to move faster, and 3) some of the fluid particles will travel along longer flow paths in the porous medium than other particles to go the same linear distance. In most groundwater flow systems, advection and dispersion are the dominant forces moving solute, and diffusion is neglected. However, at very low velocities and low permeabilities, diffusion can become a factor. To evaluate the relative contribution of diffusion to solute transport, the Peclet number is used. The Peclet number is a dimensionless number that relates the effectiveness of mass transport by dispersion to the effectiveness of mass transport by diffusion (20):

$$P = \frac{v_x d}{D_d} \tag{7}$$

where:

v_x = average linear velocity
d = average grain diameter
D_d = coefficient of molecular diffusion (1×10^{-9} to 2×10^{-9} m^2 s^{-1} (20))

When the Peclet number is less than (approximately) 0.4, diffusion is the predominant force for solute transport. For Peclet numbers between 0.4 and 6, there is a transition zone, where the effects of diffusion and longitudinal mechanical dispersion are essentially equal. If the Peclet number is greater than 6, mechanical dispersion is the dominant force. For transverse mechanical dispersion, the same ranges hold, but for Peclet numbers roughly

100 times greater (see Appendix 7 (20)). Peclet numbers were calculated (Appendix 7) using grain sizes from Chamley (11) for lithologies described in the borehole logs (30), and seepage velocities calculated by Pegram (55). For shale, the Peclet number for the transverse direction ranged from 0.08 to 2.6; for the longitudinal direction, the Peclet number ranged from 0.01 to 0.5. Therefore, for the finer grained regions within the shales, diffusion is the dominant mechanism for solute transport in both the longitudinal and transverse direction. For the slightly coarser grained regions within the shales, the effects of mechanical dispersion and diffusion on solute transport are approximately equal. In the sandstones, the Peclet number ranged from 0.01 to 0.12. As with shales, longitudinal solute transport will be dominated by diffusion where grain sizes are at the smaller end of the range, and mechanical dispersion will become more important where grain sizes are slightly larger. Transverse solute transport in sandstones will be entirely controlled by diffusion. No vertical seepage velocity was calculated for any of the sandstone units, therefore, the same Peclet number was used to estimate advection and diffusion in both the horizontal and transverse direction. In summary, the vertical movement of any electron donors from the shales to the sandstones does not depend entirely on diffusion. Where grain sizes are slightly larger, mechanical dispersion plays a role. As equation 6b shows, mechanical dispersion has a velocity component. Velocity is calculated from Darcy's Law (24):

$$v = \frac{K}{n_e}\frac{dh}{dl} \tag{8}$$

where:

K = hydraulic conductivity
n_e = effective porosity
dh/dl = head gradient

The direction (i.e. up or down) of the velocity, and therefore of any mechanical dispersion, is dependent on the direction of the head gradient. The groundwater flow study found definite downward gradients in the Mancos Shale in the area of the mine tailings, and also in the upper units on Mesa Chivato (55). Stone *et al.* (68) reports downward groundwater flow in the Dakota Sandstone and horizontal flow in the Morrison Formation. Therefore, where mechanical dispersion is a factor in transport of electron donors and acceptors, increases in microbial activity may not be seen at the interface, but below it (or above it, in cases where the hydraulic gradiant is upward). Where diffusion dominates transport, head gradients are unimportant; electron donors and electron acceptors should be able to rendezvous regardless of whether the shale overlies the sandstone or visa versa.

4.4 Microbial Influences on Geochemistry at Cerro Negro

Carbon-14 dating was one of the methods used to estimate the age of the groundwater at Cerro Negro (details of this effort are in the previously cited Master's independent study paper by Page Pegram of NMIMT) (55). This method requires that sources and sinks of "dead" carbon (carbon containing no ^{14}C because it has decayed) by chemical dissolution and precipitation of rock minerals along the flow path be considered. The computer model NETPATH was used for this. One of the tools for checking the correctness of the computer model is the $\delta^{13}C$ isotopic signature of the water. It has been observed that bacterially produced CO_2 may be either isotopically heavy (13, 48, 52), or isotopically light (9, 51) and thus may produce an isotopic signature that is different than it would be with no biological input of carbon. In the NETPATH models of the two deeper aquifers, the Paguate and the

Cubero/Morrison, the modeled calcite $\delta^{13}C$ values needed for a match between predicted and measured $\delta^{13}C$ in final waters were heavier than the measured calcite $\delta^{13}C$. One could speculate that the discrepancy is due to isotopically heavy biogenic carbon input into these aquifers. The NETPATH model of the upper sandstone aquifer, the Two Wells, predicted $\delta^{13}C$ values for calcite that were lighter than the actual values. In this case, speculation would be for input of isotopically light biogenic DIC. The NETPATH model has the ability to consider such biological input, but information on the degree of isotopic fractionation by microbial activity is required, and was not a part of this study.

As an alternative to the elaborate NETPATH modeling, a simple dissolution model was also used. This model assumed that the only source of carbon entering the groundwater is from dissolution of carbonate rocks, and that there is no carbon sink. The increase in dissolved inorganic carbon (DIC) along the flow path was used to calculate a dilution factor, which is then used to correct the initial ^{14}C activity (55). Biogenic input of dead carbon will reduce the ^{14}C activity, thus making the groundwater appear older (19). Both models, the simple dissolution model and the NETPATH model produced quite similar ages (30,000 to 40,000 yrs) for the groundwater at Cerro Negro (55). The closeness of the ages by both models suggests that the biologic influence on DIC concentration of the waters is not significant.

Terminal electron acceptors available for microbes in the deep subsurface, in order from the most energetically favorable to the least favorable are: O_2, NO_3^-, Mn^{4+}, Fe^{3+}, SO_4^{2-}, and CO_2. Organisms using a more energetically favorable electron acceptor out-compete those using less favorable electron acceptors. This competition leads to distinctive zones where one electron acceptor predominates over the others, even when all are

available. These zones will occur no matter what the scale of the ecosystem is, whether it is a Winogradsky column a few centimeters long or an aquifer flow path many kilometers long. Lovely and others (12, 45, 46) have proposed a method to determine which electron acceptor predominates at any given point along a flow path, based on the concentration of dissolved H_2. Dissolved H_2 (Table 9) was measured on four of water samples (Bibo, Moquino, Seboyeta and L-Bar, Figure 5) collected as part of the geochemical and isotopic modeling project. The data in Table 9 suggest that at the Bibo well, the succession of terminal electron accepting processes has progressed to sulfate reduction, and that in the vicinity of Cerro Negro, methanogenesis is predominant. However, several researchers have found that deep aquifer systems that have extensive mineral sources of sulfate lack significant methane production (14, 44, 58), as sulfate reduction is energetically favored

Table 9: Results of dissolved hydrogen analysis on 4 well water samples (from Stevens and Wagnon (67)). See Figure 5 for well locations. Probable electron-accepting process interpreted according to Lovely (46).

Well Name	Screened Unit	$[H_2]$ (nM)	Probable Electron-Accepting Process
Bibo	Two Wells & Paguate	2.45±0.42	Sulfate reducing
Moquino	Morrison	34.6±1.8	methanogenic (fermentation?)
Seboyeta	Cubero & Morrison	20.4±2.9	methanogenic (fermentation?)
L-Bar	Morrison	15.9±2.1	methanogenic

over methanogenesis. Sulfate is depleted in the Moquino well (<0.05 mg L^{-1}), but is abundant in the Bibo, Seboyeta and L-Bar wells (163.2, 22.97, and 236.24 mg L^{-1} respectively). It has been suggested that the dissolved hydrogen data may be affected by well casings (67).

Which ever process dominates, it must be anaerobic. The section of the aquifer flow path that was studied has low dissolved oxygen (DO) and low

redox potentials (E_h). (All well water data described in this paragraph were collected by Page Pegram, NMIMT (55). A complete table of well water analysis results are included in Appendix 1.) For oxygen to be used as the electron acceptor, the redox potential must be greater than +350 mV (2). Redox potentials of the waters from the formations of interest were well below this range (Table 10). After oxygen, NO_3^- and Fe^{3+} are the next most energetically favorable electron acceptors in low redox, anaerobic environments. The concentrations of these two species were low; NO_3^- ranged from 1.27 to <0.02 mg L^{-1}, Fe^{3+} ranged from 0.14 to <0.04 mg L^{-1}. These two species are probably not available in sufficient quantities to be the predominant electron acceptor.

There are other indirect clues which can be used to infer which electron-accepting process is occurring, such as accumulation of DIC from the oxidation of organic matter, or the accumulation of bicarbonate and sulfides associated with sulfate reduction (45), but these biological processes are often overwhelmed by geochemical ones.

Table 10: Dissolved oxygen (DO) concentrations and redox potentials (E_h) of wells along the flow path of the Cerro Negro aquifers. The Elkins and Presbyterian wells are shallow wells located on Mesa Chivato; they do not reach the sandstones being studied. Data from Page Pegram, NMIMT.

Well Name	Screened Unit	E_h (mV)	DO (mg L^{-1})
Elkins	volcanic conglomerate	229	5.91
Presbyterian	volcanic conglomerate	395	6.87
Seboyeta	Cubero & Morrison	-25	0
Bibo	Two Wells & Paguate	273	0.62
Moquino	Morrison	-8	0.05
CNV-W2	Two Wells	282	0.2
CNV-W3	Cubero	231	0.18
CNV-W5	Paguate	233	0.01
L-Bar	Morrison	103	2.39

4.5. Statistical Analyses

The ANOVA comparing results from each of the boreholes indicated that two parameters were significantly different among boreholes. The CNAR borehole was found to have significantly higher CO_2-production in shale samples, compared to shales in CNV. This is probably because the average carbonate content of shale samples from CNAR is twice that of shales from CNV (data from J. McKinley, Pacific Northwest Laboratory, see Appendix 2). The other significant difference between boreholes was in the plate counts for sandstones; CNAR was again higher than CNV. This could indicate that the smaller diameter cores from CNAR were contaminated by drilling muds. Of all 65 samples, the two with the highest plate counts were sandstones from CNAR. These samples also had the largest porethroat sizes, which would make it easier for drilling mud to penetrate the core. However, one of these samples was obtained using N_2 gas as the drilling fluid. The most sensitive parameter, glucose mineralization, showed no bias in any of the comparisons. From these data, it appears that the use of tracers to detect contamination by drilling mud was effective in eliminating microbiologically compromised samples.

The borehole from which the sample was taken proved to be a significant factor in the two-way ANOVA for moisture content. The interaction graph shows that the moisture content was indeed higher in six out of seven stratigraphic units in the CNV borehole. These results probably reflect the fact that the average time lapse between coring and processing the samples from CNV was 3.6 days, the average time lapse for CNAR samples was 19.6 days. The longer time lapse did not have a consistent, observable, effect on any of the microbial activity parameters. As part of a small experiment to investigate effects of different poison control methods, O_2-

uptake and CO_2-production analyses were repeated on seven samples after approximately six months of cold-storage. CO_2-production increased in three samples, decreased in three samples and remained unchanged in one sample. O_2-uptake decreased in four samples and remained unchanged in three (see Appendix 4).

The ANOVA results from the more sensitive assays, O_2-uptake, CO_2-production and glucose mineralization indicated a significant difference between sandstones and shales. The box and whisker plots show that, for these three parameters, sandstones have higher activity than do the shales. The limited Pearson product-moment correlation matrix also indicated a strong positive correlation of glucose-mineralization to both permeability and porosity. ANOVA also showed that the three shales and five sandstones were different from each other. The O_2-uptake and CO_2-production data were affected by abiotic processes which were probably different between sandstones and shales. Therefore, these parameters probably are not reliable indicators of different activity between lithology, even though the results seem to support the glucose-mineralization data.

The large Pearson product-moment correlation produced only a few strong correlations, either positive or negative. This matrix was produced using all of the individual data points for each parameter that was included. Data were not sorted by borehole, lithology or stratigraphy, nor were any averages used. The wide variations in most of the parameters probably masked some of the correlations that would normally be expected, such as between glucose-mineralization and viable cells.

5.0 Conclusions

All core samples from all three boreholes showed some evidence of microbial activity, even in the formations near the intrusion. There are conflicting data as to the thermal history of the rock near the intrusion; it is not known at this time whether the extreme temperatures needed to sterilize the rock were reached.

It was not possible to determine definitively whether present-day microbes that exist in deep subsurface formations are the original inhabitants. Two lines of evidence suggest that some of the microbes found in extremely tight formations may be original inhabitants: 1) the very small porethroats of many of the samples make it unlikely that bacteria were transported there via groundwater, and 2) marine microorganisms were present in many samples.

Some microbial colonization has undoubtedly occurred via groundwater advection. The sandstones, whose permeabilities averaged an order of magnitude greater than the shales, mineralized an average of 2 times more glucose than the shales. The Mancos Shale was shown to have a fairly high vertical hydraulic conductivity, probably due to fracture flow. Isotope data indicated that waters, and thus possibly the microbial colonies, in the Mancos Shale near the Cerro Negro intrusion are modern, but older than 50 yrs.

With the exception of those organisms that might have arrived at their present locations through fractures in the rocks, present day microbes (or their ancestors) at Cerro Negro have been a very long time in transit. Estimated travel times from the recharge area range from 30,000 yrs (the approximate age of the groundwater) to 91,000 yrs (based on the slowest calculated groundwater flow rate).

References

1. Alexander, M. 1977. Introduction to Soil Microbiology, 2nd ed. John Wiley & Sons, New York, pp. 467.

2. Altas, R. M., and R. Bartha. 1993. Microbial Ecology, The Benjamin/Cummings Publishing Co., Inc., Redwood City, CA, pp. 563.

3. Amy, P. S., D. L. Haldeman, D. R. Ringleberg, D. H. Hall, and C. Russel. 1992. Comparison of identification systems for classification of bacteria isolated from water and endolithic habitats from within the deep subsurface. Applied and Environmental Microbiology **58:** 3367-3373.

4. Avnimelech, Y., and A. Nevo. 1964. Biological clogging of sands. Soil Science **98:** 222-226.

5. Balkwill, D. L. 1989. Numbers, diversity and morphological characteristics of aerobic chemoheterotrophic bacteria in deep subsurface sediments from a site in South Carolina. Geomicrobiology Journal **7:** 33-52.

6. Balkwill, D. L., and W. C. Ghiorse. 1985. Characterization of bacteria associated with two shallow aquifers in Oklahoma. Applied and Environmental Microbiology **50:** 580-588.

7. Berk, K. N. 1994. Data Analysis with Student Systat, Course Technology, Inc., Cambridge, MA, pp. 480.

8. Blair, N. E., C. S. Martens, and D. J. D. Marais. 1987. Natural abundances of carbon isotopes in acetate from a coastal marine sediment. Science **236:** 66-68.

9. Brock, T. D., M. T. Madigan, J. M. Martinko, and J. Parker. 1994. Biology of Microorganisms, 7th ed. Prentice Hall, Englewood Cliff, NJ, pp. 909.

10. Brockman, F. J., B. A. Denovan, R. J. Hicks, and J. K. Fredrickson. 1989. Isolation and characterization of a quinoline degrading bacteria from subsurface sediments. Applied and Environmental Microbiology **55:** 1029-1032.

11. Chamley, H. 1990. Sedimentology, Springer-Verlag, New York, pp. 285.

12. Chapelle, F. H. 1993. Ground-water Microbiology and Geochemistry, John Wiley & Sons, New York, pp. 424.

13. Chapelle, F. H., J. T. Morris, P. B. McMahon, and J. J.L. Zelibor. 1988. Bacterial metabolism and the δ ^{13}C composition of groundwater, Floridan aquifer system, South Carolina. Geology **16:** 117-121.

14. Chapelle, J. H., and P. B. McMahon. 1991. Geochemistry of dissolved inorganic carbon in a coastal plain aquifer. 1. Sulfate from confining beds as an oxidant in microbial CO_2 production. Journal of Hydrology **127:** 85-108.

15. Colwell, F. S. 1989. Microbiological comparison of surface soil and unsaturated subsurface soil from a semiarid high desert. Applied and Environmental Microbiology **55:** 2420-2423.

16. Colwell, F. S., G. J. Stormberg, T. J. Phelps, S. A. Birnbaum, J. P. McKinley, S. A. Rawson, C. Veverka, S. Goodwin, P. E. Long, B. F. Russel, T. Garland, D. Thompson, P. Skinner, and S. Grover. 1992. Innovative techniques for collection of saturated and unsaturated subsurface basalts and sediments for microbiological characterization. Journal of Microbiological Methods **15:** 279-292.

17. Cusack, J., S. Singh, C. McMcarthy, J. Greici, M. d. Rocco, D. Nguyen, H. Lappin-Scott, and J. W. Costerton. 1992. Enhances oil recovery - three-demensional sandpack simulation of ultrmicrobacteria resuscitation in reservoir formation. Journal of General Microbiology **138:** 647-655.

18. Dockins, W. S., G. L. Olsen, G. A. McFetters, and S. C. Turbak. 1980. Dissimilartory bacterial sulfate reduction in Montana groundwaters. Geomicrobiology Journal **2:** 83-98.

19. Domenico, P. A., and F. A. Schwartz. 1990. Physical and Chemical Hydrogeology, John Wiley & Sons, New York, pp. 824.

20. Fetter, C. W. 1993. Contaminant Hydrogeology, Macmillan, New York, pp. 458.

21. Fontes, D. E., A. L. Mills, G. M. Hornberger, and J. S. Herman. 1991. Physical and chemical factors influencing transport of microorganisms through porous media. Applied and Environmental Microbiology **57:** 2473-2481.

22. Fredrickson, J. K., F. J. Brockman, D. J. Workman, S. W. Li, and T. O. Stevens. 1991. Isolation and characterization of a subsurface bacterium capable of growth on toluene, naphthalene, and other aromatic compounds. Applied and Environmental Microbiology **57:** 796-803.

23. Fredrickson, J. K., R. J. Hicks, S. W. Li, and F. J. Brockman. 1988. Plasmid incidence in bacteria from deep subsurface sediments. Applied and Environmental Microbiology **54:** 2916-2923.

24. Freeze, R. A., and J. A. Cherry. 1979. Groundwater, Prentice Hall, Englewood Cliffs, NJ, pp. 604.

25. Gannon, J. T., V. B. Manilal, and M. Alexander. 1991. Relationship between cell surface properties and transport of bacteria through soil. Applied and Environmental Microbiology **57:** 190-193.

26. Gerba, C. P. 1985. Microbial contamination of the subsurface, John Wiley & Sons, New York, pp. 547.

27. Griffiths, R. 1995. Initial analyses of Cerro Negro Data. Oregon State University.

28. Haldeman, D. L., P. S. Amy, D. R. Ringleberg, and D. C. White. 1993. Characterization of the microbiology within an 21 m^3 section of rock from the deep subsurface. Microbial Ecology **26:** 145-159.

29. Hallett, B. 1994. Geologic and Hydrologic Summary of Cerro Negro. Golder Federal Services.

30. Hallett, R. B. 1994. Lithologic results and deposition environments from Cerro Negro boreholes CNV and CNAR. Golder Federal Services.

31. Heibert, F. K., and P. C. Bennett. 1992. Microbial control of silicate weathering in organic-rich groundwater. Science **258:** 278-281.

32. Hornberger, G. M., A. L. Mills, and J. S. Herman. 1992. Bacterial transport in porous media: evaluation of a model using laboratory observations. Water Resources Research **28:** 915-938.

33. Ivanov, M. V. 1990. Presented at the First International Symposium on Microbiology of the Deep Subsurface, Orlando, FL.

34. Jenneman, G. E., M. J. McInerney, and R. M. Knapp. 1985. Microbial penetration through nutrient-saturated Berea sandstone. Applied and Environmental Microbiology **50:** 383-391.

35. Jones, R. E., R. E. Beeman, and J. M. Suflita. 1989. Anaerobic metabolic processes in the deep terrestrial subsurface. Geomicrobiology Journal **7:** 117-130.

36. Khovrychev, M. P., I. Y. Mareev, and V. F. Pomytkin. 1994. Ability of microbial biomass to sorb radionuclides. Microbiology **63:** 83-86.

37. Kieft, T. L. in press. Dwarf cells in soil and subsurface terrestrial environments. *In* R. R. Colwell and D. J. Grimes (ed.), Non-culturable Microorganisms in the Environment. Chapman & Hall, New York.

38. Kieft, T. L., P. S. Amy, F. J. Brockman, J. K. Fredrickson, B. N. Bjornstad, and L. L. Rosacker. 1993. Microbial abundance and activities in relation to water potential in the vadose zones of arid and semiarid sites. Microbial Ecology **26:** 59-78.

39. Kieft, T. L., J. K. Fredrickson, J. P. McKinley, B. N. Bjornstad, S. A. Rawson, T. J. Phelps, F. J. Brockman, and S. M. Pfiffner. 1995. Microbiological comparisons within and across contiguous lacustrine, paleosol and fluvial subsurface sediments. Applied and Environmental Microbiology **61:** 749-757.

40. Kieft, T. L., and L. L. Rosacker. 1991. Application of respiration- and adenylate-based soil microbiological assays to deep subsurface terrestrial sediments. Soil Biology and Biochemistry **23:** 563-568.

41. Lance, J. C., and C. P. Gerba. 1984. Virus movement in soil during saturated and unsaturated flow. Applied and Environmental Microbiology **47:** 335-337.

42. Long, P. E. 1993. Subsurface science program, deep microbiology subprogam: origens of microorganisms in deep subsurface environements research implementation plan. APPENDIX: Identification of sampling sites for conducting field research on the origins of subsurface microorganisms. Pacific Northwest Laboratory.

43. Long, P. E., and J. K. Fredrickson. 1995. Origins research sites: Thermal aureole hypothesis, Shale-sandstone hypothesis. Pacific Northwest Laboratory.

44. Lovely, D. R. 1985. Minimum threshold for hydrogen metabolism in methanogenic bacteria. Applied and Environmental Microbiology **49:** 1530-1531.

45. Lovely, D. R., and F. H. Chapelle. 1995. Deep subsurface microbial Processes. Reviews of Geophysics **33:** 365-381.

46. Lovley, D. R., and S. Goodwin. 1988. Hydrogen concentrations as an indicator of the predominant terminal electron accepting reactions in aquatic sediments. Geochimica Cosmochmica Acta **52:** 2993-3003.

47. McMahon, P. B., and F. H. Chapelle. 1991. Microbial production of organic acids in aquitard sediment and its role in aquifer geochemistry. Nature **349:** 233-235.

48. McMahon, P. B., D. F. Williams, and J. T. Morris. 1990. Production and carbon isotopic composition of bacterial CO_2 in deep coastal plain sediments of South Carolina. Ground Water **28:** 693-702.

49. Mitchell, R., and A. Nevo. 1964. Effect of bacterial polysaccharide accumulation on infiltration of water through sand. Applied Microbiology **12:** 219-223.

50. Mook, W. G. 1980. Carbon-14 in hydrogeological studies, Elsevier Science, New York, pp. 479.

51. Murphy, E. M., and S. N. Davis. 1989. Characterization and isotopic composition of organic and inorganic carbon in the Milk River Aquifer. Water Resources Research **25:** 1893-1905.

52. Murphy, E. M., J. A. Schramke, J. K. Fredrickson, H. W. Bledsoe, A. J. Francis, D. S. Sklarew, and J. C. Linehan. 1992. The influence of microbial activity and sedimentary organic carbon on the isotope geochemistry of the Middendorf aquifer. Water Resources Research **28:** 723-740.

53. Olsen, G. J., W. S. Dockins, G. A. McFetters, and W. P. Iverson. 1981. Sulfate-reducing and methanogenic bacteria from deep aquifers in Montana. Geomicrobiology Journal **2:** 327-341.

54. Pederson, K., and S. Evendahl. 1990. Distribution and activity of bacteria in deep granitic groundwaters of southeastern Sweden. Microbial Ecology **20:** 37-52.

55. Pegram, P. 1995. MS Thesis: An isotopic study of groundwater flow near Cerro Negro, New Mexico New Mexico Institute of Mining and Technology, Socorro, NM.

56. Phelps, T. J., C. B. Fliermans, R. T. Garland, S. M. Pfiffner, and D. C. White. 1989. Methods for recovery of deep terrestrial subsurface sediment for microbiological analysis. Journal of Microbiological Methods **9:** 15-27.

57. Phelps, T. J., S. M. Pfiffner, and D. C. White. 1994. Factors influencing the abundance and metabolic capacities of microorganisms in eastern coastal plain sediments. Microbial Ecology **28:** 351-356.

58. Plummer, L. N., J. F. Busby, R. W. Lee, and B. B. Hanshaw. 1990. Geochemical modeling of the Madison aquifer in parts of Montana, Wyoming and South Dakota. Water Resources Research **26:** 1981-2014.

59. Powelson, D. K., J. R. Simpson, and C. P. Gerba. 1991. Effects of organic matter on virus transport in unsaturated flow. Applied and Environmental Microbiology **57:** 2192-2196.

60. Reynolds, P. J., P. Sharma, G. E. Jenneman, and M. J. McInerney. 1989. Mechanisms of microbial movement in subsurface materials. Applied and Environemntal Microbiology **55:** 2280-2286.

61. Sargent, K. A., and C. B. Fliermans. 1989. Geology and hydrogeology of the deep subsurface microbiology sampling sites at the Savannah River Plant, South Carolina. Geomicrobiology Journal **7:** 3-13.

62. Scholl, M. A., and R. W. Harvey. 1992. Laboratory investigation of the role of sediment surface and groundwater chemistry in transport of bacteria through a contaminated sandy aquifer. Environmental Science and Technology **26:** 1410-1417.

63. Sharma, P. K., and M. J. McInerney. 1994. Effect of grain size on bacterial penetration, reproduction and metabolic activity in porous glass bead chambers. Applied and Environmental Microbiology **60:** 1481-1486.

64. Sharma, P. K., M. J. McInerney, and R. M. Knapp. 1993. In situ growth and activity and the modes of penetration of Escherichia coli in unconsolidated porous media. Applied and Environmental Microbiology **59:** 3686-3694.

65. Sinclair, J. L., W.C. Ghiorse. 1989. Distribution of aerobic bacteria, protozoa, algae and fungi in deep subsurface sediments. Geomicrobiology **7:** 15-31.

66. Sokal, R. R., and F. J. Rolf. 1969. Biometry, W.H. Freeman & Co., San Fransisco, pp. 469.

67. Stevens, T., and K. Wagnon. 1995. Cerro negro project - PNL assays for anaerobic bacteria. Pacific Northwest Laboratory.

68. Stone, W. J., F. P. Lyford, P. F. Frenzel, N. H. Mizell, and E. T. Padgett. 1983. Hydrogeology and water resoruces of the San Juan Basin, New Mexico. Hydrologic Report 6. New Mexico Bureau of Mines and Mineral Resources.

69. Tsezos, M., and J. P. Bell. 1989. Comparison of the biosorption and desorption of hazardous organic pollutants by live and dead biomass. Water Resources Research **23:** 561-566.

70. Tsezos, M., R. G. L. McCready, and J. P. Bell. 1989. The continuous recovery of uranium from biologically leached solutions using immobilized biomass. Biotechnology and Bioengineering **34:** 10-14.

71. Tuominen, L., T. Kairesalo, and H. Hartikainen. 1994. Comparison of methods for inhibiting bacterial activity in sediment. Applied and Environmental Microbiology **60:** 3454-3457.

72. van Beek, C. G. E. M., and D. v. d. Kooij. 1982. Sulfate-reducing bacteria in ground water from clogging and non-clogging shallow wells in the Netherlands river region. Ground Water **20:** 298-302.

73. Vandevivere, P., and P. Baveye. 1992. Effect of bacterial extracellular polymers on saturated hydraulic conductivity of sand columns. Applied and Environmental Microbiology **58:** 1690-1698.

74. vanOlphen, H. 1977. An Introduction to Clay Colliod Chemistry, John Wiley & Sons, New York, pp. 316.

75. Waksmann, S. A. 1916. Bacterial numbers in soil at different depths and in different seasons of the year. Soil Science **1:** 363-380.

76. Wan, J., J. L. Wilson, and T. L. Kieft. 1994. Influence of the gas-water interface on transport of microorganisms through unsaturated porous media. Applied and Environmental Microbiology **60:** 509-516.

77. West, J. M. 1990. Presented at the First International Symposium on Microbiology of the Deep Subsurface, Orlando, FL.

78. Wilkinson, L., M. Hill, and E. Vang. 1992. Systat: Graphics, 5.2 ed. Systat, Inc, Evanston, IL.

79. Wilson, J. T., F. S. McNabb, D. L. Balkwill, and W. C. Ghiorse. 1983. Enumeration and characterization of bacteria indigenous to a shallow aquifer. Ground Water **21:** 134-142.

Appendix 1: Data Summaries

Summary of Sample Grades and Depths

Sample ID	Stratigraphic Unit	Vertical Depth (m)	Elev. Above Sea Level (m)	Sample Grade
CNV-SURFACE	***N/A***	***0.0***	***1937.0***	***soil***
CNV-4-SC-60.5	mancos shale	60.5	1876.5	1
CNV-4-SC-127.3	two wells sandstone	127.3	1809.7	2
CNV-4-SC-140.3	whitewater arroyo shale	140.3	1796.7	2
CNV-4-SC-149.2	whitewater arroyo shale	149.2	1787.8	2
CNV-4-SC-164.2	paguatesandstone	164.2	1772.8	2
CNV-4-SC-165.8	paguatesandstone	165.8	1771.2	1
CNV-4-SC-170.4	paguatesandstone	170.4	1766.6	2
CNV-4-SC-178.9	paguatesandstone	178.9	1758.1	1
CNV-4-SC-183.9	clay mesa shale	183.9	1753.1	1
CNV-4-SC-185.7	cubero sandstone	185.7	1751.3	1
CNV-4-SC-187.1	cubero sandstone	187.1	1749.9	1
CNV-4-SC-188.5	cubero sandstone	188.5	1748.5	1
CNV-4-SC-193.1	cubero sandstone	193.1	1743.9	1
CNV-4-SC-196.3	cubero sandstone	196.3	1740.7	1
CNV-4-SC-198.1	cubero sandstone	198.1	1738.9	1
CNV-4-SC-200.3	cubero sandstone	200.3	1736.7	1
CNV-4-SC-201.0	oak canyon member (upper)	201.0	1736.0	1
CNV-4-SC-201.6	oak canyon member (upper)	201.6	1735.4	1
CNV-4-SC-202.5	***N/A***	***202.5***	***1734.5***	***sterile***
CNV-4-SC-203.3	oak canyon member (upper)	203.3	1733.7	1
CNV-4-SC-204.0	oak canyon member (upper)	204.0	1733.0	1
CNVR-4-SC-189.2	***N/A***	***189.2***	***1748.1***	***sterile***
CNVR-4-SC-196.9	cubero sandstone	196.9	1740.4	1
CNVR-4-SC-206.7	oak canyon member (upper)	206.7	1730.6	1
CNVR-4-SC-209.6	oak canyon member	209.6	1727.7	2
CNVR-4-SC-221.7	oak canyon member	221.7	1715.6	1
CNVR-4-SC-227.8	oak canyon member (lower)	227.8	1709.5	1
CNVR-4-SC-231.5	***morrison fm.***	***231.5***	***1705.8***	***3***

Ground Surface Elevation (GSE) for CNV was 1937.0 m
GSE for CNVR was 1937.3 m.
GSE for CNAR was 1960.0 m.

Samples that appear in bold are control samples, or samples that received a sample grade of "3". All have been removed from data analysis. See section 2.3.2 of text for explanation of sample grade.

Sample ID	Stratigraphic Unit	Vertical Depth (m)	Elev. Above Sea Level (m)	Sample Grade
CNAR-SURACE	***N/A***	***0.0***	***1960.0***	***soil***
CNAR-4-SC-91.8	mancos shale	48.0	1912.0	1
CNAR-4-SC-93.5	***mancos shale***		***1960.0***	***spiked***
CNAR-4-SC-200.0	mancos shale	102.0	1858.0	1
CNAR-4-SC-227.6	mancos shale	117.5	1842.5	2
CNAR-4-SC-239.9	mancos shale	124.0	1836.0	2
CNAR-4-SC-251.6	two wells sandstone	130.5	1829.5	2
CNAR-4-SC-260.5	two wells sandstone	137.5	1822.5	2
CNAR-4-SC-299.0	two wells sandstone	158.0	1802.0	1
CNAR-4-SC-310.8	whitewater arroyo shale	165.0	1795.0	1
CNAR-4-SC-315.4	whitewater arroyo shale	169.0	1791.0	1
CNAR-4-SC-319.7	whitewater arroyo shale	171.0	1789.0	1
CNAR-4-SC-329.2	whitewater arroyo shale	177.0	1783.0	1
CNAR-4-SC-333.7	paguatesandstone	179.0	1781.0	1
CNAR-4-SC-344.2	paguatesandstone	185.5	1774.5	1
CNAR-4-SC-350.5	paguatesandstone	190.0	1770.0	1
CNAR-4-SC-355.4	paguatesandstone	193.0	1767.0	1
CNAR-4-SC-361.1	paguatesandstone	198.0	1762.0	1
CNAR-4-SC-371.1	clay mesa shale	203.0	1757.0	1
CNAR-4-SC-375.3	clay mesa shale	205.8	1754.2	1
CNAR-4-SC-378.4	clay mesa shale	207.8	1752.2	1
CNAR-4-SC-381.8	clay mesa shale	210.0	1750.0	2
CNAR-4-SC-386.5	cubero sandstone	213.1	1746.9	2
CNAR-4-SC-390.9	cubero sandstone	216.0	1744.0	2
CNAR-4-SC-397.1	***cubero sandstone***	***219.0***	***1741.0***	***3***
CNAR-4-SC-405.0	oak canyon member (upper)	226.0	1734.0	1
CNAR-4-SC-409.8	oak canyon member (upper)	229.0	1731.0	2
CNAR-4-SC-417.4	oak canyon member (upper)	233.0	1727.0	1
CNAR-4-SC-425.0	oak canyon member (upper)	239.7	1720.3	1
CNAR-4-SC-426.5	oak canyon member (lower)	241.0	1719.0	2
CNAR-4-SC-436.7	oak canyon member (lower)	247.0	1713.0	2
CNAR-4-SC-451.2	***morrison fm.***	***256.0***	***1704.0***	***3***
CNAR-4-SC-457.3	basalt dike in morrison fm.	261.0	1699.0	2
CNAR-4-SC-464.2	morrison fm.	265.0	1695.0	2
CNAR-4-SC-475.3	***morrison fm.***	***272.1***	***1687.9***	***3***
CNAR-4-SC-482.9	morrison fm.	278.0	1682.0	2
CNAR-4-SC-503.9	morrison fm.	292.5	1667.5	2
CNAR-4-SC-507.3	morrison fm.	297.0	1663.0	2

Time Lapsed Between Obtaining and Processing Core Samples

Sample ID	Date Collected	Date Processed	Days Lapsed
CNV-60.5	7/10/94	7/12/94	2
CNV-127.3	7/14/94	7/17/94	3
CNV-140.3	7/15/94	7/17/94	2
CNV-149.2	7/18/94	7/19/94	1
CNV-164.2	7/18/94	7/25/94	7
CNV-165.8	7/19/94	7/25/94	6
CNV-170.4	7/19/94	7/25/94	6
CNV-178.9	7/20/94	7/25/94	5
CNV-183.9	7/20/94	7/25/94	5
CNV-185.7	7/21/94	7/25/94	4
CNV-187.1	7/21/94	7/25/94	4
CNV-188.5	7/21/94	7/25/94	4
CNV-193.1	7/22/94	7/25/94	3
CNV-196.3	7/22/94	7/25/94	3
CNV-198.1	7/22/94	7/25/94	3
CNV-200.3	7/25/94	7/28/94	3
CNV-201.0	7/27/94	7/29/94	2
CNV-201.6	7/27/94	7/29/94	2
CNV-202.5	***N/A***	***8/1/94***	***N/A***
CNV-203.3	7/27/94	7/29/94	2
CNV-204.0	7/27/94	8/1/94	5
CNVR-189.2	***11/1/94***	***11/21/94***	***20***
CNVR-196.9	11/5/94	11/21/94	16
CNVR-206.7	11/9/94	11/21/94	12
CNVR-209.6	11/9/94	11/21/94	12
CNVR-221.7	11/10/94	11/22/94	12
CNVR-227.8	11/11/94	11/22/94	11
CNVR-231.5	***11/11/94***	***11/22/94***	***11***

CNV average =	3.60
CNVR average =	13.43
CNAR average =	19.57

Sample ID	Date Collected	Date Processed	Days Lapsed
CNAR-91.8	8/29/94	9/1/94	3
CNAR-93.5	***8/30/94***	***9/1/94***	***2***
CNAR-200.0	9/13/94	9/16/94	3
CNAR-227.6	9/16/94	9/20/94	4
CNAR-239.9	9/20/94	9/22/94	2
CNAR-251.6	9/23/94	9/30/94	7
CNAR-260.5	9/25/94	9/30/94	5
CNAR-299.0	9/28/94	9/30/94	2
CNAR-310.8	9/29/94	10/7/94	8
CNAR-315.4	9/30/94	10/7/94	7
CNAR-319.7	9/30/94	10/7/94	7
CNAR-329.2	10/2/94	10/9/94	7
CNAR-333.7	10/2/94	10/9/94	7
CNAR-344.2	10/2/94	10/9/94	7
CNAR-350.3	10/3/94	10/9/94	6
CNAR-355.4	10/3/95	10/9/94	6
CNAR-361.1	10/4/95	11/1/94	28
CNAR-371.1	10/4/95	11/1/94	28
CNAR-375.3	10/5/94	11/2/94	28
CNAR-378.4	10/5/94	11/2/94	28
CNAR-381.8	10/6/94	11/4/94	29
CNAR-386.5	10/6/94	11/4/94	29
CNAR-390.9	10/7/94	11/4/94	28
CNAR-397.1	***10/7/94***	***11/11/94***	***35***
CNAR-405.5	10/9/94	11/7/94	29
CNAR-409.8	10/9/94	11/9/94	31
CNAR-417.4	10/9/94	11/9/94	31
CNAR-425.0	10/10/94	11/11/94	32
CNAR-426.5	10/10/94	11/11/94	32
CNAR-436.7	10/11/94	11/14/94	34
CNAR-451.2	***10/12/94***	***11/14/94***	***33***
CNAR-457.3	10/14/94	11/11/94	28
CNAR-464.2	10/14/94	11/11/94	28
CNAR-475.3	***10/15/94***	***11/17/94***	***33***
CNAR-482.9	10/18/94	11/17/94	33
CNAR-503.9	10/19/94	11/17/94	32
CNAR-507.3	10/19/94	11/17/94	32

Summary of Sample Moisture Content

Sample ID	Moisture Content (%)
CNV-SURFACE	7.8
CNV-4-SC-60.5	6.0
CNV-4-SC-127.3	3.2
CNV-4-SC-140.3	3.2
CNV-4-SC-149.2	3.6
CNV-4-SC-164.2	4.4
CNV-4-SC-165.4	3.1
CNV-4-SC-170.4	4.3
CNV-4-SC-178.9	3.3
CNV-4-SC-183.9	8.9
CNV-4-SC-185.7	3.9
CNV-4-SC-187.1	7.4
CNV-4-SC-188.5	7.6
CNV-4-SC-193.1	6.4
CNV-4-SC-196.3	4.6
CNV-4-SC-198.1	3.9
CNV-4-SC-200.3	8.1
CNV-4-SC-201.0	7.2
CNV-4-SC-201.6	8.5
CNV-4-SC-202.5	2.9
CNV-4-SC-203.3	7.8
CNV-4-SC-204.0	4.2
CNVR-4-SC-189.2	0.3
CNVR-4-SC-196.9	3.1
CNVR-4-SC-206.7	3.9
CNVR-4-SC-209.6	2.8
CNVR-4-SC-221.7	7.9
CNVR-4-SC-227.8	6.3
CNVR-4-SC-231.5	11.7

Sample ID	Moisture Content (%)
CNA-SURFACE	4.8
CNAR-4-SC-91.8	1.8
CNAR-4-SC-93.5	1.8
CNAR-4-SC-200.0	10.4
CNAR-4-SC-227.6	3.8
CNAR-4-SC-239.9	1.8
CNAR-4-SC-251.6	8.8
CNAR-4-SC-260.5	5.9
CNAR-4-SC-299.0	4.0
CNAR-4-SC-310.8	3.1
CNAR-4-SC-315.4	2.9
CNAR-4-SC-319.7	1.9
CNAR-4-SC-329.2	3.0
CNAR-4-SC-333.7	8.9
CNAR-4-SC-344.2	5.9
CNAR-4-SC-350.5	3.6
CNAR-4-SC-355.4	2.5
CNAR-4-SC-361.1	0.0
CNAR-4-SC-371.1	1.0
CNAR-4-SC-375.3	2.3
CNAR-4-SC-378.4	1.8
CNAR-4-SC-381.8	3.6
CNAR-4-SC-386.5	3.9
CNAR-4-SC-390.9	1.7
CNAR-4-SC-397.1	2.6
CNAR-4-SC-405.5	2.2
CNAR-4-SC-409.8	1.8
CNAR-4-SC-417.4	2.4
CNAR-4-SC-425.0	2.8
CNAR-4-SC-426.5	8.5
CNAR-4-SC-436.7	6.4
CNAR-4-SC-451.2	0.7
CNAR-4-SC-457.3	6.2
CNAR-4-SC-464.2	8.7
CNAR-4-SC-475.3	2.3
CNAR-4-SC-482.9	1.5
CNAR-4-SC-503.9	1.6
CNAR-4-SC-507.3	3.9

Sample ID	Strat. Unit	Depth (m)	% Mineral-ization	Stdev
CNAR-SURFACE	*soil*	*1960*	*21.48*	*0.60*
CNAR-91.8	M	1912	0.00	0.05
CNAR-93.5	*spiked*	*1960*	*22.62*	*1.70*
CNAR-200.0	M	1858	1.37	1.27
CNAR-227.6	M	1842.5	0.23	0.04
CNAR-239.9	M	1836	0.25	0.06
CNAR-251.6	2W	1829.5	8.99	1.40
CNAR-260.5	2W	1822.5	0.89	0.24
CNAR-299.0	2W	1802	1.78	0.37
CNAR-310.8	WW	1795	0.93	0.43
CNAR-315.4	WW	1791	1.25	0.28
CNAR-319.7	WW	1789	0.57	0.26
CNAR-329.2	WW	1783	0.76	0.79
CNAR-333.7	P	1781	5.22	0.83
CNAR-344.2	P	1774.5	9.16	3.92
CNAR-350.3	P	1770	2.05	0.37
CNAR-355.4	P	1767	0.94	0.24
CNAR-361.1	P	1762	1.79	0.69
CNAR-371.1	CM	1757	0.61	0.40
CNAR-375.3	CM	1754.2	0.45	0.24
CNAR-378.4	CM	1752.2	0.69	0.21
CNAR-381.8	CM	1750	0.01	0.16
CNAR-386.5	C	1746.9	31.08	6.92
CNAR-390.9	C	1744	4.86	1.43
CNAR-397.1	C	*1741*	*0.61*	*0.29*
CNAR-405.5	CC	1734	2.83	0.73
CNAR-409.8	CC	1731	0.17	0.19
CNAR-417.4	CC	1727	0.31	0.18
CNAR-425.0	CC	1720.3	0.22	0.13
CNAR-426.5	CC	1719	3.65	2.89
CNAR-436.7	CC	1713	6.68	5.48
CNAR-451.2	*MO*	*1704*	*7.29*	*8.87*
CNAR-457.3	basalt	1699	3.62	6.43
CNAR-464.2	MO	1695	2.56	3.30
CNAR-475.3	MO	*1687.9*	*0.36*	*0.10*
CNAR-482.9	MO	1682	22.18	2.92
CNAR-503.9	MO	1667.5	0.78	0.47
CNAR-507.3	MO	1663	0.06	0.05

Sample ID	Strat. Unit	Depth (m)	% Mineral-ization	Stdev
CNV-SURFACE	*soil*	*1937*	*15.71*	*0.31*
CNV-60.5	M	1876.5	4.16	0.19
CNV-127.3	2W	1809.7	0.49	0.03
CNV-140.3	WW	1796.7	0.15	0.02
CNV-149.2	WW	1787.8	1.17	0.01
CNV-164.2	P	1772.8	1.55	0.04
CNV-165.8	P	1771.2	2.49	0.02
CNV-170.4	P	1766.6	1.96	0.07
CNV-178.9	P	1758.1	1.29	0.07
CNV-183.9	CM	1753.1	1.44	0.02
CNV-185.7	C	1751.3	0.96	0.02
CNV-187.1	C	1749.9	0.00	0.00
CNV-188.5	C	1748.5	0.32	0.04
CNV-193.1	C	1743.9	16.04	0.50
CNV-196.3	C	1740.7	2.04	0.01
CNV-198.1	C	1738.9	0.67	0.02
CNV-200.3	C	1736.7	0.47	0.01
CNV-201.0	CC	1736	0.78	0.01
CNV-201.6	CC	1735.4	1.63	0.11
CNV-202.5	*sterile*	*1734.5*	*1.31*	*0.02*
CNV-203.3	CC	1733.7	1.20	0.01
CNV-204.0	CC	1733	1.86	0.02

Sample ID	Strat. Unit	Depth (m)	% Mineral-ization	Stdev
CNVR-189.2	*control*	*1748.1*	*2.94*	*0.08*
CNVR-196.9	C	1740.4	1.28	0.02
CNVR-206.7	CC	1730.6	0.77	0.04
CNVR-209.6	CC	1727.7	0.17	0.02
CNVR-221.7	CC	1715.6	0.35	0.01
CNVR-227.8	CC	1709.5	0.00	0.00
CNVR-231.5	CC	*1705.8*	*13.45*	*0.36*

Percent mineralization values shown are calculated % mineralization minus 0.0975 (average of 4 poisoned controls).

On Nov. 23, 1994, the prescribed procedure for collection of CO2 was not followed, leading to poor replication of data. Effected values are shaded, and have been removed from data analysis.

Summary of Plate Count Data

Sample ID	Strat. Unit	Depth (m)	Average CFU/gdw	STDEV CFU/gdw	Average of logs	STDEV of logs
CNAR-SURFACE	*soil*	*1960.0*	*3.07E+08*	*2.36E+08*	*8.35*	*0.49*
CNAR-91.8	M	1912.0	1.75E+02	2.05E+02	1.95	0.69
CNAR-93.5	*spiked*	*1960.0*	*7.67E+05*	*6.43E+05*	*5.79*	*0.34*
CNAR-200.0	M	1858.0	3.80E+02	6.27E+02	1.86	1.03
CNAR-227.6	M	1842.5	<3.00E+01*		<1.48*	0.00
CNAR-239.9	M	1836.0	<3.00E+01		<1.48	0.00
CNAR-251.6	2W	1829.5	2.90E+02	1.26E+02	2.44	0.17
CNAR-260.5	2W	1822.5	<3.00E+01		<1.48	0.00
CNAR-299.0	2W	1802.0	<3.00E+01		<1.48	0.00
CNAR-310.8	WW	1795.0	1.03E+03	0.00E+00	3.01	0.00
CNAR-315.4	WW	1791.0	<3.00E+01		<1.48	0.00
CNAR-319.7	WW	1789.0	<3.00E+01		<1.48	0.00
CNAR-329.2	WW	1783.0	<3.00E+01		<1.48	0.00
CNAR-333.7	P	1781.0	1.05E+03	6.29E+01	3.02	0.03
CNAR-344.2	P	1774.5	8.24E+01	1.12E+02	1.61	0.62
CNAR-350.3	P	1770.0	<3.00E+01		<1.48	0.00
CNAR-355.4	P	1767.0	4.55E+01	4.93E+01	1.49	0.45
CNAR-361.1	P	1762.0	<3.00E+01		<1.48	0.00
CNAR-371.1	CM	1757.0	<3.00E+01		<1.48	0.00
CNAR-375.3	CM	1754.2	<3.00E+01		<1.48	0.00
CNAR-378.4	CM	1752.2	7.35E+01	4.90E+01	1.75	0.45
CNAR-381.8	CM	1750.0	<3.00E+01		<1.48	0.00
CNAR-386.5	C	1746.9	4.02E+03	1.59E+02	3.60	0.02
CNAR-390.9	C	1744.0	4.51E+01	4.90E+01	1.49	0.45
CNAR-397.1	C	*1741.0*	*<3.00E+01*		*<1.48*	*0.00*
CNAR-405.5	CC	1734.0	<3.00E+01		<1.48	0.00
CNAR-409.8	CC	1731.0	4.52E+01	4.90E+01	1.49	0.45
CNAR-417.4	CC	1727.0	<3.00E+01		<1.48	0.00
CNAR-425.0	CC	1720.3	4.57E+01	4.95E+01	1.49	0.45
CNAR-426.5	CC	1719.0	3.62E+02	2.26E+02	2.47	0.38
CNAR-436.7	CC	1713.0	7.68E+01	5.12E+01	1.77	0.45
CNAR-451.2	*MO*	*1704.0*	*3.29E+03*	*3.81E+02*	*3.52*	*0.05*
CNAR-457.3	basalt	1699.0	<3.00E+01		<1.48	0.00
CNAR-464.2	MO	1695.0	3.70E+03	5.75E+02	3.56	0.07
CNAR-475.3	MO	*1687.9*	*<3.00E+01*		*<1.48*	*0.00*
CNAR-482.9	MO	1682.0	7.34E+03	2.11E+02	3.87	0.01
CNAR-503.9	MO	1667.5	<3.00E+01		<1.48	0.00
CNAR-507.3	MO	1663.0	<3.00E+01		<1.48	0.00

Sample ID	Strat. Unit	Depth (m)	Average CFU/gdw	STDEV CFU/gdw	Average of logs	STDEV of logs
CNV-SURFACE	*soil*	*1937.0*	*1.49E+07*	*9.36E+06*	*7.17*	*0.07*
CNV-60.5	M	1876.5	1.02E+03	5.82E+02	2.52	1.12
CNV-127.3	2W	1809.7	2.04E+03	1.76E+03	2.73	1.30
CNV-140.3	WW	1796.7	<3.33E+01		<1.52	0
CNV-149.2	WW	1787.8	1.04E+03	1.03E+03	2.52	1.12
CNV-164.2	P	1772.8	4.52E+01	5.41E+01	1.49	0.45
CNV-165.8	P	1771.2	<3.33E+01		<1.52	0
CNV-170.4	P	1766.6	8.24E+01	1.17E+02	1.61	0.62
CNV-178.9	P	1758.1	<3.33E+01		<1.52	0
CNV-183.9	CM	1753.1	<3.33E+01		<1.52	0
CNV-185.7	C	1751.3	<3.33E+01		<1.52	0
CNV-187.1	C	1749.9	7.92E+01	1.13E+02	1.59	0.62
CNV-188.5	C	1748.5	<3.33E+01		<1.52	0
CNV-193.1	C	1743.9	4.84E+01	9.29E+00	1.52	0.45
CNV-196.3	C	1740.7	<3.33E+01		<1.52	0
CNV-198.1	C	1738.9	4.60E+01	8.80E+00	1.50	0.45
CNV-200.3	C	1736.7	<3.33E+01		<1.52	0
CNV-201.0	CC	1736.0	<3.33E+01		<1.52	0
CNV-201.6	CC	1735.4	<3.33E+01		<1.52	0
CNV-202.5	*sterile*	*1734.5*	*<3.33E+01*		*<1.52*	*0*
CNV-203.3	CC	1733.7	<3.33E+01		<1.52	0
CNV-204.0	CC	1733.0	<3.33E+01		<1.52	0
CNVR-189.2	*control*	*1748.1*	*<3.33E+01*		*<1.52*	*0*
CNVR-196.9	C	1740.4	<3.33E+01		<1.52	0
CNVR-206.7	CC	1730.6	<3.33E+01		<1.52	0
CNVR-209.6	CC	1727.7	<3.33E+01		<1.52	0
CNVR-221.7	CC	1715.6	4.61E+01	5.52E+01	1.49714018	0.44952
CNVR-227.8	CC	1709.5	<3.33E+01		<1.52	0
CNVR-231.5	CC	*1705.8*	*6.56E+03*	*3.74E+03*	*3.8149945*	*0.0541*

*Limit of detection (average) is 3.00E+01 CFU/gww (log = 1.48)

Limit of detection (LOD) for method is 3.33E+01 CFU/gww (log = 1.52). When average of 3 replicates is taken, those replicates with no colonies are assigned the value of 1/2(LOD). This has the effect of lowering the average LOD.

Summary of "BacLight" Stain Direct Count Data

Sample ID	Strat. Unit	Depth (m)	Cells/gdw		log(cells/gdw)		log(stdev)		%
			Viable	Total	Viable	Total	Viable	Total	Viable
CNAR-SURF.	*soil*	*1960*	*5.75E+06*	*6.12E+06*	*6.75*	*6.78*	*0.10*	*0.08*	*93.8*
CNAR-91.8	M	1912	8.50E+04	1.70E+05	4.71	5.12	0.47	0.35	50.0
CNAR-93.5	*spiked*	*1960*	*2.90E+06*	*3.37E+06*	*6.46*	*6.53*	*0.05*	*0.03*	*86.0*
CNAR-200.0	M	1858	2.23E+05	3.97E+05	5.06	5.57	0.62	0.20	56.3
CNAR-227.6	M	1842.5	8.13E+05	1.00E+06	5.91	5.99	0.06	0.09	81.3
CNAR-239.9	M	1836	7.97E+05	9.67E+05	5.90	5.98	0.06	0.06	82.4
CNAR-251.6	2W	1829.5	1.40E+05	2.10E+05	5.09	5.31	0.26	0.12	66.7
CNAR-260.5	2W	1822.5	4.08E+05	5.44E+05	5.61	5.73	0.08	0.06	75.0
CNAR-299.0	2W	1802	4.67E+05	5.48E+05	5.66	5.74	0.08	0.06	85.4
CNAR-310.8	WW	1795	1.46E+05	2.52E+05	5.14	5.38	0.17	0.15	57.9
CNAR-315.4	WW	1791	8.72E+05	1.00E+06	5.94	6.00	0.05	0.07	86.8
CNAR-319.7	WW	1789	6.67E+05	7.20E+05	5.82	5.86	0.09	0.04	92.7
CNAR-329.2	WW	1783	8.46E+05	9.92E+05	5.92	5.99	0.09	0.07	85.3
CNAR-333.7	P	1781	8.39E+04	1.40E+05	4.78	5.12	0.41	0.16	60.0
CNAR-344.2	P	1774.5	1.50E+05	1.63E+05	5.03	5.19	0.46	0.18	91.7
CNAR-350.3	P	1770	3.06E+05	4.52E+05	5.30	5.58	0.52	0.29	67.6
CNAR-355.4	P	1767	6.71E+05	8.29E+05	5.82	5.92	0.07	0.05	81.0
CNAR-361.1	P	1762	4.65E+06	5.15E+06	6.67	6.71	0.04	0.04	90.3
CNAR-371.1	CM	1757	1.40E+06	1.72E+06	6.14	6.23	0.07	0.05	81.2
CNAR-375.3	CM	1754.2	5.12E+05	6.57E+05	5.71	5.82	0.05	0.04	78.0
CNAR-378.4	CM	1752.2	2.61E+05	3.27E+05	5.39	5.50	0.20	0.12	80.0
CNAR-381.8	CM	1750	1.46E+05	2.13E+05	5.12	5.29	0.23	0.23	68.8
CNAR-386.5	C	1746.9	4.00E+05	5.20E+05	5.60	5.71	0.07	0.07	76.9
CNAR-390.9	C	1744	1.83E+05	2.35E+05	5.25	5.36	0.13	0.14	77.8
CNAR-397.1	C	*1741*	*6.85E+05*	*8.30E+05*	*5.82*	*5.90*	*0.16*	*0.15*	*82.5*
CNAR-405.5	OC	1734	4.72E+05	5.55E+05	5.66	5.73	0.11	0.12	85.2
CNAR-409.8	OC	1731	6.54E+05	7.71E+05	5.81	5.89	0.09	0.03	84.7
CNAR-417.4	OC	1727	8.55E+05	1.04E+06	5.93	6.02	0.05	0.04	82.3
CNAR-425.0	OC	1720.3	5.71E+05	8.22E+05	5.74	5.90	0.14	0.12	69.5
CNAR-426.5	OC	1719	<3.00E+04*	<3.00E+04	<4.48	<4.48	0.17	0.17	
CNAR-436.7	OC	1713	6.83E+04	9.56E+04	4.80	4.83	0.55	0.49	71.4
CNAR-451.2	*MO*	*1704*	*7.76E+04*	*1.42E+05*	*4.63*	*5.08*	*0.60*	*0.31*	*54.5*
CNAR-457.3	basalt	1699	8.52E+04	1.36E+05	4.86	5.07	0.31	0.31	62.5
CNAR-464.2	MO	1695	<3.00E+04	<3.00E+04	<4.48	<4.48	2.13	0.09	
CNAR-475.3	MO	*1688*	*2.13E+06*	*2.39E+06*	*6.33*	*6.38*	*0.06*	*0.05*	*89.0*
CNAR-482.9	MO	1682	4.30E+05	5.08E+05	5.62	5.70	0.11	0.08	84.6
CNAR-503.9	MO	1667.5	2.22E+05	2.48E+05	5.30	5.38	0.25	0.15	89.5
CNAR-507.3	MO	1663	1.20E+05	1.47E+05	5.01	5.15	0.30	0.14	81.8

Sample ID	Strat. Unit	Depth (m)	Cells/gdw		log(cells/gdw)		log(stdev)		%
			Viable	Total	Viable	Total	Viable	Total	Viable
CNV-SURF.	*soil*	*1937*	*2.99E+06*	*3.42E+06*	*6.46*	*6.53*	*0.13*	*0.10*	*87.4*
CNV-60.5	M	1876.5	4.63E+05	7.49E+05	5.65	5.87	0.12	0.05	61.8
CNV-127.3	2W	1809.7	2.65E+05	3.97E+05	5.42	5.59	0.09	0.08	66.7
CNV-140.3	WW	1796.7	9.41E+05	1.13E+06	5.97	6.05	0.04	0.06	83.5
CNV-149.2	WW	1787.8	3.19E+05	4.52E+05	5.39	5.61	0.44	0.24	70.6
CNV-164.2	P	1772.8	1.27E+05	2.61E+05	4.96	5.25	0.43	0.55	48.8
CNV-165.8	P	1771.2	4.28E+05	6.18E+05	5.61	5.76	0.18	0.19	69.3
CNV-170.4	P	1766.6	4.96E+05	7.01E+05	5.68	5.83	0.12	0.13	70.7
CNV-178.9	P	1758.1	5.84E+05	7.83E+05	5.76	5.89	0.10	0.03	74.6
CNV-183.9	CM	1753.1	7.97E+05	1.10E+06	5.90	6.04	0.05	0.06	72.2
CNV-185.7	C	1751.3	4.56E+05	5.52E+05	5.66	5.74	0.05	0.04	82.5
CNV-187.1	C	1749.9	5.67E+04	7.67E+04	4.75	4.88	0.37	0.46	73.9
CNV-188.5	C	1748.5	2.76E+05	3.58E+05	5.43	5.55	0.11	0.08	76.9
CNV-193.1	C	1743.9	7.52E+05	9.43E+05	5.87	5.96	0.11	0.14	79.7
CNV-196.3	C	1740.7	5.50E+05	6.71E+05	5.73	5.82	0.11	0.08	82.0
CNV-198.1	C	1738.9	8.44E+05	9.87E+05	5.92	5.99	0.08	0.08	85.5
CNV-200.3	C	1736.7	6.25E+05	7.36E+05	5.77	5.85	0.17	0.13	84.9
CNV-201.0	OC	1736	7.02E+05	8.53E+05	5.84	5.92	0.10	0.09	82.3
CNV-201.6	OC	1735.4	9.75E+04	2.79E+05	4.84	5.44	0.30	0.08	35.0
CNV-202.5	*sterile*	*1734.5*	*<3.00E+04*	*<3.00E+04*	*<4.48*	*<4.48*	*0.09*	*0.40*	
CNV-203.3	OC	1733.7	8.86E+05	1.07E+06	5.94	6.03	0.08	0.05	83.1
CNV-204.0	OC	1733	2.14E+05	2.94E+05	5.24	5.43	0.31	0.21	72.7
CNVR-189.2	*control*	*1748.1*	*5.79E+04*	*6.44E+04*	*4.76*	*4.77*	*0.39*	*0.24*	*90.0*
CNVR-196.9	C	1740.4	2.12E+05	2.91E+05	5.26	5.42	0.31	0.22	72.7
CNVR-206.7	OC	1730.6	4.13E+05	5.33E+05	5.60	5.71	0.12	0.13	77.5
CNVR-209.6	OC	1727.7	2.67E+05	4.13E+05	5.39	5.59	0.23	0.18	64.5
CNVR-221.7	OC	1715.6	2.36E+05	3.88E+05	5.36	5.58	0.11	0.10	60.7
CNVR-227.8	OC	1709.5	7.92E+05	9.69E+05	5.89	5.98	0.07	0.09	81.7
CNVR-231.5	OC	*1705.8*	*8.61E+05*	*1.05E+06*	*5.93*	*6.02*	*0.05*	*0.05*	*82.2*

*Limit of detection (average) is 3.00E+04 CFU/gww (log = 4.48)

Limit of detection (LOD) for method is 5.14E+04 cells/gww (log = 4.71). When average of 4 slides is taken, those replicates with less than 5.14E+04 cells are assigned the value of 1/2(LOD). This has the effect of lowering the average LOD.

Summary of Carbon Dioxide-Production and Oxygen-Uptake

Sample ID	Depth	Sample				Poisoned Control			
		O2 (%/10 gww)		CO2 (%/10 gww)		O2 (%/10 gww)		CO2 (%/10 gww)	
		Average	Stdev	Average	Stdev	Average	Stdev	Average	Stdev
CNAR-SURF.	*1960.0*	*0.839*	*0.093*	*0.396*	*0.040*	*1.568*	*0.316*	*0.620*	*0.044*
CNAR-91.8	1912.0	5.079	0.813	0.054	0.047	4.456	0.792	0.000	0.000
CNAR-93.5	*1960.0*	*4.935*	*0.202*	*0.596*	*0.014*	*6.150*	*0.067*	*1.463*	*0.015*
CNAR-200.0	1858.0	5.938	0.362	0.000	0.000	2.412	0.118	0.000	0.000
CNAR-227.6	1842.5	4.876	1.208	0.428	0.193	1.562	0.234	0.000	0.000
CNAR-239.9	1836.0	1.950	0.519	0.158	0.013	0.672	0.257	0.000	0.000
CNAR-251.6	1829.5	1.391	0.069	0.659	0.024	0.194	0.119	0.248	0.031
CNAR-260.5	1822.5	2.392	0.517	1.333	0.186	0.417	0.062	0.280	0.050
CNAR-299.0	1802.0	3.799	0.893	0.916	0.352	2.493	0.238	0.519	0.077
CNAR-310.8	1795.0	4.437	1.424	0.472	0.313	3.570	1.037	0.378	0.137
CNAR-315.4	1791.0	3.645	0.546	0.293	0.071	3.785	1.358	0.382	0.074
CNAR-319.7	1789.0	3.943	0.878	0.298	0.101	4.172	1.121	0.245	0.202
CNAR-329.2	1783.0	3.765	0.504	0.213	0.073	2.648	0.363	0.104	0.013
CNAR-333.7	1781.0	3.074	0.199	1.024	0.071	0.931	0.873	0.324	0.358
CNAR-344.2	1774.5	3.885	0.121	1.247	0.076	1.685	0.702	0.251	0.219
CNAR-350.3	1770.0	3.154	0.460	0.609	0.060	1.685	0.702	0.251	0.219
CNAR-355.4	1767.0	1.842	0.375	0.353	0.022	0.944	0.741	0.175	0.253
CNAR-361.1	1762.0	2.002	0.937	0.700	0.175	0.361	0.355	0.047	0.053
CNAR-371.1	1757.0	2.980	0.352	0.499	0.070	0.591	0.261	0.000	0.000
CNAR-375.3	1754.2	2.592	0.916	0.205	0.026	0.201	1.437	0.000	0.000
CNAR-378.4	1752.2	Not Enough Sample							
CNAR-381.8	1750.0	2.315	0.527	0.142	0.053	2.362	0.501	0.104	0.004
CNAR-386.5	1746.9	2.234	0.084	0.887	0.030	-0.052	0.044	0.006	0.005
CNAR-390.9	1744.0	2.946	0.540	0.968	0.160	0.950	0.404	0.340	0.107
CNAR-397.1	*1741.0*	*2.434*	*1.071*	*0.832*	*0.240*	*1.712*	*0.345*	*0.647*	*0.086*
CNAR-405.5	1734.0	2.954	0.506	0.196	0.022	0.221	0.120	0.000	0.000
CNAR-409.8	1731.0	2.561	0.535	0.404	0.017	0.418	0.141	-0.045	0.039
CNAR-417.4	1727.0	3.334	0.276	0.312	0.062	0.626	0.453	0.000	0.000
CNAR-425.0	1720.3	4.015	0.119	0.102	0.089	2.471	0.339	0.121	0.020
CNAR-426.5	1719.0	2.372	0.072	0.255	0.046	0.458	0.116	0.081	0.009
CNAR-436.7	1713.0	1.932	0.069	0.401	0.002	0.374	0.132	-0.027	0.044
CNAR-451.2	*1704.0*	*0.770*	*0.142*	*0.402*	*0.013*	*0.339*	*0.109*	*0.095*	*0.127*
CNAR-457.3	1699.0	Not Enough Sample							
CNAR-464.2	1695.0	0.829	0.071	0.000	0.000	0.368	0.118	0.000	0.000
CNAR-475.3	*1687.9*	*1.306*	*0.139*	*0.000*	*0.000*	*0.878*	*0.122*	*0.000*	*0.000*
CNAR-482.9	1682.0	0.846	0.133	0.000	0.000	0.162	0.040	-0.041	0.029
CNAR-503.9	1667.5	0.716	0.170	0.000	0.000	0.412	0.131	0.000	0.000
CNAR-507.3	1663.0	0.810	0.161	0.000	0.000	0.227	0.732	0.000	0.000

Sample ID	Depth	Sample				Poisoned Control			
		O2 (%/10 gww)		CO2 (%/10 gww)		O2 (%/10 gww)		CO2 (%/10 gww)	
		Average	Stdev	Average	Stdev	Average	Stdev	Average	Stdev
CNV-SURF.	*1937.0*	*1.149*	*0.474*	*0.305*	*0.035*	*0.763*	*0.281*	*0.219*	*0.006*
CNV-60.5	1876.5	6.849	0.743	0.000	0.000	6.514	0.447	0.000	0.000
CNV-127.3	1809.7	1.510	1.310	0.525	0.013	2.803	0.419	0.564	0.084
CNV-140.3	1796.7	2.887	0.297	0.160	0.047	2.862	0.513	0.192	0.041
CNV-149.2	1787.8	2.101	0.153	0.000	0.000	2.299	0.117	0.000	0.000
CNV-164.2	1772.8	2.192	0.246	0.431	0.061	2.254	0.165	0.405	0.104
CNV-165.8	1771.2	2.531	0.383	0.188	0.082	2.533	0.138	0.204	0.016
CNV-170.4	1766.6	1.615	0.187	0.259	0.011	1.663	0.174	0.266	0.035
CNV-178.9	1758.1	1.954	0.209	0.121	0.004	1.952	0.206	0.140	0.009
CNV-183.9	1753.1	1.774	0.074	0.000	0.000	1.744	0.243	0.000	0.000
CNV-185.7	1751.3	1.609	0.314	0.713	0.073	1.754	0.508	0.744	0.152
CNV-187.1	1749.9	1.727	0.136	0.689	0.079	1.585	0.236	0.667	0.054
CNV-188.5	1748.5	1.359	0.411	0.517	0.043	1.680	0.435	0.566	0.126
CNV-193.1	1743.9	1.574	0.106	0.565	0.045	1.500	0.051	0.469	0.012
CNV-196.3	1740.7	2.001	0.030	0.349	0.031	1.935	0.103	0.317	0.028
CNV-198.1	1738.9	1.652	0.186	0.236	0.031	1.810	0.112	0.269	0.006
CNV-200.3	1736.7	2.300	0.438	0.000	0.000	2.182	0.095	0.000	0.000
CNV-201.0	1736.0	2.551	0.057	0.000	0.000	2.360	0.341	0.000	0.000
CNV-201.6	1735.4	Not Enough Sample							
CNV-202.5	*1734.5*	*1.811*	*0.184*	*0.365*	*0.021*	*1.748*	*0.136*	*0.410*	*0.066*
CNV-203.3	1733.7	2.007	0.200	0.078	0.004	2.161	0.043	0.022	0.039
CNV-204.0	1733.0	1.923	0.048	0.102	0.004	2.267	0.312	0.095	0.032
CNVR-189.2	*1748.1*	*2.785*	*0.490*	*0.219*	*0.042*	*1.531*	*0.254*	*0.026*	*0.008*
CNVR-196.9	1740.4	1.999	0.569	0.685	0.119	0.472	0.09	0.082	0.033
CNVR-206.7	1730.6	2.218	0.335	0.313	0.005	-1.810	2.634	0.000	0.000
CNVR-209.6	1727.7	2.545	0.307	0.360	0.046	0.455	0.169	0.000	0.000
CNVR-221.7	1715.6	1.312	0.315	0.019	0.011	0.250	0.191	-0.001	0.003
CNVR-227.8	1709.5	2.843	0.153	0.095	0.006	0.669	0.949	0.000	0.000
CNVR-231.5	*1705.8*	*0.529*	*0.231*	*0.000*	*0.000*	*0.055*	*0.149*	*0.000*	*0.000*

Average Result of Each Assay, for Each Stratigraphic Unit, in Each Borehole.

		O2-Uptake				CO2 Produced				% 14C-Gluc. Mineral.		Plate Counts		Direct Counts					
		Sample		Poisoned		Sample		Poisoned		Sample		log Sample		Viable (log)		Total (log)		% Viable	
	n	Avg.	Stdev	Avg.	Stdev	Avg.	Stdev	Avg.	Stdev	Avg.	Stdev	Avg.	Stdev	Avg.	Stdev	Avg.	Stdev	Avg.	Stdev
Mancos Shale																			
CNV	1	6.849		6.514		0.000		0.000		4.160		2.52		5.67		5.14		61.82	
CNVR	0																		
CNAR	4	4.461	1.736	2.276	1.618	0.160	0.190	0.000	0.000	0.462	0.607	0.95	1.10	5.39	0.70	5.70	0.37	58.18	31.50
Average		5.655	1.689	4.395	2.997	0.080	0.113	0.000	0.000	2.311	2.615	1.733		5.527		5.422		59.999	
Two Wells Sandstone																			
CNV	1	1.510		2.803		0.525		0.564		0.490		2.73		5.42		4.71		66.67	
CNVR	0																		
CNAR	3	2.527	1.210	1.035	1.268	0.969	0.340	0.349	0.148	1.336	0.821	0.81	1.41	5.48	0.29	5.60	0.24	75.68	9.37
Average		2.019	0.719	1.919	1.250	0.747	0.314	0.457	0.152	0.913	0.598	1.773	1.358	5.449	0.037	5.154	0.628	71.172	6.372
Whitewater Arroyo Shale																			
CNV	2	2.494	0.556	2.581	0.398	0.080	0.113	0.096	0.136	0.661	0.005	1.44	2.03	5.74	0.33	5.95	0.14	63.99	27.64
CNVR	0																		
CNAR	4	3.948	0.349	3.544	0.647	0.319	0.109	0.335	0.078	0.878	0.247	0.75	1.51	5.71	0.37	5.81	0.28	80.70	15.53
Average		3.221	1.028	3.062	0.681	0.200	0.169	0.216	0.169	0.770	0.154	1.096	0.485	5.726	0.018	5.884	0.099	72.343	11.817
Paguate Sandstone																			
CNV	4	2.073	0.386	2.101	0.376	0.250	0.133	0.254	0.113	1.824	0.024	0.77	0.89	5.51	0.40	5.73	0.24	64.16	19.55
CNVR	0																		
CNAR	5	2.791	0.856	1.121	0.566	0.787	0.352	0.210	0.105	3.831	3.391	1.22	1.27	5.60	0.70	5.73	0.64	76.11	17.46
Average		2.432	0.508	1.611	0.692	0.518	0.380	0.232	0.031	2.828	1.419	0.999	0.318	5.557	0.061	5.727	0.002	70.132	8.451
Clay Mesa Shale																			
CNV	1	1.774		1.744		0.000		0.000		1.440		0.00	0.00	5.90		4.92		82.61	
CNVR	0																		
CNAR	4	2.629	0.334	1.051	1.152	0.282	0.191	0.035	0.060	0.439	0.305	0.44	0.87	5.61	0.42	5.72	0.40	76.99	5.65
Average		2.202	0.605	1.398	0.490	0.141	0.199	0.017	0.025	0.940	0.708	0.219	0.309	5.756	0.206	5.322	0.569	79.798	3.974
Cubero Sandstone																			
CNV	7	1.746	0.311	1.778	0.229	0.438	0.259	0.433	0.258	2.928	5.817	0.66	0.82	4.93	2.18	5.01	2.21	70.64	31.32
CNVR	1	1.999		0.472		0.685		0.082		1.280		0	0	5.33		5.07		72.73	
CNAR	2	2.590	0.503	0.449	0.709	0.928	0.057	0.173	0.236	17.967	18.538	2.54	1.50	5.43	0.24	5.54	0.24	77.35	0.60
Average		2.168	0.597	1.114	0.761	0.683	0.245	0.303	0.182	7.392	9.196	1.067	1.321	5.229	0.265	5.206	0.294	73.572	3.435
Oak Canyon Member																			
CNV	4	2.160	0.341	2.263	0.100	0.060	0.053	0.024	0.021	1.365	0.479	0.00	0.00	5.53	0.45	5.72	0.30	68.28	22.68
CNVR	4	2.230	0.663	-0.109	1.147	0.197	0.165	0.000	0.001	0.324	0.332	0.37	0.37	5.58	0.24	5.73	0.18	71.11	10.07
CNAR	6	2.861	0.742	0.761	0.848	0.278	0.278	0.022	0.065	0.882	1.296	1.20	1.20	4.67	2.32	4.76	2.36	65.31	32.64
Average		2.417	0.496	0.972	1.200	0.178	0.110	0.015	0.013	0.857	0.521	0.526	0.616	5.260	0.509	5.404	0.555	68.231	2.897
Morrison Formation																			
CNV	0																		
CNVR	0																		
CNAR	5	0.800	0.058	0.292	0.117	0.000	0.000	-0.010	0.021	7.674	12.571	1.49	1.49	4.18	2.35	5.17	0.46	61.18	37.56

... unless otherwise specified

Sample Name	Precip	Elkins	Presbyteri	Seboyeta	Bibo#1	Moquino#	CNV-W2	CNV-W3	CNV-W5	MW-65	MW-68	MW-64	MW-60	L-Bar
Date sampled	ave	10-27-94	10-27-94	10-5-94	10-5-94	10-5-94	7-17-94	7-25-94	7-31-94	5-20-94	5-20-94	5-20-94	5-20-94	10-5-94
Temp (C)	-	16.02	12.48	22.9	19.74	17.7	20	20	20	20	19	19	19	18.41
DO (mg/L)	-	5.91	6.87	0	0.62	0.05	0.2	0.18	0.01	-	-	-	-	2.39
Conductivity (mS/cm)	0.009	0.1318	0.170	0.311	0.839	0.604	0.93	0.99	1.53	-	-	-	-	1.074
pH	4.979	7.81	7.27	7.94	8.05	8.59	8.26	8.17	8.46	7.8	8.1	7.9	8.1	8.26
Eh (mV)	-	229	395	-25	273	-8	282	231	233	-	-	-	-	103
F	-	0.19	0.17	0.23	1.03	1.57	1.85	1.38	4.53	1.81	1.71	1.53	1.84	2.15
Cl	0.099	2.96	2.73	7.75	15	4.07	13.88	5.25	11.16	305.43	61.42	34.21	42.64	15.12
NO2	-	<0.01	<0.01	<0.03	<0.03	<0.03	<0.03	<0.03	<.03	<0.01	<0.01	<0.01	<0.01	<0.03
Br	-	0.03	0.05	0.03	<0.02	<0.02	0.06	0.29	0.3	0.041	0.2	0.11	0.13	0.08
NO3	0.856	1.21	0.86	0.12	0.22	<0.02	1.27	0.08	0.07	0.04	0.04	0.39	<0.01	0.31
PO4	-	0.17	0.23	<0.06	<0.06	<0.06	<0.03	<0.03	<.06	<0.02	<0.02	<0.02	<0.02	<0.06
SO3	-	<0.05	<0.05	<0.05	<0.05	<0.05	<0.05	<0.05	<.05	-	-	-	-	<0.05
SO4	0.851	2.06	2.34	22.97	163.2	<0.05	225.59	80.76	370.42	260.25	1131.81	409.36	588.92	236.24
OX	-	<0.09	<0.09	<0.07	<0.07	<0.07	<0.07	<0.07	<.07	<0.06	<0.06	<0.06	<0.06	<0.07
HCO3 *	-	91.68	119.80	213.53	362.38	393.70	464.48	585.80	535.89	664.11	612.67	653.48	746.01	482.11
Zn	-	0.05	0.096	0.022	0.058	0.08	0.18	0.165	0.065	-	-	-	-	0.028
Ba	-	0.018	0.038	0.096	0.078	0.046	-	-	-	-	-	-	-	0.02
B	-	<.0066	<.0066	<.0066	0.096	0.126	0.33	0.34	0.655	-	-	-	-	0.222
Si	-	23.492	23.42	9.412	8.468	4.408	5.616	4.965	3.96	7.525	10.145	7.11	7.575	4.712
Mn	-	0.002	0.002	0.002	0.006	0.008	0.005	0.03	0.005	0.035	0.01	0.01	0.02	0.006
Fe	-	0.242	0.008	0.008	0.042	0.086	0.57	0.95	0	0.06	0.725	<.012	<.012	0.034
Mg	0.021	5.2	6.418	3.232	4.734	2.294	1.345	0.77	6.61	9.77	4.47	2.825	2.825	1.322
Al	-	0.026	0.042	0.034	0.034	<.015	-	-	-	-	-	-	-	0.02
Sr	-	0.082	0.104	0.374	0.576	0.296	0.185	0.22	0.565	-	-	-	-	0.228
Ca	0.184	13.668	16.132	8.468	12.78	4.314	3.335	4.98	17.425	10.06	12.995	7.97	7.97	3.626
Na	0.064	9.072	10.644	68.172	192.48	172.84	307	247.2	355.1	527.12	724.3	568.34	568.34	289.24
Li	-	0.004	0.004	0.022	0.044	0.038	<0.06	0.105	0.09	-	-	-	-	0.054
K	0.018	3.546	3.848	2.012	2.722	1.394	6.37	2.17	1.705	4.095	4.3	3.36	3.36	1.704
Fe(tot), (mg/L) onsite	-	-	-	.12	0.34	1.29	-	-	-	-	-	-	-	0.02
Fe2, (mg/L) onsite	-	-	-	<	0	0.18	-	-	-	-	-	-	-	0.02
Fe3+ (mg/L) lab	-	<.04	-	<.04	<.04	<.04	0.11	0.14	<.07	<.13	0.14	<.13	<.13	<.04
Fe2+(mg/L) lab	-	<.1	-	<.1	<.1	<.1	0.46	0.81	<.04	<.07	0.36	<.07	<.07	<.1
Fe(tot) (mg/L) lab	-	0	-	0	0	0	0.57	0.95	0	0	0.5	0	0	0
DIC (ppm)	-	18.1	23.6	42.2	71.7	78.9	92.2	116.1	106.9	131.1	121.3	129.1	147.7	95.7
dIrect (u) DOC (ppm)	-	0.67	0.78	0.75	0.66	0.71	5.29	1.84	13.85	-	-	-	-	0.86
del 13C (o/oo)	-	-13.279	-13.969	-11.317	-8.669	-7.085	-4.43	-3.08	-3.6	-6.84	-4.67	-5.65	-5.04	-5.986
14C (pmc)	-	56.45	73.33	23.96	17.84	4.61	52.29	0.74	0.28	0.25	0.11	0.28	0.17	0.16
del 18O (o/oo)	-	-	-	-11.30	-11.55	-11.50	-11.20	-11.20	-	-11.60	-12.70	-11.90	-12.80	-12.60
del D (o/oo)	-	-95	-90.6	-89.38	-94.5	-93.87	-98.6	-100.34	-88.5	-89.02	-105.39	-97.88	-105.42	-105.47
Tritium (TU)	-	0.9	<0.8	<0.8	<0.8	<0.8	<0.8	<0.8	<0.8	<0.8	<0.8	<0.8	<0.8	<0.8
34S SO4 (o/oo)	-	nes	nes	-2.25	-12.15	-6.35	-22.09	-9.95	-8.78	-14.55	-19.18	-16.61	-18.3	-8.89

NOTES

[redacted] -Estimated from data on nearby monitor wells

nes -Not enough sample

\- -Not determined

* -Calculated from DIC and pH

Appendix 2: Master Data Table

This table contains data from all of the investigators involved in the Cerro Negro Origins project.

General Distribution / Sample Number	Depth Feet	Depth meters	Stratigraphic Unit##	Tracers	Type** Microspheres	microspheres no./g
CNV						
CNV-60.5	198.5	60.5	Mancos Shale	None		
CNV-127.3	417.7	127.3	Two Wells Sandstone	LiBr, PFT, microspheres	1 micron YG	
CNV-140.3	460.3	140.3	Whitewater Arroyo Shale	microspheres	1 micron YG	1.60E+04
CNV-149.2	489.5	149.2	Whitewater Arroyo Shale	LiBr, PFT, microspheres	1 micron YG	1.05E+03
CNVC-164.2	538.7	164.2	Paguate Sandstone	LiBr, PFT, microspheres	1 micron YG	
CNV-165.8	544.0	165.8	Paguate Sandstone	LiBr, PFT, microspheres	1 micron YG	
CNV-170.4	559.1	170.4	Paguate Sandstone	LiBr, PFT, microspheres	1 micron YG	4.61E+02
CNV-178.9	586.9	178.9	Paguate Sandstone	LiBr, PFT, microspheres	1 micron NYO	
CNV-183.9	603.3	183.9	Clay Mesa Shale	LiBr, PFT, microspheres	1 micron NYO	
CNV-185.7	609.3	185.7	Cubero Sandstone	LiBr, PFT, microspheres	1 micron NYO	
CNV-187.1	614.0	187.1	Cubero Sandstone	LiBr, PFT, microspheres^	1 micron NYO#	
CNV-188.5	618.4	188.5	Cubero Sandstone	LiBr, PFT, microspheres^	1 micron NYO#	
Hetero.-189.7	622.4	189.7	Cubero Sandstone	LiBr, PFT, microspheres^	1 micron NYO#	
Hetero.-191.3	627.6	191.3	Cubero Sandstone	LiBr, PFT, microspheres^	1 micron NYO#	
CNV-193.1	633.5	193.1	Cubero Sandstone	LiBr, microspheres^	1 micron NYO#	
CNV-196.3	644.0	196.3	Cubero Sandstone	LiBr, microspheres^	1 micron NYO#	
CNV-198.1	649.9	198.1	Cubero Sandstone	LiBr, microspheres^	1 micron NYO#	
CNV-200.3	657.2	200.3	Cubero Sandstone	LiBr, PFT	none	na
CNV-201.0	659.4	201.0	Oak Canyon Member (upper)	LiBr, microspheres^	1 micron NYO#	
CNV-201.6	661.0	201.6	Oak Canyon Member (upper)	LiBr, microspheres^	1 micron NYO#	
CNV-202.5	N/A	N/A	sterile control	N/A	N/A	na
CNV-203.3	667.0	203.3	Oak Canyon Member (upper)	LiBr, PFT, microspheres^	1 micron NYO#	
CNV-204.0	669.3	204.0	Oak Canyon Member (upper)	LiBr, PFT, microspheres^	1 micron NYO#	
CNA-R						
CNAR-160.5*	160.5	23.0	Mancos Shale	@	@	
CNAR-91.8	301.2	48.0	Mancos Shale	microspheres	1 micron NYO	
CNAR-93.5	spiked control		Mancos Shale	N/A	N/A	na
CNAR-200.0	656.2	102.0	Mancos Shale	microspheres^	1 micron NYO#	
CNAR-227.6	746.5	117.5	Mancos Shale	microspheres^	1 micron NYO#	
CNAR-239.9	787.1	124.0	Mancos Shale	PFT, microspheres^	1 micron NYO#	
CNAR-251.6	825.5	130.5	Two Wells Sandstone	LiBr, PFT, microspheres^	1 micron NYO#	
CNAR-259.9	852.7	136.0	Two Wells Sandstone	LiBr, PFT, microspheres	1 micron NYO#	
CNAR-260.5	854.7	137.5	Two Wells Sandstone	LiBr, PFT, microspheres	1 micron NYO#	
CNAR-299.0	981.0	158.0	Two Wells Sandstone	LiBr, PFT	none	na
CNAR-310.8	1019.7	165.0	Whitewater Arroyo Shale	LiBr, PFT, microspheres	1 micron NYO#	
CNAR-315.4	1034.8	169.0	Whitewater Arroyo Shale	LiBr, PFT	none	na
CNAR-319.7	1048.9	171.0	Whitewater Arroyo Shale	LiBr, PFT	none	na
CNAR-329.2	1080.1	177.0	Whitewater Arroyo Shale	LiBr, PFT, microspheres	1 micron NYO#	
CNAR-333.7	1094.8	179.0	Paguate Sandstone	LiBr, PFT, microspheres	1 micron NYO#	
CNAR-344.2	1129.3	185.5	Paguate Sandstone	PFT, microspheres	1 micron BB	none
CNAR-350.3	1149.3	190.0	Paguate Sandstone	LiBr, PFT, microspheres	1 micron BB	none
CNAR-355.4	1166.0	193.0	Paguate Sandstone	LiBr, PFT, microspheres	1 micron BB	none
CNAR-361.1	1185.0	198.0	Paguate Sandstone	LiBr, PFT, microspheres	1 micron BB	none
CNAR-371.1	1217.5	203.0	Clay Mesa Shale	LiBr, PFT, microspheres^	1 micron BB#	

General Distribution Sample Number	Depth Feet	Depth meters	Stratigraphic Unit##	Tracers	Type** Microspheres	microspheres no./g
CNAR-405.5	1330.4	226.0	Oak Canyon Member (upper)	LiBr, PFT, microspheres	1 micron YG	na
CNAR-409.8	1344.5	229.0	Oak Canyon Member (upper)	LiBr, PFT, microspheres	1 micron YG	
CNAR-417.4	1369.4	233.0	Oak Canyon Member (upper)	LiBr, PFT	none	na
CNAR-425.0	1394.4	239.7	Oak Canyon Member (upper)	LiBr, PFT	none	na
CNAR-426.5	1399.3	241.0	Oak Canyon Member (lower)	LiBr, PFT	none	na
CNAR-436.7	1432.7	247.0	Oak Canyon Member (lower)	LiBr, PFT, microspheres	1 micron YG#	8.00E+01
CNAR-451.2	1480.3	256.0	Morrison Fm. (Jackpile SS)	LiBr, PFT, microspheres^	1 micron YG#	
*CNAR-457.2***						
CNAR-457.3	1500.0	261.0	Basalt dike in Morrison Fm	LiBr	none	na
CNAR-464.2	1523.0	265.0	Morrison Fm.	LiBr, PFT	none	
CNAR-472.6	1550.5	270.0	Morrison Fm.	LiBr, PFT, microspheres	1 micron YG	2.12E+02
CNAR-472.6**		270.0				
CNAR-475.3	1559.4	272.1	Morrison Fm.	LiBr, PFT, microspheres	1 micron YG	3.02E+03
*CNAR-482.1***		277.4				
CNAR-482.9	1584.3	278.0	Morrison Fm.	microspheres	1 micron YG	8.02E+02
CNAR-503.9	1653.2	292.5	Morrison Fm.	microspheres	1 micron YG	8.08E+02
CNAR-507.3	1664.4	297.0	Morrison Fm.	PFT, microspheres	1 micron YG	2.58E+02
CNV-R						
CNVR-188.0	616.8	188.0	Clay Mesa/Cubero contact	LiBr, PFT	none	na
CNVR-189.2	N/A		sterile control	N/A	N/A	na
Hetero.-192.1	630.2		Cubero Sandstone	LiBr, PFT, microspheres	1 micron YG#	
CNVR-196.9	646.0	196.9	Cubero Sandstone	LiBr, PFT, microspheres	1 micron YG#	none
CNVR-206.7	678.1	206.7	Oak Canyon Member (upper)	LiBr, PFT, microspheres	1 micron YG	none
CNVR-209.6	687.7	209.6	Oak Canyon Member	LiBr, PFT, microspheres	1 micron YG	1.81E+02
CNVR-221.7	727.4	221.7	Oak Canyon Member	LiBr, PFT, microspheres	1 micron YG#	none
*CNVR-226.5***	743.1	227.8	Oak Canyon Member (lower)	LiBr, PFT	none	
CNVR-227.8	747.4		Oak Canyon Member (lower)	LiBr, PFT, microspheres^	1 micron YG#	none
CNVR-231.5	759.5		Morrison Fm. (Jackpile SS)	LiBr, PFT, microspheres^	1 micron YG#	1.03E+04

Limited distribution samples shown in bold italics

*Common interval depth in feet instead of meters

** intact core

Hetero. = sample for hetergeneity study

(**)= microspheres used: YG~FITC filter set; NYO~rhodamine; BB = coumarin

(@)=use of tracers not documented

General Distribution Sample Number	Comments	Drill Method	Br- mg/kg	Sample Grade
CNV				
CNV-60.5		Air rotary	0.00	1
CNV-127.3		Air rotary	0.26	2
CNV-140.3	no PFT added	Air rotary	0.13	2
CNV-149.2	Partial PFT injection - leak in pump connection	Air rotary	0.21	2
CNVC-164.2	Partial PFT injection	Air rotary	0.18	2
CNV-165.8		Air rotary	0.00	1
CNV-170.4		Air rotary	0.30	2
CNV-178.9		Air rotary	0.00	1
CNV-183.9		Air rotary	0.00	1
CNV-185.7	Flow of PFT interrupted several times	Air rotary	0.00	1
CNV-187.1	PFT only during first 5 minutes of coring	Air rotary	0.07	1
CNV-188.5		Air rotary	0.00	1
Hetero.-189.7	Sample processed for heterog. exp, partial PFT injection	Air rotary	-	-
Hetero.-191.3	Sample processed for heterog. exp, partial PFT injection	Air rotary	-	-
CNV-193.1	No PFT - pump not working	Air rotary	0.00	1
CNV-196.3	No PFT - pump not working	Air rotary	0.00	1
CNV-198.1	No PFT - pump not working	Air rotary	0.00	1
CNV-200.3	Nitrogen, frozen lines, microsphere bag did not break	Nitrogen rotary	0.08	1
CNV-201.0	No PFT - pump not working	Air rotary	0.00	1
CNV-201.6	No PFT - pump not working	Air rotary	0.11	1
CNV-202.5	Sterile control, shale autoclaved 3x,depth designation fictitious	N/A	-	-
CNV-203.3		Air rotary	0.00	1
CNV-204.0		Air rotary	0.00	1
CNA-R				
CNAR-160.5*		Mud rotary	-	
CNAR-91.8		Mud rotary	0.00	1
CNAR-93.5	Arthobacter-spiked control sample	N/A	-	-
CNAR-200.0		Air rotary	0.00	1
CNAR-227.6		Air rotary	1.01	2
CNAR-239.9		Air rotary	29.10	2
CNAR-251.6		Air rotary	6.51	2
CNAR-259.9		Air rotary	-	
CNAR-260.5		Air rotary	-	2
CNAR-299.0	Microsphere bag did not break	Mud rotary	0.22	1
CNAR-310.8		Mud rotary	0.13	1
CNAR-315.4	Microsphere bag did not break	Mud rotary	0.13	1
CNAR-319.7	Microsphere bag did not break	Mud rotary	0.10	1
CNAR-329.2	leaky microsphere bag, partial PFT injection	Mud rotary	0.16	1
CNAR-333.7		Mud rotary	0.11	1
CNAR-344.2		Mud rotary	0.13	1
CNAR-350.3		Mud rotary	0.00	1
CNAR-355.4		Mud rotary	0.00	1
CNAR-361.1		Mud rotary	0.17	1
CNAR-371.1		Mud rotary	0.09	1
CNAR-375.3	no LiBr added before this run	Air rotary	0.00	1
CNAR-378.4		Air rotary	0.11	1
CNAR-381.8	Nitrogen gas	Nitrogen rotary	0.26	2
CNAR-384.3	Nitrogen gas	Nitrogen rotary	-	2
CNAR-386.5	N2 gas, microshpere bag leaking at surface	Nitrogen rotary	1.28	2
CNAR-387.5	Microsphere bag leaking at surface	Nitrogen rotary	-	2
CNAR-390.9	microspheres old	Air rotary	1.57	2
CNAR-397.1	Some microspheres left in bag	Air rotary	8.31	3

General Distribution	Comments	Drill	Br-	Sample
Sample Number		Method	mg/kg	Grade
CNAR-405.5	Microsphere bag did not break	Mud rotary	0.21	1
CNAR-409.8	Some microspheres left in bag	Mud rotary	0.11	2
CNAR-417.4	Microsphere bag did not break	Mud rotary	0.00	1
CNAR-425.0	Microsphere bag did not break	Mud rotary	0.00	1
CNAR-426.5		Mud rotary	0.11	2
CNAR-436.7		Mud rotary	0.08	2
CNAR-451.2	Significant loss of drilling fluids to formation	Mud rotary	7.05	3
*CNAR-457.2***				
CNAR-457.3	No lexan liner used, no PFT used, sulfur smell	Mud rotary	0.19	2
CNAR-464.2	sulfur smell, loss of drilling fluids	Mud rotary	0.24	2
CNAR-472.6		Mud rotary	0.59	2
CNAR-472.6''				
CNAR-475.3	Partial PFT injection	Mud rotary	1.02	3
*CNAR-482.1***				
CNAR-482.9		Mud rotary	0.09	2
CNAR-503.9	No PFT	Mud rotary	0.10	2
CNAR-507.3		Mud rotary	0.00	2
CNV-R				
CNVR-188.0	Microsphere bag did not break	Air rotary	-	1
CNVR-189.2	Sterile Control	N/A	-	-
Hetero.-192.1		Air rotary	-	-
CNVR-196.9		Mud rotary	0.48	1
CNVR-206.7		Mud rotary	0.07	1
CNVR-209.6		Mud rotary	0.08	2
CNVR-221.7	Smells of SO2	Mud rotary	0.00	1
*CNVR-226.5***	PFT injected by hand	Mud rotary	-	-
CNVR-227.8	PFT injected by hand	Mud rotary	0.00	1
CNVR-231.5	PFT injected by hand	Mud rotary	0.24	3

General Distribution Sample Number	Why	Date Collected	PNL/Fredrickson, Acetate Mineralization aerobic, ave. cum. % of added (n=3)				
			d 1, ave.	sd	d 3, ave.	sd	d 7, ave
CNV							
CNV-60.5	unsaturated, low perm, air-drilled	7/10/94	0.218	0.064	0.309	0.065	0.425
CNV-127.3	microspheres moderate, PFT bd	7/14/94	0.190	0.008	12.815	1.760	51.715
CNV-140.3	microspheres high (for air-drilled), moderate Br	7/15/94	0.178	0.012	0.289	0.010	5.302
CNV-149.2	microspheres mod high, Br mod high	7/18/94	0.175	0.006	0.324	0.014	13.521
CNVC-164.2	microsphere low, Br moderate	7/18/94	0.100	0.011	6.457	10.609	15.485
CNV-165.8	microsphere low, Br below detect	7/19/94	0.063	0.008	0.256	0.080	26.668
CNV-170.4	microspheres present, Br moderately high	7/19/94	0.133	0.011	17.942	15.228	31.995
CNV-178.9	Br below detect	7/20/94	0.141	0.001	0.276	0.036	0.431
CNV-183.9	Br below detect	7/20/94	0.120	0.028	0.217	0.044	0.339
CNV-185.7	Br below detect	7/21/94	0.136	0.004	0.270	0.006	0.538
CNV-187.1	Br low	7/21/94	0.140	0.005	0.275	0.005	20.190
CNV-188.5	Br below detect	7/21/94	0.175	0.015	0.325	0.014	0.614
Hetero.-189.7		7/21/94					
Hetero.-191.3		7/21/94					
CNV-193.1	Br below detect	7/22/94	4.600	0.721	28.400	0.500	51.713
CNV-196.3	Br below detect	7/22/94	0.199	0.019	3.259	4.843	38.723
CNV-198.1	Br below detect	7/22/94	0.055	0.003	0.133	0.009	13.140
CNV-200.3	Br low	7/25/94	0.075	0.005	0.155	0.007	0.279
CNV-201.0	Br below detect	7/27/94	0.102	0.039	0.159	0.057	0.242
CNV-201.6	Br low, PFT bd	7/27/94	0.169	0.051	0.222	0.064	0.268
CNV-202.5		N/A	0.141	0.119	0.288	0.072	0.386
CNV-203.3	Br below detect	7/27/94	0.207	0.033	0.389	0.029	0.665
CNV-204.0	Br below detect	7/27/94	0.137	0.038	0.255	0.038	0.467
CNA-R			d 1, ave.	sd	2/3/4/5, av	sd	d 6/7, ave
CNAR-160.5*		8/26/94					
CNAR-91.8	Br below detect	8/29/94	0.010	0.000	0.023	0.001	0.093
CNAR-93.5		8/30/94	12.885	0.449	27.305	0.478	45.593
CNAR-200.0	Br below detect	9/13/94	0.025	0.002	0.054	0.007	0.075
CNAR-227.6	High Br	9/16/94	0.014	0.003	4.794	4.528	12.346
CNAR-239.9	Very high Br	9/20/94	0.015	0.001	0.045	0.003	0.060
CNAR-251.6	High Br	9/23/94	3.777	1.129	13.564	7.539	37.083
CNAR-259.9		9/25/94	0.102	0.097	15.756	1.680	38.241
CNAR-260.5	detectable PFT	9/25/94	0.014	0.001	5.796	9.947	16.188
CNAR-299.0	low Br	9/28/94	0.021	0.005	0.151	0.137	11.923
CNAR-310.8	low Br	9/29/94	0.017	0.003	0.062	0.004	1.064
CNAR-315.4	low Br	9/30/94	0.017	0.000	0.057	0.007	0.173
CNAR-319.7	low Br	9/30/94	0.017	0.002	4.139	7.073	13.292
CNAR-329.2	low Br	10/2/94	0.011	0.000	6.911	5.963	27.210
CNAR-333.7	low Br, PFT bd	10/2/94	4.150	1.770	21.432	7.421	40.862
CNAR-344.2	No microspheres, low Br, PFT bd	10/2/94	2.410	0.350	25.345	0.197	52.756
CNAR-350.3	No microsphere, Br bd, PFT, bd	10/3/94	0.018	0.001	0.064	0.005	0.172
CNAR-355.4	No microsphere, Br bd, PFT bd	10/3/95	0.726	0.377	22.267	1.202	42.249
CNAR-361.1	No microspheres, low Br, PFT bd	10/4/95	0.419	0.109	23.420	1.227	48.120
CNAR-371.1	No microspheres, low Br, PFT bd	10/4/95	0.011	0.001	0.070	0.030	0.226
CNAR-375.3	No microspheres, Br bd, PFT bd	10/5/94	0.049	0.004	0.089	0.011	0.367
CNAR-378.4	No microspheres, low Br, PFT bd	10/5/94	0.044	0.013	0.079	0.003	0.331
CNAR-381.8	Low microspheres, moderate Br, PFT bd	10/6/94	0.060	0.004	0.083	0.005	0.131
CNAR-384.3	Moderate microspheres, pFT bd	10/6/94	5.466	0.348	19.620	0.598	41.418
CNAR-386.5	High Br, Low microspheres, PFT bd	10/6/94	7.353	0.588	25.520	0.446	49.338
CNAR-387.5	Low microspheres, PFT bd	10/6/94	8.747	0.290	21.137	0.258	32.773
CNAR-390.9	No microspheres, high Br	10/7/94	0.070	0.016	16.752	0.383	47.991
CNAR-397.1	moderate microspheres, high Br	10/7/94	1.174	0.184	23.904	0.654	52.041

General Distribution Sample Number	Why	Date Collected	PNL/Fredrickson, Acetate Mineralization aerobic, ave. cum. % of added (n=3)				
			d 1, ave.	sd	d 3, ave.	sd	d 7, ave
CNAR-405.5	Br low, PFT bd	10/9/94	0.028	0.001	0.054	0.002	0.418
CNAR-409.8	Microspheres present, Br low, PFTs bd	10/9/94	0.028	0.000	0.062	0.004	0.328
CNAR-417.4	Br, PFT below detect	10/9/94	0.026	0.004	2.825	4.497	33.331
CNAR-425.0	Br, PFT below detect	10/10/94	0.242	0.044	0.410	0.024	13.145
CNAR-426.5	Br low, no microspheres, PFT bd	10/10/94	6.637	0.868	27.940	0.310	50.376
CNAR-436.7	Br low, microspheres low, PFTs bd	10/11/94	4.140	0.309	24.558	0.584	44.628
CNAR-451.2	high Br, high PFT, loss of mud to formation	10/12/94	7.162	0.592	21.557	0.935	30.021
*CNAR-457.2***		10/14/94					
CNAR-457.3	moderate Br, (no microspheres, no PFT)	10/14/94	5.397	0.343	18.522	0.174	34.526
CNAR-464.2	moderate Br, low PFT, no microspheres used,	10/14/94	1.161	0.269	17.532	0.421	33.825
CNAR-472.6	Low microspheres, moderate Br	10/15/94	0.187	0.003	4.230	0.055	31.227
CNAR-472.6**		10/15/94					
CNAR-475.3	high PFT, high microspheres, high Br	10/15/94	0.180	0.011	3.578	2.717	12.785
*CNAR-482.1***		10/18/94					
CNAR-482.9	high microspheres, low Br	10/18/94	8.665	0.205	21.944	0.461	33.223
CNAR-503.9	Br below background, microspheres low	10/19/94	0.113	0.006	0.232	0.007	0.327
CNAR-507.3	Microspheres moderate, Br low	10/19/94	5.506	1.216	16.028	1.695	25.060
CNV-R			d 1, ave.	sd	d 3/4, ave.	sd	d 7, ave
CNVR-188.0		10/27/94	0.080	0.003	0.177	0.002	0.352
CNVR-189.2		11/1/94	0.185	0.018	0.286	0.025	14.912
Hetero.-192.1		11/5/94					
CNVR-196.9	no microspheres, moderate Br	11/5/94	0.162	0.004	0.274	0.003	0.457
CNVR-206.7	no microspheres, low Br, PFT bd	11/9/94	0.203	0.027	0.342	0.023	0.475
CNVR-209.6	PFT below detect, low microspheres, Br low	11/9/94	0.231	0.006	0.358	0.007	0.662
CNVR-221.7	no microspheres, Br below detect, PFT bd	11/10/94	0.283	0.070	18.332	0.805	47.266
*CNVR-226.5***		11/10/94					
CNVR-227.8	no microspheres, Br below detect, PFT low	11/11/94	0.142	0.016	0.221	0.020	0.318
CNVR-231.5	high microspheres, Br, PFT moderate	11/11/94	6.180	0.021	17.839	0.358	27.036

General		Acetate Mineralization								
Distribution		anaerobic, ave. cum. % of added (n=3)						log(cfu/gs)		35SO4 red.
Sample Number	sd	d 1/2.2, ave.	sd	d 3/5, ave.	sd	d 7/8, ave.	sd	marine agar	salty PTYG	dpm*/14 d
CNV										
CNV-60.5	0.066							NG	NG	bd
CNV-127.3	0.419	0.246	0.022	0.576	0.422	15.160	25.515	3.22	3.43	bd
CNV-140.3	8.419	0.274	0.008	0.346	0.014	0.727	0.072	NG	NG	bd
CNV-149.2	20.818	0.246	0.037	0.307	0.047	0.344	0.051	NG	NG	bd
CNVC-164.2	26.114	0.312	0.052	0.553	0.277	1.200	0.937	NG	NG	bd
CNV-165.8	24.228	0.431	0.045	0.607	0.068	0.659	0.078	NG	NG	bd
CNV-170.4	27.246	0.318	0.111	0.483	0.198	0.906	0.855	NG	2.8 (nv)	bd
CNV-178.9	0.071	0.507	0.076	0.671	0.082	0.723	0.088	NG	NG	bd
CNV-183.9	0.055	0.068	0.004	0.094	0.007	0.139	0.050	NG	NG	bd
CNV-185.7	0.174	0.072	0.002	0.105	0.013	0.123	0.009	NG	NG	bd
CNV-187.1	18.300	0.069	0.001	10.467	17.960	16.886	29.043	1.5 (nv)	NG	bd
CNV-188.5	0.106	0.069	0.009	0.123	0.028	0.140	0.030	NG	NG	953
Hetero.-189.7										
Hetero.-191.3										
CNV-193.1	1.129	12.572	2.392	39.556	5.207	47.711	4.392	3.52	3.42	bd
CNV-196.3	3.824	0.222	0.005	0.304	0.004	0.681	0.604	3.58	3.53	bd
CNV-198.1	22.311	0.213	0.119	0.296	0.128	0.364	0.168	NG	NG	bd
CNV-200.3	0.020	0.284	0.007	0.370	0.019	0.417	0.021	NG	NG	bd
CNV-201.0	0.076	1.366	2.352	11.403	19.653	14.638	25.182	NG	NG	1152
CNV-201.6	0.069	0.025	0.002	0.169	0.013	0.229	0.020	3.7 (nv)	3.8 (nv)	
CNV-202.5	0.156	0.028	0.018	0.189	0.026	0.236	0.017	2.2 (nv)	1.5 (nv)	bd
CNV-203.3	0.039	0.019	0.001	0.159	0.014	0.223	0.017	NG	NG	bd
CNV-204.0	0.074	0.034	0.006	0.174	0.093	0.235	0.116	NG	NG	bd
CNA-R	sd	d 2/5, ave.	sd	d 7/8, ave.	sd			log(cfu/gs)		
CNAR-160.5*								marine agar	salty PTYG	
CNAR-91.8	0.005	0.026	0.001	0.042	0.004			NG	NG	
CNAR-93.5	0.440							6.32	6.45	
CNAR-200.0	0.007	0.025	0.003	0.049	0.003			NG	NG	670
CNAR-227.6	10.637	0.515	0.051	0.658	0.052			NG	NG	bd
CNAR-239.9	0.007	0.260	0.032	0.345	0.029			NG	NG	bd
CNAR-251.6	7.850	45.536	3.543	58.378	3.845			3.01	3.04	308
CNAR-259.9	0.698	12.678	10.340	49.323	3.826			NG	2.00	bd
CNAR-260.5	27.823	2.940	3.966	15.360	25.059			NG	NG	bd
CNAR-299.0	20.324	0.153	0.007	0.496	0.012			NG	NG	bd
CNAR-310.8	1.608	0.182	0.096	0.403	0.232			6.03	6.50	bd
CNAR-315.4	0.081	0.230	0.010	0.507	0.019			NG	NG	205
CNAR-319.7	22.807	0.282	0.084	2.352	2.548			NG	NG	bd
CNAR-329.2	23.484	3.021	3.539	30.415	22.480			1.8 (nv)	NG	bd
CNAR-333.7	10.843	22.579	0.868	48.566	2.004			3.79	3.40	2109
CNAR-344.2	0.282	22.630	0.901	48.493	5.479			3.24	3.26	330
CNAR-350.3	0.013	0.541	0.257	6.277	4.930			NG	NG	240
CNAR-355.4	1.171	46.141	1.339	59.125	0.655			2.5 (nv)	2.3 (nv)	bd
CNAR-361.1	1.212	47.783	1.911	58.148	5.283			2.7 (nv)	3.0 (nv)	184
CNAR-371.1	0.214	0.597	0.002	0.765	0.010			NG	NG	bd
CNAR-375.3	0.364	0.553	0.060	0.831	0.221			1.5 (nv)	NG	129
CNAR-378.4	0.254	0.590	0.031	0.869	0.193			NG	NG	bd
CNAR-381.8	0.011	0.608	0.061	1.026	0.253			NG	NG	bd
CNAR-384.3	0.187	42.049	0.052	54.520	2.921			3.90	3.86	3566123
CNAR-386.5	0.179	42.034	3.909	52.288	6.039			5.52	5.47	35125
CNAR-387.5	0.236							nd	5.93	
CNAR-390.9	0.312	29.172	3.993	40.480	3.707			2.5 (nv)	2.4 (nv)	bd
CNAR-397.1	0.199	39.386	0.728	48.373	1.702			2.92	3.09	bd

General		Acetate Mineralization								
Distribution		anaerobic, ave. cum. % of added (n=3)						log(cfu/gs)		35SO4 red.
Sample Number	sd	d 1/2.2, ave.	sd	d 3/5, ave.	sd	d 7/8, ave.	sd	marine agar	salty PTYG	dpm*/14 d
CNAR-405.5	0.275	0.502	0.005	1.615	1.484			NG	NG	11782
CNAR-409.8	0.326	8.682	14.174	15.796	23.647			3.77	3.65	10571
CNAR-417.4	13.544	13.308	14.018	38.960	3.238			4.18	4.04	17207
CNAR-425.0	9.302	0.148	0.002	25.153	21.538			4.00	4.12	bd
CNAR-426.5	0.853	11.362	5.006	39.525	1.025			4.16	4.15	592226
CNAR-436.7	1.252	0.794	0.413	41.850	2.413			4.03	3.78	673887
CNAR-451.2	1.267	0.016	0.006	0.035	0.006			6.17	6.10	1269684
*CNAR-457.2***										
CNAR-457.3	0.820	32.555	9.464	45.559	10.012			4.93	5.01	95360
CNAR-464.2	0.784	30.172	12.146	50.572	4.155			3.29	3.04	15843
CNAR-472.6	1.582	0.573	0.011	17.425	23.210			4.41	4.91	bd
CNAR-472.6**										
CNAR-475.3	2.406	12.896	19.008	47.246	5.909			4.58	4.55	3050
*CNAR-482.1***										
CNAR-482.9	2.648	35.201	8.479	48.496	9.256			4.29	4.41	232399
CNAR-503.9	0.130	0.483	0.022	0.604	0.025			NG	NG	bd
CNAR-507.3	0.728	36.187	1.593	49.529	1.787			2.6 (nv)	2.6 (nv)	24445
CNV-R	sd	d 2/3, ave.	sd	d 7/8, ave.	sd	d 15, ave.	sd	marine agar	salty PTYG	
CNVR-188.0	0.014	0.251	0.015	0.428	0.024			NG	NG	19940
CNVR-189.2	10.774	7.231	12.129	16.568	27.797			NG	NG	
Hetero.-192.1										
CNVR-196.9	0.005	0.217	0.003	0.518	0.012			NG	NG	4772
CNVR-206.7	0.018			0.086	0.010			NG	NG	7738
CNVR-209.6	0.328			0.092	0.005			NG	NG	7123
CNVR-221.7	1.581	34.258	4.529			55.163	1.337	NG	NG	8132
*CNVR-226.5***										
CNVR-227.8	0.020	0.219	0.010			0.314	0.014	NG	NG	141455
CNVR-231.5	1.426	31.057	16.373			51.574	3.761	6.00	6.00	879765

General	PNL anaerobes-Stevens/Wagnon, *number of cells per gram sample								
Distribution	denitrifiers		DIRB/hetero.		DIRB/litho.		SRB/hetero.		SRB/litho.
Sample Number	turbidity	acet blk	turbidity	Fe(III) red.	turbidity	Fe(III) red.	turbidity	sulfide	turbidity
CNV									
CNV-60.5	0	0	0		0		0		0
CNV-127.3	1	0	10000		1		0		0
CNV-140.3	0	0	1000		10		0		0
CNV-149.2	0	0	10000		10		0		0
CNVC-164.2	0	0	10		10		0		0
CNV-165.8	0	0	10		10		0		1
CNV-170.4	0	0	10		10		0		0
CNV-178.9	1	0	10		0		0		0
CNV-183.9	10	0	10		10		0		0
CNV-185.7	1	0	10		0		0		0
CNV-187.1	1	0	1		0		0		0
CNV-188.5	1	0	0		0		0		0
Hetero.-189.7									
Hetero.-191.3									
CNV-193.1	-	-	-		-		-		-
CNV-196.3	1	1	0		10		0		0
CNV-198.1	-	-	-		-		-		-
CNV-200.3	1	0	10		10		1		0
CNV-201.0	1	0	10		10		1		0
CNV-201.6	1	1	10		10		1		0
CNV-202.5	0	0	1		10		1		10
CNV-203.3	0	0	10		10		0		0
CNV-204.0	1	0	1		10		0		0
CNA-R									
CNAR-160.5*									
CNAR-91.8							0		
CNAR-93.5									
CNAR-200.0									
CNAR-227.6									
CNAR-239.9									
CNAR-251.6	10	10	1		0		0		0
CNAR-259.9	0	10	100		10		0		0
CNAR-260.5	1	0	10000		0		1		0
CNAR-299.0	0	0	10000	10000	10000	10000	0		1
CNAR-310.8	1	0	10		0		1		1
CNAR-315.4	100	10000	10000		0		1		100
CNAR-319.7	0	1	10000		0		0		1
CNAR-329.2	0	0	10000		0		0		1000
CNAR-333.7	0	1	10000		0		10		10000
CNAR-344.2	1	1	10000		0		0		10000
CNAR-350.3	0	1	10000		0		0		10000
CNAR-355.4	0	1	10000		0		0		1
CNAR-361.1	0	0	10000		1		0		1000
CNAR-371.1	0	10	10000		1		0		1000
CNAR-375.3	1	1	10000		1		0		1
CNAR-378.4	1	1	10		10		0		1
CNAR-381.8	0	0	1000		10		0		10
CNAR-384.3	1000	1000	100	100	0		100		1
CNAR-386.5	10000	10000	10000	10000	0		100		0
CNAR-387.5									
CNAR-390.9	10	10000	100		0		100		0
CNAR-397.1	0	0	10		0		0		0

General	PNL anaerobes-Stevens/Wagnon, *number of cells per gram sample								
Distribution	denitrifiers		DIRB/hetero.		DIRB/litho.		SRB/hetero.		SRB/litho.
Sample Number	turbidity	acet blk	turbidity	Fe(III) red.	turbidity	Fe(III) red.	turbidity	sulfide	turbidity
CNAR-405.5	0	1	10		0		0		0
CNAR-409.8	0	1	0		1		0		0
CNAR-417.4	1	1	0		0		0		0
CNAR-425.0	1	1000	10		10		0		0
CNAR-426.5	10	10	100		0		10		0
CNAR-436.7	10	1	10		1		100		0
CNAR-451.2	1000	1000	100	10	1		1000		1
*CNAR-457.2***	see below								
CNAR-457.3	1	10	10		0		0		0
CNAR-464.2	1000	1000	100	10	0		1000		0
CNAR-472.6	0	10	10		10		0		1
CNAR-472.6**	0	10	1		0		0		1
CNAR-475.3	100	100	10		10		1		1
*CNAR-482.1***	see below								
CNAR-482.9									
CNAR-503.9	0	1	1		0		0		0
CNAR-507.3	10	10	10		0		0		0
CNV-R									
CNVR-188.0									
CNVR-189.2	1	0	10000		0		0		0
Hetero.-192.1									
CNVR-196.9	10000	0	1000	1000	1000		0		0
CNVR-206.7	0	0	1		0		0		0
CNVR-209.6	1	0	0		0		0		1
CNVR-221.7	1	0	0		0		0		0
*CNVR-226.5***									
CNVR-227.8	10	0	0		0		0		0
CNVR-231.5	10000	10000	10000	10000	0		10000		0
							0		
	0	0	0		0		0		1
	100	100	10		0		100		10

Activity Assays:

denitrification:acetylene block assay

Fe(III) reduction: production of excess Fe(II)

SO4-reduction:production of excess acid volatile sulfide

Methanogenesis:production of methane in headspace

Acetogenesis:production of acetate and or butyrate

FB Flame=exterior flamed & enriched for fermenter's turbi

General							
Distribution		CO2 reducers		Fermenters			
Sample Number	sulfide	turbidity	methane	turbidity	methane	FB Flame	Marine Broth
CNV							
CNV-60.5		0	10	0	1		10
CNV-127.3		0	10	0	bd		0
CNV-140.3		0	1	0	bd		1
CNV-149.2		0	1	0	bd		0
CNVC-164.2		0	1	0	bd		0
CNV-165.8		0	1	0	bd		0
CNV-170.4		0	1	0	bd		0
CNV-178.9		1	1	0	bd		10
CNV-183.9		0	1	0	bd		0
CNV-185.7		0	1	0	bd		0
CNV-187.1		0	1	0	1		0
CNV-188.5		0		0			0
Hetero.-189.7							
Hetero.-191.3							
CNV-193.1		-	ns	-	1	0	-
CNV-196.3		1	bd	0	bd	0	0
CNV-198.1		-		-			-
CNV-200.3		1	bd	1	bd	0	1
CNV-201.0		0	bd	0	bd		1000
CNV-201.6		0	1	1	bd	0	1
CNV-202.5		1	bd	1	bd		0
CNV-203.3		0	1	0	bd	0	10
CNV-204.0		0	bd	0	bd		0
CNA-R							
CNAR-160.5*							
CNAR-91.8							0
CNAR-93.5							
CNAR-200.0							
CNAR-227.6							
CNAR-239.9							
CNAR-251.6		0	bd	0	bd		0
CNAR-259.9		0	bd	0	bd		0
CNAR-260.5		0	bd	0	bd		0
CNAR-299.0		10	1	0	bd		0
CNAR-310.8		0	1	0	bd		0
CNAR-315.4		0	1	0	bd		0
CNAR-319.7		1	1	100	bd		0
CNAR-329.2		0	1	0	bd		0
CNAR-333.7		0	1	0	bd		0
CNAR-344.2		0	1	0	bd		0
CNAR-350.3		1	1	0	bd		0
CNAR-355.4		10	1	10	bd		0
CNAR-361.1		100	bd	10	bd		0
CNAR-371.1		100	1	10	bd		0
CNAR-375.3		10000	1	10	bd		10000
CNAR-378.4		10000	1	10	bd		1
CNAR-381.8		10000	1	0	bd		100
CNAR-384.3		0	1	1000	1		100
CNAR-386.5		10000	1	10000	bd		0
CNAR-387.5							
CNAR-390.9		0	1	1000	1		0
CNAR-397.1		0	1	1	bd		0

General							
Distribution		CO2 reducers		Fermenters			
Sample Number	sulfide	turbidity	methane	turbidity	methane	FB Flame	Marine Broth
CNAR-405.5		1000	1	0	bd		0
CNAR-409.8		0	1	0	bd		0
CNAR-417.4		0	1	0	bd		0
CNAR-425.0		0	1	0	bd		0
CNAR-426.5		0	1	100	bd		0
CNAR-436.7		1	1	0	bd		0
CNAR-451.2		1	bd	100	bd		100
*CNAR-457.2***							
CNAR-457.3		0	100	10	bd		0
CNAR-464.2		0	1	100	bd		1000
CNAR-472.6		0	100	0	bd		0
CNAR-472.6**		0	1	0	bd		
CNAR-475.3		0	1	0	bd		0
*CNAR-482.1***							
CNAR-482.9							
CNAR-503.9		0	bd	0	bd		0
CNAR-507.3		0	bd	0	bd		0
CNV-R							
CNVR-188.0							
CNVR-189.2		0	1	10	bd		0
Hetero.-192.1							
CNVR-196.9		0	1	1	bd		0
CNVR-206.7		0	1	0	bd		0
CNVR-209.6		0	1	0	bd		0
CNVR-221.7		0	1	0	bd		0
*CNVR-226.5***							
CNVR-227.8		0	1	0	bd		0
CNVR-231.5		0	1	10000	1		10000
							0
		0	1	1	1		
		0	1	10	bd		

IC=intact core,
INT=interface
SS=sandstone, 1ss/2ss=1cm/2cm into the sandstone part of the intact core
B=basalt; 1B= 1 cm into the basalt section of the intact core
P=pyrite
SO=sample of opportunity

General	PLFA (pmole/g) from White/Ringelberg					Percent Composition (mol%)				
Distribution	total	prok.	euk.	prok/	DGFA/	NSat	TerBrSat	MidBrSat	BrMono	Mono
Sample Number				euk	PLFA					
CNV										
CNV-60.5	2.46	1.75	0.71	2.47	0.42	77.80	3.59	-	-	16.87
CNV-127.3	5.81	4.16	1.65	2.52	0.43	85.07	8.11	2.45	-	3.16
CNV-140.3	4.41	2.89	1.52	1.91	0.55	78.11	9.47	2.04	2.75	7.13
CNV-149.2	7.97	3.84	4.13	0.93	0.50	86.27	4.05	-	-	1.88
CNVC-164.2	3.13	2.38	0.75	3.17	0.33	90.90	-	2.57	-	3.51
CNV-165.8	4.66	3.33	1.33	2.51	0.26	85.72	3.44	1.83	-	6.72
CNV-170.4	3.18	2.29	0.89	2.59	0.58	88.35	3.97	1.72	-	5.97
CNV-178.9	38.15	31.91	6.24	5.11	0.05	91.24	1.82	0.50	-	1.36
CNV-183.9	7.52	5.61	1.91	2.94	0.23	83.70	10.10	3.77	-	2.43
CNV-185.7	1.59	1.09	0.51	2.15	1.66	87.66	6.50	-	-	5.84
CNV-187.1	1.28	0.89	0.39	2.30	2.74	87.53	4.17	3.60	-	4.70
CNV-188.5	2.59	1.23	1.36	0.90	1.26	93.76	1.71	-	-	4.54
Hetero.-189.7										
Hetero.-191.3										
CNV-193.1	1.81	1.23	0.58	2.11	0.40	76.42	10.15	-	-	10.64
CNV-196.3	2.53	1.51	1.01	1.49	0.61	80.08	13.47	-	-	6.45
CNV-198.1	1.34	1.01	0.33	3.07	1.21	100.00	-	-	-	-
CNV-200.3	5.33	3.92	1.41	2.79	0.34	63.71	12.31	-	-	23.98
CNV-201.0	2.83	1.81	1.03	1.76	1.22	76.05	16.62	-	-	7.33
CNV-201.6	1.66	1.32	0.34	3.89	2.07	72.12	-	-	-	27.88
CNV-202.5	1.81	1.46	0.35	4.14	1.22	93.13	1.68	-	-	4.65
CNV-203.3	1.84	1.49	0.35	4.31	1.40	80.75	6.51	2.89	-	9.84
CNV-204.0	4.05	2.57	1.48	1.74	0.45	78.64	14.04	-	-	7.32
CNA-R										
CNAR-160.5*										
CNAR-91.8	22.31	19.56	2.76	7.10		46.27	17.06	-	-	36.67
CNAR-93.5	36.83	35.69	1.14	31.30		22.19	57.90	-	3.69	16.18
CNAR-200.0	10.63	8.26	2.37	3.49		69.66	18.95	-	6.40	4.99
CNAR-227.6										
CNAR-239.9	6.77	6.21	0.56	11.14		66.53	13.61	-	5.90	13.96
CNAR-251.6	0.84	0.54	0.30	1.82		100.00	-	-	-	-
CNAR-259.9	0.40	0.40	-	-		100.00	-	-	-	-
CNAR-260.5	2.91	2.43	0.48	5.08		93.15	6.85	-	-	-
CNAR-299.0										
CNAR-310.8	0.62	0.40	0.22	1.78		100.00	-	-	-	-
CNAR-315.4	3.73	1.83	1.90	0.97		85.57	14.43	-	-	-
CNAR-319.7										
CNAR-329.2	7.35	3.89	3.46	1.12		88.98	8.38	-	-	2.64
CNAR-333.7	1.92	1.22	0.70	1.73		81.19	8.24	3.65		6.92
CNAR-344.2										
CNAR-350.3	1.69	1.17	0.52	2.26		100.00	-	-	-	-
CNAR-355.4										
CNAR-361.1	1.35	0.69	0.66	1.05		91.66	8.34	0.00		0.00
CNAR-371.1										
CNAR-375.3										
CNAR-378.4	0.40	0.40	0.00	0.00		100.00	0.00	0.00		0.00
CNAR-381.8	1.76	1.10	0.66	1.67		89.61	0.00	0.00		10.39
CNAR-384.3										
CNAR-386.5	0.48	0.32	0.16	1.99		100.00	0.00	0.00		0.00
CNAR-387.5	0.52	0.24	0.28	0.85		96.33	2.36	0.00		1.31
CNAR-390.9										
CNAR-397.1										

General	PLFA (pmole/g) from White/Ringelberg					Percent Composition (mol%)				
Distribution	total	prok.	euk.	prok/	DGFA/	NSat	TerBrSat	MidBrSat	BrMono	Mono
Sample Number				euk	PLFA					
CNAR-405.5										
CNAR-409.8										
CNAR-417.4										
CNAR-425.0										
CNAR-426.5										
CNAR-436.7										
CNAR-451.2	5.48	2.10	3.38	0.62		58.52	4.30	0.54	-	32.68
*CNAR-457.2***										
CNAR-457.3	0.03	0.03	0.00	0.00		100.00	0.00	0.00		0.00
CNAR-464.2	8.20	5.26	2.93	1.80		100.00	-	-	-	-
CNAR-472.6	6.43	3.42	3.01	1.14		100.00	-	-	-	-
CNAR-472.6**	0.08	0.03	0.05	0.60		100.00	-	-	-	-
CNAR-475.3	0.03	0.02	0.01	1.34		100.00	-	-	-	-
*CNAR-482.1***										
CNAR-482.9	0.07	0.07	0.00	0.00		100.00	0.00	0.00		0.00
CNAR-503.9	0.14	0.07	0.07	0.89		100.00	-	-	-	-
CNAR-507.3	0.00	0.00	0.00	0.00		0.00	0.00	0.00		0.00
CNV-R										
CNVR-188.0										
CNVR-189.2	0.11	0.06	0.05	1.23		100.00	-	-	-	-
Hetero.-192.1										
CNVR-196.9										
CNVR-206.7	1.63	1.48	0.17	6.61		91.64	8.36	0.00		0.00
CNVR-209.6										
CNVR-221.7	2.15	1.23	0.92	1.34		74.10	25.90	-	-	-
*CNVR-226.5***										
CNVR-227.8										
CNVR-231.5	0.15	0.11	0.04	2.80		100.00	0.00	0.00		0.00
	0.39	0.27	0.12	1.42		90.08	0.15	-	-	0.68
	0.30	0.27	0.13	1.54		30.00	0.50	-	-	2.25
	847	728	120	6.08	0.01	13.60	24.46	30.43	7.18	24.33
	311	256	55	4.70	0.01	13.97	19.02	38.22	6.14	22.65
	3073	2575	498	5.18	0.00	14.55	18.82	23.72	8.49	34.42
	Key:									
	total=total pmol PLFA/gram					NSat=normal saturates				
	euk.=eukaryotic PLFA/gram					TerBrSat=terminally branched saturates				
	prok=prokaryotic PLFA/gram					MidBrSat=mid-chain branched saturates				
						BrMono=branched monounsaturates				
						Mono=monounsaturates				
	0.00	0.00	0.00	0.00		0	0.00	0.00		0.00
	0.06	0.02	0.04	0.45		100.00	0.00	0.00		0.00

General	Balkwill-counts on dilution plates				Balkwill-"sprinkle" plates				No. of colony types		
Distribution	log CFU/g	log CFU/g	log CFU/g	log CFU/g	no. colony types on 2 plates				seen on dilution plat		
Sample Number	HM	LM	HF	LF	HM	LM	HF	LF	HM	LM	HF
CNV											
CNV-60.5											
CNV-127.3	ng	ng	2.2 (nv)	ng	ng	ng	ng	ng	0	0	5
CNV-140.3	ng	ng	ng	ng	ng	ng	ng	ng	0	0	0
CNV-149.2	ng	ng	1.8 (NV)	ng	ng	ng	ng	ng	0	0	2
CNVC-164.2	ng	ng	ng	ng	ng	ng	ng	ng	0	0	0
CNV-165.8	ng	ng	ng	1.8(nv)	ng	ng	ng	ng	0	0	0
CNV-170.4	ng	ng	ng	ng	ng	ng	ng	ng	0	0	0
CNV-178.9	ng	1.5 (NV)	ng	ng	ng	ng	ng	ng	0	1	0
CNV-183.9	ng	ng	ng	1.5(nv)	ng	ng	ng	ng	0	0	0
CNV-185.7	ng	ng	ng	ng	ng	ng	ng	ng	0	0	0
CNV-187.1	ng	ng	1.8 (NV)	ng	ng	ng	ng	ng	0	0	2
CNV-188.5	ng	ng	1.8 (NV)	ng	ng	ng	ng	ng	0	0	2
Hetero.-189.7											
Hetero.-191.3											
CNV-193.1	ng	ng	ng	ng	8	6	3	6	0	0	0
CNV-196.3	ng	ng	1.8 (NV)	ng	ng	ng	ng	ng	0	0	2
CNV-198.1	ng	ng	1.8 (NV)	1.5(nv)	ng	ng	ng	ng	0	0	2
CNV-200.3	ng	ng	ng	ng	ng	ng	ng	1	0	0	0
CNV-201.0	ng	ng	1.5 (nv)	ng	ng	ng	1	ng	0	0	0
CNV-201.6											
CNV-202.5	ng	ng	1.5 (nv)	ng	ng	ng	ng	ng	0	0	1
CNV-203.3	ng	1.5 (nv)	1.5 (nv)	ng	1	ng	ng	ng	0	1	1
CNV-204.0	ng	ng	ng	ng	ng	ng	ng	ng	0	0	0
CNA-R											
CNAR-160.5*	ng	ng	ng	ng	ng	ng	ng	ng	0	0	0
CNAR-91.8	ng	ng	1.5 (nv)	ng	ng	ng	ng	ng	0	0	1
CNAR-93.5	spiked sample										
CNAR-200.0	ng	ng	ng	ng	ng	ng	ng	ng	0	0	0
CNAR-227.6	ng	ng	ng	1.5 (nv)	ng	1	ng	ng	0	0	0
CNAR-239.9	ng	ng	ng	ng	ng	1	ng	ng	0	0	0
CNAR-251.6	1.5(nv)	ng	2.8 (ap)	2.6 (ap)	n/a	n/a	n/a	n/a	1	0	8
CNAR-259.9	ng	ng	ng	ng	ng	ng	1	ng	0	0	0
CNAR-260.5	ng	ng	ng	1.8(nv)	ng	ng	1	ng	0	0	0
CNAR-299.0	ng	ng	ng	ng	ng	ng	ng	ng	0	0	0
CNAR-310.8	ng	ng	ng	ng	ng	ng	ng	ng	0	0	0
CNAR-315.4	ng	ng	ng	ng	ng	ng	ng	ng	0	0	0
CNAR-319.7	ng	ng	1.5 (nv)	ng	ng	ng	ng	ng	0	0	1
CNAR-329.2	ng	ng	ng	ng	ng	ng	ng	ng	0	0	0
CNAR-333.7	ng	ng	2.6 (ap)	ng	n/a	n/a	n/a	n/a	0	0	3
CNAR-344.2	ng	ng	ng	ng	ng	1	2	ng	0	0	0
CNAR-350.3	ng	ng	ng	ng	ng	ng	ng	ng	0	0	0
CNAR-355.4	1.5(nv)	ng	2.4 (ap)	2.1 (ap)	n/a	1	n/a	n/a	1	0	2
CNAR-361.1	ng	1.5 (nv)	ng	1.5 (nv)	ng	ng	1	ng	0	1	0
CNAR-371.1	ng	1.5 (nv)	1.8 (nv)	ng	1	ng	ng	ng	0	1	1
CNAR-375.3	ng	ng	ng	ng	1	ng	1	ng	0	0	0
CNAR-378.4	1.5 (nv)	ng	ng	1.5 (nv)	ng	ng	1	ng	1	0	0
CNAR-381.8	1.5 (nv)	ng	ng	ng	1	ng	ng	ng	1	0	0
CNAR-384.3											
CNAR-386.5	1.5 (nv)	1.5 (nv)	3.7	2.6 (ap)	n/a	n/a	n/a	n/a	1	1	13
CNAR-387.5											
CNAR-390.9	ng	ng	ng	ng	1	ng	1	ng	0	0	0
CNAR-397.1	ng	ng	ng	ng	ng	ng	ng	ng	0	0	0

General	Balkwill-counts on dilution plates				Balkwill-"sprinkle" plates				No. of colony types		
Distribution	log CFU/g	log CFU/g	log CFU/g	log CFU/g	no. colony types on 2 plates				seen on dilution plat		
Sample Number	HM	LM	HF	LF	HM	LM	HF	LF	HM	LM	HF
CNAR-405.5	ng	ng	ng	ng	ng	ng	ng	ng	0	0	0
CNAR-409.8	ng	ng	ng	ng	ng	1	1	ng	0	0	0
CNAR-417.4	1.5 (nv)	ng	1.5 (nv)	ng	ng	ng	ng	ng	1	0	1
CNAR-425.0	ng	1.5 (nv)	2.0 (ap)	ng	0	0	7	6	0	1	3
CNAR-426.5	2.1 (ap)	2.1 (ap)	3	2.9 (ap)	n/a	n/a	n/a	n/a	2	5	5
CNAR-436.7	ng	ng	2.0 (ap)	2.3 (ap)	ng	2	3	1	0	0	3
CNAR-451.2	2.2 (ap)	2.0 (ap)	4.2	3.8	n/a	n/a	n/a	n/a	6	2	20
*CNAR-457.2***											
CNAR-457.3	ng	ng	2.1 (nv)	1.5 (nv)	1	1	6	1	0	0	2
CNAR-464.2	2.2 (nv)	1.8 (nv)	3.9	3.2	n/a	n/a	n/a	n/a	4	3	9
CNAR-472.6	ng	ng	ng	ng	1	0	2	0	0	0	0
CNAR-472.6**											
CNAR-475.3	ng	ng	ng	ng	1	ng	1	ng	0	0	0
*CNAR-482.1***											
CNAR-482.9	3.2	3.2	4.6	4.3	n/a	n/a	n/a	n/a	4	2	8
CNAR-503.9	ng	ng	ng	ng	ng	ng	ng	1	0	0	0
CNAR-507.3	1.5 (nv)	ng	2.5 (ap)	2.0 (nv)	1	0	2	0	1	0	2
CNV-R											
CNVR-188.0	ng	ng	1.8 (nv)	ng	0	0	1	0	0	0	2
CNVR-189.2	ng	ng	ng	ng	ng	ng	ng	ng	0	0	0
Hetero.-192.1											
CNVR-196.9	ng	ng	ng	ng	ng	ng	ng	ng	0	0	0
CNVR-206.7	ng	ng	ng	ng	ng	ng	ng	ng	0	0	0
CNVR-209.6	ng	ng	ng	ng	ng	ng	ng	ng	0	0	0
CNVR-221.7	ng	ng	ng	ng	ng	ng	ng	ng	0	0	0
*CNVR-226.5***											
CNVR-227.8	ng	ng	ng	ng	ng	ng	ng	ng	0	0	0
CNVR-231.5	3.5	3.4	4.2	4.5	n/a	n/a	n/a	n/a	9	8	12
	6.5	6.5	6.4	6	n/a	n/a	n/a	n/a	28	33	26

LF=low-carbon freshwater medium

ng= no growth on any of the plates

(nv)= not a valid count due to no real dilution pattern, it is <2 or "below detect"

(ap)= Approximate count. Had reasonable dilution pattern but colony numbers on plates were too low to get a statistically good count.

n/a= sprinkle plates were not analyzed because ther was sufficient growth on dilution plates

s=isolates indicated are considered suspicious, because no valid dilution pattern or the isolates came from dilution plates when no colonies were seen on the sprinkle plates for the same sample

General		Isolates from dilution plates				Isolates from sprinkle plates			
Distribution	es	No. of types (total no. of isolates)				No. of types (total no. of isolates)			
Sample Number	LF	HM	LM	HF	LF	HM	LM	HF	LF
CNV									
CNV-60.5									
CNV-127.3	0	0 (0)	0 (0)	2 (2) s	0 (0)	0 (0)	0 (0)	0 (0)	0 (0)
CNV-140.3	0	0 (0)	0 (0)	0 (0)	0 (0)	0 (0)	0 (0)	0 (0)	0 (0)
CNV-149.2	0	0 (0)	0 (0)	1 (1) s	0 (0)	0 (0)	0 (0)	0 (0)	0 (0)
CNVC-164.2	0	0 (0)	0 (0)	0 (0)	0 (0)	0 (0)	0 (0)	0 (0)	0 (0)
CNV-165.8	2	0 (0)	0 (0)	0 (0)	2 (2) s	0 (0)	0 (0)	0 (0)	0 (0)
CNV-170.4	0	0 (0)	0 (0)	0 (0)	0 (0)	0 (0)	0 (0)	0 (0)	0 (0)
CNV-178.9	0	0 (0)	1 (1) s	0 (0)	0 (0)	0 (0)	0 (0)	0 (0)	0 (0)
CNV-183.9	1	0 (0)	0 (0)	1 (1) s	0 (0)	0 (0)	0 (0)	0 (0)	0 (0)
CNV-185.7	0	0 (0)	0 (0)	0 (0)	0 (0)	0 (0)	0 (0)	0 (0)	0 (0)
CNV-187.1	0	0 (0)	0 (0)	2 (2) s	0 (0)	0 (0)	0 (0)	0 (0)	0 (0)
CNV-188.5	0	0 (0)	0 (0)	1 (1) s	0 (0)	0 (0)	0 (0)	0 (0)	0 (0)
Hetero.-189.7									
Hetero.-191.3									
CNV-193.1	0	0 (0)	0 (0)	0 (0)	0 (0)	7 (9)	6 (7)	3 (4)	6 (6)
CNV-196.3	0	0 (0)	0 (0)	2 (2) s	0 (0)	0 (0)	0 (0)	0 (0)	0 (0)
CNV-198.1	1	0 (0)	0 (0)	1 (1) s	1 (1) s	0 (0)	0 (0)	0 (0)	0 (0)
CNV-200.3	0	0 (0)	0 (0)	0 (0)	0 (0)	0 (0)	0 (0)	0 (0)	0 (0)
CNV-201.0	0	0 (0)	0 (0)	1 (1) s	0 (0)	0 (0)	0 (0)	0 (0)	0 (0)
CNV-201.6									
CNV-202.5	0	0 (0)	0 (0)	1 (1) s	0 (0)	0 (0)	0 (0)	1 (1) s	0 (0)
CNV-203.3	0	0 (0)	1 (1) s	1 (1) s	0 (0)	1 (1) s	0 (0)	0 (0)	0 (0)
CNV-204.0	0	0 (0)	0 (0)	0 (0)	0 (0)	0 (0)	0 (0)	0 (0)	0 (0)
CNA-R									
CNAR-160.5*	0	0 (0)	0 (0)	0 (0)	0 (0)	0 (0)	0 (0)	0 (0)	0 (0)
CNAR-91.8	0	0 (0)	0 (0)	1 (1) s	0 (0)	0 (0)	0 (0)	0 (0)	0 (0)
CNAR-93.5									
CNAR-200.0	0	0 (0)	0 (0)	0 (0)	0 (0)	0 (0)	0 (0)	0 (0)	0 (0)
CNAR-227.6	1	0 (0)	0 (0)	0 (0)	1 (1)	0 (0)	1 (11)	0 (0)	0 (0)
CNAR-239.9	0	0 (0)	0 (0)	0 (0)	0 (0)	0 (0)	1 (1)	0 (0)	0 (0)
CNAR-251.6	4	1 (2)	0 (0)	8 (17)	3 (14)	n/a	n/a	n/a	n/a
CNAR-259.9	0	0 (0)	0 (0)	0 (0)	0 (0)	0 (0)	0 (0)	1 (1)	0 (0)
CNAR-260.5	1	0 (0)	0 (0)	0 (0)	1 (1)	0 (0)	0 (0)	1 (1)	0 (0)
CNAR-299.0	0	0 (0)	0 (0)	0 (0)	0 (0)	0 (0)	0 (0)	0 (0)	0 (0)
CNAR-310.8	0	0 (0)	0 (0)	0 (0)	0 (0)	0 (0)	0 (0)	0 (0)	0 (0)
CNAR-315.4	0	0 (0)	0 (0)	0 (0)	0 (0)	0 (0)	0 (0)	0 (0)	0 (0)
CNAR-319.7	0	0 (0)	0 (0)	1 (1) s	0 (0)	0 (0)	0 (0)	0 (0)	0 (0)
CNAR-329.2	0	0 (0)	0 (0)	0 (0)	0 (0)	0 (0)	0 (0)	0 (0)	0 (0)
CNAR-333.7	0	0 (0)	0 (0)	3 (7)	0 (0)	n/a	n/a	n/a	n/a
CNAR-344.2	0	0 (0)	0 (0)	0 (0)	0 (0)	0 (0)	1 (1)	2 (2)	0 (0)
CNAR-350.3	0	0 (0)	0 (0)	0 (0)	0 (0)	0 (0)	0 (0)	0 (0)	0 (0)
CNAR-355.4	1	1 (1)	0 (0)	2 (7)	1 (4)	n/a	1 (1)	n/a	n/a
CNAR-361.1	1	0 (0)	1 (1)	0 (0)	1 (1)	0 (0)	0 (0)	1 (2)	0 (0)
CNAR-371.1	0	0 (0)	1 (1) s	1 (2) s	0 (0)	1 (1) s	0 (0)	0 (0)	0 (0)
CNAR-375.3	0	0 (0)	0 (0)	0 (0)	0 (0)	1 (1) s	0 (0)	1 (1) s	0 (0)
CNAR-378.4	1	1 (1) s	0 (0)	0 (0)	1 (1) s	0 (0)	0 (0)	1 (1) s	0 (0)
CNAR-381.8	0	1 (1) s	0 (0)	0 (0)	0 (0)	1 (1) s	0 (0)	0 (0)	0 (0)
CNAR-384.3									
CNAR-386.5	1	1 (1)	1 (1)	10 (59)	1 (11)	n/a	n/a	n/a	n/a
CNAR-387.5									
CNAR-390.9	0	0 (0)	0 (0)	0 (0)	0 (0)	0 (0)	0 (0)	0 (0)	0 (0)
CNAR-397.1	0	0 (0)	0 (0)	0 (0)	0 (0)	0 (0)	0 (0)	0 (0)	0 (0)

General		Isolates from dilution plates				Isolates from sprinkle plates			
Distribution	es	No. of types (total no. of isolates)				No. of types (total no. of isolates)			
Sample Number	LF	HM	LM	HF	LF	HM	LM	HF	LF
CNAR-405.5	0	0 (0)	0 (0)	0 (0)	0 (0)	0 (0)	0 (0)	0 (0)	0 (0)
CNAR-409.8	0	0 (0)	0 (0)	0 (0)	0 (0)	0 (0)	1 (1) s	1 (1) s	0 (0)
CNAR-417.4	0	1 (1) s	0 (0)	1 (1) s	0 (0)	0 (0)	0 (0)	0 (0)	0 (0)
CNAR-425.0	0	0 (0)	1 (1)	3 (3)	0 (0)	0 (0)	0 (0)	7 (10)	6 (8)
CNAR-426.5	1	2 (4)	4 (5)	5 (19)	1 (11)	0 (0)	0 (0)	0 (0)	0 (0)
CNAR-436.7	4	0 (0)	0 (0)	3 (4)	4 (7)	0 (0)	1 (1)	3 (7)	1 (7)
CNAR-451.2	8	6 (6)	1 (2)	20 (76)	7 (44)	n/a	n/a	n/a	n/a
*CNAR-457.2***									
CNAR-457.3	1	0 (0)	0 (0)	2 (6)	1 (1)	1 (1)	1 (1)	6 (10)	1 (2)
CNAR-464.2	5	4 (6)	2 (2)	9 (74)	5 (25)	n/a	n/a	n/a	n/a
CNAR-472.6	0	0 (0)	0 (0)	0 (0)	0 (0)	1 (1)	0 (0)	2 (2)	0 (0)
CNAR-472.6**									
CNAR-475.3	0	0 (0)	0 (0)	0 (0)	0 (0)	0 (0)	0 (0)	0 (0)	0 (0)
*CNAR-482.1***									
CNAR-482.9	3	4 (23)	1 (21)	8 (57)	3 (34)	n/a	n/a	n/a	n/a
CNAR-503.9	0	0 (0)	0 (0)	0 (0)	0 (0)	0 (0)	0 (0)	0 (0)	1 (1)
CNAR-507.3	1	1 (1)	0 (0)	2 (3)	1 (3)	1 (1)	0 (0)	2 (2)	0 (0)
CNV-R									
CNVR-188.0	0	0 (0)	0 (0)	2 (3) s	0 (0)	0 (0)	0 (0)	1(1) s	0 (0)
CNVR-189.2	0	0 (0)	0 (0)	0 (0)	0 (0)	0 (0)	0 (0)	0 (0)	0 (0)
Hetero.-192.1									
CNVR-196.9	0	0 (0)	0 (0)	0 (0)	0 (0)	0 (0)	0 (0)	0 (0)	0 (0)
CNVR-206.7	0	0 (0)	0 (0)	0 (0)	0 (0)	0 (0)	0 (0)	0 (0)	0 (0)
CNVR-209.6	0	0 (0)	0 (0)	0 (0)	0 (0)	0 (0)	0 (0)	0 (0)	0 (0)
CNVR-221.7	0	0 (0)	0 (0)	0 (0)	0 (0)	0 (0)	0 (0)	0 (0)	0 (0)
*CNVR-226.5***									
CNVR-227.8	0	0 (0)	0 (0)	0 (0)	0 (0)	0 (0)	0 (0)	0 (0)	0 (0)
CNVR-231.5	13	9 (40)	6 (18)	12 (38)	8 (11)	n/a	n/a	n/a	n/a
	23	23 (27)	30 (57)	20 (56)	22 (83)	n/a	n/a	n/a	n/a

General Distribution Sample Number	Conclusions re:validity of isolates	Direct counts/Marc Frischer & Sandra Nierzwicki-Bauer/RPI cells/g total	cells/g active	% active	# of total cells enumerated total	active
CNV						
CNV-60.5		3.27E+06	9.80E+05	30.00	20	6
CNV-127.3	no valid isolates	1.96E+06	3.27E+05	16.70	12	2
CNV-140.3	n/a	1.80E+06	3.27E+05	18.20	11	2
CNV-149.2	no valid isolates	3.27E+06	6.53E+05	20.00	20	4
CNVC-164.2	n/a	2.61E+06	4.90E+05	18.80	16	3
CNV-165.8	no valid isolates	2.94E+06	6.53E+05	22.20	18	4
CNV-170.4	n/a	2.61E+06	3.27E+05	12.50	16	2
CNV-178.9	no valid isolates	2.78E+06	3.27E+05	11.80	17	2
CNV-183.9	no valid isolates	2.45E+06	3.27E+05	13.30	15	2
CNV-185.7	n/a	1.31E+06	3.27E+05	25.00	8	2
CNV-187.1	no valid isolates	1.31E+06	3.27E+05	25.00	8	2
CNV-188.5	no valid isolates	1.96E+06	1.63E+05	8.30	12	1
Hetero.-189.7						
Hetero.-191.3						
CNV-193.1	OK (26 isolates)	7.19E+06	8.17E+05	11.30	44	5
CNV-196.3	no valid isolates	3.10E+06	1.63E+05	5.30	19	1
CNV-198.1	no valid isolates	4.74E+06	ND	NA	29	0
CNV-200.3	n/a	4.90E+06	1.63E+05	3.30	30	1
CNV-201.0	no valid isolates	4.74E+06	3.27E+05	6.90	29	2
CNV-201.6		3.27E+06	ND	NA	20	0
CNV-202.5	no valid isolates	2.21E+06	3.27E+05	15.40	13	2
CNV-203.3	no valid isolates	5.72E+06	1.63E+05	2.90	35	1
CNV-204.0	n/a	1.02E+07	7.08E+05	6.90	63	4
CNA-R						
CNAR-160.5*	n/a					
CNAR-91.8	no valid isolates	2.29E+06	ND	NA	14	0
CNAR-93.5		2.83E+07	5.44E+06	19.20	52	10
CNAR-200.0	n/a	SAMPLE MISSING				
CNAR-227.6	????	4.41E+06	6.53E+05	14.80	27	4
CNAR-239.9	no valid isolates	2.45E+06	8.17E+05	33.30	15	5
CNAR-251.6	OK (33 isolates)	6.37E+06	1.14E+06	17.90	39	7
CNAR-259.9	no valid isolates	5.39E+06	6.53E+05	12.10	33	4
CNAR-260.5	no valid isolates	3.43E+06	4.90E+05	14.30	21	3
CNAR-299.0	n/a	4.90E+06	1.63E+05	3.30	30	1
CNAR-310.8	n/a	8.00E+06	4.90E+05	6.10	49	3
CNAR-315.4	n/a	3.76E+06	1.63E+05	4.30	23	1
CNAR-319.7	no valid isolates	3.59E+06	6.53E+05	18.20	22	4
CNAR-329.2	no valid isolates	5.06E+06	6.53E+05	12.90	31	4
CNAR-333.7	OK (7 isolates)	3.10E+06	3.27E+05	10.50	19	2
CNAR-344.2	??? (3 isolates)	1.80E+06	ND	NA	11	0
CNAR-350.3	n/a	4.41E+06	6.53E+05	14.80	27	4
CNAR-355.4	OK (13 isolates)	3.27E+06	ND	NA	20	0
CNAR-361.1	??? (4 isolates)	4.25E+06	8.17E+05	19.20	26	5
CNAR-371.1	no valid isolates	9.80E+05	1.63E+05	16.70	6	1
CNAR-375.3	no valid isolates	3.67E+06	1.63E+05	4.30	23	1
CNAR-378.4	no valid isolates	4.41E+06	8.17E+05	18.50	27	5
CNAR-381.8	no valid isolates	1.96E+06	1.63E+05	8.30	12	1
CNAR-384.3						
CNAR-386.5	OK (72 isolates)	2.94E+06	1.63E+05	5.60	18	1
CNAR-387.5						
CNAR-390.9	n/a	2.94E+06	3.27E+05	11.10	18	2
CNAR-397.1	n/a	9.80E+05	ND	NA	6	0

General Distribution	SO4-reducing	sulfur-	fermentors	MnO2	Fe(III)	Porosity (%)		Bulk Density
Sample Number	bacteria	reducers		reducers	reducers	Boyle's law	Resaturation	(g/cc)
CNAR-405.5	<0.7	<0.7	2.3	2.3	<0.7			
CNAR-409.8	<0.7	<0.7	>6	<0.7	<0.7			
CNAR-417.4	<0.7	<0.7	<0.7	<0.7	<0.7			
CNAR-425.0	<0.7	<0.7	0.9	<0.7	<0.7			
CNAR-426.5	<0.7	<0.7	>6	2.3	0.9			
CNAR-436.7	<0.7	<0.7	>6	<0.7	<0.7			
CNAR-451.2	>6	>6	>6	>6	>6			
*CNAR-457.2***								
CNAR-457.3	2.3	>6	>6	2.3	0.9			
CNAR-464.2	0.9	2.3	2.3	2.3	2.3			
CNAR-472.6								
CNAR-472.6**								
CNAR-475.3	<0.7	<0.7	>6	>6	<0.7			
*CNAR-482.1***								
CNAR-482.9	2.3	2.3	>6	>6	>6	1.99	1.87	2.67
CNAR-503.9	<0.7	<0.7	<0.7	<0.7	<0.7			
CNAR-507.3	<0.7	<0.7	<0.7	<0.7	<0.7			
CNV-R								
CNVR-188.0	<0.7	<0.7	<0.7	<0.7	<0.7			
CNVR-189.2								
Hetero.-192.1								
CNVR-196.9	<0.7	<0.7	<0.7	<0.7	<0.7	15.28	15.03	2.39
CNVR-206.7	<0.7	<0.7	<0.7	<0.7	<0.7	11.62	11.83	2.48
CNVR-209.6	<0.7	<0.7	<0.7	<0.7	<0.7	11.17	10.96	2.49
CNVR-221.7	<0.7	<0.7	0.9	<0.7	<0.7	17.97	17.37	2.34
*CNVR-226.5***								
CNVR-227.8	<0.7	<0.7	<0.7	<0.7	<0.7	20.29	20.26	2.30
CNVR-231.5	>6	>6	>6	>6	>6			
						12.00	12.16	2.46
						12.28	12.01	2.46

General Distribution	Grain Density	Permeability (mD)		Hydraulic Cond. (cm/s)		Magnetic susceptibility by TC Onstott/Witold
Sample Number	(g/cc)	Kair (mD)	Kliq. (mD)	Kair (cm/s)	Kliq (cm/s)	unit=cgs x 10^-6
CNV						
CNV-60.5	2.69	4.189	0.010	4.05E-06	9.27E-09	
CNV-127.3	2.67	0.049	0.005	4.73E-08	5.02E-09	1.7
CNV-140.3	2.68	0.008	0.004	7.73E-09	3.38E-09	9.46
CNV-149.2						7.96
CNVC-164.2						11.88
CNV-165.8	2.67	0.012	0.004	1.16E-08	3.57E-09	11.66
CNV-170.4	2.67	0.043	0.004	4.15E-08	3.48E-09	5.98
CNV-178.9						14.09
CNV-183.9						11.94
CNV-185.7	2.63	1.980	0.006	1.91E-06	5.51E-09	17.41
CNV-187.1	2.64	153.000	60.200	1.48E-04	5.82E-05	7.96
CNV-188.5						6.47
Hetero.-189.7						
Hetero.-191.3						
CNV-193.1						4.77
CNV-196.3	2.65	0.199	0.004	1.92E-07	3.38E-09	10.37
CNV-198.1	2.66	0.212	0.006	2.05E-07	5.51E-09	11.04
CNV-200.3	2.66	0.201	0.010	1.94E-07	9.27E-09	9.75
CNV-201.0						10.4
CNV-201.6						
CNV-202.5						
CNV-203.3	2.62	0.460	0.012	2.17E-05	1.13E-08	8.9
CNV-204.0	2.66	0.498	0.007	4.81E-07	6.38E-09	8.9
CNA-R						
*CNAR-160.5**						12.1
CNAR-91.8						11.2
CNAR-93.5						12.2
CNAR-200.0						13.9
CNAR-227.6						6.9
CNAR-239.9						3.2
CNAR-251.6						1
CNAR-259.9						2.8
CNAR-260.5						5.5 or 1.7
CNAR-299.0						5
CNAR-310.8						7
CNAR-315.4						7.4
CNAR-319.7						6.7
CNAR-329.2						8.9
CNAR-333.7						2.9
CNAR-344.2						4
CNAR-350.3						5.4
CNAR-355.4						6.5 or 2.8
CNAR-361.1						4.6
CNAR-371.1						7.3
CNAR-375.3						7.3
CNAR-378.4						6.6
CNAR-381.8						6.6
CNAR-384.3						
CNAR-386.5						2
CNAR-387.5						
CNAR-390.9						2
CNAR-397.1						2.4

General Distribution	Grain Density	Permeability (mD)		Hydraulic Cond. (cm/s)		Magnetic susceptibility by TC Onstott/Witold
Sample Number	(g/cc)	Kair (mD)	Kliq. (mD)	Kair (cm/s)	Kliq (cm/s)	unit=cgs x 10^-6
CNAR-405.5						5.7
CNAR-409.8						5.5
CNAR-417.4						5.9
CNAR-425.0						7
CNAR-426.5						6.8
CNAR-436.7						1
CNAR-451.2						
*CNAR-457.2***						
CNAR-457.3						
CNAR-464.2						
CNAR-472.6						
CNAR-472.6**						
CNAR-475.3						
*CNAR-482.1***						
CNAR-482.9	2.70	0.009	0.004	8.69E-09	4.06E-09	
CNAR-503.9						
CNAR-507.3						
CNV-R						
CNVR-188.0						
CNVR-189.2						
Hetero.-192.1						
CNVR-196.9	2.64	0.530	0.021	5.12E-07	2.03E-08	
CNVR-206.7	2.68	0.092	0.007	8.89E-08	6.67E-09	
CNVR-209.6	2.68	0.051	0.005	4.93E-08	4.64E-09	
CNVR-221.7	2.64	2.892	0.163	2.79E-06	1.57E-07	
*CNVR-226.5***						
CNVR-227.8	2.64	21.868	2.546	2.11E-05	2.46E-06	
CNVR-231.5						
	2.66	0.039	0.005	3.77E-08	5.22E-09	
	2.66	0.056	0.008	5.41E-08	7.25E-09	

General Distribution Sample Number	Virtinite reflectance by Phil Long , PNL % reflectance	grain size index by Bruce Bjornstad (normalized resitivity/gamma ray intensity)	Geochemistry from J. McKinley Depth Feet	Depth m	Depth (v) m	TC (C%)	TOC (C%)
CNV							
CNV-60.5		0.067	198.5		60.5	0.90	0.73
CNV-127.3		0.972	417.7		127.3	1.67	0.37
CNV-140.3		0.222	460.3		140.3	2.62	0.68
CNV-149.2	0.825	0.131	489.5		149.2	1.94	0.88
CNVC-164.2		0.649	538.7		164.2	1.16	0.37
CNV-165.8		0.397	544.0		165.8	1.36	0.53
CNV-170.4		0.180	559.1		170.4	1.19	0.20
CNV-178.9		0.206	586.9		178.9	2.11	0.95
CNV-183.9	0.843	0.092	603.3		183.9	2.70	1.47
CNV-185.7	0.852	0.095	609.3		185.7	1.57	0.40
CNV-187.1		0.063	614.0		187.1	0.24	0.21
CNV-188.5		0.612	618.4		188.5	0.29	0.24
Hetero.-189.7		1.758	622.4		189.7		
Hetero.-191.3		0.942	627.6		191.3		
CNV-193.1		0.829	633.5		193.1	0.530	0.17
CNV-196.3		1.235	644.0		196.3	0.660	0.39
CNV-198.1		0.690	649.9		198.1	0.770	0.52
CNV-200.3		0.305	657.2		200.3	0.950	0.48
CNV-201.0		0.447	659.4		201.0	0.890	0.45
CNV-201.6		0.555	661.0		201.6	0.890	0.15
CNV-202.5			N/A			1.930	0.51
CNV-203.3		0.115	667.0		667.0	0.800	0.40
CNV-204.0		0.051	669.3		669.3	0.910	0.40
CNA-R							
CNAR-160.5*			160.5	160.5	80.2		
CNAR-91.8		0.036	301.2	91.8	40.4	0.59	0.46
CNAR-93.5			N/A	93.5	41.4		
CNAR-200.0		0.036	656.2	200	103.2	1.60	1.16
CNAR-227.6		0.128	746.5	227.6	119.2	8.73	3.68
CNAR-239.9		0.066	787.1	239.9	126.3	8.73	0.69
CNAR-251.6		0.974	825.5	251.6	133.1	0.87	0.23
CNAR-259.9	1.404	3.978	852.7	259.9	137.9		
CNAR-260.5		2.865	854.7	260.5	138.2		
CNAR-299.0	1.024	0.534	981.0	299.0	160.6	2.01	0.39
CNAR-310.8		0.187	1019.7	310.8	167.4	2.68	0.72
CNAR-315.4		0.136	1034.8	315.4	170.1	2.67	0.80
CNAR-319.7		0.220	1048.9	319.7	172.6	2.04	0.54
CNAR-329.2		0.199	1080.1	329.2	178.1	2.29	0.78
CNAR-333.7		2.350	1094.8	333.7	180.7	1.02	0.14
CNAR-344.2	0.949	0.627	1129.3	344.2	186.6	1.03	0.28
CNAR-350.3		0.321	1149.3	350.3	190.7	1.85	0.08
CNAR-355.4		0.720	1166.0	355.4	194.1	1.26	0.38
CNAR-361.1		0.408	1185.0	361.1	197.9	1.42	0.33
CNAR-371.1		0.164	1217.5	371.1	204.6	1.91	0.73
CNAR-375.3		0.085	1231.3	375.3	207.4	2.26	1.04
CNAR-378.4		0.070	1241.5	378.4	209.5	2.60	1.32
CNAR-381.8		0.777	1252.6	381.8	211.8	2.64	1.47
CNAR-384.3	1.128	1.358	1261.0	384.3	213.5		
CNAR-386.5		0.942	1268.0	386.5	214.9	0.43	0.11
CNAR-387.5		0.862	1271.0	387.5	215.6		
CNAR-390.9		1.908	1282.5	390.9	217.9	0.61	0.44
CNAR-397.1		0.719	1302.8	397.1	222.0	0.80	0.47

General	Virtinite reflectance	grain size index	Geochemistry from J. McKinley				
Distribution	by Phil Long , PNL	by Bruce Bjornstad (normalized	Depth	Depth	Depth (v)	TC	TOC
Sample Number	% reflectance	resitivity/gamma ray intensity)	Feet	m	m	(C%)	(C%)
CNAR-405.5		0.327	1330.4	405.5	227.7	0.93	0.42
CNAR-409.8		0.309*	1344.5	409.8	230.6	1.21	0.38
CNAR-417.4		0.193	1369.4	417.4	235.6	1.20	0.60
CNAR-425.0		1.084	1394.4	425.0	240.7	1.00	0.99
CNAR-426.5		0.901	1399.3	426.5	241.7	0.21	0.21
CNAR-436.7			1432.7	436.7	248.6	0.35	0.35
CNAR-451.2	1.812		1480.3	451.2	258.3	0.04	0.04
*CNAR-457.2***							
CNAR-457.3	0.901		1500.0	457.3	262.4	0.02	0.01
CNAR-464.2	1.539		1523.0	464.2	267.0	0.02	0.12
CNAR-472.6			1550.5	472.6	272.6	0.03	0.02
CNAR-472.6**							
CNAR-475.3			1559.4	475.3	274.4	0.17	0.07
*CNAR-482.1***	1.833		1581.7	482.1	279.0		
CNAR-482.9	1.998		1584.3	482.9	279.5	0.03	0.01
CNAR-503.9	2.272		1653.2	503.9	293.6	3.71	<0.05
CNAR-507.3			1664.4	507.3	295.9	0.07	0.02
CNV-R							
CNVR-188.0		1.358	616.8		188.0		
CNVR-189.2			N/A		189.2		
Hetero.-192.1			630.2		192.1		
CNVR-196.9		0.415	646.0		196.9	0.730	0.39
CNVR-206.7		0.154	678.1		206.7	1.030	0.51
CNVR-209.6		0.239	687.7		209.6	1.280	0.58
CNVR-221.7	1.036		727.4		221.7	0.290	0.29
*CNVR-226.5***	0.908		743.1		226.5		
CNVR-227.8	0.930		747.4		227.8	0.630	0.62
CNVR-231.5			759.5		231.5	0.019	0.02
		* average of 0.358 & 0.259					
	0.861		surface			1.14	0.48
	0.921		surface			0.72	0.41

General Distribution	CC	Total S	Org+Pyr S	Org S	Sulfate S	Sulf + Pyr S	Sulfide S	Geochemistry from J. F	Cl
Sample Number	(C%)	(S%)	"S, %"	"S,%"	"S, %"	"S, %"	"S, %"	(mg/K)	(mg/K)
CNV									
CNV-60.5	0.170	1.15	0.979	0.051	0.018	0.658	0.001	16.84	22.99
CNV-127.3	1.300	0.31	0.334	0.006	<0.00	0.351	0.001	6.92	31.35
CNV-140.3	1.940	0.72	0.659	0.038	<0.00	0.605	0.001	9.91	28.69
CNV-149.2	1.060	0.61	0.403	0.036	<0.00	0.511	0.001	15.63	20.50
CNVC-164.2	0.790	0.61	0.480	0.025	<0.00	0.535	0.001	7.05	21.14
CNV-165.8	0.830	0.56	0.370	0.028	0.011	0.591	0	8.22	17.18
CNV-170.4	0.990	0.23	0.318	0.003	0.017	0.346	0.001	5.43	23.27
CNV-178.9	1.160	0.91	0.876	0.041	0.007	0.847	0.001	10.90	20.29
CNV-183.9	1.230	1.17	1.032	0.061	0.005	0.894	0.001	12.29	9.63
CNV-185.7	1.170	0.70	0.687	0.021	<0.00	0.685	0.001	6.27	15.52
CNV-187.1	0.030	0.51	0.442	0.008	<0.00	0.534	0.001	3.64	14.36
CNV-188.5	0.050	0.39	0.387	0.008	0.055	0.264	0.001	5.17	12.88
Hetero.-189.7									
Hetero.-191.3									
CNV-193.1	0.36	0.30	0.252	0.004	0.030	0.357	0.001	3.65	10.62
CNV-196.3	0.27	0.54	0.347	0.005	0.017	0.409	0.001	6.11	10.71
CNV-198.1	0.25	0.64	0.597	0.03	0.012	0.657	0.001	6.78	10.66
CNV-200.3	0.47	0.40	0.311	0.02	<0.00	0.429	0.001	10.34	17.55
CNV-201.0	0.44	0.35	0.312	0.005	<0.00	0.410	0.001	14.68	14.93
CNV-201.6	0.74	0.24	0.177	0.005	<0.00	0.303	0.002	15.68	1.25
CNV-202.5	1.42	0.51	0.384	0.014	0.038	0.435	0.001	8.12	31.62
CNV-203.3	0.4	0.32	0.323	0.007	0.012	0.226	0.001	8.93	13.64
CNV-204.0	0.51	0.37	0.334	0.007	0.011	0.446	0	8.48	12.27
CNA-R									
*CNAR-160.5**									
CNAR-91.8	0.130	0.47	0.432	0.007	0.017	0.439	0.001	17.23	31.26
CNAR-93.5									
CNAR-200.0	0.440	0.71	0.299	0.033	0.013	0.672	0.001	26.04	14.45
CNAR-227.6	5.050	1.18	1.138	0.108	0.030	1.115	0.002	26.06	14.11
CNAR-239.9	8.040	0.01	0.806	0.066	0.022	0.977	0.001	15.28	6.70
CNAR-251.6	0.640	0.37	0.281	0.01	0.007	0.323	0	6.42	23.77
CNAR-259.9									
CNAR-260.5									
CNAR-299.0	1.620	0.39	0.318	0.01	0.022	0.285	0.001	7.84	30.95
CNAR-310.8	1.960	0.78	0.702	0.037	0.015	0.614	0.001	11.32	21.45
CNAR-315.4	1.870	0.70	0.431	0.034	0.002	0.571	0.001	11.69	24.58
CNAR-319.7	1.500	0.83	0.693	0.035	0.024	0.887	0.001	11.36	18.42
CNAR-329.2	1.510	0.63	0.562	0.031	0.019	0.569	0.001	13.05	26.61
CNAR-333.7	0.880	0.21	0.192	0.005	0.024	0.243	0.001	3.70	12.60
CNAR-344.2	0.750	0.38	0.337	0.011	0.036	0.496	0.001	5.62	21.58
CNAR-350.3	1.770	<0.01	0.146	0.002	0.025	0.216	0.001	7.44	21.48
CNAR-355.4	0.880	0.47	0.369	0.014	0.030	0.443	0.001	3.60	15.95
CNAR-361.1	1.090	0.43	0.389	0.035	0.022	0.404	0.001	5.02	22.60
CNAR-371.1	1.180	0.97	0.934	0.034	0.017	0.788	0.001	10.39	19.82
CNAR-375.3	1.220	1.18	0.965	0.035	0.014	1.007	0.001	11.80	11.42
CNAR-378.4	1.280	1.05	0.963	0.059	0.017	0.880	0.001	13.51	18.80
CNAR-381.8	1.170	1.22	1.227	0.059	0.019	1.529	0.001	13.28	7.16
CNAR-384.3									
CNAR-386.5	0.320	0.30	0.294	0.005	0.009	0.405	0.004	2.84	14.61
CNAR-387.5									
CNAR-390.9	0.170	0.50	0.435	0.014	0.019	0.446	0	5.46	9.55
CNAR-397.1	0.330	0.50	0.515	0.015	0.014	0.447	0.001	62.56	105.15

General								Geochemistry from J. I	
Distribution	CC	Total S	Org+Pyr S	Org S	Sulfate S	Sulf + Pyr S	Sulfide S	F	Cl
Sample Number	(C%)	(S%)	"S, %"	"S,%"	"S, %"	"S, %"	"S, %"	(mg/K)	(mg/K)
CNAR-405.5	0.510	0.31	0.327	0.007	0.095	0.437	0.001	11.75	12.71
CNAR-409.8	0.830	0.43	0.429	0.01	0.032	0.422	0.001	7.84	11.50
CNAR-417.4	0.600	0.61	0.568	0.031	0.028	0.589	0.001	9.44	14.87
CNAR-425.0	0.011	1.50	1.325	0.06	0.017	1.375	0	10.30	5.24
CNAR-426.5	<0.005	0.27	0.272	0.004	0.010	0.353	0	4.52	6.29
CNAR-436.7	<0.005	0.27	0.272	0.007	0.010	0.016	0	4.07	7.27
CNAR-451.2	<0.005	0.02	0.005	0.004	0.021	0.080	0	0.96	12.36
*CNAR-457.2***									
CNAR-457.3	0.010	0.03	0.018	0.002	0.046	0.124	0	6.89	8.89
CNAR-464.2	0.009	0.10	0.045	0.002	0.019	0.138	0	4.03	9.51
CNAR-472.6	0.110	0.09	0.098	0.002	0.006	0.125	0	5.62	4.61
CNAR-472.6**									
CNAR-475.3	0.100	0.19	0.171	0.001	0.015	0.212	0	15.33	1.89
*CNAR-482.1***									
CNAR-482.9	0.017	<0.01	0.020	0.001	0.007	0.042	0	4.23	10.90
CNAR-503.9	3.710	<0.01	0.003	0	0.014	0.007	0	4.70	3.21
CNAR-507.3	0.050	<0.01	0.012	0.001	0.009	0.071	0	8.25	8.54
CNV-R									
CNVR-188.0									
CNVR-189.2									
Hetero.-192.1									
CNVR-196.9	0.34	0.58	0.514	0.019	0.015	0.182	0.001	5.25	10.42
CNVR-206.7	0.52	0.61	0.590	0.014	0.005	0.446	0.001	9.97	12.89
CNVR-209.6	0.7	0.57	0.497	0.025	<0.005	0.464	0.001	9.91	14.70
CNVR-221.7	0	0.26	0.269	0.006	<0.005	0.315	0.001	3.45	8.47
*CNVR-226.5***									
CNVR-227.8	0.014	0.97	0.926	0.034	<0.005	0.607	0.001	8.40	4.59
CNVR-231.5	0.005	0.04	0.018	0	<0.005	0.196	0	5.46	10.76
	0.660	0.15	0.012	0.0	0.058	0.164	0.0	7.39	2.51
	0.310	<0.01	0.001	0.0	0.008	0.006	0.0	6.14	10.47

General	McKinley							NH2OH-HCl extraction	
Distribution	NO2	Br	NO3	PO4	SO4	Ox	moisture	Fe3+	Fe2+
Sample Number	(mg/K)	(mg/K)	(mg/K)	(mg/K)	(mg/K)	(mg/K)	(g/g)	(mg/Kg)	(mg/Kg)
CNV									
CNV-60.5	0.00	0.00	0.42	0.21	690.52	5.55	0.1031	296.05	8343.05
CNV-127.3	0.00	0.26	0.45	0.00	225.75	1.57	0.0837	175.65	4983.07
CNV-140.3	0.00	0.13	0.39	0.00	268.28	2.59	0.0664	167.06	4452.79
CNV-149.2	0.00	0.21	0.31	0.00	258.20	3.64	0.0864	156.55	4011.50
CNVC-164.2	0.00	0.18	0.26	0.00	285.24	1.29	0.0791	155.99	4360.96
CNV-165.8	0.00	0.00	0.32	0.00	895.28	1.32	0.0776	155.65	4473.28
CNV-170.4	0.00	0.30	0.27	0.00	1037.16	0.62	0.1007	140.15	4158.02
CNV-178.9	0.00	0.00	0.33	0.00	337.37	2.34	0.0660	166.05	4578.90
CNV-183.9	0.08	0.00	0.27	0.00	411.39	3.18	0.0862	138.58	3864.98
CNV-185.7	0.00	0.00	0.37	0.00	301.42	0.88	0.0804	157.03	4098.81
CNV-187.1	0.00	0.07	0.29	0.00	246.03	0.88	0.1085	158.25	4101.13
CNV-188.5	0.00	0.00	0.50	0.00	1735.53	0.00	0.0888	181.39	4515.35
Hetero.-189.7								-	
Hetero.-191.3								-	
CNV-193.1	0.00	0.00	0.26	0.00	908.83	0.00	0.0827	145.03	3745.31
CNV-196.3	0.00	0.00	0.23	0.00	1266.36	0.00	0.0617	104.16	3652.14
CNV-198.1	0.00	0.00	0.34	0.00	712.95	1.07	0.0725	119.17	4024.97
CNV-200.3	0.00	0.08	0.33	0.00	246.74	2.93	0.0904	128.53	4352.66
CNV-201.0	0.00	0.00	0.39	0.00	273.99	3.47	0.1167	91.10	2908.61
CNV-201.6	0.20	0.11	0.43	0.00	134.15	2.36	0.0803	54.27	1562.02
CNV-202.5	0.00	1.14	0.24	0.00	1586.25	0.84	0.0831	111.04	4243.02
CNV-203.3	0.00	0.00	0.38	0.00	499.92	0.84	0.0816	92.65	3389.60
CNV-204.0	0.00	0.00	0.30	0.00	926.57	1.56	0.0805	113.33	3960.09
CNA-R									
CNAR-160.5*									
CNAR-91.8	0.00	0.00	0.49	0.64	319.66	4.77	0.0686	254.53	6099.50
CNAR-93.5									
CNAR-200.0	0.00	0.00	0.36	0.43	301.17	7.23	0.1018	314.31	8741.09
CNAR-227.6	0.51	1.01	0.22	0.00	433.15	2.11	0.0554	64.51	1556.37
CNAR-239.9	0.00	29.10	0.28	0.00	265.89	2.01	0.0356	67.09	1535.19
CNAR-251.6	0.00	6.51	0.26	0.00	209.23	1.16	0.1024	153.26	2635.58
CNAR-259.9							0.0479		
CNAR-260.5							0.0608		
CNAR-299.0	0.00	0.22	0.32	0.00	385.85	1.40	0.0525	182.22	4391.60
CNAR-310.8	0.00	0.13	0.25	0.00	266.24	2.24	0.0452	137.88	2912.43
CNAR-315.4	0.00	0.13	0.46	0.00	329.60	2.48	0.0486	183.05	5170.50
CNAR-319.7	0.00	0.10	0.29	0.00	247.58	2.35	0.0414	134.88	2693.74
CNAR-329.2	0.12	0.16	0.30	0.00	385.03	2.21	0.0468	155.80	2937.18
CNAR-333.7	0.00	0.11	0.35	0.00	695.35	0.40	0.0968	159.50	2637.39
CNAR-344.2	0.00	0.13	0.36	0.00	737.87	0.71	0.0872	160.68	2942.66
CNAR-350.3	0.00	0.00	0.38	0.00	686.00	1.08	0.0582	169.63	4799.54
CNAR-355.4	0.00	0.00	0.18	0.00	447.86	0.50	0.0400	129.50	2362.84
CNAR-361.1	0.00	0.17	0.28	0.00	439.06	0.77	0.0537	140.17	2426.35
CNAR-371.1	0.00	0.09	0.31	0.00	302.12	2.11	0.0406	159.81	4172.93
CNAR-375.3	0.00	0.00	0.29	0.00	301.15	2.78	0.0520	146.88	3535.61
CNAR-378.4	0.00	0.11	0.25	0.00	390.36	2.69	0.0536	137.20	3801.28
CNAR-381.8	0.00	0.26	0.40	0.00	455.30	2.64	0.0576	148.59	4311.46
CNAR-384.3									
CNAR-386.5	0.00	1.28	0.30	0.00	241.32	0.38	0.0838	177.67	4712.38
CNAR-387.5									
CNAR-390.9	0.00	1.57	0.32	0.00	175.76	1.14	0.0569	105.41	2418.59
CNAR-397.1	0.00	8.31	2.52	0.00	2143.50	11.87	0.0621	116.81	2605.20

General	McKinley							NH2OH-HCl extraction	
Distribution	NO2	Br	NO3	PO4	SO4	Ox	moisture	Fe3+	Fe2+
Sample Number	(mg/K)	(mg/K)	(mg/K)	(mg/K)	(mg/K)	(mg/K)	(g/g)	(mg/Kg)	(mg/Kg)
CNAR-405.5	0.00	0.12	0.36	0.00	188.22	2.81	0.0665	111.92	2547.42
CNAR-409.8	0.00	0.11	0.48	0.00	197.20	1.42	0.0540	138.61	3614.98
CNAR-417.4	0.00	0.00	0.32	0.00	290.16	1.70	0.0532	145.71	3982.85
CNAR-425.0	0.30	0.00	0.44	0.00	612.70	1.11	0.0820	130.66	4032.42
CNAR-426.5	0.00	0.11	0.25	0.35	176.82	0.73	0.1275	132.72	3100.26
CNAR-436.7	0.00	0.08	0.27	0.00	199.71	0.73	0.0859	117.89	2759.00
CNAR-451.2	0.00	7.35	0.33	0.36	65.83	0.72	0.0737	106.41	2149.38
*CNAR-457.2***									
CNAR-457.3	0.37	0.19	0.38	0.57	76.99	0.20	0.1100	93.95	1861.58
CNAR-464.2	0.21	0.24	0.30	0.00	87.18	0.00	0.1189	99.47	1861.60
CNAR-472.6	0.30	0.59	0.00	0.00	70.58	0.78	0.0602	172.00	2469.00
CNAR-472.6**									
CNAR-475.3	0.19	1.02	0.32	0.25	122.52	1.10	0.1012	61.54	1286.64
*CNAR-482.1***									
CNAR-482.9	0.00	0.09	0.33	0.68	98.65	0.42	0.0872	97.97	2478.30
CNAR-503.9	0.11	0.10	0.35	0.00	48.09	1.06	0.0307	84.67	1998.02
CNAR-507.3	0.11	0.00	0.51	0.34	37.08	0.98	0.0677	175.46	3136.32
CNV-R									
CNVR-188.0									
CNVR-189.2									
Hetero.-192.1									
CNVR-196.9	0.00	0.48	0.27	0.00	230.94	1.03	0.0644	118.48	3685.95
CNVR-206.7	0.00	0.07	0.21	0.00	232.22	1.90	0.0545	91.56	2864.50
CNVR-209.6	0.00	0.08	0.30	0.00	248.02	2.69	0.0524	107.91	3763.92
CNVR-221.7	0.00	0.00	0.25	0.00	188.87	0.78	0.1051	98.25	2828.39
*CNVR-226.5***									
CNVR-227.8	0.00	0.00	0.30	0.00	289.35	1.77	0.0652	108.08	3367.18
CNVR-231.5	0.18	0.24	1.31	41.25	0.65	0.65	0.1312	103.29	3061.76
	0.00	0.00	3.79	0.00	2553.28	0.00	0.1713	128.41	2998.11
	0.23	0.16	4.59	0.00	371.12	1.72	0.1203	308.32	2952.74
							0.0550 ±		
				(± = estimated moisture determination)					

General Distribution	0.5 M HCl extraction		
Sample Number	Fe3+ (mg/Kg)	Fe2+ (mg/Kg)	Soil pH
CNV			
CNV-60.5	1073.61	2704.60	8.56
CNV-127.3	671.76	3240.68	8.21
CNV-140.3	610.43	2202.46	8.29
CNV-149.2	571.60	1723.46	8.41
CNVC-164.2	601.56	2309.07	8.18
CNV-165.8	700.90	1892.96	8.09
CNV-170.4	657.21	2410.58	8.26
CNV-178.9	645.76	2104.78	8.25
CNV-183.9	570.33	1544.92	8.20
CNV-185.7	498.56	2979.34	8.09
CNV-187.1	455.20	3291.21	7.53
CNV-188.5	582.64	3409.46	7.42
Hetero.-189.7			
Hetero.-191.3			
CNV-193.1	535.14	3013.75	8.05
CNV-196.3	690.63	2237.50	7.81
CNV-198.1	600.49	2579.49	7.92
CNV-200.3	664.92	2121.97	8.43
CNV-201.0	426.36	1400.97	8.84
CNV-201.6	154.67	1009.91	8.71
CNV-202.5	805.70	2280.97	8.14
CNV-203.3	513.42	1846.85	8.35
CNV-204.0	699.58	1987.72	8.13
CNA-R			
*CNAR-160.5**			
CNAR-91.8	844.59	1992.58	8.66
CNAR-93.5			
CNAR-200.0	820.30	2510.93	8.75
CNAR-227.6	516.16	2111.83	8.39
CNAR-239.9	343.31	1934.71	8.38
CNAR-251.6	515.91	2092.39	8.29
CNAR-259.9			
CNAR-260.5			
CNAR-299.0	653.35	2410.90	8.28
CNAR-310.8	445.58	1594.38	8.42
CNAR-315.4	626.92	2396.91	8.33
CNAR-319.7	440.09	1628.72	8.45
CNAR-329.2	557.58	1779.98	8.29
CNAR-333.7	675.14	2245.87	8.19
CNAR-344.2	674.83	2207.18	8.17
CNAR-350.3	726.67	2540.08	8.18
CNAR-355.4	598.72	2170.32	
CNAR-361.1	581.98	1583.79	8.15
CNAR-371.1	601.01	2080.85	8.31
CNAR-375.3	456.30	1499.36	8.42
CNAR-378.4	524.81	1653.55	8.27
CNAR-381.8	558.81	1709.47	8.25
CNAR-384.3			
CNAR-386.5	477.31	3723.16	8.15
CNAR-387.5			
CNAR-390.9	442.12	1127.32	7.97
CNAR-397.1	380.26	1348.59	8.03

General	0.5 M HCl extraction		
Distribution	Fe3+	Fe2+	
Sample Number	(mg/Kg)	(mg/Kg)	Soil pH
CNAR-405.5	386.24	1062.82	8.68
CNAR-409.8	536.24	1605.79	8.27
CNAR-417.4	578.98	1297.57	8.26
CNAR-425.0	492.98	1435.70	7.99
CNAR-426.5	460.39	1751.86	7.70
CNAR-436.7	439.92	1697.05	7.84
CNAR-451.2	325.56	1541.70	7.43
*CNAR-457.2***			
CNAR-457.3	371.48	1384.05	8.45
CNAR-464.2	418.72	1480.14	8.00
CNAR-472.6	569.19	1187.58	8.39
CNAR-472.6**			
CNAR-475.3	461.74	652.96	8.89
*CNAR-482.1***			
CNAR-482.9	396.53	1963.73	8.22
CNAR-503.9	632.50	1697.54	8.49
CNAR-507.3	627.34	1928.91	8.53
CNV-R			
CNVR-188.0			
CNVR-189.2			
Hetero.-192.1			
CNVR-196.9	505.64	2882.59	8.05
CNVR-206.7	423.38	1339.44	8.47
CNVR-209.6	637.32	1731.04	8.35
CNVR-221.7	420.70	2254.73	7.41
*CNVR-226.5***			
CNVR-227.8	470.94	1631.60	8.64
CNVR-231.5	433.52	2090.08	8.01
	1018.33	887.16	7.59
	1011.45	1159.22	7.84

Appendix 3: Geophysical and Geological Borehole Logs

Geophysical Borehole Log Performed on CNVR, by Schlumberger Well Services

COMPANY:BATTELLE - PNL
WELL: CNV-R
FIELD: CERRA NEGRO
COUNTY:CIBOLA
STATE: NEW MEXICO
DATE LOGGED: 16-NOV-1994
SERVICE COMPANY: ,,SCHLUMBERGER WELL SERVICES
DEPTH LOGGER: 767
BOTTOM HOLE TEMPERATURE: 79
BIT SIZE:-999.25
MUD SAMPLE TEMP:80
NEUTRON LOG MATRIX:LIME
START DEPTH: 70
STOP DEPTH: 738
SAMPLING RATE: 0.5

SUMMARY

	k	n
Mancos	0.0013	10.67
2 Wells	0.1167	8.57
Wt. Water	0.0054	4.61
Paguate	0.0937	8.88
Clay Mesa	0.0248	4.75
Cubero	0.1675	11.79
Oak Can.	0.098	11.08

Permeability is a function of porosity and irreducible water saturation derived from the logging tools. It is a relative measurement that was then calibrated to absolute laboratory measurements. Density porosity is equal to matrix density minus the bulk density, divided by the matrix density minus the formation density.

Depth (ft)	Depth (m)	Gamma Ray	Caliper	Perm. (mD)
70.0	21.34	90.836	10.088	0.000001
70.5	21.49	92.807	10.153	0.000001
71.0	21.64	92.748	10.201	0.000001
71.5	21.79	93.605	10.203	0.000001
72.0	21.95	93.497	10.203	0.000001
72.5	22.10	98.492	10.204	0.000001
73.0	22.25	98.716	10.204	0.000001
73.5	22.40	100.677	10.203	0.000001
74.0	22.56	94.997	10.203	0.0003
74.5	22.71	96.095	10.197	0.000001
75.0	22.86	93.098	10.181	0.000001
75.5	23.01	92.672	10.163	0.000001
76.0	23.16	90.184	10.161	0.000001
76.5	23.32	89.468	10.16	0.000001
77.0	23.47	90.91	10.161	0.0002
77.5	23.62	95.193	10.173	0.000001
78.0	23.77	97.79	10.193	0.000001
78.5	23.93	94.319	10.205	0.000001
79.0	24.08	90.262	10.226	0.000001
79.5	24.23	89.839	10.239	0.000001
80.0	24.38	92.016	10.244	0.000001
80.5	24.54	96.88	10.298	0.000001
81.0	24.69	95.336	10.327	0.000001
81.5	24.84	95.264	10.356	0.000001
82.0	24.99	94.365	10.389	0.000001
82.5	25.15	95.421	10.399	0.000001
83.0	25.30	96.866	10.4	0.000001
83.5	25.45	97.734	10.402	0.000001
84.0	25.60	99.787	10.402	0.000001
84.5	25.76	100.995	10.403	0.000001
85.0	25.91	99.439	10.455	0.000001
85.5	26.06	98.927	10.509	0.000001
86.0	26.21	98.508	10.536	0.000001
86.5	26.37	100.261	10.547	0.000001
87.0	26.52	100.687	10.541	0.000001

Depth (ft)	Depth (m)	Gamma Ray	Caliper	Perm. (mD)
87.5	26.67	101.234	10.525	0.000001
88.0	26.82	98.479	10.492	0.000001
88.5	26.97	101.043	10.449	0.000001
89.0	27.13	100.33	10.395	0.000001
89.5	27.28	101.952	10.395	0.000001
90.0	27.43	98.041	10.397	0.000001
90.5	27.58	101.386	10.413	0.000001
91.0	27.74	104.991	10.413	0.000001
91.5	27.89	108.714	10.417	0.000001
92.0	28.04	107.352	10.438	0.000001
92.5	28.19	107.544	10.45	0.000001
93.0	28.35	108.805	10.449	0.000001
93.5	28.50	107.896	10.449	0.000001
94.0	28.65	105.991	10.45	0.000001
94.5	28.80	102.757	10.45	0.000001
95.0	28.96	103.188	10.451	0.000001
95.5	29.11	103.517	10.451	0.000001
96.0	29.26	104.094	10.449	0.000001
96.5	29.41	105.644	10.449	0.000001
97.0	29.57	104.962	10.451	0.000001
97.5	29.72	105.987	10.411	0.000001
98.0	29.87	104.424	10.359	0.000001
98.5	30.02	103.661	10.288	0.000001
99.0	30.18	103.288	10.251	0.000001
99.5	30.33	101.212	10.246	0.000001
100.0	30.48	104.295	10.254	0.000001
100.5	30.63	105.814	10.258	0.000001
101.0	30.78	107.404	10.255	0.000001
101.5	30.94	108.646	10.242	0.000001
102.0	31.09	108.29	10.207	0.000001
102.5	31.24	110.519	10.205	0.000001
103.0	31.39	111.497	10.204	0.000001
103.5	31.55	110.892	10.196	0.000001
104.0	31.70	111.197	10.152	0.000001
104.5	31.85	107.807	10.114	0.000001

Depth (ft)	Depth (m)	Gamma Ray	Caliper	Permeability (mD)
105.0	32.00	107.172	10.071	0.000001
105.5	32.16	108.005	10.025	0.000001
106.0	32.31	108.984	9.987	0.000001
106.5	32.46	109.987	9.963	0.000001
107.0	32.61	108.354	9.953	0.000001
107.5	32.77	109.225	9.937	0.000001
108.0	32.92	110.001	9.912	0.000001
108.5	33.07	112.234	9.881	0.000001
109.0	33.22	113.947	9.772	0.000001
109.5	33.38	114.712	9.738	0.000001
110.0	33.53	112.636	9.75	0.000001
110.5	33.68	110.54	9.751	0.000001
111.0	33.83	108.126	9.753	0.000001
111.5	33.99	110.744	9.751	0.000001
112.0	34.14	111.072	9.848	0.000001
112.5	34.29	111.032	9.901	0.000001
113.0	34.44	112.654	9.915	0.000001
113.5	34.59	113.31	9.916	0.000001
114.0	34.75	116.124	9.945	0.000001
114.5	34.90	114.667	9.942	0.000001
115.0	35.05	114.173	9.954	0.000001
115.5	35.20	113.232	9.956	0.000001
116.0	35.36	115.171	9.957	0.000001
116.5	35.51	122.679	9.958	0.000001
117.0	35.66	126.261	9.957	0.000001
117.5	35.81	124.358	9.946	0.000001
118.0	35.97	115.752	9.903	0.000001
118.5	36.12	109.605	9.914	0.000001
119.0	36.27	104.648	9.91	0.000001
119.5	36.42	103.016	9.909	0.000001
120.0	36.58	101.536	9.914	0.000001
120.5	36.73	100.542	9.914	0.000001
121.0	36.88	99.072	9.877	0.000001
121.5	37.03	100.452	9.851	0.000001
122.0	37.19	105.389	9.773	0.000001
122.5	37.34	111.163	9.512	0.000001
123.0	37.49	114.384	9.644	0.000001
123.5	37.64	112.508	9.779	0.000001
124.0	37.80	109.695	9.781	0.000001
124.5	37.95	109.342	9.778	0.000001
125.0	38.10	111.403	9.787	0.000001
125.5	38.25	111.962	9.858	0.000001
126.0	38.40	113.224	9.855	0.000001
126.5	38.56	113.531	9.836	0.000001
127.0	38.71	116.141	9.834	0.000001
127.5	38.86	115.048	9.808	0.000001
128.0	39.01	113.521	9.844	0.000001
128.5	39.17	112.211	9.914	0.000001
129.0	39.32	113.035	9.896	0.000001
129.5	39.47	114.398	9.868	0.000001
130.0	39.62	113.186	9.827	0.000001
130.5	39.78	111.206	9.775	0.000001
131.0	39.93	111.777	9.71	0.000001
131.5	40.08	109.625	9.712	0.000001
132.0	40.23	104.302	9.719	0.000001
132.5	40.39	100.736	9.842	0.000001
133.0	40.54	102.085	9.871	0.000001
133.5	40.69	104.518	9.972	0.000001
134.0	40.84	106.341	10.029	0.000001
134.5	41.00	104.913	10.029	0.000001
135.0	41.15	104.9	9.993	0.000001

Depth (ft)	Depth (m)	Gamma Ray	Caliper	Permeability (mD)
135.5	41.30	102.199	9.978	0.000001
136.0	41.45	102.212	9.988	0.000001
136.5	41.61	104.619	10.014	0.000001
137.0	41.76	103.468	10.031	0.000001
137.5	41.91	102.327	10.02	0.000001
138.0	42.06	102.083	9.99	0.000001
138.5	42.21	104.313	9.931	0.000001
139.0	42.37	106.149	9.825	0.000001
139.5	42.52	103.867	9.792	0.000001
140.0	42.67	103.39	9.761	0.000001
140.5	42.82	102.298	9.774	0.000001
141.0	42.98	101.822	9.803	0.000001
141.5	43.13	102.731	9.831	0.000001
142.0	43.28	105.136	9.835	0.000001
142.5	43.43	108.327	9.835	0.000001
143.0	43.59	113.24	9.832	0.000001
143.5	43.74	113.431	9.813	0.000001
144.0	43.89	111.456	9.771	0.000001
144.5	44.04	102.558	9.677	0.000001
145.0	44.20	95.95	9.526	0.000001
145.5	44.35	95.013	9.508	0.000001
146.0	44.50	98.909	9.654	0.000001
146.5	44.65	105.468	9.789	0.000001
147.0	44.81	103.605	9.807	0.000001
147.5	44.96	101.554	9.789	0.000001
148.0	45.11	98.297	9.807	0.000001
148.5	45.26	100.03	9.806	0.000001
149.0	45.42	97.616	9.77	0.000001
149.5	45.57	101.934	9.669	0.000001
150.0	45.72	107.096	9.56	0.000001
150.5	45.87	111.689	9.516	0.000001
151.0	46.02	108.789	9.565	0.000001
151.5	46.18	104.518	9.715	0.000001
152.0	46.33	101.401	9.849	0.000001
152.5	46.48	101.547	9.861	0.000001
153.0	46.63	102.757	9.881	0.000001
153.5	46.79	108.089	9.914	0.000001
154.0	46.94	108.786	9.977	0.000001
154.5	47.09	108.55	9.998	0.000001
155.0	47.24	109.412	9.989	0.000001
155.5	47.40	110.754	9.919	0.000001
156.0	47.55	108.471	9.908	0.000001
156.5	47.70	104.687	9.862	0.000001
157.0	47.85	103.469	9.761	0.000001
157.5	48.01	105.087	9.738	0.000001
158.0	48.16	104.93	9.665	0.000001
158.5	48.31	103.401	9.541	0.000001
159.0	48.46	97.535	9.456	0.000001
159.5	48.62	95.174	9.562	0.000001
160.0	48.77	94.59	9.67	0.000001
160.5	48.92	98.388	9.7	0.000001
161.0	49.07	97.945	9.69	0.000001
161.5	49.23	101.041	9.708	0.000001
162.0	49.38	102.117	9.732	0.000001
162.5	49.53	109.114	9.636	0.000001
163.0	49.68	112.446	9.612	0.000001
163.5	49.83	116.337	9.623	0.000001
164.0	49.99	113.021	9.626	0.000001
164.5	50.14	121.171	9.642	0.000001
165.0	50.29	123.065	9.664	0.000001
165.5	50.44	121.718	9.551	0.000001

Depth (ft)	Depth (m)	Gamma Ray	Caliper	Permeability (mD)
166.0	50.60	114.814	9.576	0.000001
166.5	50.75	112.461	9.658	0.000001
167.0	50.90	113.229	9.64	0.000001
167.5	51.05	110.807	9.554	0.000001
168.0	51.21	111.156	9.546	0.000001
168.5	51.36	112.215	9.637	0.000001
169.0	51.51	112.323	9.809	0.000001
169.5	51.66	112.247	9.9	0.000001
170.0	51.82	109.904	9.901	0.000001
170.5	51.97	107.222	9.889	0.000001
171.0	52.12	106.927	9.867	0.000001
171.5	52.27	109.691	9.946	0.000001
172.0	52.43	111.695	9.999	0.000001
172.5	52.58	109.052	9.964	0.000001
173.0	52.73	104.573	9.997	0.000001
173.5	52.88	100.777	9.997	0.000001
174.0	53.04	100.513	9.935	0.000001
174.5	53.19	99.149	9.915	0.000001
175.0	53.34	100.545	10.035	0.000001
175.5	53.49	100.353	10.041	0.000001
176.0	53.64	101.645	10.055	0.000001
176.5	53.80	103.18	10.093	0.000001
177.0	53.95	104.323	10.087	0.000001
177.5	54.10	103.452	10.067	0.000001
178.0	54.25	97.232	10.013	0.000001
178.5	54.41	94.231	10.027	0.000001
179.0	54.56	95.691	10.027	0.000001
179.5	54.71	100.327	10.047	0.000001
180.0	54.86	104.147	10.079	0.000001
180.5	55.02	104.403	10.07	0.000001
181.0	55.17	103.983	10.076	0.000001
181.5	55.32	104.81	10.065	0.000001
182.0	55.47	105.435	10.041	0.000001
182.5	55.63	108.742	10.042	0.000001
183.0	55.78	105.681	10.041	0.000001
183.5	55.93	104.117	10.053	0.000001
184.0	56.08	100.952	10.07	0.000001
184.5	56.24	101.816	10.068	0.000001
185.0	56.39	103.438	10.071	0.000001
185.5	56.54	104.155	10.074	0.000001
186.0	56.69	107.462	10.066	0.000001
186.5	56.85	104.7	10.046	0.000001
187.0	57.00	101.073	10.028	0.000001
187.5	57.15	95.871	10.047	0.000001
188.0	57.30	93.588	10.076	0.000001
188.5	57.45	94.29	10.092	0.000001
189.0	57.61	96.284	10.014	0.000001
189.5	57.76	97.928	10.095	0.000001
190.0	57.91	99.038	10.078	0.000001
190.5	58.06	97.002	10.082	0.000001
191.0	58.22	98.733	10.101	0.000001
191.5	58.37	98.346	10.107	0.000001
192.0	58.52	100.983	10.108	0.000001
192.5	58.67	101.476	10.109	0.000001
193.0	58.83	103.405	10.109	0.000001
193.5	58.98	103.112	10.108	0.000001
194.0	59.13	103.897	10.108	0.000001
194.5	59.28	102.751	10.107	0.000001
195.0	59.44	102.22	10.108	0.000001
195.5	59.59	102.613	10.158	0.000001
196.0	59.74	104.473	10.233	0.000001

Depth (ft)	Depth (m)	Gamma Ray	Caliper	Permeability (mD)
196.5	59.89	107.225	10.314	0.000001
197.0	60.05	105.962	10.317	0.000001
197.5	60.20	104.837	10.404	0.000001
198.0	60.35	104.775	10.46	0.000001
198.5	60.50	105.24	10.582	0.000001
199.0	60.66	107.503	10.731	0.000001
199.5	60.81	109.462	10.864	0.000001
200.0	60.96	108.799	10.963	0.000001
200.5	61.11	110.682	10.982	0.000001
201.0	61.26	108.64	10.885	0.000001
201.5	61.42	108.98	10.746	0.000001
202.0	61.57	107.272	10.59	0.000001
202.5	61.72	105.802	10.431	0.000001
203.0	61.87	107.563	10.176	0.000001
203.5	62.03	105.31	10.155	0.000001
204.0	62.18	100.9	10.07	0.000001
204.5	62.33	89.642	9.601	0.000001
205.0	62.48	81.463	9.074	0.000001
205.5	62.64	78.35	9.25	0.000001
206.0	62.79	77.907	9.474	0.000001
206.5	62.94	78.015	9.834	0.000001
207.0	63.09	82.169	10.163	0.000001
207.5	63.25	91.949	10.256	0.000001
208.0	63.40	102.919	10.201	0.000001
208.5	63.55	108.241	10.305	0.000001
209.0	63.70	112.06	10.285	0.000001
209.5	63.86	111.31	10.214	0.000001
210.0	64.01	113.851	10.203	0.000001
210.5	64.16	111.154	10.263	0.000001
211.0	64.31	111.224	10.358	0.000001
211.5	64.47	108.737	10.342	0.000001
212.0	64.62	109.847	10.377	0.000001
212.5	64.77	110.366	10.345	0.000001
213.0	64.92	114.193	10.317	0.000001
213.5	65.07	112.065	10.264	0.000001
214.0	65.23	110.119	10.245	0.000001
214.5	65.38	106.181	10.209	0.000001
215.0	65.53	108.472	10.16	0.000001
215.5	65.68	110.803	10.138	0.000001
216.0	65.84	107.726	10.114	0.000001
216.5	65.99	101.104	10.091	0.000001
217.0	66.14	98.405	10.034	0.000001
217.5	66.29	98.791	10.109	0.000001
218.0	66.45	101.434	10.263	0.000001
218.5	66.60	99.407	10.139	0.000001
219.0	66.75	97.173	9.822	0.000001
219.5	66.90	94.591	10.195	0.000001
220.0	67.06	91.701	10.67	0.000001
220.5	67.21	92.167	11.583	0.000001
221.0	67.36	93.723	11.031	0.000001
221.5	67.51	96.965	10.425	0.000001
222.0	67.67	98.808	10.918	0.000001
222.5	67.82	99.335	10.767	0.000001
223.0	67.97	102.266	10.544	0.000001
223.5	68.12	103.092	10.512	0.000001
224.0	68.28	101.886	10.546	0.000001
224.5	68.43	99.76	10.901	0.000001
225.0	68.58	100.941	10.776	0.000001
225.5	68.73	102.528	10.653	0.000001
226.0	68.88	105.238	10.521	0.000001
226.5	69.04	100.959	10.487	0.000001

Depth (ft)	Depth (m)	Gamma Ray	Caliper	Permeability (mD)
227.0	69.19	100.865	10.41	0.000001
227.5	69.34	102.029	10.363	0.000001
228.0	69.49	104.917	10.355	0.000001
228.5	69.65	105.645	10.367	0.000001
229.0	69.80	103.511	10.391	0.000001
229.5	69.95	104.318	10.39	0.000001
230.0	70.10	105.185	10.316	0.000001
230.5	70.26	102.072	10.251	0.000001
231.0	70.41	102.479	10.156	0.000001
231.5	70.56	103.34	10.195	0.000001
232.0	70.71	103.307	10.325	0.000001
232.5	70.87	100.849	10.423	0.000001
233.0	71.02	96.798	10.369	0.000001
233.5	71.17	98.515	10.226	0.000001
234.0	71.32	98.904	10.256	0.000001
234.5	71.48	100.467	10.283	0.000001
235.0	71.63	103.633	10.316	0.000001
235.5	71.78	103.196	10.359	0.000001
236.0	71.93	101.788	10.374	0.000001
236.5	72.09	96.058	10.373	0.000001
237.0	72.24	96.786	10.378	0.000001
237.5	72.39	99.284	10.399	0.000001
238.0	72.54	100.794	10.446	0.000001
238.5	72.69	99.703	10.492	0.000001
239.0	72.85	97.434	10.334	0.000001
239.5	73.00	97.959	10.257	0.000001
240.0	73.15	95.294	10.344	0.000001
240.5	73.30	97.632	10.368	0.000001
241.0	73.46	98.305	10.349	0.000001
241.5	73.61	103.321	10.318	0.000001
242.0	73.76	103.048	10.288	0.000001
242.5	73.91	102.153	10.283	0.000001
243.0	74.07	100.766	10.288	0.000001
243.5	74.22	100.539	10.288	0.000001
244.0	74.37	100.233	10.291	0.000001
244.5	74.52	100.73	10.382	0.000001
245.0	74.68	100.785	10.346	0.000001
245.5	74.83	101.698	10.331	0.000001
246.0	74.98	101.244	10.331	0.000001
246.5	75.13	100.763	10.334	0.000001
247.0	75.29	102.519	10.335	0.000001
247.5	75.44	100.703	10.337	0.000001
248.0	75.59	100.377	10.34	0.000001
248.5	75.74	98.402	10.343	0.000001
249.0	75.90	99.326	10.359	0.000001
249.5	76.05	98.783	10.403	0.000001
250.0	76.20	99.682	10.455	0.000001
250.5	76.35	98.735	10.677	0.000001
251.0	76.50	95.688	12.064	0.000001
251.5	76.66	90.906	11.793	0.000001
252.0	76.81	90.174	10.618	0.000001
252.5	76.96	91.776	10.534	0.000001
253.0	77.11	96.19	10.493	0.000001
253.5	77.27	99.066	10.31	0.000001
254.0	77.42	100.177	10.311	0.000001
254.5	77.57	97.623	10.359	0.000001
255.0	77.72	94.893	10.21	0.000001
255.5	77.88	91.566	9.928	0.000001
256.0	78.03	89.605	9.9	0.000001
256.5	78.18	89.372	9.909	0.000001
257.0	78.33	87.65	9.933	0.000001

Depth (ft)	Depth (m)	Gamma Ray	Caliper	Permeability (mD)
257.5	78.49	87.816	9.895	0.000001
258.0	78.64	86.183	9.882	0.000001
258.5	78.79	88.506	9.911	0.000001
259.0	78.94	91.142	10.001	0.000001
259.5	79.10	92.755	10.011	0.000001
260.0	79.25	93.427	10.012	0.000001
260.5	79.40	92.615	9.913	0.000001
261.0	79.55	93.66	9.725	0.000001
261.5	79.71	93.989	9.639	0.000001
262.0	79.86	94.236	9.729	0.000001
262.5	80.01	93.27	9.722	0.000001
263.0	80.16	94.317	9.832	0.000001
263.5	80.31	93.836	9.863	0.000001
264.0	80.47	94.819	9.679	0.000001
264.5	80.62	93.825	9.545	0.000001
265.0	80.77	92.887	9.528	0.000001
265.5	80.92	93.424	9.652	0.000001
266.0	81.08	96.485	9.846	0.000001
266.5	81.23	100.811	9.886	0.000001
267.0	81.38	102.904	9.993	0.000001
267.5	81.53	99.698	9.997	0.000001
268.0	81.69	96.122	9.924	0.000001
268.5	81.84	92.63	9.831	0.000001
269.0	81.99	92.166	9.867	0.000001
269.5	82.14	94.772	9.868	0.000001
270.0	82.30	99.122	9.877	0.000001
270.5	82.45	101.555	9.944	0.000001
271.0	82.60	100.231	9.993	0.000001
271.5	82.75	97.848	9.993	0.000001
272.0	82.91	97.299	10.012	0.000001
272.5	83.06	102.594	10.008	0.000001
273.0	83.21	104.582	9.967	0.000001
273.5	83.36	103.956	10.021	0.000001
274.0	83.52	100.676	10.029	0.000001
274.5	83.67	99.517	10.036	0.000001
275.0	83.82	100.256	10.007	0.000001
275.5	83.97	98.403	10.034	0.000001
276.0	84.12	96.542	10.001	0.000001
276.5	84.28	95.802	9.938	0.000001
277.0	84.43	97.522	9.899	0.000001
277.5	84.58	100.506	9.925	0.000001
278.0	84.73	101.929	9.957	0.000001
278.5	84.89	103.386	9.957	0.000001
279.0	85.04	102.963	9.965	0.000001
279.5	85.19	103.232	9.96	0.000001
280.0	85.34	103.677	9.957	0.000001
280.5	85.50	102.117	9.898	0.000001
281.0	85.65	98.304	9.846	0.000001
281.5	85.80	96.166	9.877	0.000001
282.0	85.95	95.124	9.893	0.000001
282.5	86.11	96.341	9.854	0.000001
283.0	86.26	95.697	9.822	0.000001
283.5	86.41	96.07	9.801	0.000001
284.0	86.56	100.063	9.787	0.000001
284.5	86.72	99.236	9.791	0.000001
285.0	86.87	100.316	9.816	0.000001
285.5	87.02	97.742	9.847	0.000001
286.0	87.17	101.12	9.866	0.000001
286.5	87.33	102.979	9.799	0.000001
287.0	87.48	106.216	9.722	0.000001
287.5	87.63	110.572	9.696	0.0008

Depth (ft)	Depth (m)	Gamma Ray	Caliper	Permeability (mD)
288.0	87.78	113.421	9.837	0.0613
288.5	87.93	114.06	9.883	0.000001
289.0	88.09	111.605	9.901	0.000001
289.5	88.24	108.509	9.903	0.000001
290.0	88.39	103.606	9.909	0.000001
290.5	88.54	99.007	9.957	0.000001
291.0	88.70	92.487	9.955	0.000001
291.5	88.85	90.327	9.99	0.000001
292.0	89.00	83.761	9.997	0.0003
292.5	89.15	81.102	9.999	0.001
293.0	89.31	78.106	9.999	0.000001
293.5	89.46	78.725	9.989	0.000001
294.0	89.61	75.357	9.993	0.000001
294.5	89.76	75.509	9.963	0.000001
295.0	89.92	76.285	10.035	0.000001
295.5	90.07	78.834	10.041	0.000001
296.0	90.22	79.77	10.039	0.000001
296.5	90.37	80.569	10.035	0.000001
297.0	90.53	82.028	10.042	0.000001
297.5	90.68	83.165	10.007	0.000001
298.0	90.83	85.236	10.015	0.000001
298.5	90.98	88.628	10.027	0.000001
299.0	91.14	86.43	10.01	0.000001
299.5	91.29	84.411	10	0.0012
300.0	91.44	80.393	9.997	0.000001
300.5	91.59	79.76	9.998	0.003
301.0	91.74	79.251	9.998	0.0063
301.5	91.90	77.044	9.998	0.007
302.0	92.05	74.567	9.998	0.0085
302.5	92.20	72.134	10	0.0198
303.0	92.35	72.842	9.989	0.0114
303.5	92.51	73.551	9.958	0.008
304.0	92.66	77.99	9.957	0.0125
304.5	92.81	79.119	9.957	0.0076
305.0	92.96	80.284	9.956	0.0063
305.5	93.12	79.973	9.956	0.0064
306.0	93.27	79.379	9.957	0.0082
306.5	93.42	77.995	9.967	0.0074
307.0	93.57	73.167	9.984	0.0117
307.5	93.73	67.129	9.986	0.0137
308.0	93.88	66.903	9.997	0.0166
308.5	94.03	71.821	10	0.0121
309.0	94.18	76.997	9.997	0.0028
309.5	94.34	79.38	9.998	0.0022
310.0	94.49	77.659	9.998	0.0007
310.5	94.64	74.894	9.977	0.0135
311.0	94.79	70.082	9.996	0.0216
311.5	94.95	68.572	10.034	0.0059
312.0	95.10	66.196	10.032	0.0183
312.5	95.25	70.271	10.027	0.0285
313.0	95.40	69.469	10.029	0.0333
313.5	95.55	70.57	10.028	0.0227
314.0	95.71	69.384	10.061	0.0235
314.5	95.86	70.449	10.091	0.004
315.0	96.01	71.621	10.153	0.005
315.5	96.16	71.326	10.166	0.0058
316.0	96.32	72.442	10.228	0.0032
316.5	96.47	74.951	10.346	0.0014
317.0	96.62	77.41	10.358	0.000001
317.5	96.77	80.306	10.395	0.000001
318.0	96.93	80	10.409	0.000001

Depth (ft)	Depth (m)	Gamma Ray	Caliper	Permeability (mD)
318.5	97.08	72.987	10.439	0.000001
319.0	97.23	62.264	10.502	0.000001
319.5	97.38	55.954	10.569	0.000001
320.0	97.54	59.917	10.575	0.000001
320.5	97.69	64.18	10.577	0.000001
321.0	97.84	73.223	10.612	0.000001
321.5	97.99	80.724	10.503	0.000001
322.0	98.15	76.149	10.563	0.0062
322.5	98.30	63.429	10.618	0.000001
323.0	98.45	51.473	10.655	0.000001
323.5	98.60	46.014	10.656	0.000001
324.0	98.76	46.65	10.658	0.000001
324.5	98.91	49.794	10.654	0.000001
325.0	99.06	56.85	10.643	0.000001
325.5	99.21	61.376	10.627	0.0059
326.0	99.36	66.562	10.62	0.0069
326.5	99.52	69.222	10.607	0.000001
327.0	99.67	77.045	10.566	0.000001
327.5	99.82	82.717	10.924	0.0341
328.0	99.97	87.604	12.046	0.0145
328.5	100.13	82.751	11.427	0.0257
329.0	100.28	72.992	11.191	0.0234
329.5	100.43	64.245	11.078	0.000001
330.0	100.58	60.1	11.015	0.000001
330.5	100.74	63.478	11.001	0.000001
331.0	100.89	65.921	10.961	0.000001
331.5	101.04	66.6	10.883	0.000001
332.0	101.19	66.537	10.753	0.000001
332.5	101.35	63.548	10.613	0.000001
333.0	101.50	57.471	10.452	0.000001
333.5	101.65	49.559	10.214	0.000001
334.0	101.80	44.596	9.943	0.000001
334.5	101.96	47.536	9.873	0.000001
335.0	102.11	59.276	9.883	0.0298
335.5	102.26	69.96	10.109	0.048
336.0	102.41	77.007	10.763	0.0286
336.5	102.57	79.27	10.385	0.0434
337.0	102.72	77.993	9.941	0.000001
337.5	102.87	71.921	9.924	0.000001
338.0	103.02	63.915	9.677	0.000001
338.5	103.17	62.768	9.815	0.000001
339.0	103.33	67.309	10.02	0.000001
339.5	103.48	74.541	9.932	0.000001
340.0	103.63	78.36	9.972	0.000001
340.5	103.78	81.698	10.302	0.000001
341.0	103.94	85.956	10.053	0.000001
341.5	104.09	91.076	9.907	0.000001
342.0	104.24	92.397	9.886	0.000001
342.5	104.39	87.59	10.117	0.000001
343.0	104.55	78.313	9.927	0.000001
343.5	104.70	72.745	9.916	0.0025
344.0	104.85	80.47	10.038	0.000001
344.5	105.00	92.186	10.108	0.000001
345.0	105.16	100.46	10.204	0.000001
345.5	105.31	98.567	10.236	0.000001
346.0	105.46	95.873	10.258	0.000001
346.5	105.61	97.665	10.29	0.000001
347.0	105.77	97.944	10.272	0.000001
347.5	105.92	98.758	10.328	0.0001
348.0	106.07	98.092	10.387	0.0025
348.5	106.22	100.511	10.408	0.0009

Depth (ft)	Depth (m)	Gamma Ray	Caliper	Permeability (mD)
349.0	106.38	101.369	10.384	0.0008
349.5	106.53	102.136	10.342	0.0004
350.0	106.68	102.492	10.351	0.0007
350.5	106.83	101.481	10.383	0.000001
351.0	106.98	100.575	10.375	0.000001
351.5	107.14	100.055	10.356	0.000001
352.0	107.29	99.538	10.272	0.000001
352.5	107.44	91.169	10.189	0.0102
353.0	107.59	79.964	10.063	0.024
353.5	107.75	71.973	9.945	0.000001
354.0	107.90	67.194	9.933	0.000001
Mancos Shale average				*0.0015846*
354.5	108.05	62.799	9.912	0.0834
355.0	108.20	60.193	9.887	0.1082
355.5	108.36	58.29	9.833	0.13
356.0	108.51	56.685	9.754	0.1448
356.5	108.66	53.772	9.688	0.1666
357.0	108.81	53.593	9.698	0.1761
357.5	108.97	54.243	9.735	0.1779
358.0	109.12	50.645	9.738	0.1912
358.5	109.27	45.993	9.689	0.2045
359.0	109.42	41.012	9.596	0.2147
359.5	109.58	39.693	9.528	0.2223
360.0	109.73	39.095	9.555	0.2281
360.5	109.88	41.864	9.666	0.2289
361.0	110.03	42.919	9.666	0.2275
361.5	110.19	42.402	9.669	0.2336
362.0	110.34	40.768	9.671	0.2341
362.5	110.49	39.16	9.7	0.2059
363.0	110.64	39.53	9.734	0.1906
363.5	110.79	38.787	9.692	0.175
364.0	110.95	42.378	9.652	0.1506
364.5	111.10	48.203	9.638	0.1357
365.0	111.25	54.745	9.636	0.1134
365.5	111.40	59.723	9.626	0.0859
366.0	111.56	59.856	9.625	0.0727
366.5	111.71	61.525	9.627	0.0654
367.0	111.86	61.81	9.625	0.0588
367.5	112.01	64.597	9.595	0.0476
368.0	112.17	64.843	9.53	0.0565
368.5	112.32	62.409	9.512	0.0639
369.0	112.47	54.225	9.541	0.0973
369.5	112.62	41.914	9.555	0.1177
370.0	112.78	30.81	9.549	0.1591
370.5	112.93	26.599	9.528	0.1932
371.0	113.08	24.31	9.518	0.2182
371.5	113.23	24.931	9.51	0.2276
372.0	113.39	24.423	9.49	0.2389
372.5	113.54	24.929	9.496	0.2467
373.0	113.69	24.664	9.516	0.2406
373.5	113.84	23.888	9.504	0.2379
374.0	114.00	25.305	9.502	0.233
374.5	114.15	25.868	9.486	0.2305
375.0	114.30	26.478	9.432	0.223
375.5	114.45	28.178	9.314	0.2175
376.0	114.60	32.615	8.996	0.2149
376.5	114.76	39.675	8.884	0.2056
377.0	114.91	41.865	8.883	0.2032
377.5	115.06	41.14	8.91	0.2011
378.0	115.21	40.488	8.917	0.2145
378.5	115.37	42.103	8.91	0.2227

Depth (ft)	Depth (m)	Gamma Ray	Caliper	Permeability (mD)
379.0	115.52	41.787	8.936	0.2238
379.5	115.67	39.141	9.038	0.2353
380.0	115.82	35.781	9.178	0.2373
380.5	115.98	34.849	9.247	0.2288
381.0	116.13	34.7	9.293	0.2276
381.5	116.28	37.031	9.351	0.223
382.0	116.43	41.177	9.386	0.2252
382.5	116.59	44.799	9.455	0.2038
383.0	116.74	45.241	9.579	0.2039
383.5	116.89	44.857	9.679	0.2071
384.0	117.04	41.618	9.743	0.2218
384.5	117.20	38.487	9.763	0.2241
385.0	117.35	35.945	9.756	0.242
385.5	117.50	37.177	9.723	0.2507
386.0	117.65	39.283	9.75	0.2513
386.5	117.81	39.624	9.797	0.2298
387.0	117.96	38.523	9.808	0.216
387.5	118.11	37.539	9.798	0.2172
388.0	118.26	37.808	9.801	0.2146
388.5	118.41	40.295	9.882	0.1955
389.0	118.57	42.258	9.938	0.1791
389.5	118.72	42.253	9.956	0.1722
390.0	118.87	42.837	9.966	0.1731
390.5	119.02	43.652	9.974	0.1585
391.0	119.18	46.338	9.975	0.1407
391.5	119.33	48.072	9.971	0.1473
392.0	119.48	48.273	9.962	0.1498
392.5	119.63	47.283	9.97	0.1455
393.0	119.79	46.782	9.998	0.1436
393.5	119.94	48.19	9.999	0.1408
394.0	120.09	49.858	10.006	0.1326
394.5	120.24	50.166	10.06	0.1271
395.0	120.40	52.571	10.102	0.1229
395.5	120.55	53.886	10.165	0.111
396.0	120.70	55.445	10.22	0.0994
396.5	120.85	56.719	10.269	0.109
397.0	121.01	59.504	10.308	0.0863
397.5	121.16	62.117	10.33	0.0829
398.0	121.31	64.361	10.341	0.0758
398.5	121.46	65.288	10.341	0.076
399.0	121.62	67.536	10.34	0.0682
399.5	121.77	68.114	10.342	0.0666
400.0	121.92	69.626	10.336	0.0583
400.5	122.07	69.383	10.328	0.0588
401.0	122.22	66.289	10.28	0.0749
401.5	122.38	65.577	10.23	0.0873
402.0	122.53	65.412	10.105	0.0941
402.5	122.68	68.837	9.998	0.0842
403.0	122.83	69.046	9.905	0.0812
403.5	122.99	66.956	9.83	0.0795
404.0	123.14	65.552	9.817	0.0805
404.5	123.29	65.209	9.799	0.0708
405.0	123.44	69.553	9.773	0.0322
405.5	123.60	68.961	9.754	0.0385
406.0	123.75	64.677	9.734	0.0603
406.5	123.90	60.74	9.719	0.0815
407.0	124.05	59.678	9.713	0.0818
407.5	124.21	64.347	9.705	0.0694
408.0	124.36	63.138	9.688	0.0829
408.5	124.51	65.431	9.683	0.0657
409.0	124.66	63.033	9.698	0.0706

Depth (ft)	Depth (m)	Gamma Ray	Caliper	Permeability (mD)
409.5	124.82	62.939	9.734	0.0796
410.0	124.97	58.047	9.748	0.1082
410.5	125.12	56.082	9.746	0.1319
411.0	125.27	56.298	9.722	0.1263
411.5	125.43	57.346	9.71	0.1099
412.0	125.58	55.853	9.711	0.1254
412.5	125.73	54.05	9.716	0.1201
413.0	125.88	52.678	9.722	0.106
413.5	126.03	52.18	9.722	0.0981
414.0	126.19	50.345	9.72	0.0913
414.5	126.34	45.874	9.671	0.0433
415.0	126.49	43.896	9.627	0.031
415.5	126.64	41.28	9.652	0.035
416.0	126.80	45.101	9.709	0.0234
416.5	126.95	46.791	9.685	0.0625
417.0	127.10	48.53	9.658	0.0883
417.5	127.25	49.555	9.566	0.0997
418.0	127.41	52.217	9.537	0.1027
418.5	127.56	56.06	9.523	0.0986
419.0	127.71	56.007	9.555	0.0812
419.5	127.86	58.664	9.541	0.0688
420.0	128.02	61.29	9.509	0.0581
420.5	128.17	64.698	9.519	0.0378
421.0	128.32	63.502	9.466	0.0447
421.5	128.47	62.97	9.497	0.0542
422.0	128.63	61.489	9.51	0.0613
422.5	128.78	60.949	9.519	0.06
423.0	128.93	61.595	9.63	0.0596
423.5	129.08	60.073	9.587	0.048
424.0	129.24	61.643	9.58	0.0452
424.5	129.39	59.363	9.567	0.0536
425.0	129.54	61.951	9.578	0.047
425.5	129.69	62.106	9.589	0.0473
426.0	129.84	61.24	9.614	0.061
426.5	130.00	61.522	9.602	0.0486
427.0	130.15	60.752	9.589	0.0566
427.5	130.30	61.992	9.598	0.066
428.0	130.45	63.954	9.633	0.0675
428.5	130.61	64.332	9.631	0.0735
429.0	130.76	66.566	9.598	0.0922
429.5	130.91	64.39	9.619	0.1001
430.0	131.06	62.026	9.771	0.1051
430.5	131.22	57.498	10.011	0.1242
431.0	131.37	56.451	10.056	0.1245
431.5	131.52	56.435	10.008	0.0986
432.0	131.67	52.341	10.021	0.0458
432.5	131.83	48.264	10.039	0.0166
433.0	131.98	47.575	10.056	0.0565
433.5	132.13	55.325	10.098	0.0639
434.0	132.28	60.836	10.095	0.0597
434.5	132.44	62.401	10.113	0.0598
435.0	132.59	62.17	10.123	0.0535
435.5	132.74	62.581	10.13	0.0404
436.0	132.89	64.879	10.134	0.0371
436.5	133.05	64.871	10.134	0.0323
437.0	133.20	63.077	10.127	0.0365
437.5	133.35	62.214	10.105	0.0488
438.0	133.50	61.607	10.096	0.0542
438.5	133.65	61.431	10.096	0.0711
439.0	133.81	61.615	10.096	0.071
439.5	133.96	60.104	10.072	0.0776
440.0	134.11	59.716	10.044	0.0801
440.5	134.26	57.457	10.01	0.0923
441.0	134.42	56.802	9.981	0.1003
441.5	134.57	56.205	9.969	0.092
442.0	134.72	57.513	9.981	0.0833
442.5	134.87	58.723	9.967	0.0886
443.0	135.03	61.937	9.92	0.0819
443.5	135.18	61.218	9.879	0.0867
444.0	135.33	58.433	9.887	0.0908
444.5	135.48	53.681	9.991	0.0815
445.0	135.64	51.397	10.062	0.0447
445.5	135.79	51.728	10.175	0.039
446.0	135.94	55.16	10.283	0.0352
446.5	136.09	58.316	10.379	0.0496
447.0	136.25	63.194	10.47	0.069
447.5	136.40	64.044	10.522	0.0757
448.0	136.55	65.243	10.606	0.0708
448.5	136.70	65.452	10.747	0.0735
449.0	136.86	67.23	10.884	0.0564
449.5	137.01	68.587	11.01	0.0463
450.0	137.16	71.074	11.068	0.034
450.5	137.31	74.893	11.101	0.0109
451.0	137.46	75.701	11.132	0.0107
451.5	137.62	77.984	11.161	0.0039
452.0	137.77	79.725	11.161	0.0113
Two Wells sandstone average				*0.116617*
452.5	137.92	83.651	11.161	0.000001
453.0	138.07	85.803	11.181	0.000001
453.5	138.23	86.985	11.184	0.000001
454.0	138.38	87.463	11.159	0.000001
454.5	138.53	90.351	11.121	0.000001
455.0	138.68	91.655	11.04	0.000001
455.5	138.84	92.74	10.987	0.000001
456.0	138.99	94.29	10.783	0.000001
456.5	139.14	92.509	10.54	0.000001
457.0	139.29	90.919	10.344	0.000001
457.5	139.45	85.933	10.194	0.000001
458.0	139.60	84.052	10.148	0.000001
458.5	139.75	84.109	10.107	0.000001
459.0	139.90	85.533	10.053	0.000001
459.5	140.06	85.396	10.018	0.000001
460.0	140.21	87.119	10.007	0.000001
460.5	140.36	85.975	9.996	0.000001
461.0	140.51	86.687	9.98	0.000001
461.5	140.67	85.887	9.964	0.000001
462.0	140.82	85.397	9.958	0.000001
462.5	140.97	85.573	9.938	0.000001
463.0	141.12	84.832	9.927	0.000001
463.5	141.27	87.404	9.93	0.000001
464.0	141.43	87.781	9.929	0.000001
464.5	141.58	87.984	9.89	0.0009
465.0	141.73	85.134	9.926	0.0008
465.5	141.88	81.518	9.956	0.0063
466.0	142.04	80.738	9.958	0.0041
466.5	142.19	80.602	9.971	0.003
467.0	142.34	81.371	9.974	0.000001
467.5	142.49	82.005	9.9	0.000001
468.0	142.65	82.694	9.96	0.000001
468.5	142.80	84.63	10.022	0.000001
469.0	142.95	84.72	10.048	0.000001
469.5	143.10	85.721	10.089	0.000001

Depth (ft)	Depth (m)	Gamma Ray	Caliper	Permeability (mD)
470.0	143.26	86.059	10.093	0.000001
470.5	143.41	85.49	10.096	0.000001
471.0	143.56	83.157	10.066	0.0078
471.5	143.71	86.694	10.084	0.0007
472.0	143.87	88.62	10.085	0.0023
472.5	144.02	89.959	10.096	0.0008
473.0	144.17	89.427	10.069	0.000001
473.5	144.32	90.066	10.048	0.000001
474.0	144.48	91.048	10.053	0.000001
474.5	144.63	92.432	10.061	0.0052
475.0	144.78	97.676	10.042	0.000001
475.5	144.93	101.905	10	0.0175
476.0	145.08	99.279	10.033	0.000001
476.5	145.24	93.193	10.021	0.000001
477.0	145.39	88.176	10.067	0.000001
477.5	145.54	86.597	10.096	0.000001
478.0	145.69	84.629	10.085	0.000001
478.5	145.85	80.775	10.062	0.000001
479.0	146.00	80.974	10.021	0.000001
479.5	146.15	81.445	10.064	0.000001
480.0	146.30	86.557	10.072	0.000001
480.5	146.46	86.966	10.052	0.000001
481.0	146.61	89.066	10.043	0.000001
481.5	146.76	89.974	10.04	0.000001
482.0	146.91	91.837	10.041	0.000001
482.5	147.07	96.059	10.032	0.000001
483.0	147.22	100.151	10.003	0.000001
483.5	147.37	101.148	9.967	0.000001
484.0	147.52	95.89	9.945	0.000001
484.5	147.68	85.679	9.948	0.000001
485.0	147.83	81.116	9.913	0.000001
485.5	147.98	78.058	10.002	0.000001
486.0	148.13	83.496	10.007	0.000001
486.5	148.29	85.336	10.033	0.000001
487.0	148.44	90.724	10.07	0.000001
487.5	148.59	90.977	10.087	0.000001
488.0	148.74	92.202	10.136	0.000001
488.5	148.89	87.526	10.104	0.0256
489.0	149.05	79.948	10.1	0.031
489.5	149.20	70.279	10.133	0.0458
490.0	149.35	68.662	10.233	0.0334
490.5	149.50	71.791	10.344	0.0194
491.0	149.66	77.885	10.536	0.0085
491.5	149.81	79.84	10.664	0.0093
492.0	149.96	80.939	10.724	0.0106
492.5	150.11	82.372	10.807	0.0222
493.0	150.27	87.337	10.838	0.0221
493.5	150.42	93.574	10.778	0.000001
494.0	150.57	97.951	10.691	0.000001
494.5	150.72	96.684	10.652	0.000001
495.0	150.88	95.96	10.584	0.000001
495.5	151.03	101.577	10.544	0.000001
496.0	151.18	110.09	10.509	0.0026
496.5	151.33	108.709	10.529	0.0707
497.0	151.49	104.841	10.426	0.000001
497.5	151.64	96.843	10.426	0.000001
498.0	151.79	99.544	10.425	0.000001
498.5	151.94	100.593	10.426	0.000001
499.0	152.10	109.455	10.483	0.000001
499.5	152.25	117.184	10.512	0.000001
500.0	152.40	123.291	10.529	0.000001

Depth (ft)	Depth (m)	Gamma Ray	Caliper	Permeability (mD)
500.5	152.55	118.01	10.535	0.000001
501.0	152.70	107.275	10.52	0.000001
501.5	152.86	97.761	10.501	0.0217
502.0	153.01	93.307	10.452	0.0176
502.5	153.16	89.884	10.283	0.0164
503.0	153.31	83.423	10.179	0.0404
503.5	153.47	80.863	10.137	0.0477
504.0	153.62	81.734	10.136	0.0437
504.5	153.77	84.631	10.137	0.0253
White Water Shale average				*0.005501*
505.0	153.92	87.61	10.136	0.0075
505.5	154.08	90.301	10.136	0.0001
506.0	154.23	94.573	10.137	0.000001
506.5	154.38	96.673	10.138	0.000001
507.0	154.53	99.177	10.138	0.000001
507.5	154.69	95.833	10.138	0.000001
508.0	154.84	91.892	10.135	0.000001
508.5	154.99	89.134	10.123	0.0056
509.0	155.14	89.38	10.104	0.000001
509.5	155.30	90.448	10.097	0.000001
510.0	155.45	90.077	10.076	0.000001
510.5	155.60	91.521	10.052	0.000001
511.0	155.75	90.896	10.017	0.0064
511.5	155.91	86.895	9.981	0.0096
512.0	156.06	76.769	9.915	0.0497
512.5	156.21	65.929	9.807	0.0992
513.0	156.36	56.25	9.704	0.1416
513.5	156.51	50.563	9.645	0.1648
514.0	156.67	48.161	9.633	0.1693
514.5	156.82	45.53	9.656	0.1716
515.0	156.97	44.115	9.666	0.1701
515.5	157.12	41.289	9.688	0.1822
516.0	157.28	38.987	9.716	0.1993
516.5	157.43	37.226	9.717	0.222
517.0	157.58	35.641	9.702	0.2437
517.5	157.73	36.076	9.62	0.2596
518.0	157.89	37.113	9.446	0.2683
518.5	158.04	40.227	9.32	0.2657
519.0	158.19	41.222	9.492	0.2558
519.5	158.34	40.344	9.591	0.2495
520.0	158.50	37.996	9.667	0.2452
520.5	158.65	38.916	9.742	0.2385
521.0	158.80	42.85	9.709	0.2196
521.5	158.95	46.867	9.9	0.1933
522.0	159.11	51.575	9.968	0.1621
522.5	159.26	51.769	9.957	0.1493
523.0	159.41	53.807	9.989	0.1454
523.5	159.56	54.171	10.006	0.1324
524.0	159.72	56.71	10	0.1068
524.5	159.87	58.034	9.971	0.0899
525.0	160.02	60.235	9.935	0.0713
525.5	160.17	60.873	9.895	0.0803
526.0	160.32	56.353	9.806	0.1131
526.5	160.48	54.476	9.641	0.1356
527.0	160.63	54.092	9.555	0.145
527.5	160.78	57.31	9.545	0.1354
528.0	160.93	55.047	9.586	0.1437
528.5	161.09	49.389	9.686	0.1715
529.0	161.24	48.491	9.794	0.1677
529.5	161.39	46.84	9.917	0.1721
530.0	161.54	51.108	10.029	0.15

Depth (ft)	Depth (m)	Gamma Ray	Caliper	Permeability (mD)
530.5	161.70	50.792	10.044	0.1744
531.0	161.85	51.983	10.044	0.1839
531.5	162.00	51.109	10.041	0.1868
532.0	162.15	51.873	10.039	0.18
532.5	162.31	53.349	10.021	0.1795
533.0	162.46	52.176	9.947	0.1885
533.5	162.61	52.518	9.869	0.1854
534.0	162.76	52.589	9.763	0.1879
534.5	162.92	51.957	9.696	0.1908
535.0	163.07	51.839	9.667	0.1695
535.5	163.22	54.761	9.669	0.1495
536.0	163.37	58.005	9.761	0.124
536.5	163.53	61.767	9.896	0.0991
537.0	163.68	62.687	9.951	0.0918
537.5	163.83	63.44	9.986	0.0879
538.0	163.98	62.903	10.012	0.0934
538.5	164.13	59.936	10.039	0.0984
539.0	164.29	59.456	10.048	0.1047
539.5	164.44	59.283	10.049	0.117
540.0	164.59	59.546	10.066	0.0957
540.5	164.74	59.527	10.113	0.0968
541.0	164.90	60.414	10.158	0.099
541.5	165.05	62.262	10.169	0.0944
542.0	165.20	64.904	10.173	0.0861
542.5	165.35	66.695	10.166	0.0776
543.0	165.51	68.969	10.081	0.0843
543.5	165.66	71.357	10.135	0.0598
544.0	165.81	71.187	10.263	0.0571
544.5	165.96	69.598	10.245	0.0787
545.0	166.12	66.229	10.197	0.1039
545.5	166.27	65.262	10.144	0.0999
546.0	166.42	65.328	9.983	0.0991
546.5	166.57	66.639	9.87	0.0878
547.0	166.73	69.126	9.708	0.0828
547.5	166.88	71.061	9.669	0.0674
548.0	167.03	72.841	9.697	0.0584
548.5	167.18	71.889	9.869	0.0384
549.0	167.34	67.305	9.98	0.0668
549.5	167.49	66.526	9.967	0.0771
550.0	167.64	67.066	9.945	0.0755
550.5	167.79	72.359	9.902	0.0484
551.0	167.94	74.247	9.881	0.0498
551.5	168.10	78.862	9.891	0.0416
552.0	168.25	80.021	9.908	0.0362
552.5	168.40	81.584	9.918	0.035
553.0	168.55	79.897	9.928	0.0359
553.5	168.71	80.31	9.93	0.0356
554.0	168.86	81.128	9.931	0.044
554.5	169.01	82.247	9.924	0.0418
555.0	169.16	84.298	9.842	0.0237
555.5	169.32	85.179	9.809	0.0327
556.0	169.47	86.089	9.885	0.0385
556.5	169.62	85.027	10.059	0.0516
557.0	169.77	85.722	10.06	0.0538
557.5	169.93	86.204	10.11	0.0428
558.0	170.08	86.694	10.064	0.0513
558.5	170.23	87.479	10.058	0.047
559.0	170.38	89.861	10.123	0.0434
559.5	170.54	91.523	10.132	0.0299
560.0	170.69	91.851	10.13	0.0403
560.5	170.84	91.575	10.075	0.0546
561.0	170.99	95.68	10.032	0.0595
561.5	171.15	88.486	10.062	0.082
562.0	171.30	73.532	10.109	0.1256
562.5	171.45	56.881	10.134	0.1659
563.0	171.60	51.99	10.165	0.1762
563.5	171.75	51.333	10.178	0.1665
564.0	171.91	51.609	10.168	0.1638
564.5	172.06	51.759	10.077	0.1663
565.0	172.21	54.609	10.042	0.1835
565.5	172.36	55.59	10.041	0.1652
566.0	172.52	53.616	10.045	0.1574
566.5	172.67	51.982	10.024	0.1498
567.0	172.82	54.478	9.996	0.1414
567.5	172.97	57.198	9.982	0.1381
568.0	173.13	57.304	9.981	0.1357
568.5	173.28	53.047	9.953	0.1551
569.0	173.43	51.959	9.874	0.1578
569.5	173.58	55.521	9.806	0.148
570.0	173.74	58.586	9.806	0.1193
570.5	173.89	61.232	9.806	0.1029
571.0	174.04	59.961	9.796	0.0844
571.5	174.19	57.358	9.77	0.0588
572.0	174.35	52.252	9.918	0.0587
572.5	174.50	48.758	9.993	0.0747
573.0	174.65	53.254	9.971	0.1031
573.5	174.80	62.588	10.001	0.0889
574.0	174.96	67.658	10.006	0.0644
574.5	175.11	69.898	10.012	0.0548
575.0	175.26	66.679	9.977	0.0646
575.5	175.41	68.423	9.948	0.0586
576.0	175.56	68.805	9.932	0.0583
576.5	175.72	71.291	9.915	0.026
577.0	175.87	69.614	9.928	0.016
577.5	176.02	67.323	9.942	0.0267
578.0	176.17	69.361	9.954	0.0117
578.5	176.33	74.873	9.967	0.000001
579.0	176.48	76.47	10	0.000001
579.5	176.63	75.817	9.998	0.000001
580.0	176.78	74.645	9.97	0.000001
580.5	176.94	78.159	9.972	0.000001
581.0	177.09	80.66	10	0.000001
581.5	177.24	84.319	10	0.000001
582.0	177.39	86.594	10.001	0.000001
582.5	177.55	86.548	10.008	0.000001
583.0	177.70	85.668	10.012	0.000001
583.5	177.85	85.851	10.014	0.000001
584.0	178.00	88.366	10.012	0.000001
584.5	178.16	92.335	9.987	0.000001
585.0	178.31	93.969	9.908	0.000001
585.5	178.46	92.17	9.898	0.000001
586.0	178.61	89.302	9.981	0.000001
586.5	178.77	87.356	10.006	0.000001
Paguate sandstone average				*0.08782*
587.0	178.92	88.966	10.004	0.000001
587.5	179.07	91.292	9.954	0.000001
588.0	179.22	90.45	9.92	0.000001
588.5	179.37	87.514	9.898	0.000001
589.0	179.53	85.358	9.906	0.000001
589.5	179.68	86.153	9.98	0.000001
590.0	179.83	87.408	10.013	0.000001
590.5	179.98	87.787	10.017	0.000001

Depth (ft)	Depth (m)	Gamma Ray	Caliper	Permeability (mD)
591.0	180.14	87.335	10.013	0.000001
591.5	180.29	89.082	10.007	0.000001
592.0	180.44	91.35	10.012	0.000001
592.5	180.59	92.678	10.011	0.000001
593.0	180.75	95.278	10.011	0.000001
593.5	180.90	94.27	10.012	0.000001
594.0	181.05	94.838	10.009	0.000001
594.5	181.20	93.071	9.996	0.000001
595.0	181.36	96.062	9.967	0.000001
595.5	181.51	93.464	9.905	0.000001
596.0	181.66	92.217	9.89	0.0057
596.5	181.81	93.502	9.887	0.0085
597.0	181.97	93.391	9.888	0.0326
597.5	182.12	94.325	9.881	0.0378
598.0	182.27	94.755	9.87	0.0358
598.5	182.42	95.614	9.865	0.0291
599.0	182.58	88.649	9.874	0.0395
599.5	182.73	84.954	9.852	0.0566
600.0	182.88	85.04	9.815	0.0518
600.5	183.03	90.112	9.751	0.041
601.0	183.18	91.446	9.793	0.023
601.5	183.34	95.93	9.859	0.0129
602.0	183.49	97.31	9.929	0.0064
602.5	183.64	100.601	9.985	0.0016
603.0	183.79	99.439	10.013	0.0106
603.5	183.95	101.532	10.075	0.0286
604.0	184.10	101.913	10.079	0.0378
604.5	184.25	102.06	10.125	0.0503
605.0	184.40	98.008	10.136	0.0494
605.5	184.56	93.212	10.14	0.0594
606.0	184.71	92.961	10.152	0.0475
606.5	184.86	94.502	10.171	0.074
607.0	185.01	94.92	10.182	0.057
607.5	185.17	94.902	10.178	0.0965
608.0	185.32	95.713	10.192	0.0763
608.5	185.47	96.683	10.22	0.1012
609.0	185.62	98.727	10.18	0.0443
Clay Mesa shale average				*0.0301408*
609.5	185.78	101.481	10.178	0.042
610.0	185.93	102.032	10.15	0.065
610.5	186.08	103.918	10.138	0.0467
611.0	186.23	107.473	10.134	0.0485
611.5	186.39	109.013	10.125	0.0215
612.0	186.54	107.415	10.124	0.0356
612.5	186.69	105.5	10.068	0.0217
613.0	186.84	110.601	10.026	0.0078
613.5	186.99	112.514	10.012	0.0101
614.0	187.15	113.781	10.033	0.018
614.5	187.30	110.429	10.035	0.0449
615.0	187.45	112.515	10.014	0.0565
615.5	187.60	111.261	10.007	0.0635
616.0	187.76	107.497	9.982	0.0728
616.5	187.91	92.286	9.907	0.0794
617.0	188.06	75.036	9.89	0.1445
617.5	188.21	62.317	9.891	0.1605
618.0	188.37	57.15	9.879	0.1582
618.5	188.52	53.987	9.78	0.1702
619.0	188.67	45.593	9.678	0.2125
619.5	188.82	41.21	9.648	0.229
620.0	188.98	36.917	9.655	0.226
620.5	189.13	38.246	9.671	0.2131

Depth (ft)	Depth (m)	Gamma Ray	Caliper	Permeability (mD)
621.0	189.28	35.013	9.722	0.2108
621.5	189.43	35.904	9.8	0.2078
622.0	189.59	34.594	9.852	0.2069
622.5	189.74	37.338	9.858	0.2039
623.0	189.89	40.085	9.849	0.1919
623.5	190.04	40.834	9.823	0.194
624.0	190.20	41.498	9.77	0.1923
624.5	190.35	39.449	9.772	0.1889
625.0	190.50	38.341	9.806	0.1898
625.5	190.65	37.688	9.806	0.1903
626.0	190.80	38.7	9.83	0.1822
626.5	190.96	40.794	9.862	0.168
627.0	191.11	42.308	9.876	0.1623
627.5	191.26	45.086	9.888	0.1538
628.0	191.41	46.311	9.894	0.1456
628.5	191.57	46.097	9.892	0.1438
629.0	191.72	42.717	9.883	0.1398
629.5	191.87	43.158	9.885	0.1459
630.0	192.02	43.76	9.887	0.1467
630.5	192.18	44.708	9.883	0.1418
631.0	192.33	44.173	9.88	0.16
631.5	192.48	43.163	9.889	0.1589
632.0	192.63	43.911	9.878	0.1527
632.5	192.79	45.243	9.848	0.146
633.0	192.94	46.792	9.854	0.1402
633.5	193.09	48.033	9.812	0.1381
634.0	193.24	46.782	9.809	0.1573
634.5	193.40	48.548	9.778	0.1525
635.0	193.55	49.372	9.763	0.1362
635.5	193.70	50.4	9.758	0.1325
636.0	193.85	46.161	9.741	0.1416
636.5	194.01	40.808	9.686	0.1761
637.0	194.16	35.639	9.569	0.2166
637.5	194.31	34.796	9.389	0.2176
638.0	194.46	35.165	9.143	0.2389
638.5	194.61	35.696	9.191	0.2388
639.0	194.77	35.622	9.258	0.2283
639.5	194.92	34.723	9.169	0.2286
640.0	195.07	35.056	9.229	0.2338
640.5	195.22	34.445	9.243	0.2376
641.0	195.38	35.048	9.255	0.2358
641.5	195.53	35.087	9.235	0.2432
642.0	195.68	35.235	9.124	0.2475
642.5	195.83	36.22	9.013	0.258
643.0	195.99	39.417	8.92	0.2606
643.5	196.14	41.553	9.028	0.2595
644.0	196.29	44.182	9.354	0.2528
644.5	196.44	43.587	9.215	0.2428
645.0	196.60	44.909	9.475	0.2608
645.5	196.75	47.342	9.79	0.2154
646.0	196.90	47.987	9.774	0.225
646.5	197.05	49.329	9.971	0.2269
647.0	197.21	48.443	9.972	0.2096
647.5	197.36	48.507	9.953	0.2241
648.0	197.51	48.622	10.003	0.2001
648.5	197.66	46.727	10.002	0.2192
649.0	197.82	49.176	9.924	0.2117
649.5	197.97	51.357	10.011	0.2115
650.0	198.12	54.998	10.015	0.2066
650.5	198.27	57.051	10.015	0.1849
651.0	198.42	57.44	9.939	0.1821

Depth (ft)	Depth (m)	Gamma Ray	Caliper	Permeability (mD)
651.5	198.58	59.151	9.968	0.17
Cubero sandstone average				*0.0965833*
652.0	198.73	61.743	10.044	0.1749
652.5	198.88	64.252	10.042	0.1561
653.0	199.03	64.115	9.937	0.1366
653.5	199.19	61.462	9.952	0.1489
654.0	199.34	62.792	9.928	0.1518
654.5	199.49	65.94	9.903	0.1444
655.0	199.64	69.021	9.966	0.1603
655.5	199.80	70.39	9.942	0.1261
656.0	199.95	68.385	9.958	0.123
656.5	200.10	66.079	9.857	0.1189
657.0	200.25	63.175	9.897	0.1427
657.5	200.41	62.64	9.871	0.1386
658.0	200.56	61.241	9.873	0.1404
658.5	200.71	58.426	9.796	0.164
659.0	200.86	56.612	9.768	0.1632
659.5	201.02	55.844	9.75	0.1434
660.0	201.17	55.181	9.795	0.1366
660.5	201.32	56.668	9.806	0.1148
661.0	201.47	58.218	9.918	0.1009
661.5	201.63	62.654	9.916	0.0503
662.0	201.78	63.742	9.807	0.0843
662.5	201.93	67.821	9.862	0.1081
663.0	202.08	68.648	9.774	0.1006
663.5	202.23	73.749	9.652	0.0971
664.0	202.39	76.635	9.532	0.099
664.5	202.54	80.894	9.319	0.0816
665.0	202.69	82.376	9.438	0.0843
665.5	202.84	81.497	8.625	0.0977
666.0	203.00	86.151	8.601	0.0714
666.5	203.15	97.492	8.678	0.046
667.0	203.30	119.447	8.471	0.000001
667.5	203.45	143.784	9.223	0.000001
668.0	203.61	149.721	9.763	0.000001
668.5	203.76	132.227	6.972	0.000001
669.0	203.91	97.86	7.236	0.000001
669.5	204.06	74.28	8.648	0.0145
670.0	204.22	65.762	9.624	0.0355
670.5	204.37	62.495	9.788	0.0673
671.0	204.52	60.47	9.806	0.067
671.5	204.67	59.52	9.91	0.0909
672.0	204.83	61.386	9.997	0.0965
672.5	204.98	64.429	9.999	0.0922
673.0	205.13	64.057	10	0.1034
673.5	205.28	63.275	10.005	0.1089
674.0	205.44	64.221	9.999	0.1129
674.5	205.59	66.451	9.999	0.1058
675.0	205.74	68.777	10.026	0.1226
675.5	205.89	69.802	10.041	0.1011
676.0	206.04	70.347	10.009	0.0949
676.5	206.20	69.947	9.975	0.0942
677.0	206.35	70.493	9.9	0.0815
677.5	206.50	68.436	10.03	0.0905
678.0	206.65	62.803	10.001	0.094
678.5	206.81	55.421	9.965	0.0994
679.0	206.96	51.614	9.923	0.0753
679.5	207.11	55.964	9.913	0.0675
680.0	207.26	61.526	9.901	0.0617
680.5	207.42	66.722	9.989	0.078
681.0	207.57	68.489	10.01	0.0827

Depth (ft)	Depth (m)	Gamma Ray	Caliper	Permeability (mD)
681.5	207.72	69.683	9.788	0.1062
682.0	207.87	71.162	9.511	0.0913
682.5	208.03	75.919	9.461	0.0722
683.0	208.18	80.324	9.528	0.0558
683.5	208.33	83.819	9.597	0.0532
684.0	208.48	86.801	9.592	0.0413
684.5	208.64	87.909	9.613	0.0406
685.0	208.79	86.183	9.824	0.0314
685.5	208.94	83.168	9.978	0.0361
686.0	209.09	82.3	10.044	0.0242
686.5	209.25	82.147	10.035	0.0371
687.0	209.40	81.543	10.01	0.0313
687.5	209.55	82.697	9.958	0.0359
688.0	209.70	82.791	9.904	0.0424
688.5	209.85	80.153	9.846	0.0432
689.0	210.01	77.073	9.816	0.0382
689.5	210.16	78.455	9.875	0.0442
690.0	210.31	83.266	9.964	0.0348
690.5	210.46	84.61	9.999	0.0235
691.0	210.62	83.169	9.965	0.0209
691.5	210.77	78.831	9.935	0.0348
692.0	210.92	79.332	9.894	0.0287
692.5	211.07	82.016	9.877	0.029
693.0	211.23	85.237	9.875	0.0358
693.5	211.38	82.781	9.877	0.0273
694.0	211.53	81.627	9.877	0.0274
694.5	211.68	78.992	9.848	0.0223
695.0	211.84	81.999	9.771	0.0055
695.5	211.99	87.79	9.73	0.000001
696.0	212.14	101.328	9.611	0.000001
696.5	212.29	111.217	9.35	0.000001
697.0	212.45	108.429	9.337	0.000001
697.5	212.60	99.164	9.283	0.000001
698.0	212.75	91.103	9.393	0.000001
698.5	212.90	88.312	9.49	0.000001
699.0	213.06	86.998	9.536	0.000001
699.5	213.21	90.026	9.546	0.000001
700.0	213.36	91.225	9.56	0.000001
700.5	213.51	92.097	9.59	0.000001
701.0	213.66	94.885	9.614	0.000001
701.5	213.82	95.203	9.625	0.000001
702.0	213.97	101.088	9.65	0.000001
702.5	214.12	105.221	9.671	0.000001
703.0	214.27	109.719	9.703	0.000001
703.5	214.43	110.957	9.747	0.000001
704.0	214.58	110.095	9.75	0.000001
704.5	214.73	106.498	9.752	0.000001
705.0	214.88	101.437	9.752	0.0221
705.5	215.04	91.178	9.758	0.0406
706.0	215.19	73.003	9.785	0.0793
706.5	215.34	55.884	9.793	0.1193
707.0	215.49	46.292	9.637	0.1513
707.5	215.65	46.882	9.533	0.1561
708.0	215.80	48.411	9.514	0.1413
708.5	215.95	49.485	9.515	0.1432
709.0	216.10	51.315	9.51	0.1559
709.5	216.26	52.716	9.518	0.159
710.0	216.41	54.127	9.563	0.1433
710.5	216.56	56.15	9.63	0.1289
711.0	216.71	56.411	9.635	0.1359
711.5	216.87	58.706	9.6	0.1433

Depth (ft)	Depth (m)	Gamma Ray	Caliper	Permeability (mD)
712.0	217.02	57.989	9.607	0.1481
712.5	217.17	57.55	9.712	0.1445
713.0	217.32	52.321	9.836	0.1488
713.5	217.47	48.564	9.877	0.1607
714.0	217.63	47.957	9.91	0.1733
714.5	217.78	48.105	9.988	0.1695
715.0	217.93	48.812	10.033	0.1633
715.5	218.08	49.494	10.036	0.1512
716.0	218.24	52.027	10.112	0.1439
716.5	218.39	54.281	10.251	0.1421
717.0	218.54	54.751	10.261	0.1326
717.5	218.69	54.91	10.256	0.1147
718.0	218.85	52.494	10.231	0.1252
718.5	219.00	51.82	10.227	0.1383
719.0	219.15	51.009	10.252	0.1461
719.5	219.30	53.773	10.282	0.1435
720.0	219.46	53.785	10.289	0.1579
720.5	219.61	56.026	10.3	0.1591
721.0	219.76	56.211	10.3	0.156
721.5	219.91	58.405	10.288	0.1448
722.0	220.07	57.675	10.262	0.1376
722.5	220.22	56.575	10.237	0.1507
723.0	220.37	55.614	10.215	0.1537
723.5	220.52	54.255	10.186	0.1585
724.0	220.68	52.032	10.178	0.1729
724.5	220.83	50.287	10.179	0.1671
725.0	220.98	49.821	10.179	0.1604
725.5	221.13	49.602	10.179	0.1469
726.0	221.28	45.327	10.179	0.152
726.5	221.44	39.045	10.179	0.1771
727.0	221.59	34.581	10.174	0.1702
727.5	221.74	36.392	10.092	0.1635
728.0	221.89	39.382	10.018	0.1599
728.5	222.05	42.568	9.974	0.1649
729.0	222.20	44.036	9.952	0.1771
729.5	222.35	45.151	9.94	0.1831
730.0	222.50	45.863	9.907	0.1813
730.5	222.66	47.515	9.85	0.1804
731.0	222.81	49.502	9.835	0.1762
731.5	222.96	49.366	9.843	0.1746
732.0	223.11	48.171	9.836	0.1706
732.5	223.27	47.646	9.816	0.1596
733.0	223.42	47.573	9.819	0.1439
733.5	223.57	46.848	9.89	0.1391
734.0	223.72	45.466	9.969	0.1508
734.5	223.88	45.466	10.002	0.1544
735.0	224.03	45.466	9.985	0.1547
735.5	224.18	45.466	9.917	0.1606
736.0	224.33	45.466	9.851	0.1698
736.5	224.49	45.466	9.878	0.1814
737.0	224.64	45.466	9.873	0.1948
737.5	224.79	45.466	9.821	0.2112
738.0	224.94	45.466	9.756	0.2178
Oak Canyon sandstone average				*0.1261134*

Depth (m)	Density porosity
17.6	18.491
17.8	25.535
17.9	29.878
18.1	27.730
18.2	20.963
18.4	13.733
18.5	11.376
18.7	11.043
18.8	11.647
19.0	12.493
19.1	12.796
19.3	13.117
19.4	13.565
19.6	14.083
19.8	14.499
19.9	14.449
20.1	14.664
20.2	14.933
20.4	14.699
20.5	14.046
20.7	13.734
20.8	13.838
21.0	13.130
21.1	12.366
21.3	12.531
21.4	13.305
21.6	13.918
21.7	14.271
21.9	14.457
22.0	14.669
22.2	14.751
22.3	15.073
22.5	14.482
22.6	13.727
22.8	13.363
23.0	13.655
23.1	14.306
23.3	14.720
23.4	15.128
23.6	15.886
23.7	16.664
23.9	16.734
24.0	16.044
24.2	15.042
24.3	14.626
24.5	13.269
24.6	11.673
24.8	10.106
24.9	10.492
25.1	11.200
25.2	11.989
25.4	12.298
25.5	13.216
25.7	14.428
25.8	15.288
26.0	15.385
26.2	14.434
26.3	13.374
26.5	12.255
26.6	10.928
26.8	9.142
26.9	8.584

Depth (m)	Density porosity
27.1	8.512
27.2	9.388
27.4	9.562
27.5	10.016
27.7	10.447
27.8	10.894
28.0	10.573
28.1	10.580
28.3	10.432
28.4	11.194
28.6	12.042
28.7	12.522
28.9	12.990
29.0	12.646
29.2	12.585
29.4	12.285
29.5	12.520
29.7	12.680
29.8	12.102
30.0	11.836
30.1	11.659
30.3	12.249
30.4	12.870
30.6	13.629
30.7	14.403
30.9	14.148
31.0	13.624
31.2	12.439
31.3	11.335
31.5	10.443
31.6	9.683
31.8	10.027
31.9	10.460
32.1	11.427
32.2	11.459
32.4	11.224
32.6	10.560
32.7	10.372
32.9	9.947
33.0	10.541
33.2	11.031
33.3	12.171
33.5	12.147
33.6	10.935
33.8	9.056
33.9	8.140
34.1	8.359
34.2	8.121
34.4	7.646
34.5	7.285
34.7	7.823
34.8	9.121
35.0	10.244
35.1	9.796
35.3	9.166
35.4	8.271
35.6	9.417
35.8	9.212
35.9	9.346
36.1	7.761
36.2	7.898
36.4	7.751

Depth (m)	Density porosity
36.5	8.044
36.7	7.142
36.8	7.208
37.0	7.412
37.1	7.741
37.3	7.833
37.4	7.544
37.6	7.219
37.7	5.963
37.9	5.708
38.0	5.755
38.2	6.747
38.3	8.091
38.5	8.896
38.6	10.482
38.8	10.985
39.0	11.304
39.1	11.181
39.3	10.727
39.4	10.375
39.6	10.637
39.7	11.507
39.9	12.111
40.0	11.428
40.2	10.882
40.3	10.284
40.5	10.046
40.6	10.152
40.8	10.309
40.9	10.448
41.1	10.853
41.2	11.101
41.4	11.336
41.5	11.267
41.7	9.949
41.8	8.833
42.0	6.608
42.2	4.585
42.3	5.464
42.5	6.496
42.6	5.838
42.8	6.019
42.9	5.823
43.1	7.306
43.2	8.333
43.4	9.654
43.5	9.944
43.7	10.026
43.8	9.010
44.0	7.387
44.1	6.406
44.3	6.968
44.4	7.795
44.6	7.907
44.7	7.996
44.9	8.033
45.0	8.989
45.2	8.746
45.4	8.941
45.5	9.139
45.7	10.151
45.8	10.684

Depth (m)	Density porosity
46.0	11.355
46.1	10.106
46.3	7.866
46.4	6.748
46.6	8.925
46.7	11.278
46.9	11.203
47.0	10.878
47.2	10.352
47.3	11.957
47.5	13.832
47.6	14.367
47.8	14.540
47.9	15.121
48.1	15.549
48.2	15.097
48.4	13.109
48.6	11.170
48.7	10.746
48.9	9.908
49.0	9.367
49.2	8.383
49.3	8.335
49.5	7.869
49.6	7.326
49.8	7.120
49.9	6.718
50.1	6.496
50.2	5.308
50.4	4.690
50.5	3.905
50.7	3.824
50.8	5.202
51.0	6.144
51.1	8.393
51.3	9.893
51.4	11.905
51.6	12.806
51.8	12.137
51.9	8.758
52.1	6.710
52.2	6.993
52.4	10.038
52.5	11.567
52.7	12.253
52.8	12.265
53.0	12.445
53.1	12.144
53.3	11.842
53.4	11.303
53.6	11.224
53.7	11.516
53.9	12.148
54.0	12.086
54.2	12.132
54.3	12.240
54.5	12.157
54.7	12.114
54.8	12.213
55.0	12.745
55.1	13.948
55.3	13.662

Depth (m)	Density porosity
55.4	12.326
55.6	10.412
55.7	9.977
55.9	9.893
56.0	9.939
56.2	10.729
56.3	10.919
56.5	10.804
56.6	10.283
56.8	10.203
56.9	10.528
57.1	10.732
57.2	10.186
57.4	9.480
57.5	8.902
57.7	8.249
57.9	7.329
58.0	7.110
58.2	8.262
58.3	9.172
58.5	9.412
58.6	9.605
58.8	9.229
58.9	8.979
59.1	9.239
59.2	9.964
59.4	10.775
59.5	10.832
59.7	10.644
59.8	10.439
60.0	11.075
60.1	13.190
60.3	16.428
60.4	14.278
60.6	6.446
60.7	0.839
60.9	3.673
61.1	7.942
61.2	8.311
61.4	8.183
61.5	8.131
61.7	7.836
61.8	8.204
62.0	8.445
62.1	9.090
62.3	9.580
62.4	10.351
62.6	10.465
62.7	9.894
62.9	8.433
63.0	8.010
63.2	8.085
63.3	9.364
63.5	10.012
63.6	10.200
63.8	10.308
63.9	11.111
64.1	12.140
64.3	12.934
64.4	13.077
64.6	11.596
64.7	8.494

Depth (m)	Density porosity
64.9	7.417
65.0	11.323
65.2	13.244
65.3	13.513
65.5	11.916
65.6	11.867
65.8	11.266
65.9	11.327
66.1	11.455
66.2	11.489
66.4	11.390
66.5	11.349
66.7	11.783
66.8	11.544
67.0	10.951
67.1	9.924
67.3	9.634
67.5	9.677
67.6	10.595
67.8	11.044
67.9	11.409
68.1	10.422
68.2	9.967
68.4	9.546
68.5	9.232
68.7	7.714
68.8	6.562
69.0	6.473
69.1	7.621
69.3	8.727
69.4	10.092
69.6	10.345
69.7	9.496
69.9	8.036
70.0	8.682
70.2	8.721
70.3	7.306
70.5	3.265
70.7	0.327
70.8	1.874
71.0	4.947
71.1	6.699
71.3	6.947
71.4	7.383
71.6	7.062
71.7	6.610
71.9	6.554
72.0	6.745
72.2	6.735
72.3	6.829
72.5	7.379
72.6	7.787
72.8	8.738
72.9	9.074
73.1	8.715
73.2	8.183
73.4	8.194
73.5	8.642
73.7	8.218
73.9	6.363
74.0	6.076
74.2	8.792

Depth (m)	Density porosity
74.3	11.743
74.5	12.695
74.6	11.915
74.8	11.269
74.9	11.006
75.1	10.179
75.2	11.717
75.4	16.958
75.5	27.170
75.7	33.765
75.8	34.074
76.0	28.055
76.1	20.912
76.3	14.670
76.4	12.818
76.6	12.836
76.7	14.018
76.9	16.415
77.1	19.966
77.2	20.988
77.4	19.883
77.5	17.040
77.7	16.031
77.8	15.868
78.0	16.143
78.1	15.223
78.3	14.430
78.4	14.623
78.6	15.684
78.7	16.190
78.9	15.210
79.0	14.433
79.2	13.614
79.3	13.458
79.5	12.123
79.6	10.997
79.8	10.686
79.9	11.971
80.1	12.698
80.3	12.788
80.4	11.660
80.6	11.159
80.7	10.941
80.9	10.815
81.0	10.108
81.2	9.504
81.3	10.054
81.5	9.773
81.6	9.461
81.8	8.079
81.9	8.357
82.1	8.581
82.2	10.180
82.4	11.273
82.5	12.019
82.7	12.012
82.8	11.720
83.0	11.809
83.1	11.841
83.3	11.807
83.5	11.998
83.6	11.601

Depth (m)	Density porosity
83.8	11.173
83.9	10.345
84.1	10.351
84.2	9.903
84.4	10.076
84.5	10.152
84.7	10.294
84.8	10.309
85.0	10.527
85.1	15.499
85.3	20.563
85.4	22.079
85.6	18.426
85.7	14.092
85.9	12.370
86.0	12.056
86.2	11.057
86.3	10.012
86.5	8.788
86.7	7.842
86.8	7.601
87.0	8.061
87.1	8.133
87.3	8.551
87.4	8.219
87.6	7.977
87.7	7.372
87.9	7.706
88.0	8.107
88.2	9.199
88.3	9.450
88.5	9.725
88.6	8.848
88.8	8.439
88.9	8.129
89.1	8.202
89.2	7.656
89.4	6.486
89.5	6.148
89.7	6.540
89.9	6.354
90.0	6.006
90.2	5.936
90.3	7.125
90.5	7.714
90.6	8.290
90.8	8.262
90.9	8.494
91.1	8.375
91.2	8.094
91.4	8.112
91.5	8.356
91.7	8.815
91.8	9.338
92.0	9.507
92.1	9.434
92.3	8.618
92.4	7.133
92.6	5.587
92.8	6.232
92.9	7.164
93.1	8.308

Depth (m)	Density porosity
93.2	7.936
93.4	7.433
93.5	7.282
93.7	7.517
93.8	8.648
94.0	8.998
94.1	9.351
94.3	9.984
94.4	9.950
94.6	8.960
94.7	5.473
94.9	2.133
95.0	1.189
95.2 *	2.167
95.3	3.360
95.5	4.893
95.6	6.834
95.8	6.699
96.0	4.106
96.1	1.899
96.3	1.460
96.4	0.822
96.6	1.519
96.7	3.118
96.9	5.307
97.0	5.587
97.2	6.052
97.3	11.615
97.5	26.651
97.6	32.946
97.8	30.128
97.9	15.953
98.1	4.742
98.2	2.930
98.4	3.048
98.5	3.802
98.7	3.894
98.8	3.884
99.0	2.356
99.2	0.637
99.3	0.597
99.5	2.822
99.6	7.831
99.8	17.743
99.9	29.336
100.1	31.630
100.2	26.539
100.4	13.284
100.5	9.143
100.7	12.603
100.8	14.173
101.0	14.338
101.1	16.470
101.3	22.571
101.4	28.238
101.6	28.310
101.7	22.354
101.9	12.375
102.0	4.704
102.2	5.337
102.4	7.064
102.5	8.543

Depth (m)	Density porosity
102.7	8.911
102.8	9.213
103.0	7.612
103.1	6.053
103.3	5.157
103.4	5.859
103.6	6.523
103.7	7.586
103.9	7.828
104.0	7.768
104.2	7.165
104.3	6.986
104.5	6.886
104.6	8.385
104.8	8.941
104.9	8.410
105.1	5.411
105.2	4.109
105.4	3.588
105.6	5.815
105.7	9.027
105.9	11.884
106.0	13.724
106.2	13.569
106.3	13.927
106.5	13.803
106.6	14.414
106.8	15.142
106.9	15.571
107.1	15.921
107.2	15.965
107.4	16.279
107.5	16.890
107.7	17.417
107.8	17.938
108.0	17.708
Mancos	*11.399*
108.1	17.316
108.3	15.688
108.4	13.938
108.6	12.008
108.8	10.936
108.9	9.875
109.1	9.659
109.2	9.914
109.4	9.943
109.5	9.816
109.7	7.989
109.8	6.851
110.0	8.306
110.1	13.065
110.3	16.212
110.4	17.447
110.6	16.871
110.7	16.961
110.9	17.796
111.0	18.385
111.2	18.094
111.3	18.670
111.5	19.114
111.6	19.657
111.8	18.543

Depth (m)	Density porosity
112.0	17.472
112.1	16.172
112.3	15.305
112.4	13.996
112.6	13.127
112.7	12.890
112.9	13.771
113.0	13.909
113.2	13.847
113.3	14.118
113.5	14.902
113.6	15.210
113.8	14.995
113.9	14.341
114.1	13.260
114.2	12.366
114.4	12.248
114.5	13.167
114.7	13.478
114.8	15.268
115.0	15.831
115.2	16.106
115.3	14.942
115.5	16.387
115.6	16.843
115.8	17.396
115.9	16.801
116.1	16.128
116.2	15.189
116.4	14.591
116.5	13.742
116.7	13.030
116.8	12.408
117.0	11.829
117.1	11.047
117.3	10.664
117.4	10.766
117.6	11.316
117.7	11.145
117.9	11.153
118.0	11.051
118.2	10.310
118.4	9.667
118.5	8.598
118.7	8.083
118.8	7.710
119.0	7.371
119.1	6.517
119.3	5.140
119.4	5.198
119.6	5.433
119.7	5.815
119.9	5.367
120.0	5.567
120.2	6.267
120.3	6.687
120.5	6.779
120.6	6.816
120.8	6.557
120.9	6.592
121.1	6.413
121.2	6.916

Depth (m)	Density porosity
121.4	7.163
121.6	8.408
121.7	8.951
121.9	9.431
122.0	9.038
122.2	8.883
122.3	8.598
122.5	9.316
122.6	10.002
122.8	10.862
122.9	10.468
123.1	10.920
123.2	11.155
123.4	11.571
123.5	10.913
123.7	10.308
123.8	8.769
124.0	6.221
124.1	3.799
124.3	3.227
124.4	5.040
124.6	7.592
124.8	10.250
124.9	12.036
125.1	12.424
125.2	11.340
125.4	9.105
125.5	8.019
125.7	7.656
125.8	7.161
126.0	7.033
126.1	7.437
126.3	8.227
126.4	8.686
126.6	8.365
126.7	8.504
126.9	8.559
127.0	8.564
127.2	8.435
127.3	8.027
127.5	8.085
127.6	7.684
127.8	7.637
128.0	7.458
128.1	7.409
128.3	7.042
128.4	6.814
128.6	7.264
128.7	6.997
128.9	6.747
129.0	5.985
129.2	4.691
129.3	2.307
129.5	-0.007
129.6	-0.816
129.8	1.670
129.9	3.534
130.1	4.831
130.2	4.721
130.4	4.784
130.5	4.819
130.7	4.909

Depth (m)	Density porosity
130.9	4.758
131.0	4.321
131.2	4.504
131.3	4.571
131.5	4.713
131.6	4.744
131.8	4.922
131.9	5.344
132.1	6.366
132.2	6.232
132.4	6.683
132.5	5.989
132.7	6.319
132.8	5.865
133.0	4.626
133.1	1.541
133.3	-1.335
133.4	-2.564
133.6	-1.761
133.7	0.118
133.9	2.127
134.1	2.761
134.2	3.362
134.4	3.286
134.5	3.536
134.7	3.010
134.8	2.664
135.0	2.616
135.1	2.436
135.3	2.850
135.4	2.345
135.6	2.807
135.7	2.909
135.9	2.603
136.0	2.159
136.2	1.866
136.3	2.234
136.5	2.069
136.6	1.814
136.8	1.085
136.9	0.685
137.1	1.175
137.3	1.545
137.4	2.182
137.6	2.408
137.7	3.205
2 Wells	*2.993*
137.9	2.938
138.0	3.143
138.2	2.676
138.3	2.776
138.5	2.144
138.6	2.062
138.8	2.428
138.9	3.551
139.1	4.808
139.2	4.603
139.4	3.277
139.5	2.214
139.7	2.192
139.8	2.344
140.0	2.174

Depth (m)	Density porosity
140.1	2.449
140.3	2.753
140.5	2.630
140.6	2.026
140.8	2.132
140.9	2.521
141.1	2.023
141.2	1.311
141.4	1.831
141.5	2.471
141.7	3.239
141.8	2.989
142.0	3.562
142.1	4.093
142.3	5.979
142.4	9.750
142.6	12.166
142.7	10.480
142.9	6.479
143.0	4.075
143.2	4.295
143.3	4.702
143.5	4.127
143.7	3.195
143.8	2.701
144.0	2.972
144.1	3.281
144.3	3.473
144.4	3.758
144.6	4.008
144.7	4.694
144.9	5.096
145.0	5.437
145.2	4.669
145.3	3.807
145.5	3.101
145.6	3.123
145.8	3.196
145.9	3.529
146.1	3.835
146.2	4.998
146.4	5.724
146.5	5.653
146.7	4.588
146.9	3.265
147.0	3.033
147.2	3.696
147.3	3.523
147.5	2.951
147.6	2.815
147.8	3.483
147.9	4.464
148.1	5.418
148.2	5.983
148.4	4.797
148.5	4.701
148.7	9.226
148.8	15.541
149.0	17.408
149.1	13.926
149.3	8.152
149.4	6.184

Depth (m)	Density porosity
149.6	7.106
149.7	7.195
149.9	7.228
150.1	7.650
150.2	7.913
150.4	6.915
150.5	5.004
150.7	4.450
150.8	4.188
151.0	4.350
151.1	3.888
151.3	3.392
151.4	3.293
151.6	4.210
151.7	5.263
151.9	5.110
152.0	4.284
152.2	3.640
152.3	3.250
152.5	3.799
152.6	4.169
152.8	3.805
152.9	3.623
153.1	3.391
153.3	3.657
153.4	3.841
153.6	5.975
153.7	8.908
Wt.Water	*2.889*
153.9	12.830
154.0	14.372
154.2	14.906
154.3	13.215
154.5	12.076
154.6	12.592
154.8	13.832
154.9	14.845
155.1	15.988
155.2	17.526
155.4	18.143
155.5	17.490
155.7	16.866
155.8	17.061
156.0	17.589
156.1	17.360
156.3	17.244
156.5	16.351
156.6	15.393
156.8	13.623
156.9	12.715
157.1	11.760
157.2	10.086
157.4	8.800
157.5	7.819
157.7	7.927
157.8	8.220
158.0	9.736
158.1	11.928
158.3	14.251
158.4	15.708
158.6	17.118
158.7	17.084

Depth (m)	Density porosity
158.9	16.107
159.0	14.456
159.2	15.317
159.3	16.274
159.5	16.552
159.7	15.942
159.8	15.770
160.0	16.402
160.1	16.501
160.3	16.319
160.4	15.743
160.6	15.229
160.7	15.035
160.9	13.747
161.0	12.548
161.2	11.744
161.3	11.519
161.5	11.447
161.6	11.328
161.8	11.873
161.9	11.863
162.1	11.743
162.2	10.989
162.4	10.821
162.5	9.980
162.7	9.552
162.9	8.022
163.0	7.227
163.2	6.390
163.3	7.888
163.5	8.875
163.6	10.204
163.8	10.345
163.9	9.984
164.1	9.024
164.2	8.709
164.4	7.873
164.5	7.553
164.7	7.836
164.8	8.802
165.0	8.570
165.1	7.298
165.3	6.211
165.4	6.230
165.6	6.119
165.7	6.641
165.9	6.309
166.1	6.754
166.2	5.997
166.4	5.476
166.5	4.402
166.7	4.425
166.8	5.440
167.0	5.610
167.1	5.110
167.3	3.951
167.4	3.100
167.6	3.557
167.7	4.084
167.9	4.489
168.0	4.666
168.2	4.714

Depth (m)	Density porosity
168.3	5.606
168.5	7.896
168.6	10.492
168.8	12.616
169.0	13.429
169.1	13.417
169.3	12.690
169.4	11.965
169.6	11.504
169.7	12.014
169.9	12.760
170.0	12.560
170.2	11.698
170.3	10.153
170.5	10.422
170.6	11.313
170.8	12.635
170.9	12.366
171.1	11.167
171.2	10.985
171.4	10.454
171.5	9.184
171.7	6.204
171.8	2.341
172.0	0.752
172.2	2.698
172.3	5.191
172.5	6.626
172.6	6.534
172.8	5.876
172.9	5.368
173.1	5.465
173.2	5.050
173.4	4.712
173.5	3.634
173.7	3.971
173.8	3.733
174.0	3.867
174.1	3.394
174.3	3.571
174.4	4.005
174.6	3.853
174.7	3.780
174.9	3.360
175.0	3.234
175.2	3.475
175.4	3.203
175.5	3.094
175.7	2.515
175.8	1.641
176.0	1.511
176.1	1.763
176.3	2.406
176.4	2.869
176.6	2.660
176.7	2.937
176.9	2.448
177.0	2.392
177.2	2.042
177.3	2.339
177.5	2.026
177.6	2.110

Depth (m)	Density porosity
177.8	2.923
177.9	3.339
178.1	3.128
178.2	2.260
178.4	2.026
178.6	1.368
178.7	0.756
Paguate	*6.225*
178.9	1.195
179.0	1.868
179.2	2.580
179.3	2.630
179.5	2.908
179.6	2.792
179.8	3.152
179.9	2.967
180.1	3.089
180.2	3.212
180.4	3.707
180.5	4.113
180.7	4.303
180.8	3.940
181.0	4.314
181.1	3.642
181.3	3.421
181.4	3.274
181.6	4.171
181.8	4.881
181.9	4.647
182.1	3.826
182.2	3.711
182.4	3.569
182.5	4.227
182.7	4.354
182.8	5.186
183.0	5.344
183.1	5.817
183.2756	5.613
183.428	6.432
183.5804	6.451
183.7328	6.629
183.8852	6.820
184.0376	6.692
184.19	6.415
184.3424	6.246
184.4948	6.561
184.6472	6.705
184.7996	6.617
184.952	6.981
185.1044	7.439
185.2568	7.911
185.4092	6.701
185.5616	6.685
ClayMesa	*4.750*
185.714	7.921
185.8664	8.607
186.0188	8.319
186.1712	7.816
186.3236	10.246
186.476	12.763
186.6284	14.254
186.7808	14.082

Depth (m)	Density porosity
186.933	13.534
187.086	13.161
187.238	13.406
187.39	13.512
187.543	13.994
187.695	14.407
187.848	14.418
188	14.979
188.152	14.686
188.305	15.029
188.457	14.554
188.61	14.445
188.762	13.617
188.914	13.057
189.067	12.677
189.219	12.945
189.372	12.395
189.524	12.541
189.676	12.696
189.829	13.285
189.981	13.362
190.134	13.168
190.286	12.438
190.438	11.867
190.591	11.481
190.743	12.084
190.896	12.414
191.048	12.236
191.2	10.787
191.353	9.320
191.505	9.972
191.658	12.128
191.81	14.521
191.962	15.774
192.115	16.389
192.267	16.356
192.42	15.732
192.572	15.339
192.724	15.154
192.877	15.288
193.029	14.815
193.182	14.973
193.334	15.669
193.486	16.147
193.639	15.565
193.791	14.422
193.944	14.604
194.096	13.892
194.248	13.569
194.401	12.061
194.553	11.853
194.706	11.375
194.858	10.229
195.01	9.626
195.163	9.223
195.315	9.607
195.468	9.834
195.62	9.993
195.772	9.589
195.925	9.104
196.077	9.232
196.23	9.191

Depth (m)	Density porosity
196.382	9.187
196.5344	8.972
196.6868	8.241
196.8392	7.875
196.9916	8.032
197.144	8.389
197.2964	7.360
197.4488	6.598
197.6012	5.731
197.7536	6.297
197.906	6.338
198.0584	6.977
198.2108	7.851
198.3632	8.929
198.5156	9.451
198.668	9.775
Cubero	*11.790*
198.8204	9.548
198.9728	8.056
199.1252	4.978
199.2776	3.954
199.43	5.920
199.5824	8.701
199.7348	8.637
199.8872	8.187
200.0396	7.979
200.192	8.992
200.3444	10.680
200.4968	13.748
200.6492	16.508
200.8016	18.900
200.954	20.955
201.1064	22.733
201.2588	22.844
201.4112	19.925
201.5636	14.731
201.716	8.704
201.8684	6.871
202.0208	7.479
202.1732	7.355
202.3256	7.424
202.478	7.128
202.6304	6.474
202.7828	6.372
202.9352	6.590
203.0876	6.652
203.24	6.572
203.3924	6.473
203.5448	6.319
203.6972	6.011
203.8496	6.309
204.002	5.936
204.1544	5.876
204.3068	5.480
204.4592	4.567
204.6116	3.182
204.764	2.393
204.9164	2.661
205.0688	3.829
205.2212	4.762
205.3736	5.715
205.526	7.180

Depth (m)	Density porosity
205.6784	8.514
205.8308	8.743
205.9832	7.857
206.1356	7.467
206.288	6.929
206.4404	7.249
206.5928	7.514
206.7452	8.309
206.8976	7.543
207.05	6.024
207.2024	4.344
207.3548	5.163
207.5072	6.020
207.6596	6.818
207.812	6.929
207.9644	6.632
208.1168	5.799
208.2692	5.627
208.4216	5.450
208.574	5.314
208.7264	5.228
208.8788	4.885
209.0312	3.818
209.1836	3.360
209.336	3.372
209.4884	3.328
209.6408	3.667
209.7932	4.802
209.9456	7.706
210.098	9.503
210.2504	9.490
210.4028	7.110
210.5552	5.653
210.7076	5.507
210.86	5.928
211.0124	5.872
211.1648	6.079
211.3172	5.931
211.4696	6.311
211.622	6.456
211.7744	6.812
211.9268	7.130
212.0792	7.620
212.2316	8.262
212.384	8.802
212.5364	8.712
212.6888	7.133
212.8412	6.351
212.9936	7.912
213.146	11.661
213.2984	14.710
213.4508	16.683
213.6032	17.935
213.7556	18.560
213.908	18.513
214.0604	17.710
214.2128	17.583
214.3652	17.289
214.5176	16.848
214.67	15.896
214.8224	14.377
214.9748	13.088
215.1272	13.874
215.2796	15.687
215.432	17.072
215.5844	16.619
215.7368	15.583
215.8892	14.986
216.0416	14.095
216.194	14.626
216.3464	14.229
216.4988	14.507
216.6512	14.429
216.8036	15.055
216.956	15.775
217.1084	16.043
217.2608	15.424
217.4132	14.740
217.5656	14.557
217.718	14.385
217.8704	14.239
218.0228	14.024
218.1752	13.912
218.3276	13.067
218.48	12.191
218.6324	11.573
218.7848	11.746
218.9372	11.292
219.0896	11.183
219.242	11.363
219.3944	12.247
219.5468	13.896
219.6992	16.151
219.8516	18.694
220.004	20.027
220.1564	19.806
220.3088	19.204
220.4612	18.846
220.6136	19.078
220.766	19.169
220.9184	18.591
221.0708	17.530
221.2232	16.599
221.3756	16.666
221.528	16.928
221.6804	16.252
221.8328	16.526
221.9852	17.522
222.1376	19.495
222.29	20.038
222.4424	20.734
222.5948	20.983
222.7472	21.851
222.8996	21.210
223.052	20.601
OakCan	***8.514***

Box	Lithologic Description	Thickness (m)	Total Depth (m) (bottom of unit)	Microbiology Samples
	Mancos Shale, main body (incomplete). Depositional Environment - marine, transgressive, deposition occurred on or near edge of continental shelf. Transgression most likely caused by eustatic sea-level rise in middle- to upper-Cenomanian time (~96 to 91 Ma) (Vail and others, 1977). This section of the main body is upper-Cenomanian to lower-Turonain in age (Fig. 1) based on ammonite index fossils (Cobban and Hook, 1989).			
1-5†	Mudstone, silty, moderate olive brown (5Y 3/2), well sorted, laminar bedded, minor lithic fragments, weakly calcite cemented, fossiliferous. 50-60% clay, 30-40% silt, 0-5% lithics. Minor pyrite occurrences associated with organic fragments.	60.5	60.5	CNV-X-SC-60.5
5-7	Claystone, silty, grayish-black to olive black (N2 to 5Y 6/1), very well sorted, laminar bedded, moderately calcite cemented, fossiliferous. Occasional biotite-rich silt laminations.	3.5	64.0	
8-9	Mudstone, silty, olive-black to greenish-gray (5GY 2/1 to 5GY 4/1), well sorted, laminar bedded, moderately calcite cemented.	1.7	65.7	
9	Limestone, clay-rich, greenish-gray (5GY 2/1), laminar bedded, moderately calcite cemented, fossiliferous with fine-grained organic fragments.	0.1	65.8	
9	Mudstone, moderate dark gray (N4), well sorted, finely laminated, moderately calcite cemented, fossil indentations.	0.7	66.5	
9	Claystone, olive black(5Y 2/2), well sorted, finely laminated, weakly calcite cemented, fossil indentations.	0.2	66.7	
9-10	Mudstone, moderate dark gray (N4), well sorted, finely laminated, moderately calcite cemented, fossil indentations.	1.6	68.3	
10	Claystone, grayish-black (5GY 2/1), well sorted, fissile, moderately calcite cemented.	0.3	68.6	
10	Mudstone, (5GY 4/1), well sorted, fissile, moderately calcite cemented.	0.2	68.8	
10	Claystone, grayish-black (N2), well sorted, homogenous, weakly calcite cemented.	0.4	69.2	
11	Mudstone, grayish-black (5Y 2/1),well sorted, finely laminated, weakly calcite cemented.	0.3	69.5	
11	Claystone, grayish-black (N2), well sorted, massive, weakly calcite cemented.	0.5	70.0	
11-12†	Mudstone, olive-black (5Y 2/1), well sorted, finely laminated, weakly calcite cemented, minor shell fragments.	3.6	73.6	
13-15†	Mudstone, olive gray to greenish-black (5Y 4/1 to 5GY 2/1) moderate to well sorted, massive, weakly calcite cemented, 0-15% lithic fragments.	41.5	115.1	
	Totals (incomplete)		**115.1**	

† some portion of drilled interval advanced by tricone bit (no core taken)

Box	Lithologic Description	Thickness (m)	Total Depth (m) (bottom of unit)	Microbiology Samples
	Twowells Sandstone Tongue of the Dakota Sandstone. Depositional Environment - Marine, regressive, deposited as part of an extensive offshore, shallow-water marine shelf sandstone (Landis and others, 1973). The relative amounts of bioturbation observed throughout the Dakota Sandstone tongues may indicate slow regressive cycles as opposed to fast transgressive cycles in the intertonguing shales (Owen, 1989). The Twowells Sandstone is early upper-Cenomanian in age (Fig. 1) based on ammonite index fossils (Cobban and Hook, 1989).			
16	Sandstone, silty, light olive gray (5Y 5/2), cross bedded, very well sorted, subangular, fine to very fine grained sand (80% fine and very fine sand, 20% clay), moderately to strongly calcite cemented, trace of gluaconite.	0.7	115.8	
16	Sandstone, clay-rich, light olive gray (5Y 5/2), cross bedded, very well sorted, subangular, fine to very fine grained sand (60% fine and very fine sand, 40% clay), moderately to strongly calcite cemented.	0.3	116.1	
16-21	Sandstone, silty, light olive gray (5Y 5/2), very well sorted, subangular, fine to very fine grained sand (80% fine to very fine sand, 20% clay), moderately to strongly calcite cemented, occasional shell fragments. Moderate bioturbation overprints primary cross stratification (mottled).	4.7	120.6	
21	Sandstone, silty, light olive gray (5Y 5/2), very well sorted, subangular, fine to very fine grained sand (80% fine to very fine sand, 20% clay), moderately to strongly calcite cemented. Moderate bioturbation overprints primary lamination (mottled).	1.8	122.4	
21-23	Sandstone, silty, dark gray (N3), very well sorted, subangular, fine to very fine grained sand (80% fine to very fine sand, 20% clay), moderately to strongly calcite cemented, finely laminated. Moderate bioturbation overprints primary cross stratification (mottled).	3.1	125.5	
23-24	Sandstone, silty, grayish-black (N2), very well sorted, subangular, fine to very fine grained sand, moderately to strongly calcite cemented, finely laminated, occasional shell fragment. Moderate bioturbation overprints primary planar and cross laminations (mottled). Fibrous calcite veins (secondary).	1.0	126.5	
24	Sandstone, silty, dark gray (N3), very well sorted, subangular, fine to very fine grained sand, moderately to strongly calcite cemented, finely laminated. Moderate bioturbation overprints primary planar and cross laminations (mottled).	0.3	126.8	
24-25	Sandstone, silty, medium dark gray (N4), very well sorted, subangular, fine to very fine grained sand, moderately to strongly calcite cemented, finely laminated. Moderate bioturbation overprints primary planar and cross laminations (mottled).	1.0	127.8	CNV-X-SC-127.3
25	Sandstone, silty, medium gray (N5), very well sorted, subangular, fine to very fine grained sand, moderately to strongly calcite cemented, finely laminated. Moderate bioturbation overprints primary planar and cross laminations (mottled).	0.1	127.9	
25	Sandstone, silty, medium dark gray (N4), very well sorted, subangular, fine to very fine grained sand, moderately to strongly calcite cemented, finely laminated. Moderate bioturbation overprints primary planar and cross laminations (mottled).	0.2	128.1	

Box	Lithologic Description	Thickness (m)	Total Depth (m) (bottom of unit)	Microbiology Samples
25-33	Sandstone, silty, dark gray to medium dark gray (N3 to N4), well sorted, subangular, fine to very fine grained sand, moderately to strongly calcite cemented, finely laminated, finely disseminated pyrite. Moderate bioturbation overprints primary planar and cross laminations (mottled).	9.4	137.5	
34	Sandstone, silty, grayish-black (N2), well sorted, subangular, fine to very fine grained sand, moderately to strongly calcite cemented, finely laminated. Moderate bioturbation overprints primary planar and cross laminations (mottled).	0.4	137.9	
	Totals		**22.8**	
	Whitewater Arroyo Shale Tongue of the Mancos Shale. Depositional Environment - marine, transgressive, deposited in a shallow-water marine shelf environment that was quieter and deeper than the over- and underlying sandstone tongues (Landis and others, 1973). The Whitewater Arroyo Shale is late middle- to early upper-Cenomanian in age (Fig. 1) based on ammonite index fossils (Cobban and Hook, 1989).			
34-36	Siltstone, sandy, grayish-black (N2), well sorted, subrounded, moderately to strongly calcite cemented, finely laminated. Moderate bioturbation overprints primary planar laminations (mottled), occasional massive fine-grained pyrite, more carbonaceous than above Twowells Sandstone.	2.2	140.1	
36A	Mudstone, sandy, grayish-black (N2), well sorted, clay to fine sand, subrounded, moderately calcite cemented, occasional shell fragments, finely laminated, bioturbated, mottled.	1.3	141.4	CNV-X-SC-140.3
36-37	Siltstone, sandy, dark gray (N3), well sorted, subrounded, clay to fine sand, moderately to strongly calcite cemented, occasional shell fragments, finely laminated, bioturbated, mottled.	1.1	142.5	
37	Bentonite, very light gray (N8), well sorted, homogeneous.	0.1	142.6	
37-42	Siltstone, clay-rich, dark gray to grayish-black (N3 to N2), well sorted, subrounded, clay to fine sand, moderately to strongly calcite cemented, occasional shell fragments, finely laminated, bioturbated, mottled.	6.5	149.1	
42	Bentonite, very light gray (N8), well sorted, homogeneous.	0.2	149.3	CNV-X-SC-149.2
42	Siltstone, clay-rich, grayish-black (N2), well sorted, subrounded, clay to fine sand, moderately to strongly calcite cemented, occasional shell fragments, finely laminated, bioturbated, mottled.	0.6	149.9	
42-43	Mudstone, silty, grayish-black (N2), well sorted, clay (30%) to silt (70%), weakly calcite cemented, laminated, bioturbated.	0.3	150.2	
43	Claystone, silty, grayish black (N2), very well sorted, clay (90%) to silt (10%), weakly calcite cemented, laminated, bioturbated.	0.1	150.3	
43-46	Mudstone, silty, grayish-black (N2), well sorted, clay (30%) to silt (70%), weakly calcite cemented, occasional shell fragment, disseminated pyrite, laminated, bioturbated.	3.2	153.5	
46	Mudstone, sandy, grayish-black (N2), well sorted, clay (70%) to fine sand (30%), weakly calcite cemented, occasional shell fragment, laminated, bioturbated, calcite veining.	0.2	153.7	
	Totals		**15.6**	

Box	Lithologic Description	Thickness (m)	Total Depth (m) (bottom of unit)	Microbiology Samples
	Paguate Sandstone Tongue of the Dakota Sandstone. Depositional Environment - marine, regression. The interbedding of sandstones and mudstones in this unit represent a mixture of open-marine shelf and nearshore marine environments (Landis and other, 1973). The upper silty sandstones were deposited on an open-marine shelf while the more sandy mudstones are indicative of nearshore marine environments. The Paguate Sandstone tongue is late middle-Cenomanian in age (Fig. 1) based on ammonite index fossils (Cobban and Hook, 1989).			
46-49	Sandstone, silty, medium gray to medium dark gray (N5 to N4), very well sorted, silt (30%) to very fine sand (70%), subangular to subrounded grains, moderately calcite cemented, laminated, bioturbated; abundant dark streaks of organic carbon near top of unit, trace of gluaconite.	3.8	157.5	
49-50	Mudstone, sandy, dark gray (N3), very well sorted, clay (50%) to very fine sand (50%), subrounded grains, weakly to moderately calcite cemented, cross laminated, bioturbated.	1.3	158.8	
50-53	Sandstone, silty, dark gray to medium dark gray (N3 to N4), very well sorted, silt (30%) to very fine sand (70%), subangular to subrounded grains, moderately calcite cemented, homogeneous to thinly cross-laminated, bioturbated; dark organic-rich laminations, occasional shell fragment.	3.4	162.2	
53-57	Mudstone, sandy, grayish-black (N2), very well sorted, clay (60-70%) to very fine sand (30-40%), subrounded grains, weakly to moderately calcite cemented, cross laminated, bioturbated; disseminated pyrite, dark organic-rich laminations, occasional chert fragments.	5.8	168.0	CNV-X-SC-164.2 CNV-X-SC-165.8
57-61	Sandstone, clay-rich, dark gray (N3 to N4), very well sorted, silt (40%) to very fine sand (60%), weakly calcite cemented, thinly cross-laminated, bioturbated, occasional shell fragment, occasional disseminated pyrite.	8.6	176.6	CNV-X-SC-170.4
	Totals		**22.9**	

	Clay Mesa Shale Tongue of the Mancos Shale. Depositional Environment - marine, transgressive. The lower, finer-grained (i.e. mudstones and claystones) Clay Mesa Shale units are indicative of open-marine, shelf environments. The coarser-grained siltstones near the top of the Clay Mesa section are shallower, nearshore deposits (Landis and others, 1973). The Clay Mesa Shale is middle-Cenomanian in age (Fig. 1) based on ammonite index fossils (Cobban and Hook, 1989).			
62	Siltstone, clay-rich, dark gray (N3), very well sorted, silt (50%) to very fine sand (50%), moderately calcite cemented, thinly cross-laminated, bioturbated.	2.4	179.0	CNV-X-SC-178.9
62	Mudstone, dark gray (N3), very well sorted, moderately calcite cemented, thinly cross-laminated, bioturbated, occasional shell fragments.	2.5	181.5	
63-64	Claystone, grayish-black (N2), very well sorted, clay (70%) to silt (30%), moderately calcite cemented, thin organic-rich laminations, occasional mollusk shells and fragments.	1.8	183.3	
64-65	Mudstone, grayish black (N2), very well sorted, silt and clay (90%) to very fine sand (10%), moderately calcite cemented, thin organic-rich laminations, occasional mollusk shells fragments.	1.7	185.0	CNV-X-SC-183.9

Box	Lithologic Description	Thickness (m)	Total Depth (m) (bottom of unit)	Microbiology Samples
65	Claystone, grayish-black (N2), very well sorted, clay (70%) to silt (30%), moderately calcite cemented, thin organic-rich laminations, fissile, occasional mollusk shells and fragments.	0.7	185.7	CNV-X-SC-185.7
	Totals		9.1	
	Cubero Sandstone Tongue of the Dakota Sandstone. Depositional Environment - marine, regressive. The lower muddy sandstone represents a deeper nearshore environment while the silty sandstones near the top are indicative of shallow nearshore environments. The general coarsening upward sequence observed in the Cubero is characteristic of all three Dakota Sandstone tongues and represents a shallowing (upwards) sea (Landis and others, 1973). The Cubero Sandstone is middle-Cenomanian in age (Fig. 1) based on ammonite index fossils (Cobban and Hook, 1989).			
65-66	Sandstone, silty, moderate dark gray to medium gray (N4 to N5), very well sorted, moderately calcite cemented, thin organic-rich laminations, fossiliferous.	0.6	186.3	
66-71	Sandstone, dark gray to light gray (N3 to N6), very well sorted, subrounded, 1 mm mud drapes; clean, medium-grained quartz sand (95%), very bioturbated, mottled.	9.0	197.3	CNV-X-SC-187.1 CNV-X-SC-188.5 Heterogeneity-189.7 Heterogeneity-191.3 CNV-X-SC-193.1 CNV-X-SC-196.3 CNV-X-SC-196.1
71-72	Sandstone, muddy, dark gray to light gray (N3 to N6), very well sorted, subangular to subrounded, medium-grained quartz sand, very bioturbated, mottled.	1.4	198.7	
	Totals		13.0	
	Oak Canyon Member of the Dakota Sandstone (incomplete). Depositional Environment - terrestrial and marine. Although the full section was not drilled, the sequence of shales, silty sandstone, and sandstones in the Oak Canyon represent a complex assemblage of fluviatile, lagoonal, estuarine and open-marine depositional environments. The muddy sandstone and sandy mudstone sequence drilled below is entirely in the upper, transgressive marine unit of the Oak Canyon and were deposited in an open-marine to nearshore environment. The Oak Canyon Member is early middle-Cenomanian in age (Fig. 1) based on ammonite index fossils (Cobban and Hook, 1989).			
72-73	Sandstone, muddy, medium dark gray (N4), very well sorted, subangular, moderately calcite cemented, fossiliferous, muddy laminations, bioturbated.	2.4	201.0	CNV-X-SC-200.3 CNV-X-SC-201.0
74	Mudstone, sandy, olive black (5Y 2/1), very well sorted, clay to fine sand, homogeneous, moderately cemented, calcite filled fractures.	0.8	201.8	CNV-X-SO-201.6
74	Sandstone, muddy, medium dark gray (N4), very well sorted, subangular, moderately calcite cemented, fossiliferous, muddy laminations, bioturbated.	0.4	202.2	

Box	Lithologic Description	Thickness (m)	Total Depth (m) (bottom of unit)	Microbiology Samples
74	Bentonite, light olive gray (5Y 6/1), well cemented.	0.1	202.3	
74-76	Sandstone, muddy, medium dark gray (N4), very well sorted, subangular, moderately calcite cemented, fossiliferous, muddy laminations, bioturbated, occurrences of pyrite.	3.1	205.2	CNV-X-SC-202.5 CNV-X-SC-203.3 CNV-X-SC-204.0
	Totals (incomplete)		**6.5**	

END OF HOLE

Box	Lithologic Description	Thickness (ft)	Total Depth (ft) (bottom of unit)	Microbiology Samples
	Soil.			
1	Soil, silty, unconsolidated, light olive gray (5Y 5/2), very well sorted, homogeneous. 75% silt, 25% clay. Occasional gypsum-filled fracture.	19.2	19.2	
	Total	19.2		
	Mancos Shale, main body (incomplete). Depositional Environment - marine, transgressive, deposition occurred on or near edge of continental shelf. Transgression most likely caused by eustatic sea-level rise in middle- to upper-Cenomanian time (~96 to 91 Ma) (Vail and others, 1977). This section of the main body is upper-Cenomanian to lower-Turonain in age (Fig. 1) based on ammonite index fossils (Cobban and Hook, 1989).			
2-11	Mudstone, clay-rich, light olive gray (5Y 5/2), very well sorted, laminar bedded (0.5 to 2.0 mm), weakly to moderately consolidated and weak to moderately calcite cemented. Gypsum-filled fractures common near the top of unit and hell fragments common near the base of unit. Occasional interbedded muddy sandstone or sandy mudstone not more than 1 foot thick. Septarian concretion at 70.5 ft.	93.3	112.5	
12-18	Claystone, grayish-black (N2), very well sorted, fissile, homogeneous, moderate to strongly calcite cemented, shell fragments throughout section.	56.5	169.0	CNA-R-X-SC-160.5
18-19	Claystone, grayish-black to medium gray (N2 to N5), sandy near the top with gypsum-filled fractures, very well sorted, fissile, homogeneous, moderate to strongly calcite cemented.	14.0	183.0	
19-21	Claystone, grayish-black (N2), very well sorted, fissile, homogeneous, moderate to strongly calcite cemented, shell fragments throughout section.	12.5	195.5	
21	Sandstone, muddy, grayish-black to medium gray (N2 to N5), very well sorted, finely laminated and cross-bedded, bioturbated, moderate to strongly calcite cemented, pyrite at 198.0 ft.	4.5	200.0	
	MUD MOTOR DRILLING - NO CORE	80.0	280.0	
22	Claystone, grayish-black (N2), very well sorted, fissile, homogeneous, moderate to strongly calcite cemented, shell fragments throughout section.	4.0	284.0	
22	Mudstone, sandy, grayish-black to moderate dark gray (N2 to N4), very well sorted, laminated, bioturbated, moderate to strongly calcite cemented.	2.0	286.0	
23-24A	Sandstone, muddy, grayish-black to moderate light gray (N2 to N6), very well sorted, finely laminated, bioturbated, moderate to strongly calcite cemented, shell fragments throughout, pyrite at 295.0 ft.	17.5	303.5	CNA-R-X-SC-91.6
24A-24B	Mudstone, sandy, grayish-black to moderate dark gray (N2 to N4), very well sorted, laminated, bioturbated, moderate to strongly calcite cemented, shell fragments throughout, pyrite at 307.5 ft.	11.0	314.5	CNA-R-X-SC-93.5
24B	Bentonite, (5GY 6/1), well sorted, calcite cemented.	1.0	315.5	
24B-25	Mudstone, sandy, dark gray (N3), very well sorted, laminated, moderate to strongly calcite cemented, shell fragments throughout.	11.0	326.5	
25-26	Claystone, grayish-black (N2), very well sorted (<5% sand), laminated, moderate to strongly calcite cemented, shell fragments throughout section.	2.3	328.8	

Box	Lithologic Description	Thickness (ft)	Total Depth (ft) (bottom of unit)	Microbiology Samples
26	Mudstone, sandy, dark gray (N3), moderately sorted (sand grades in and out), laminated, moderate to strongly calcite cemented, shell fragments throughout.	6.2	335.0	
26-27	Claystone, grayish-black (N2), very well sorted, laminated, fissile, moderate to strongly calcite cemented, shell fragments throughout section.	3.2	338.2	
27	Sandstone, light gray (N7), very well sorted, laminated, bioturbated, moderate to strongly calcite cemented.	0.3	338.5	
27	Mudstone, sandy, grayish-black (N2), very well sorted, laminated, moderate to strongly calcite cemented, shell fragments and disseminated pyrite throughout.	7.5	346.0	
27	Sandstone, (N8), very well sorted, laminated, cross-bedded, bioturbated, moderate to strongly calcite cemented.	0.3	346.3	
27-28	Mudstone, sandy, grayish-black to dark gray (N2 to N3), very well sorted, small bioturbated sandstone lenses, laminated, moderate to strongly calcite cemented, shell fragments throughout.	4.1	350.4	
28	Sandstone, muddy, dark gray to medium gray (N3 to N5), very well sorted, laminated, cross-bedded, bioturbated, moderate to strongly calcite cemented, shell fragments throughout, pyrite at 358.0 ft.	9.1	359.5	
29	Mudstone, sandy, grayish-black to dark gray (N2 to N3), very well sorted, laminated, moderate to strongly calcite cemented, shell fragments throughout.	2.5	362.0	
29-35	Claystone, grayish-black (N2), very well sorted, homogeneous, fissile, moderate to strongly cemented, occasional fossil, organic material, and sandstone lens.	55.0	417.0	
35-37	Mudstone, sandy, grayish-black to moderate dark gray (N2 to N4), very well sorted, laminated, cross-bedded, bioturbated, weakly calcite cemented.	13.5	430.5	
37-40	Claystone, grayish-black (N2), very well sorted, homogeneous to laminated, fissile, weakly cemented, occasional fossil, organic material, and sandstone lenses.	17.5	448.0	
	MUD MOTOR DRILLING - NO CORE	162.0	610.0	
39-51†	Claystone, dark gray to olive black (N3 to 5Y 2/1), very well sorted, homogeneous to laminated, fissile, weakly calcite cemented, occasional fossil and organic material throughout unit. Mica flakes common near top of unit, interbedded thin silty sandstone layers common over the lower 2/3 of the unit	123.0	733.0	CNA-R-X-SC-200.0
51-54	Siltstone, dark gray to olive black (N3 to 5Y 2/1), moderate to well sorted, homogeneous to laminated, moderate to strongly calcite cemented. Shell fragments and sparry calcite laminae (1 to 4 laminae every foot) present in the lower 10 feet of the unit. Silvery (sulfide) replacement on shell fragment at 764.0 feet.	35.5	768.5	CNA-R-X-SC-227.6
54	Claystone, dark gray (N3), well sorted, laminated, moderate to strongly cemented, occasional fossil.	2.5	771.0	
55	Siltstone, moderate dark gray (N4), moderately sorted, blocky to laminated, moderate to strongly calcite cemented.	1.5	772.5	

† some portion of interval lost in coring

Box	Lithologic Description	Thickness (ft)	Total Depth (ft) (bottom of unit)	Microbiology Samples
55†	Mudstone, grayish-black (N2), moderately sorted, blocky to laminated, weakly calcite cemented. Fine-grained, disseminated organic material on biotite flakes near base of section.	5.3	777.8	
55-57†	Siltstone, olive black (5Y 2/1), moderately sorted, homogeneous to laminated, moderate to strongly calcite cemented. Shell fragments prominent throughout unit. Pyrite occurs at 790.3 and 809.5 feet.	39.2	817.0	CNA-R-X-SC-239.9
	Totals (incomplete)		797.8	

	Twowells Sandstone Tongue of the Dakota Sandstone. Depositional Environment - Marine, regressive, deposited as part of an extensive offshore, shallow-water marine shelf sandstone (Landis and others, 1973). The relative amounts of bioturbation observed throughout the Dakota Sandstone tongues may indicate slow regressive cycles as opposed to fast transgressive cycles in the intertonguing shales (Owen, 1989). The Twowells Sandstone is early upper-Cenomanian in age (Fig. 1) based on ammonite index fossils (Cobban and Hook, 1989).			
57-58†	Sandstone, medium dark gray (N4), poorly sorted, shells throughout base of section, subangular, medium to very fine grained sand (30% medium sand, 40% fine sand, and 30% very fine sand to clay), moderately to strongly calcite cemented. The unit generally fines downward.	8.8	825.8	CNA-R-X-SC-251.6
58-60†	Sandstone, silty, dark gray to medium dark gray (N4 to N3), well sorted, subangular, fine sand to clay (80-90% fine and very fine sand, 10-20% clay), moderately to strongly calcite cemented. Gluaconite occurs throughout the upper and middle portion of the unit. Shell fragments are common near the top. Organic laminations common in the lower 1/2 of unit.	26.7	852.5	
60	Sandstone, medium dark gray (N3), moderately sorted, subangular, medium to very fine grained sand (50% medium sand, 30% fine sand, and 20% very fine sand), laminated, bioturbated, mottled, moderately to strongly calcite cemented, occasional shell fragments. Gluaconite present throughout interval.	1.0	853.5	CNA-R-X-SC-259.9
60	Sandstone, silty, medium dark gray (N4), well sorted, subangular, laminated, fine sand to silt, moderately to strongly calcite cemented. Moderate bioturbation overprints primary lamination (mottled).	3.3	856.8	CNA-R-X-SC-260.5
60	Sandstone, medium dark gray (N4), moderately sorted, subangular, medium to fine grained sand, moderately to strongly calcite cemented. Moderate bioturbation overprints primary bedding (mottled).	1.4	858.2	

† some portion of interval lost in coring

Box	Lithologic Description	Thickness (ft)	Total Depth (ft) (bottom of unit)	Microbiology Samples
60-63†	Sandstone, medium dark gray (N4), moderately sorted, subangular, medium to very fine grained sand (40% medium sand and 40% fine sand near top; 60% fine sand, 30% very fine sand, and 10 clay near the base), moderately to strongly calcite cemented, finely laminated. Moderate bioturbation overprints primary planar laminations (mottled). Gluaconite is common throughout the lower 3/4 of unit; organic-rich laminations common over the lower 10 ft.; pyrite occurs at 867.0 ft.	35.8	894.0	CNA-R-X-SC-299.0
63-73	Sandstone, silty, dark gray to medium gray (N3 to N5), moderate to well sorted, subangular, fine sand to clay (10-60% fine sand, 50-60% very fine sand, and 10-40% clay),weak to moderately calcite cemented, finely laminated (organic-rich laminations). Moderate bioturbation overprints primary planar laminations (mottled). Gluaconite and shell fragments scattered throughout section. Pyrite occurs at 975.4, 978.0, and 991.5 ft.	99.2	993.2	
	Totals		176.2	
	Whitewater Arroyo Shale Tongue of the Mancos Shale. Depositional Environment - marine, transgressive, deposited in a shallow-water marine shelf environment that was quieter and deeper than the over- and underlying sandstone tongues (Landis and others, 1973). The Whitewater Arroyo Shale is late middle- to early upper-Cenomanian in age (Fig. 1) based on ammonite index fossils (Cobban and Hook, 1989).			
73-76	Siltstone, sandy, grayish-black to olive black (N2 to 5Y 2/1), moderately sorted, very fine sand to silt (20-40% very fine sand and 60-80% silt), weak to moderately calcite cemented, finely laminated. Moderate bioturbation overprints primary planar laminations (mottled); gluaconitic near the top; occasional shell fragment. Disseminated pyrite occurs at 993.5, 1003.0, and 1008.0 ft. This first siltstone unit in the Whitewater is comparably finer-grained than above Twowells Sandstone.	16.3	1009.5	
75	Bentonite, very light gray (N8), well sorted, homogeneous.	0.1	1009.6	
75-76	Siltstone, grayish-black to olive black (N3 to 5Y 2/1), moderately sorted, very fine sand to clay (20% very fine sand and 80% silt and clay),weak to moderately calcite cemented, occasional shell fragments near the top of section, finely laminated, bioturbated, mottled. Pyrite occurs at 1014.8 and 1018.2 ft.	17.6	1027.2	CNA-R-X-SC-310.8
76	Bentonite, very light gray (N8), well sorted, homogeneous.	0.2	1027.4	
76-81	Siltstone, olive black (5Y 2/1), moderately sorted, very fine sand to clay (20-40% very fine sand and 60-80% silt and clay), weak to moderately calcite cemented, shell fragments throughout, finely laminated and bioturbated. Pyrite occurs at 1029.5,1043.8, and 1061.8 ft.	55.8	1083.2	CNA-R-X-SC-315.4 CNA-R-X-SC-319.7 CNA-R-X-SC-329.2

† some portion of interval lost in coring

Box	Lithologic Description	Thickness (m)	Total Depth (m) (bottom of unit)	Microbiology Samples
81	Mudstone, sandy, grayish-black to moderate dark gray (N2 to N4), moderately sorted, very fine sand to clay (30-40% very fine sand and 60-70% silt and clay), weakly calcite cemented, shell fragments, laminated, and bioturbated.	4.8	1088.0	
	Totals		**94.8**	
	Paguate Sandstone Tongue of the Dakota Sandstone. Depositional Environment - marine, regression. The interbedding of sandstones and mudstones in this unit represent a mixture of open-marine shelf and nearshore marine environments (Landis and other, 1973). The upper silty sandstones were deposited on an open-marine shelf while the more sandy mudstones are indicative of nearshore marine environments. The Paguate Sandstone tongue is late middle-Cenomanian in age (Fig. 1) based on ammonite index fossils (Cobban and Hook, 1989).			
82-88	Sandstone, muddy, medium gray to grayish black (N5 to N2), well sorted, very fine sand to clay, subangular to subrounded grains, moderate to strongly calcite cemented, laminated, bioturbated (mottled); abundant dark laminations of organic carbon, disseminated gluaconite and shell fragments throughout section. Pyrite at 1135.3 and 1138.2 feet.	77.6	1165.6	CNA-R-X-SC-338.7 CNA-R-X-SC-344.2 CNA-R-X-SC-350.3
88	Sandstone, limy, medium light gray (N6), well sorted, very fine sand to clay, subangular to subrounded grains, strongly calcite cemented, abundant mollusk shells.	1.0	1166.6	CNA-R-X-SC-355.4
88-89	Sandstone, muddy, medium gray to grayish black (N5 to N2), well sorted, very fine sand to clay, subangular to subrounded grains, moderate to strongly calcite cemented, laminated, bioturbated (mottled); abundant dark laminations of organic carbon, shell fragments throughout section.	11.9	1178.5	
89-90	Sandstone, limy, medium light gray (N6), very well sorted, very fine sand to clay, subangular to subrounded grains, strongly calcite cemented; 2 inch layer of carbonaceous shale at top.	2.5	1181.0	
90	Sandstone, muddy, medium gray to grayish black (N5 to N2), well sorted, very fine sand to clay, subangular to subrounded grains, moderate to strongly calcite cemented, laminated, bioturbated (mottled), and cross-bedded; shell fragments.	3.0	1184.0	
90	Sandstone, limy, medium light gray (N6), very well sorted, very fine sand to clay, subangular to subrounded grains, laminated, strongly calcite cemented.	0.3	1184.3	
90-92	Sandstone, muddy, medium gray to grayish black (N5 to N2), well sorted, very fine sand to clay, subangular to subrounded grains, moderate to strongly calcite cemented, laminated, bioturbated (mottled), and cross-bedded; shell fragments common near top.	25.7	1210.0	CNA-R-X-SC-361.1
	Totals		**122.0**	

Box	Lithologic Description	Thickness (m)	Total Depth (m) (bottom of unit)	Microbiology Samples
	Clay Mesa Shale Tongue of the Mancos Shale. Depositional Environment - marine, transgressive. The lower, finer-grained (i.e. mudstones and claystones) Clay Mesa Shale units are indicative of open-marine, shelf environments. The coarser-grained siltstones near the top of the Clay Mesa section are shallower, nearshore deposits (Landis and others, 1973). The Clay Mesa Shale is middle-Cenomanian in age (Fig. 1) based on ammonite index fossils (Cobban and Hook, 1989).			
92-93	Mudstone, sandy, dark gray to grayish black (N3 to N2), very well sorted, very fine sand to clay, weakly calcite cemented, thinly cross-laminated, bioturbated, shell fragments throughout Pyrite at 1222.5 feet.	20.5	1230.5	CNA-R-X-SC-371.1
93-95	Claystone, grayish-black to black (N2 to N1), very well sorted, clay to silt, moderately cemented, laminated and fissile, occasional mollusk shells and fragments throughout section.	29.5	1260.0	CNA-R-X-SC-375.3 CNA-R-X-SC-378.4 CNA-R-X-SC-381.8
	Totals		**50.0**	
	Cubero Sandstone Tongue of the Dakota Sandstone. Depositional Environment - marine, regressive. The lower muddy sandstone represents a deeper nearshore environment while the silty sandstones near the top are indicative of shallow nearshore environments. The general coarsening upward sequence observed in the Cubero is characteristic of all three Dakota Sandstone tongues and represents a shallowing (upwards) sea (Landis and others, 1973). The Cubero Sandstone is middle-Cenomanian in age (Fig. 1) based on ammonite index fossils (Cobban and Hook, 1989).			
95-96	Sandstone, silty, medium gray to gray black (N5 to N2), well sorted, medium sand to clay (majority is fine to very fine sand), subangular to subrounded grains, moderately calcite cemented, laminated, bioturbated, and cross-bedded.	11.5	1271.5	CNA-R-X-SC-384.3 CNA-R-X-SC-388.5 CNA-R-X-SC-387.5
96-98	Sandstone, muddy, dark gray to moderate dark gray (N3 to N4), well sorted, subangular to subrounded, moderately calcite cemented, cross-laminated (silt-rich), very bioturbated (mottled).	20.5	1292.0	CNA-R-X-SC-390.9
98	Sandstone, limy, dark gray to moderate dark gray (N3 to N4), very well sorted, subangular, strongly calcite cemented, laminated.	0.3	1292.3	
98-100	Sandstone, muddy, dark gray to moderate dark gray (N3 to N4), well sorted, medium sand to clay (majority fine to very fine sand), subangular, moderately calcite cemented, cross-laminated, bioturbated.	17.7	1310.0	CNA-R-X-SC-397.1
100-101	Sandstone, muddy with limy interbeds, dark gray to light gray (N3 to N6), very well sorted, subangular, medium-grained quartz sand to clay (mostly fine to very fine sand), cross-laminated (shale-rich), very bioturbated, mottled. Limy sections are calcite cemented, muddy sections are weakly calcite cemented.	11.0	1321.0	
	Totals		**61.0**	

Box	Lithologic Description	Thickness (m)	Total Depth (m) (bottom of unit)	Microbiology Samples
	Oak Canyon Member of the Dakota Sandstone. Depositional Environment - terrestrial and marine. Although the full section was not drilled, the sequence of shales, silty sandstone, and sandstones in the Oak Canyon represent a complex assemblage of fluviatile, lagoonal, estuarine and open-marine depositional environments. The muddy sandstone and sandy mudstone sequence drilled below is entirely in the upper, transgressive marine unit of the Oak Canyon and were deposited in an open-marine to nearshore environment. The Oak Canyon Member is early middle-Cenomanian in age (Fig. 1) based on ammonite index fossils (Cobban and Hook, 1989).			
101-102	Sandstone, muddy, medium dark gray (N4), very well sorted, subangular, clay to silt, moderately calcite cemented, cross-laminated, bioturbated. Limy near top.	12.2	1333.2	CNA-R-X-SC-405.5
102	Bentonite, moderate dark gray (N4), well cemented calcite veined. Contains a lime concretion.	2.8	1336.0	
102	Sandstone, muddy, medium dark gray (N4), very well sorted, subangular, moderately calcite cemented, fossiliferous, laminated, bioturbated.	2.5	1338.5	
102-103	Sandstone, limy, medium dark gray (N4), very well sorted, subangular, clay to fine sand, moderately calcite cemented, laminated.	1.5	1340.0	
103	Sandstone, muddy, medium gray to medium dark gray (N5 to N4), well sorted, clay to fine sand (mostly very fine sand), moderately calcite cemented, cross-laminated, bioturbated.	10.5	1350.5	CNA-R-X-SC-409.8
103-104	Sandstone, limy, moderate light gray to dark gray (N6 to N4), well sorted, clay to fine sand, strongly calcite cemented, cross-laminated, bioturbated.	4.5	1355.0	
104	Sandstone, muddy, dark gray to medium dark gray (N3 to N4), well sorted, clay to fine sand, moderately calcite cemented, cross-laminated.	4.0	1359.0	
104-105	Mudstone, sandy, dark gray to grayish black (N3 to N2), well sorted, clay to fine sand, weakly calcite cemented, laminated, bioturbated, mollusk shells near the base.	5.0	1364.0	
105	Mudstone, dark gray to grayish black (N3 to N2), well sorted, clay to very fine sand, weakly calcite cemented, laminated, bioturbated, mollusk shells throughout.	8.5	1372.5	CNA-R-X-SC-417.4
105	Mudstone, sandy, dark gray to grayish black (N3 to N2), well sorted, clay to very fine sand, moderately calcite cemented, laminated, bioturbated, mollusk shells throughout.	2.5	1375.0	
106	Sandstone, muddy with limy interbeds, dark gray to moderate light gray (N3 to N6), well sorted, clay to very fine sand, moderate to strongly calcite cemented, cross-laminated, bioturbated, mollusk shells throughout.	5.5	1380.5	
106	Bentonite, moderate light gray (N6), well cemented.	1.0	1381.5	
106-107	Mudstone, sandy, dark gray to grayish black (N3 to N2), well sorted, clay to very fine sand, moderately calcite cemented, laminated, bioturbated, mollusk shells near top. Pyrite occurs at 1383.0,1385.0, and 1389.0 ft.	9.5	1391.0	
107-108	Shale, grayish black (N2), very well sorted, clay to very fine sand, weakly calcite cemented, laminated, fissile. Pyrite occurs at 1392.5 ft.	8.0	1399.0	CNA-R-X-SC-425.0
108-110	Sandstone, muddy, moderate dark gray to medium gray (N4 to N5), well sorted, subangular, clay to medium sand, weakly calcite cemented, cross-laminated, bioturbated, thin silty laminations throughout.	25.0	1424.0	CNA-R-X-SC-426.5

Box	Lithologic Description	Thickness (m)	Total Depth (m) (bottom of unit)	Microbiology Samples
110	Sandstone, medium gray (N5), very well sorted (quartz arenite), subangular, clay to medium sand (mostly medium sand), weakly calcite cemented, few laminations.	4.0	1428.0	
110-112	Sandstone, muddy, moderate dark gray to medium gray (N4 to N5), well sorted, subangular, clay to medium sand, weakly calcite cemented, cross-laminated, bioturbated.	19.0	1447.0	CNA-R-X-SC-436.7
112	Bentonite, moderate light gray (N6), well cemented.	0.5	1447.5	
112-113	Sandstone, muddy, moderate dark gray to medium gray (N4 to N5), well sorted, subangular, clay to medium sand, weakly calcite cemented, cross-laminated, bioturbated.	4.5	1452.0	
113	Basalt, grayish black (N2), fine grained, vesicular, calcite veined. Vesicles filled with white mineral (zeolite ?).	4.0	1456.0	
113	Sandstone, muddy, moderate dark gray to medium gray (N4 to N5), well sorted, subangular, clay to medium sand, weakly calcite cemented, cross-laminated, bioturbated.	5.5	1461.5	
	Totals		**140.5**	

	Jackpile Sandstone of the Morrison Formation (incomplete). Depositional Environment - terrestrial, braided-stream. The Jackpile sandstone was deposited by a low-energy braided stream system, probably on the distal portion of a low-gradient alluvial fan (Owen, 1982). Alteration minerals (primarily kaolinite) indicate the climate was arid and located far from the sea (Bell, 1981). Overbank and floodplain deposits (i.e. siltstones) generally are minor components (Flesch, 1974).			
114-115	Sandstone, moderate light gray (N6), very well sorted, subangular, fine to medium sand, strongly cemented, massive.	23.0	1484.5	CNA-R-X-SC-451.2
115-116	Sandstone, muddy (high kaolinite content), moderate light gray (N6), moderately sorted, subangular, clay to fine sand, weak to moderately cemented, massive.	14.0	1498.5	
116	Basalt, grayish black (N2), fine grained, vesicular.	1.0	1499.5	
117-121	Sandstone, muddy (high kaolinite content), moderate light gray to light gray (N6 to N7), well sorted, subangular, clay to fine sand, moderately cemented, massive to few laminations. Occasional dark blue-green laminations up to 0.5 inch thick.	47.5	1547.0	CNA-R-X-SC-457.3 CNA-R-X-SC-464.2
121	Basalt, grayish black (N2), fine grained, vesicular.	3.5	1550.5	CNA-R-X-SC-472.6
121	Siltstone, (5GY 4/1), moderately sorted, clay to silt, moderately cemented, few laminations.	3.5	1554.0	
121	Sandstone, muddy (high kaolinite content), greenish gray (5GY 6/1), moderately sorted, subangular, clay to fine sand, moderately cemented, massive to few laminations.	5.5	1559.5	CNA-R-X-SC-475.3
122-124	Siltstone, greenish black to brownish black (5GY 2/1 to 5YR 2/1), moderately sorted, clay to silt, moderately cemented, few laminations.	16.2	1575.7	
124	Basalt, grayish black (N2), fine grained, vesicular.	0.5	1576.2	
124-125	Sandstone, muddy (high kaolinite content), greenish gray (5GY 6/1), moderately sorted, subangular, clay to fine sand, moderately cemented, massive to few laminations.	4.7	1580.9	CNA-R-03-SC-481.2 CNA-R-03-SC-481.34 CNA-R-03-SC-481.7
125	Basalt, grayish black (N2), fine grained, vesicular.	0.7	1581.6	

Box	Lithologic Description	Thickness (m)	Total Depth (m) (bottom of unit)	Microbiology Samples
125-126	Sandstone, muddy (high kaolinite content), greenish gray (5GY 6/1), moderately sorted, subangular, clay to fine sand, moderately cemented, massive to few laminations.	9.4	1591.0	CNA-R-02-SC-482.1 CNA-R-X-SC-482.9
	Totals (incomplete)		129.5	
				CNA-R-X-SC-503.9 CNA-R-X-SC-507.3

END OF HOLE

Appendix 4: Results of O_2-Uptake Methods Development Experiments

Trial 1:

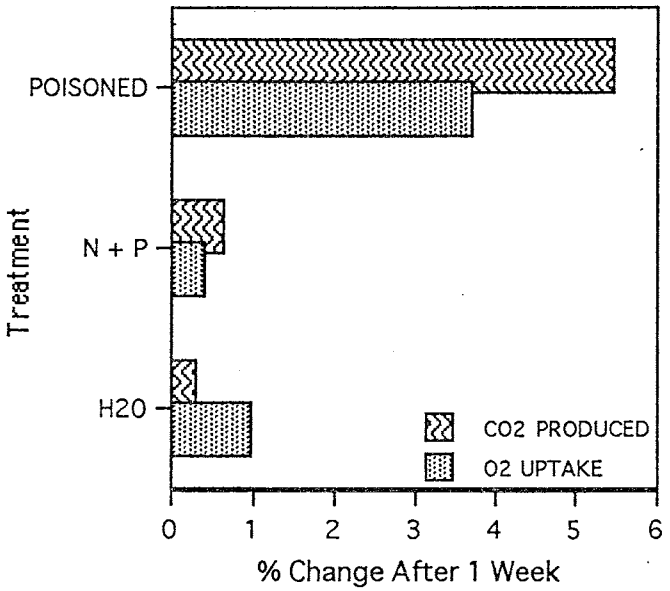

Vials set up according to procedure. Poison was 3.7% formadehyde. N + P had added nitrogen and phosphorous. Vials incubated for 1 week.

	SAMPLE ID: GAV 5					
	H_2O					
REPLICATE	CO_2 INITIAL	CO_2 FINAL	CO_2 PRODUCED	O_2 INITIAL	O_2 FINAL	O_2 UPTAKE
a	0.103	0.352	0.249	21.998	21.049	0.949
b	0.097	0.374	0.277	21.983	21.205	0.778
c	0.109	0.442	0.333	21.97	20.971	0.999
AVERAGE	0.106	0.397	0.291	21.984	21.010	0.974
STDEV	0.004	0.064	0.059	0.020	0.055	0.035

	N + P					
	CO_2 INITIAL	CO_2 FINAL	CO_2 PRODUCED	O_2 INITIAL	O_2 FINAL	O_2 UPTAKE
a	0.662	1.214	0.552	21.617	21.387	0.230
b	0.419	1.096	0.677	21.899	21.476	0.423
c	0.470	1.161	0.691	21.905	21.315	0.590
AVERAGE	0.566	1.187	0.621	21.761	21.351	0.410
STDEV	0.136	0.037	0.098	0.204	0.051	0.255

	FORMALDEHYDE POISONED					
	CO_2 INITIAL	CO_2 FINAL	CO_2 PRODUCED	O_2 INITIAL	O_2 FINAL	O_2 UPTAKE
a	0.200	5.653	5.453	21.564	18.209	3.355
b	0.301	5.810	5.509	21.766	17.732	4.034
c	No Third Replicate					
AVERAGE	0.250	5.735	5.481	21.665	17.970	3.694
STDEV	0.071	0.111	0.040	0.143	0.337	0.480

Trial 2:

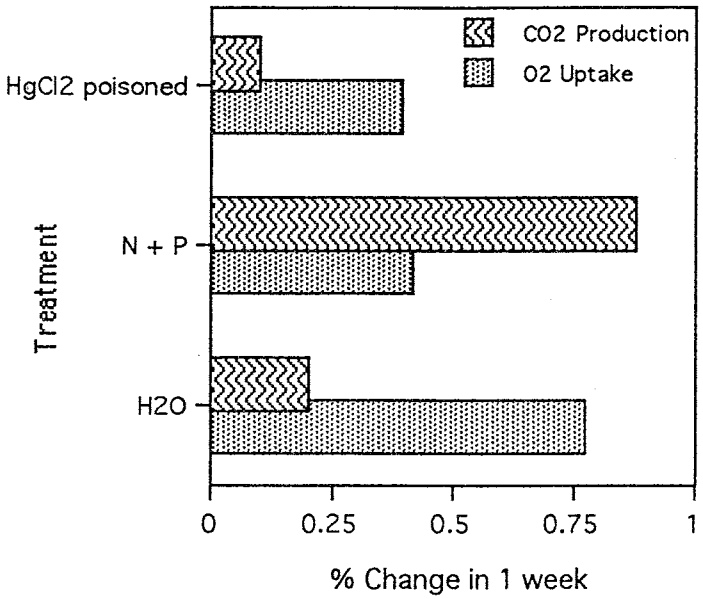

Vials set up according to procedure. Poison was 500 μg ml^{-1} $HgCl_2$. N + P had added nitrogen and phosphorous. Vials incubated for 1 week.

	SAMPLE ID: GAV 8					
	H_2O					
REPLICATE	CO_2 INITIAL	CO_2 FINAL	CO_2 PRODUCED	O_2 INITIAL	O_2 FINAL	O_2 UPTAKE
a	0.073	0.281	0.208	21.773	21.173	0.600
b	0.074	0.268	0.194	22.018	21.182	0.836
c	0.075	0.278	0.203	22.018	21.077	0.941
AVERAGE	0.074	0.279	0.205	21.895	21.125	0.770
STDEV	0.001	0.002	0.004	0.173	0.068	0.241

	N + P					
	CO_2 INITIAL	CO_2 FINAL	CO_2 PRODUCED	O_2 INITIAL	O_2 FINAL	O_2 UPTAKE
a	0.309	1.188	0.879	21.906	21.496	0.41
b	0.296	1.153	0.857	21.946	21.285	0.661
c	0.293	1.166	0.873	21.949	21.53	0.419
AVERAGE	0.301	1.177	0.876	21.927	21.513	0.414
STDEV	0.011	0.016	0.004	0.030	0.024	0.006

	$HgCl_2$ POISONED (500 ug/ml)					
	CO_2 INITIAL	CO_2 FINAL	CO_2 PRODUCED	O_2 INITIAL	O_2 FINAL	O_2 UPTAKE
a	0.082	0.189	0.107	22.002	21.494	0.508
b	0.068	0.165	0.097	22.011	21.726	0.285
c	No Third Replicate					
AVERAGE	0.075	0.177	0.102	22.006	21.61	0.396
STDEV	0.010	0.017	0.007	0.006	0.164	0.158

Trial 3:

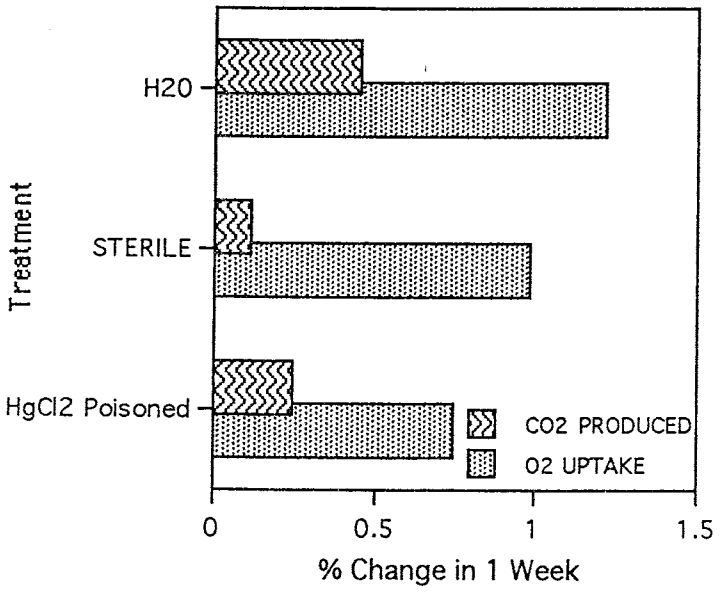

Vials set up according to procedure. Poison was 500 $\mu g\ ml^{-1}\ HgCl_2$. Sterile control was autoclaved for 1 hr on 3 consecutive days. N + P had added nitrogen and phosphorous. Vials incubated 1 week.

	SAMPLE ID: GAV 9					
	H_2O					
REPLICATE	CO_2 INITIAL	CO_2 FINAL	CO_2 PRODUCED	O_2 INITIAL	O_2 FINAL	O_2 UPTAKE
a	0.077	0.492	0.415	22.067	20.681	1.386
b	0.069	0.588	0.519	22.233	20.632	1.601
c	0.073	0.550	0.477	21.831	20.789	1.042
AVERAGE	0.075	0.521	0.446	21.949	20.735	1.214
STDEV	0.003	0.041	0.044	0.167	0.076	0.243

	Sterile Control					
	CO_2 INITIAL	CO_2 FINAL	CO_2 PRODUCED	O_2 INITIAL	O_2 FINAL	O_2 UPTAKE
a	0	0.115	0.115	21.594	20.780	0.814
b	0.060	0.112	0.052	21.526	20.836	0.690
c	0	0.094	0.094	21.872	20.721	1.151
AVERAGE	0	0.104	0.104	21.733	20.750	0.983
STDEV	0.000	0.015	0.015	0.197	0.042	0.238

	$HgCl_2$ POISONED					
	CO_2 INITIAL	CO_2 FINAL	CO_2 PRODUCED	O_2 INITIAL	O_2 FINAL	O_2 UPTAKE
a	0.087	0.345	0.258	21.834	21.132	0.702
b	0.087	0.313	0.226	22.024	21.241	0.783
c	0.087	0.339	0.252	21.907	21.159	0.748
AVERAGE	0.087	0.329	0.242	21.922	21.177	0.744
STDEV	0.000	0.023	0.023	0.096	0.057	0.041

Summary of Poisoned Control Repeats

After running all of the Cerro Negro samples using HgCl2 for the poisoned controls, these samples were selected for repeat, using formaldehyde as the poison. Under "unpoisoned cultures", "first" is the unpoisoned cultures run as part of the original experiment. "Second" is the unpoisoned cultures from the repeat run, 6 mo. later. Values are avg. of 3 replicates.

	UNPOISONED CULTURES				POISONED CULTURES			
	TOTAL CO_2 PRODUCTION (%)		TOTAL O_2 UPTAKE (%)		TOTAL CO_2 PRODUCTION (%)		TOTAL O_2 UPTAKE (%)	
SAMPLE ID	FIRST	SECOND	FIRST	SECOND	FIRST ($HgCl_2$)	SECOND (HCHO)	FIRST ($HgCl_2$)	SECOND (HCHO)
CNV-149.2 (WW)	0±0	0.06±0.007	2.101±0.153	2.212±0.345	0±0	6.857±0.876	2.299±0.117	8.037±1.611
CNV-183.9 (CM)	0±0	0.288±0.035	1.744±0.074	1.477±0.353	0±0	6.228±0.394	1.744±0.243	5.569±0.587
CNAR-239.9 (M)	0.158±0.013	0.3±0.012	1.950±0.519	1.409±0.203	0±0	5.182±0.269	0.672±0.257	4.842±0.218
CNV-164.2 (P)	0.431±0.061	0.211±0.005	2.192±0.246	0.622±0.004	0.405±0.104	3.380±0.073	2.254±0.165	3.084±0.017
CNV-185.7 (C)	0.713±0.073	0.300±0.013	1.609±0.314	0.106±0.051	0.774±0.152	3.832±0.1	1.753±0.509	3.889±0.358
CNV-201.0 (OC)	0±0	0±0	2.551±0.057	1.366±0.259	0±0	7.128±0.3	2.360±0.341	9.808±0.449
CNAR-426.5 (OC)	0.255±0.046	0.057±0.049	2.372±0.072	1.544±0.008	0.081±0.009	0.177±0.012	0.458±0.116	1.912±0.210

Comparison of $HgCl_2$ and Formaldehyde Poisoned Controls
2 Week Incubation

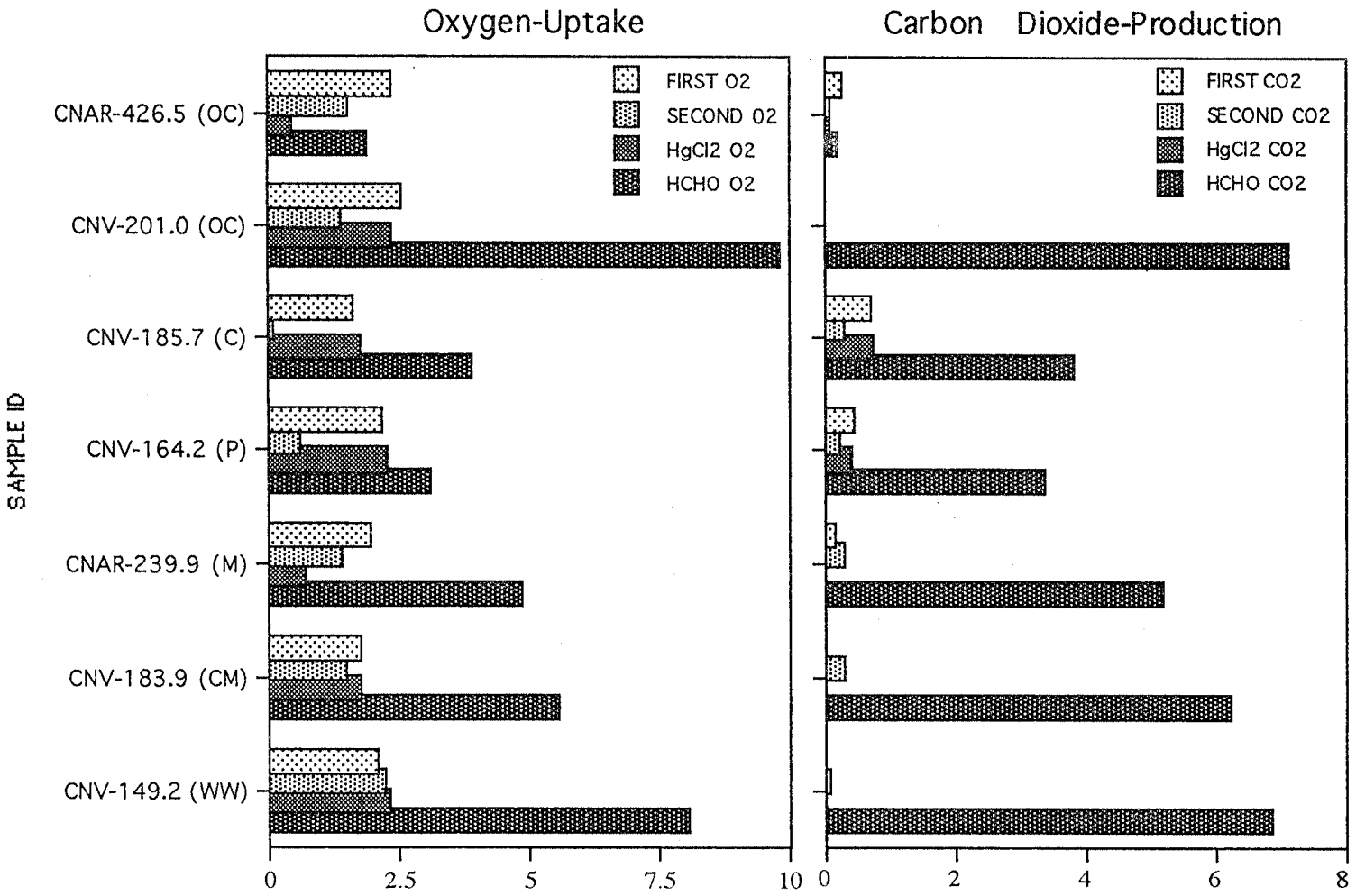

Appendix 5: Complete ANOVA Computer Printouts

TWO-WAY ANOVA: Comparison of Total Viable Cells by Borehole and Stratigraphy

LEVELS ENCOUNTERED DURING PROCESSING ARE:
HOLE$
CNAR CNV
ROCK$
CLAYMESA CUBERO MANCOS OAKCAN PAGUATE TWOWELLS
WTWATER

ANALYSIS OF VARIANCE

SOURCE	SUM-OF-SQUARES	DF	MEAN-SQUARE	F-RATIO	P
HOLE$	0.403	1	0.403	1.545	0.216
ROCK$	1.790	6	0.298	1.144	0.339
HOLE$*ROCK$	0.545	6	0.091	0.348	0.910
ERROR	46.133	177	0.261		

ADJUSTED LEAST SQUARES MEANS.

		ADJ. LS MEAN	SE	N
HOLE$	=CNAR	5.489	0.051	112
HOLE$	=CNV	5.601	0.074	79
ROCK$	=CLAYMESA	5.743	0.143	20
ROCK$	=CUBERO	5.503	0.102	37
ROCK$	=MANCOS	5.523	0.143	20
ROCK$	=OAKCAN	5.414	0.084	39
ROCK$	=PAGUATE	5.506	0.087	35
ROCK$	=TWOWELLS	5.434	0.147	16
ROCK$	=WTWATER	5.692	0.111	24

HOLE$ =CNAR ROCK$ =CLAYMESA	5.589	0.128	16
HOLE$ =CNAR ROCK$ =CUBERO	5.424	0.180	8
HOLE$ =CNAR ROCK$ =MANCOS	5.394	0.128	16
HOLE$ =CNAR ROCK$ =OAKCAN	5.338	0.104	24
HOLE$ =CNAR ROCK$ =PAGUATE	5.520	0.114	20
HOLE$ =CNAR ROCK$ =TWOWELLS	5.453	0.147	12
HOLE$ =CNAR ROCK$ =WTWATER	5.704	0.128	16
HOLE$ =CNV ROCK$ =CLAYMESA	5.898	0.255	4
HOLE$ =CNV ROCK$ =CUBERO	5.581	0.095	29
HOLE$ =CNV ROCK$ =MANCOS	5.653	0.255	4
HOLE$ =CNV ROCK$ =OAKCAN	5.489	0.132	15
HOLE$ =CNV ROCK$ =PAGUATE	5.491	0.132	15
HOLE$ =CNV ROCK$ =TWOWELLS	5.415	0.255	4
HOLE$ =CNV ROCK$ =WTWATER	5.680	0.180	8

TWO-WAY ANOVA: Comparison of CO2-Production by Borehole and Stratigraphy

LEVELS ENCOUNTERED DURING PROCESSING ARE:
HOLE$
CNAR CNV
ROCK$
CLAYMESA CUBERO MANCOS OAKCAN PAGUATE TWOWELLS
WTWATER

ANALYSIS OF VARIANCE

SOURCE	SUM-OF-SQUARES	DF	MEAN-SQUARE	F-RATIO	P
HOLE$	3.233	1	3.233	75.173	.199840E-13
ROCK$	6.455	6	1.076	25.018	.999201E-15
HOLE$*ROCK$	0.567	6	0.095	2.199	0.047
ERROR	5.332	124	0.043		

ADJUSTED LEAST SQUARES MEANS.

		ADJ. LS MEAN	SE	N
HOLE$	=CNAR	0.564	0.025	81
HOLE$	=CNV	0.193	0.035	57
ROCK$	=CLAYMESA	0.141	0.069	12
ROCK$	=CUBERO	0.683	0.048	27
ROCK$	=MANCOS	0.126	0.066	16
ROCK$	=OAKCAN	0.177	0.042	27
ROCK$	=PAGUATE	0.518	0.040	27
ROCK$	=TWOWELLS	0.806	0.070	11
ROCK$	=WTWATER	0.200	0.052	18

HOLE$ =CNAR ROCK$ =CLAYMESA	0.282	0.069	9
HOLE$ =CNAR ROCK$ =CUBERO	0.928	0.085	6
HOLE$ =CNAR ROCK$ =MANCOS	0.252	0.058	13
HOLE$ =CNAR ROCK$ =OAKCAN	0.293	0.049	18
HOLE$ =CNAR ROCK$ =PAGUATE	0.786	0.054	15
HOLE$ =CNAR ROCK$ =TWOWELLS	1.090	0.073	8
HOLE$ =CNAR ROCK$ =WTWATER	0.319	0.060	12
HOLE$ =CNV ROCK$ =CLAYMESA	.166533E-14	0.120	3
HOLE$ =CNV ROCK$ =CUBERO	0.438	0.045	21
HOLE$ =CNV ROCK$ =MANCOS	.110328E-14	0.120	3
HOLE$ =CNV ROCK$ =OAKCAN	0.060	0.069	9
HOLE$ =CNV ROCK$ =PAGUATE	0.249	0.060	12
HOLE$ =CNV ROCK$ =TWOWELLS	0.521	0.120	3
HOLE$ =CNV ROCK$ =WTWATER	0.080	0.085	6

TWO-WAY ANOVA: Comparison of CFU by Borehole and Stratigraphy

LEVELS ENCOUNTERED DURING PROCESSING ARE:
HOLE$
CNAR CNV
ROCK$
CLAYMESA CUBERO MANCOS OAKCAN PAGUATE TWOWELLS
WTWATER

ANALYSIS OF VARIANCE

SOURCE	SUM-OF-SQUARES	DF	MEAN-SQUARE	F-RATIO	P
HOLE$	0.012	1	0.012	0.030	0.864
ROCK$	8.420	6	1.403	3.468	0.003
HOLE$*ROCK$	12.349	6	2.058	5.086	.106524E-03
ERROR	50.181	124	0.405		

ADJUSTED LEAST SQUARES MEANS.

		ADJ. LS MEAN	SE	N
HOLE$	=CNAR	1.735	0.075	81
HOLE$	=CNV	1.757	0.108	57
ROCK$	=CLAYMESA	1.308	0.212	12
ROCK$	=CUBERO	1.950	0.147	27
ROCK$	=MANCOS	2.026	0.204	16
ROCK$	=OAKCAN	1.415	0.130	27
ROCK$	=PAGUATE	1.549	0.123	27
ROCK$	=TWOWELLS	2.204	0.215	11
ROCK$	=WTWATER	1.770	0.159	18

HOLE$	=CNAR			
ROCK$	=CLAYMESA	1.397	0.212	9
HOLE$	=CNAR			
ROCK$	=CUBERO	2.543	0.260	6
HOLE$	=CNAR			
ROCK$	=MANCOS	1.535	0.176	13
HOLE$	=CNAR			
ROCK$	=OAKCAN	1.610	0.150	18
HOLE$	=CNAR			
ROCK$	=PAGUATE	1.713	0.164	15
HOLE$	=CNAR			
ROCK$	=TWOWELLS	1.678	0.225	8
HOLE$	=CNAR			
ROCK$	=WTWATER	1.668	0.184	12
HOLE$	=CNV			
ROCK$	=CLAYMESA	1.220	0.367	3
HOLE$	=CNV			
ROCK$	=CUBERO	1.356	0.139	21
HOLE$	=CNV			
ROCK$	=MANCOS	2.517	0.367	3
HOLE$	=CNV			
ROCK$	=OAKCAN	1.220	0.212	9
HOLE$	=CNV			
ROCK$	=PAGUATE	1.385	0.184	12
HOLE$	=CNV			
ROCK$	=TWOWELLS	2.730	0.367	3
HOLE$	=CNV			
ROCK$	=WTWATER	1.873	0.260	6

TWO-WAY ANOVA: Comparison of Glucose Mineralization by Borehole and Stratigraphy

LEVELS ENCOUNTERED DURING PROCESSING ARE:

HOLE$
CNAR CNV

ROCK$
CLAYMESA CUBERO MANCOS OAKCAN PAGUATE TWOWELLS
WATER

ANALYSIS OF VARIANCE

SOURCE	SUM-OF-SQUARES	DF	MEAN-SQUARE	F-RATIO	P
HOLE$	0.019	1	0.019	2.891	0.092
ROCK$	0.407	6	0.068	10.188	.402858E-08
HOLE$*ROCK$	0.414	6	0.069	10.360	.292326E-08
ERROR	0.813	122	0.007		

ADJUSTED LEAST SQUARES MEANS.

		ADJ. LS MEAN	SE	N
HOLE$	=CNAR	0.154	0.010	78
HOLE$	=CNV	0.124	0.015	58
ROCK$	=CLAYMESA	0.096	0.026	15
ROCK$	=CUBERO	0.267	0.019	27
ROCK$	=MANCOS	0.132	0.026	15
ROCK$	=OAKCAN	0.102	0.017	23
ROCK$	=PAGUATE	0.160	0.016	27
ROCK$	=TWOWELLS	0.128	0.032	11
ROCK$	=WATER	0.087	0.020	18

HOLE$ =CNAR ROCK$ =CLAYMESA	0.067	0.024	12
HOLE$ =CNAR ROCK$ =CUBERO	0.407	0.033	6
HOLE$ =CNAR ROCK$ =MANCOS	0.060	0.024	12
HOLE$ =CNAR ROCK$ =OAKCAN	0.085	0.024	12
HOLE$ =CNAR ROCK$ =PAGUATE	0.182	0.021	15
HOLE$ =CNAR ROCK$ =TWOWELLS	0.181	0.027	9
HOLE$ =CNAR ROCK$ =WATER	0.094	0.024	12
HOLE$ =CNV ROCK$ =CLAYMESA	0.124	0.047	3
HOLE$ =CNV ROCK$ =CUBERO	0.127	0.018	21
HOLE$ =CNV ROCK$ =MANCOS	0.204	0.047	3
HOLE$ =CNV ROCK$ =OAKCAN	0.119	0.025	11
HOLE$ =CNV ROCK$ =PAGUATE	0.137	0.024	12
HOLE$ =CNV ROCK$ =TWOWELLS	0.076	0.058	2
HOLE$ =CNV ROCK$ =WATER	0.081	0.033	6

TWO-WAY ANOVA: Comparison of Oxygen-Uptake by Borehole and Stratigraphy

LEVELS ENCOUNTERED DURING PROCESSING ARE:
HOLE$
 CNAR CNV
ROCK$
 CLAYMESA CUBERO MANCOS OAKCAN PAGUATE TWOWELLS
 WTWATER

1 CASES DELETED DUE TO MISSING DATA.

ANALYSIS OF VARIANCE

SOURCE	SUM-OF-SQUARES	DF	MEAN-SQUARE	F-RATIO	P
HOLE$	7.645	1	7.645	10.988	0.001
ROCK$	104.908	6	17.485	25.131	.999201E-15
HOLE$*ROCK$	25.429	6	4.238	6.092	.130416E-04
ERROR	85.576	123	0.696		

ADJUSTED LEAST SQUARES MEANS.

		ADJ. LS MEAN	SE	N
HOLE$	=CNAR	3.198	0.099	80
HOLE$	=CNV	2.625	0.141	57
ROCK$	=CLAYMESA	2.201	0.278	12
ROCK$	=CUBERO	2.168	0.193	27
ROCK$	=MANCOS	5.723	0.269	15
ROCK$	=OAKCAN	2.511	0.170	27
ROCK$	=PAGUATE	2.432	0.162	27
ROCK$	=TWOWELLS	2.125	0.282	11
ROCK$	=WTWATER	3.221	0.209	18

HOLE$	=CNAR			
ROCK$	=CLAYMESA	2.629	0.278	9
HOLE$	=CNAR			
ROCK$	=CUBERO	2.590	0.341	6
HOLE$	=CNAR			
ROCK$	=MANCOS	4.598	0.241	12
HOLE$	=CNAR			
ROCK$	=OAKCAN	2.861	0.197	18
HOLE$	=CNAR			
ROCK$	=PAGUATE	2.791	0.215	15
HOLE$	=CNAR			
ROCK$	=TWOWELLS	2.968	0.295	8
HOLE$	=CNAR			
ROCK$	=WTWATER	3.948	0.241	12
HOLE$	=CNV			
ROCK$	=CLAYMESA	1.774	0.482	3
HOLE$	=CNV			
ROCK$	=CUBERO	1.746	0.182	21
HOLE$	=CNV			
ROCK$	=MANCOS	6.849	0.482	3
HOLE$	=CNV			
ROCK$	=OAKCAN	2.160	0.278	9
HOLE$	=CNV			
ROCK$	=PAGUATE	2.073	0.241	12
HOLE$	=CNV			
ROCK$	=TWOWELLS	1.282	0.482	3
HOLE$	=CNV			
ROCK$	=WTWATER	2.494	0.341	6

TWO-WAY ANOVA: Comparison of Percent Moisture by Borehole and Stratigraphy

LEVELS ENCOUNTERED DURING PROCESSING ARE:

UNIT$

CLAYMESA CUBERO MANCOS OAKCAN PAGUATE TWOWELLS WTWATER

HOLE$

CNAR CNV

ANALYSIS OF VARIANCE

SOURCE	SUM-OF-SQUARES	DF	MEAN-SQUARE	F-RATIO	P
UNIT$	0.015	6	0.003	0.683	0.665
HOLE$	0.017	1	0.017	4.643	0.038
UNIT$*HOLE$	0.026	6	0.004	1.174	0.343
ERROR	0.127	34	0.004		

ADJUSTED LEAST SQUARES MEANS.

		ADJ. LS MEAN	SE	N
UNIT$	=CLAYMESA	0.224	0.034	5
UNIT$	=CUBERO	0.205	0.024	9
UNIT$	=MANCOS	0.223	0.034	5
UNIT$	=OAKCAN	0.229	0.020	10
UNIT$	=PAGUATE	0.187	0.020	9
UNIT$	=TWOWELLS	0.215	0.035	4
UNIT$	=WTWATER	0.175	0.026	6
HOLE$	=CNAR	0.185	0.012	28
HOLE$	=CNV	0.231	0.018	20

UNIT$ =CLAYMESA HOLE$ =CNAR	0.145	0.031	4
UNIT$ =CLAYMESA HOLE$ =CNV	0.303	0.061	1
UNIT$ =CUBERO HOLE$ =CNAR	0.165	0.043	2
UNIT$ =CUBERO HOLE$ =CNV	0.245	0.023	7
UNIT$ =MANCOS HOLE$ =CNAR	0.199	0.031	4
UNIT$ =MANCOS HOLE$ =CNV	0.247	0.061	1
UNIT$ =OAKCAN HOLE$ =CNAR	0.193	0.025	6
UNIT$ =OAKCAN HOLE$ =CNV	0.264	0.031	4
UNIT$ =PAGUATE HOLE$ =CNAR	0.180	0.027	5
UNIT$ =PAGUATE HOLE$ =CNV	0.195	0.031	4
UNIT$ =TWOWELLS HOLE$ =CNAR	0.249	0.035	3
UNIT$ =TWOWELLS HOLE$ =CNV	0.180	0.061	1
UNIT$ =WTWATER HOLE$ =CNAR	0.165	0.031	4
UNIT$ =WTWATER HOLE$ =CNV	0.186	0.043	2

ONE-WAY ANOVA: Comparison of CFU by Borehole (sandstones only)

LEVELS ENCOUNTERED DURING PROCESSING ARE:
HOLE$
CNAR CNV CNVR

ANALYSIS OF VARIANCE

SOURCE	SUM-OF-SQUARES	DF	MEAN-SQUARE	F-RATIO	P
HOLE$	9.192	2	4.596	10.794	.393052E-04
ERROR	70.256	165	0.426		

CELL MEANS AND STANDARD DEVIATIONS.

		MEAN	SD	N
HOLE$	=CNAR	1.850	0.910	65
HOLE$	=CNV	1.383	0.452	75
HOLE$	=CNVR	1.340	0.283	28

COL/
ROW HOLE$
1 CNAR
2 CNV
3 CNVR

USING LEAST SQUARES MEANS. POST HOC TEST OF CFU

USING MODEL MSE OF 0.426 WITH 165. DF. MATRIX OF PAIRWISE MEAN DIFFERENCES:

	1	2	3
1	0.000		
2	-0.468	0.000	
3	-0.510	-0.043	0.000

TUKEY HSD MULTIPLE COMPARISONS. MATRIX OF PAIRWISE COMPARISON PROBABILITIES:

	1	2	3
1	1.000		
2	.882745E-04	1.000	
3	0.002	0.953	1.000

ONE-WAY ANOVA: Comparison of CFU by Stratigraphy

LEVELS ENCOUNTERED DURING PROCESSING ARE:
ROCK$
CLAYMESA CUBERO MANCOS MORRISON OAKCAN PAGUATE
TWOWELLS WTWATER

ANALYSIS OF VARIANCE

SOURCE	SUM-OF-SQUARES	DF	MEAN-SQUARE	F-RATIO	P
ROCK$	7.105	7	1.015	1.827	0.085
ERROR	89.994	162	0.556		

CELL MEANS AND STANDARD DEVIATIONS.

		MEAN	SD	N
ROCK$	=CLAYMESA	1.353	0.307	12
ROCK$	=CUBERO	1.580	0.749	30
ROCK$	=MANCOS	1.719	0.794	16
ROCK$	=MORRISON	2.052	1.214	18
ROCK$	=OAKCAN	1.449	0.429	38
ROCK$	=PAGUATE	1.567	0.627	27
ROCK$	=TWOWELLS	1.965	0.930	11
ROCK$	=WTWATER	1.736	0.856	18

COL/
ROW ROCK$
1 CLAYMESA
2 CUBERO
3 MANCOS
4 MORRISON
5 OAKCAN
6 PAGUATE
7 TWOWELLS
8 WTWATER

USING LEAST SQUARES MEANS. POST HOC TEST OF CFU

USING MODEL MSE OF 0.556 WITH 162. DF. MATRIX OF PAIRWISE MEAN DIFFERENCES:

	1	2	3	4	5
1	0.000				
2	0.227	0.000			
3	0.366	0.139	0.000		
4	0.699	0.472	0.333	0.000	
5	0.096	-0.131	-0.270	-0.603	0.000
6	0.215	-0.013	-0.152	-0.485	0.118
7	0.612	0.385	0.246	-0.087	0.516
8	0.384	0.156	0.017	-0.316	0.287

	6	7	8
6	0.000		
7	0.398	0.000	
8	0.169	-0.228	0.000

TUKEY HSD MULTIPLE COMPARISONS. MATRIX OF PAIRWISE COMPARISON PROBABILITIES:

	1	2	3	4	5
1	1.000				
2	0.987	1.000			
3	0.904	0.999	1.000		
4	0.188	0.399	0.899	1.000	
5	1.000	0.996	0.928	0.089	1.000
6	0.991	1.000	0.998	0.391	0.998
7	0.504	0.826	0.991	1.000	0.468
8	0.866	0.997	1.000	0.910	0.881

	6	7	8
6	1.000		
7	0.813	1.000	
8	0.996	0.993	1.000

ONE-WAY ANOVA: Comparison of CFU by Lithology

LEVELS ENCOUNTERED DURING PROCESSING ARE:
LITH$
SANDSTONE SHALE

ANALYSIS OF VARIANCE

SOURCE	SUM-OF-SQUARES	DF	MEAN-SQUARE	F-RATIO	P
LITH$	0.003	1	0.003	0.005	0.942
ERROR	97.096	168	0.578		

CELL MEANS AND STANDARD DEVIATIONS.

		MEAN	SD	N
LITH$	=SANDSTONE	1.640	0.770	124
LITH$	=SHALE	1.630	0.734	46

COL/
ROW LITH$
1 SANDSTONE
2 SHALE

USING LEAST SQUARES MEANS. POST HOC TEST OF CFU

USING MODEL MSE OF 0.578 WITH 168. DF. MATRIX OF PAIRWISE MEAN DIFFERENCES:

	1	2
1	0.000	
2	-0.010	0.000

TUKEY HSD MULTIPLE COMPARISONS. MATRIX OF PAIRWISE COMPARISON PROBABILITIES:

	1	2
1	1.000	
2	0.942	1.000

ONE-WAY ANOVA: Comparison of CO2-Production by Borehole (sandstones only)

LEVELS ENCOUNTERED DURING PROCESSING ARE:
HOLE$
CNAR CNV CNVR

ANALYSIS OF VARIANCE

SOURCE	SUM-OF-SQUARES	DF	MEAN-SQUARE	F-RATIO	P
HOLE$	1.244	2	0.622	4.862	0.009
ERROR	15.347	120	0.128		

CELL MEANS AND STANDARD DEVIATIONS.

		MEAN	SD	N
HOLE$	=CNAR	0.509	0.436	64
HOLE$	=CNV	0.318	0.239	45
HOLE$	=CNVR	0.280	0.259	14

COL/ ROW	HOLE$
1	CNAR
2	CNV
3	CNVR

USING LEAST SQUARES MEANS. POST HOC TEST OF CO2

USING MODEL MSE OF 0.128 WITH 120. DF. MATRIX OF PAIRWISE MEAN DIFFERENCES:

	1	2	3
1	0.000		
2	-0.191	0.000	
3	-0.229	-0.038	0.000

TUKEY HSD MULTIPLE COMPARISONS. MATRIX OF PAIRWISE COMPARISON PROBABILITIES:

	1	2	3
1	1.000		
2	0.019	1.000	
3	0.081	0.936	1.000

ONE-WAY ANOVA: Comparison of CO2 by Stratigraphy

LEVELS ENCOUNTERED DURING PROCESSING ARE:
ROCK$
CLAYMESA CUBERO MANCOS MORRISON OAKCAN PAGUATE
TWOWELLS WTWATER

ANALYSIS OF VARIANCE

SOURCE	SUM-OF-SQUARES	DF	MEAN-SQUARE	F-RATIO	P
ROCK$	9.079	7	1.297	19.547	.999201E-15
ERROR	10.682	161	0.066		

CELL MEANS AND STANDARD DEVIATIONS.

		MEAN	SD	N
ROCK$	=CLAYMESA	0.211	0.194	12
ROCK$	=CUBERO	0.561	0.294	30
ROCK$	=MANCOS	0.205	0.243	16
ROCK$	=MORRISON	0.071	0.158	17
ROCK$	=OAKCAN	0.202	0.154	38
ROCK$	=PAGUATE	0.548	0.376	27
ROCK$	=TWOWELLS	0.935	0.362	11
ROCK$	=WTWATER	0.239	0.190	18

COL/ ROW	ROCK$
1	CLAYMESA
2	CUBERO
3	MANCOS
4	MORRISON
5	OAKCAN
6	PAGUATE
7	TWOWELLS
8	WTWATER

USING LEAST SQUARES MEANS. POST HOC TEST OF CO2PROD

USING MODEL MSE OF 0.066 WITH 161. DF. MATRIX OF PAIRWISE MEAN DIFFERENCES:

	1	2	3	4	5
1	0.000				
2	0.349	0.000			
3	-0.006	-0.356	0.000		
4	-0.140	-0.490	-0.134	0.000	
5	-0.009	-0.359	-0.003	0.131	0.000
6	0.336	-0.013	0.343	0.477	0.345
7	0.724	0.374	0.730	0.864	0.733
8	0.028	-0.321	0.035	0.169	0.037

	6	7	8
6	0.000		
7	0.387	0.000	
8	-0.308	-0.696	0.000

TUKEY HSD MULTIPLE COMPARISONS. MATRIX OF PAIRWISE COMPARISON PROBABILITIES:

	1	2	3	4	5
1	1.000				
2	0.002	1.000			
3	1.000	.238299E-03	1.000		
4	0.836	.321865E-04	0.811	1.000	
5	1.000	.323653E-04	1.000	0.655	1.000
6	0.004	1.000	.663400E-03	.321865E-04	.343919E-04
7	.321269E-04	.992060E-03	.321269E-04	.321269E-04	.321269E-04
8	1.000	.761509E-03	1.000	0.527	1.000

	6	7	8
6	1.000		
7	.703514E-03	1.000	
8	0.002	.321269E-04	1.000

ONE-WAY ANOVA: Comparison of CO2 by Lithology

LEVELS ENCOUNTERED DURING PROCESSING ARE:
LITH$
SANDSTONE SHALE

ANALYSIS OF VARIANCE

SOURCE	SUM-OF-SQUARES	DF	MEAN-SQUARE	F-RATIO	P
LITH$	1.245	1	1.245	11.232	.994448E-03
ERROR	18.515	167	0.111		

CELL MEANS AND STANDARD DEVIATIONS.

		MEAN	SD	N
LITH$	=SANDSTONE	0.413	0.369	123
LITH$	=SHALE	0.220	0.207	46

COL/
ROW LITH$
1 SANDSTONE
2 SHALE

USING LEAST SQUARES MEANS. POST HOC TEST OF CO2PROD

USING MODEL MSE OF 0.111 WITH 167. DF. MATRIX OF PAIRWISE MEAN DIFFERENCES:

	1	2
1	0.000	
2	-0.193	0.000

TUKEY HSD MULTIPLE COMPARISONS. MATRIX OF PAIRWISE COMPARISON PROBABILITIES:

	1	2
1	1.000	
2	.809252E-03	1.000

ONE-WAY ANOVA: Comparison of Glucose Mineralization
by Borehole (sandstones only)

LEVELS ENCOUNTERED DURING PROCESSING ARE:
HOLE$
CNAR CNV CNVR

ANALYSIS OF VARIANCE

SOURCE	SUM-OF-SQUARES	DF	MEAN-SQUARE	F-RATIO	P
HOLE$	0.188	2	0.094	6.360	0.002
ERROR	1.612	109	0.015		

CELL MEANS AND STANDARD DEVIATIONS.

		MEAN	SD	N
HOLE$	=CNAR	0.190	0.156	51
HOLE$	=CNV	0.125	0.087	46
HOLE$	=CNVR	0.077	0.064	15

COL/
ROW HOLE$
1 CNAR
2 CNV
3 CNVR

USING LEAST SQUARES MEANS. POST HOC TEST OF GLUCOSE

USING MODEL MSE OF 0.015 WITH 109. DF. MATRIX OF PAIRWISE MEAN DIFFERENCES:

	1	2	3
1	0.000		
2	-0.064	0.000	
3	-0.113	-0.049	0.000

TUKEY HSD MULTIPLE COMPARISONS. MATRIX OF PAIRWISE COMPARISON PROBABILITIES:

	1	2	3
1	1.000		
2	0.028	1.000	
3	0.006	0.376	1.000

ONE-WAY ANOVA: Comparison of Glucose Mineralization by Stratigraphy

LEVELS ENCOUNTERED DURING PROCESSING ARE:
ROCK$
CLAYMESA CUBERO MANCOS MORRISON OAKCAN PAGUATE
TWOWELLS WATER

ANALYSIS OF VARIANCE

SOURCE	SUM-OF-SQUARES	DF	MEAN-SQUARE	F-RATIO	P
ROCK$	0.327	7	0.047	4.134	.344594E-03
ERROR	1.719	152	0.011		

CELL MEANS AND STANDARD DEVIATIONS.

		MEAN	SD	N
ROCK$	=CLAYMESA	0.079	0.036	15
ROCK$	=CUBERO	0.182	0.178	30
ROCK$	=MANCOS	0.089	0.074	15
ROCK$	=MORRISON	0.207	0.215	9
ROCK$	=OAKCAN	0.089	0.055	35
ROCK$	=PAGUATE	0.162	0.067	27
ROCK$	=TWOWELLS	0.162	0.096	11
ROCK$	=WATER	0.090	0.034	18

COL/
ROW ROCK$
1 CLAYMESA
2 CUBERO
3 MANCOS
4 MORRISON
5 OAKCAN
6 PAGUATE
7 TWOWELLS
8 WATER

USING LEAST SQUARES MEANS. POST HOC TEST OF GLUCOSE

USING MODEL MSE OF 0.011 WITH 152. DF. MATRIX OF PAIRWISE MEAN DIFFERENCES:

	1	2	3	4	5
1	0.000				
2	0.104	0.000			
3	0.010	-0.093	0.000		
4	0.129	0.025	0.118	0.000	
5	0.011	-0.093	.571429E-04	-0.118	0.000
6	0.084	-0.020	0.073	-0.045	0.073
7	0.083	-0.021	0.073	-0.046	0.073
8	0.011	-0.093	.500000E-03	-0.118	.442857E-03

	6	7	8
6	0.000		
7	-.400673E-03	0.000	
8	-0.073	-0.072	0.000

TUKEY HSD MULTIPLE COMPARISONS. MATRIX OF PAIRWISE COMPARISON PROBABILITIES:

	1	2	3	4	5
1	1.000				
2	0.043	1.000			
3	1.000	0.102	1.000		
4	0.079	0.999	0.143	1.000	
5	1.000	0.010	1.000	0.059	1.000
6	0.223	0.997	0.394	0.956	0.129
7	0.503	0.999	0.674	0.981	0.499
8	1.000	0.068	1.000	0.119	1.000

	6	7	8
6	1.000		
7	1.000	1.000	
8	0.327	0.639	1.000

ONE-WAY ANOVA: Comparison of Viable Cells by Borehole (sandstones only)

LEVELS ENCOUNTERED DURING PROCESSING ARE:
HOLE$
CNAR CNV CNVR

ANALYSIS OF VARIANCE

SOURCE	SUM-OF-SQUARES	DF	MEAN-SQUARE	F-RATIO	P
HOLE$	0.595	2	0.298	1.070	0.345
ERROR	45.623	164	0.278		

CELL MEANS AND STANDARD DEVIATIONS.

		MEAN	SD	N
HOLE$	=CNAR	5.403	0.631	84
HOLE$	=CNV	5.527	0.420	63
HOLE$	=CNVR	5.501	0.288	20

COL/
ROW HOLE$
1 CNAR
2 CNV
3 CNVR

USING LEAST SQUARES MEANS. POST HOC TEST OF VIABLE

USING MODEL MSE OF 0.278 WITH 164. DF. MATRIX OF PAIRWISE MEAN DIFFERENCES:

	1	2	3
1	0.000		
2	0.125	0.000	
3	0.098	-0.026	0.000

TUKEY HSD MULTIPLE COMPARISONS. MATRIX OF PAIRWISE COMPARISON PROBABILITIES:

	1	2	3
1	1.000		
2	0.331	1.000	
3	0.734	0.979	1.000

ONE-WAY ANOVA: Comparison of Glucose Mineralization by Lithology

LEVELS ENCOUNTERED DURING PROCESSING ARE:
LITH4$
SANDSTONE SHALE

ANALYSIS OF VARIANCE

SOURCE	SUM-OF-SQUARES	DF	MEAN-SQUARE	F-RATIO	P
LITH4$	0.130	1	0.130	10.759	0.001
ERROR	1.916	158	0.012		

CELL MEANS AND STANDARD DEVIATIONS.

	MEAN	SD	N
LITH4$ =SANDSTONE	0.148	0.127	112
LITH4$ =SHALE	0.086	0.050	48

COL/
ROW LITH4$
1 SANDSTONE
2 SHALE

USING LEAST SQUARES MEANS. POST HOC TEST OF GLUCOSE

USING MODEL MSE OF 0.012 WITH 158. DF. MATRIX OF PAIRWISE MEAN DIFFERENCES:

	1	2
1	0.000	
2	-0.062	0.000

TUKEY HSD MULTIPLE COMPARISONS. MATRIX OF PAIRWISE COMPARISON PROBABILITIES:

	1	2
1	1.000	
2	0.001	1.000

ONE-WAY ANOVA: Comparison of Total Viable Cells by Stratigraphy

LEVELS ENCOUNTERED DURING PROCESSING ARE:
ROCK$
CLAYMESA CUBERO MANCOS MORRISON OAKCAN PAGUATE
TWOWELLS WTWATER

ANALYSIS OF VARIANCE

SOURCE	SUM-OF-SQUARES	DF	MEAN-SQUARE	F-RATIO	P
ROCK$	2.294	7	0.328	1.256	0.273
ERROR	58.170	223	0.261		

CELL MEANS AND STANDARD DEVIATIONS.

	MEAN	SD	N
ROCK$ =CLAYMESA	5.651	0.392	20
ROCK$ =CUBERO	5.519	0.407	41
ROCK$ =MANCOS	5.446	0.585	20
ROCK$ =MORRISON	5.324	0.698	20
ROCK$ =OAKCAN	5.445	0.535	55
ROCK$ =PAGUATE	5.508	0.624	35
ROCK$ =TWOWELLS	5.443	0.265	16
ROCK$ =WTWATER	5.696	0.370	24

COL/
ROW ROCK$
1 CLAYMESA
2 CUBERO
3 MANCOS
4 MORRISON
5 OAKCAN
6 PAGUATE
7 TWOWELLS
8 WTWATER

USING LEAST SQUARES MEANS. POST HOC TEST OF VIABLE

USING MODEL MSE OF 0.261 WITH 223. DF. MATRIX OF PAIRWISE MEAN DIFFERENCES
:

	1	2	3	4	5
1	0.000				
2	-0.132	0.000			
3	-0.205	-0.073	0.000		
4	-0.327	-0.195	-0.122	0.000	
5	-0.206	-0.074	-.954545E-03	0.121	0.000
6	-0.143	-0.011	0.062	0.184	0.063
7	-0.207	-0.076	-0.002	0.119	-0.001
8	0.046	0.177	0.251	0.372	0.252

	6	7	8
6	0.000		
7	-0.065	0.000	
8	0.189	0.253	0.000

TUKEY HSD MULTIPLE COMPARISONS. MATRIX OF PAIRWISE COMPARISON PROBABILITIES:

	1	2	3	4	5
1	1.000				
2	0.982	1.000			
3	0.910	1.000	1.000		
4	0.467	0.858	0.995	1.000	
5	0.783	0.997	1.000	0.986	1.000
6	0.975	1.000	1.000	0.905	0.999
7	0.929	1.000	1.000	0.997	1.000
8	1.000	0.879	0.737	0.238	0.472

	6	7	8
6	1.000		
7	1.000	1.000	
8	0.861	0.788	1.000

ONE-WAY ANOVA: Comparison of Total Viable Cells by Lithology

LEVELS ENCOUNTERED DURING PROCESSING ARE:
LITH$
SANDSTONE SHALE

ANALYSIS OF VARIANCE

SOURCE	SUM-OF-SQUARES	DF	MEAN-SQUARE	F-RATIO	P
LITH$	0.935	1	0.935	3.597	0.059
ERROR	59.529	229	0.260		

CELL MEANS AND STANDARD DEVIATIONS.

		MEAN	SD	N
LITH$	=SANDSTONE	5.461	0.528	167
LITH$	=SHALE	5.604	0.460	64

COL/
ROW LITH$
1 SANDSTONE
2 SHALE

USING LEAST SQUARES MEANS. POST HOC TEST OF VIABLE

USING MODEL MSE OF 0.260 WITH 229. DF. MATRIX OF PAIRWISE MEAN DIFFERENCES:

	1	2
1	0.000	
2	0.142	0.000

TUKEY HSD MULTIPLE COMPARISONS. MATRIX OF PAIRWISE COMPARISON PROBABILITIES:

	1	2
1	1.000	
2	0.058	1.000

ONE-WAY ANOVA: Comparison of Oxygen-Uptake by Borehole (sandstones only)

LEVELS ENCOUNTERED DURING PROCESSING ARE:
HOLE$
CNAR CNV CNVR

ANALYSIS OF VARIANCE

SOURCE	SUM-OF-SQUARES	DF	MEAN-SQUARE	F-RATIO	P
HOLE$	7.102	2	3.551	4.699	0.011
ERROR	86.915	115	0.756		

CELL MEANS AND STANDARD DEVIATIONS.

		MEAN	SD	N
HOLE$	=CNAR	2.413	1.081	59
HOLE$	=CNV	1.885	0.562	45
HOLE$	=CNVR	2.181	0.637	14

COL/
ROW HOLE$
1 CNAR
2 CNV
3 CNVR

USING LEAST SQUARES MEANS. POST HOC TEST OF O2

USING MODEL MSE OF 0.756 WITH 115. DF. MATRIX OF PAIRWISE MEAN DIFFERENCES:

	1	2	3
1	0.000		
2	-0.527	0.000	
3	-0.232	0.296	0.000

TUKEY HSD MULTIPLE COMPARISONS. MATRIX OF PAIRWISE COMPARISON PROBABILITIES:

	1	2	3
1	1.000		
2	0.008	1.000	
3	0.644	0.509	1.000

ONE-WAY ANOVA: Comparison of Oxygen-Uptake by Stratigraphy

LEVELS ENCOUNTERED DURING PROCESSING ARE:
ROCK$
CLAYMESA CUBERO MANCOS MORRISON OAKCAN PAGUATE
TWOWELLS WTWATER

ANALYSIS OF VARIANCE

SOURCE	SUM-OF-SQUARES	DF	MEAN-SQUARE	F-RATIO	P
ROCK$	156.149	7	22.307	26.529	.999201E-15
ERROR	130.335	155	0.841		

CELL MEANS AND STANDARD DEVIATIONS.

		MEAN	SD	N
ROCK$	=CLAYMESA	2.415	0.661	12
ROCK$	=CUBERO	1.940	0.529	30
ROCK$	=MANCOS	5.048	1.816	15
ROCK$	=MORRISON	0.807	0.131	12
ROCK$	=OAKCAN	2.513	0.717	38
ROCK$	=PAGUATE	2.472	0.802	27
ROCK$	=TWOWELLS	2.508	1.339	11
ROCK$	=WTWATER	3.463	1.012	18

COL/ ROW	ROCK$
1	CLAYMESA
2	CUBERO
3	MANCOS
4	MORRISON
5	OAKCAN
6	PAGUATE
7	TWOWELLS
8	WTWATER

USING LEAST SQUARES MEANS. POST HOC TEST OF O2PROD

USING MODEL MSE OF 0.841 WITH 155. DF. MATRIX OF PAIRWISE MEAN DIFFERENCES:

	1	2	3	4	5
1	0.000				
2	-0.475	0.000			
3	2.632	3.108	0.000		
4	-1.608	-1.133	-4.241	0.000	
5	0.097	0.573	-2.535	1.706	0.000
6	0.057	0.532	-2.576	1.665	-0.041
7	0.093	0.568	-2.539	1.701	-0.004
8	1.048	1.523	-1.585	2.656	0.950

	6	7	8
6	0.000		
7	0.036	0.000	
8	0.991	0.955	0.000

TUKEY HSD MULTIPLE COMPARISONS. MATRIX OF PAIRWISE COMPARISON PROBABILITIES:

	1	2	3	4	5
1	1.000				
2	0.798	1.000			
3	.321269E-04	.321269E-04	1.000		
4	.479937E-03	0.007	.321269E-04	1.000	
5	1.000	0.172	.321269E-04	.326037E-04	1.000
6	1.000	0.359	.321269E-04	.360012E-04	1.000
7	1.000	0.648	.321269E-04	.258088E-03	1.000
8	0.045	.327229E-04	.507832E-04	.321269E-04	0.007

	6	7	8
6	1.000		
7	1.000	1.000	
8	0.009	0.116	1.000

ONE-WAY ANOVA: Comparison of Oxygen-Uptake by Lithology

LEVELS ENCOUNTERED DURING PROCESSING ARE:
LITH$
SANDSTONE SHALE

ANALYSIS OF VARIANCE

SOURCE	SUM-OF-SQUARES	DF	MEAN-SQUARE	F-RATIO	P
LITH$	76.053	1	76.053	58.188	.196143E-11
ERROR	210.431	161	1.307		

CELL MEANS AND STANDARD DEVIATIONS.

	MEAN	SD	N
LITH$ =SANDSTONE	2.184	0.896	118
LITH$ =SHALE	3.712	1.627	45

COL/ ROW	LITH$
1	SANDSTONE
2	SHALE

USING LEAST SQUARES MEANS. POST HOC TEST OF O2PROD

USING MODEL MSE OF 1.307 WITH 161. DF. MATRIX OF PAIRWISE MEAN DIFFERENCES:

	1	2
1	0.000	
2	1.528	0.000

TUKEY HSD MULTIPLE COMPARISONS. MATRIX OF PAIRWISE COMPARISON PROBABILITIES:

	1	2
1	1.000	
2	.876188E-05	1.000

ONE-WAY ANOVA: Comparison of Percent Moisture by Borehole (sandstones only)

LEVELS ENCOUNTERED DURING PROCESSING ARE:
HOLE$
CNAR
CNV
CNVR

ANALYSIS OF VARIANCE

SOURCE	SUM-OF-SQUARES	DF	MEAN-SQUARE	F-RATIO	P
HOLE$	0.014	2	0.007	2.108	0.136
ERROR	0.128	38	0.003		

CELL MEANS AND STANDARD DEVIATIONS.

		MEAN	SD	N
HOLE$	=CNAR	0.204	0.062	20
HOLE$	=CNV	0.233	0.044	16
HOLE$	=CNVR	0.178	0.079	5

COL/
ROW HOLE$
1 CNAR
2 CNV
3 CNVR

USING LEAST SQUARES MEANS. POST HOC TEST OF MOIST

USING MODEL MSE OF 0.003 WITH 38. DF. MATRIX OF PAIRWISE MEAN DIFFERENCES:

	1	2	3
1	0.000		
2	0.029	0.000	
3	-0.025	-0.055	0.000

TUKEY HSD MULTIPLE COMPARISONS. MATRIX OF PAIRWISE COMPARISON PROBABILITIES:

	1	2	3
1	1.000		
2	0.297	1.000	
3	0.659	0.169	1.000

ONE-WAY ANOVA: Comparison of Percent Moisture by Stratigraphy

LEVELS ENCOUNTERED DURING PROCESSING ARE:

UNIT$

CLAYMESA CUBERO MANCOS MORRISON OAKCAN PAGUATE TWOWELLS WTWATER

ANALYSIS OF VARIANCE

SOURCE	SUM-OF-SQUARES	DF	MEAN-SQUARE	F-RATIO	P
UNIT$	0.020	7	0.003	0.623	0.735
ERROR	0.228	49	0.005		

CELL MEANS AND STANDARD DEVIATIONS.

		MEAN	SD	N
UNIT$	=CLAYMESA	0.176	0.078	5
UNIT$	=CUBERO	0.222	0.051	10
UNIT$	=MANCOS	0.208	0.082	5
UNIT$	=MORRISON	0.188	0.082	4
UNIT$	=OAKCAN	0.209	0.073	14
UNIT$	=PAGUATE	0.186	0.082	9
UNIT$	=TWOWELLS	0.232	0.054	4
UNIT$	=WTWATER	0.172	0.018	6

COL/ ROW	UNIT$
1	CLAYMESA
2	CUBERO
3	MANCOS
4	MORRISON
5	OAKCAN
6	PAGUATE
7	TWOWELLS
8	WTWATER

USING LEAST SQUARES MEANS. POST HOC TEST OF MOIST

USING MODEL MSE OF 0.005 WITH 49. DF. MATRIX OF PAIRWISE MEAN DIFFERENCES:

	1	2	3	4	5
1	0.000				
2	0.046	0.000			
3	0.032	-0.014	0.000		
4	0.011	-0.035	-0.021	0.000	
5	0.033	-0.013	0.001	0.022	0.000
6	0.010	-0.036	-0.022	-0.001	-0.023
7	0.056	0.010	0.024	0.044	0.022
8	-0.004	-0.050	-0.036	-0.016	-0.038

	6	7	8
6	0.000		
7	0.045	0.000	
8	-0.015	-0.060	0.000

TUKEY HSD MULTIPLE COMPARISONS. MATRIX OF PAIRWISE COMPARISON PROBABILITIES:

	1	2	3	4	5
1	1.000				
2	0.920	1.000			
3	0.995	1.000	1.000		
4	1.000	0.989	1.000	1.000	
5	0.981	1.000	1.000	0.999	1.000
6	1.000	0.945	0.999	1.000	0.993
7	0.924	1.000	1.000	0.983	0.999
8	1.000	0.841	0.987	1.000	0.947

	6	7	8
6	1.000		
7	0.953	1.000	
8	1.000	0.870	1.000

ONE-WAY ANOVA: Comparison of Percent Moisture by Lithology

LEVELS ENCOUNTERED DURING PROCESSING ARE:
LITH$
SANDSTONE SHALE

ANALYSIS OF VARIANCE

SOURCE	SUM-OF-SQUARES	DF	MEAN-SQUARE	F-RATIO	P
LITH$	0.018	1	0.018	4.294	0.043
ERROR	0.231	55	0.004		

CELL MEANS AND STANDARD DEVIATIONS.

		MEAN	SD	N
LITH$	=SANDSTONE	0.212	0.060	41
LITH$	=SHALE	0.173	0.077	16

COL/
ROW LITH$
1 SANDSTONE
2 SHALE

USING LEAST SQUARES MEANS. POST HOC TEST OF MOIST

USING MODEL MSE OF 0.004 WITH 55. DF. MATRIX OF PAIRWISE MEAN DIFFERENCES:

	1	2
1	0.000	
2	-0.040	0.000

TUKEY HSD MULTIPLE COMPARISONS. MATRIX OF PAIRWISE COMPARISON PROBABILITIES:

	1	2
1	1.000	
2	0.043	1.000

ONE-WAY ANOVA: Comparison of CFU by Borehole (shales only)

LEVELS ENCOUNTERED DURING PROCESSING ARE:
HOLE$
CNAR CNV

ANALYSIS OF VARIANCE

SOURCE	SUM-OF-SQUARES	DF	MEAN-SQUARE	F-RATIO	P
HOLE$	0.942	1	0.942	1.780	0.189
ERROR	23.281	44	0.529		

CELL MEANS AND STANDARD DEVIATIONS.

		MEAN	SD	N
HOLE$	=CNAR	1.545	0.631	34
HOLE$	=CNV	1.871	0.960	12

COL/
ROW HOLE$
1 CNAR
2 CNV

USING LEAST SQUARES MEANS. POST HOC TEST OF CFU

USING MODEL MSE OF 0.529 WITH 44. DF. MATRIX OF PAIRWISE MEAN DIFFERENCES:

	1	2
1	0.000	
2	0.326	0.000

TUKEY HSD MULTIPLE COMPARISONS. MATRIX OF PAIRWISE COMPARISON PROBABILITIES:

	1	2
1	1.000	
2	0.189	1.000

ONE-WAY ANOVA: Comparison of CO2-Production by Borehole (shales only)

LEVELS ENCOUNTERED DURING PROCESSING ARE:
HOLE$
CNAR CNV

ANALYSIS OF VARIANCE

SOURCE	SUM-OF-SQUARES	DF	MEAN-SQUARE	F-RATIO	P
HOLE$	0.527	1	0.527	16.577	.191453E-03
ERROR	1.398	44	0.032		

CELL MEANS AND STANDARD DEVIATIONS.

		MEAN	SD	N
HOLE$	=CNAR	0.284	0.201	34
HOLE$	=CNV	0.040	0.075	12

COL/
ROW HOLE$
1 CNAR
2 CNV

USING LEAST SQUARES MEANS. POST HOC TEST OF CO2

USING MODEL MSE OF 0.032 WITH 44. DF. MATRIX OF PAIRWISE MEAN DIFFERENCES:

	1	2
1	0.000	
2	-0.244	0.000

TUKEY HSD MULTIPLE COMPARISONS. MATRIX OF PAIRWISE COMPARISON PROBABILITIES:

	1	2
1	1.000	
2	.302672E-03	1.000

ONE-WAY ANOVA: Comparison of Glucose Mineralization by Borehole (shales only)

LEVELS ENCOUNTERED DURING PROCESSING ARE:
HOLE$
CNAR
CNV

ANALYSIS OF VARIANCE

SOURCE	SUM-OF-SQUARES	DF	MEAN-SQUARE	F-RATIO	P
HOLE$	0.021	1	0.021	10.436	0.002
ERROR	0.094	46	0.002		

CELL MEANS AND STANDARD DEVIATIONS.

		MEAN	SD	N
HOLE$	=CNAR	0.074	0.039	36
HOLE$	=CNV	0.123	0.062	12

COL/
ROW HOLE$
1 CNAR
2 CNV

USING LEAST SQUARES MEANS. POST HOC TEST OF GLUCOSE

USING MODEL MSE OF 0.002 WITH 46. DF. MATRIX OF PAIRWISE MEAN DIFFERENCES:

	1	2
1	0.000	
2	0.049	0.000

TUKEY HSD MULTIPLE COMPARISONS. MATRIX OF PAIRWISE COMPARISON PROBABILITIES:

	1	2
1	1.000	
2	0.002	1.000

ONE-WAY ANOVA: Comparison of Viable Cells by Borehole (shales only)

LEVELS ENCOUNTERED DURING PROCESSING ARE:
HOLE$
CNAR
CNV

ANALYSIS OF VARIANCE

SOURCE	SUM-OF-SQUARES	DF	MEAN-SQUARE	F-RATIO	P
HOLE$	0.328	1	0.328	1.564	0.216
ERROR	12.982	62	0.209		

CELL MEANS AND STANDARD DEVIATIONS.

	MEAN	SD	N
HOLE$ =CNAR	5.562	0.495	48
HOLE$ =CNV	5.728	0.313	16

COL/
ROW HOLE$
1 CNAR
2 CNV

USING LEAST SQUARES MEANS. POST HOC TEST OF VIABLE

USING MODEL MSE OF 0.209 WITH 62. DF. MATRIX OF PAIRWISE MEAN DIFFERENCES:

	1	2
1	0.000	
2	0.165	0.000

TUKEY HSD MULTIPLE COMPARISONS. MATRIX OF PAIRWISE COMPARISON PROBABILITIES:

	1	2
1	1.000	
2	0.216	1.000

ONE-WAY ANOVA: Comparison of Oxygen-Uptake by Borehole (shales only)

LEVELS ENCOUNTERED DURING PROCESSING ARE:
HOLE$
CNAR
CNV

ANALYSIS OF VARIANCE

SOURCE	SUM-OF-SQUARES	DF	MEAN-SQUARE	F-RATIO	P
HOLE$	1.566	1	1.566	0.586	0.448
ERROR	114.849	43	2.671		

CELL MEANS AND STANDARD DEVIATIONS.

		MEAN	SD	N
HOLE$	=CNAR	3.824	1.415	33
HOLE$	=CNV	3.403	2.149	12

COL/
ROW HOLE$
1 CNAR
2 CNV

USING LEAST SQUARES MEANS. POST HOC TEST OF O2

USING MODEL MSE OF 2.671 WITH 43. DF. MATRIX OF PAIRWISE MEAN DIFFERENCES:

	1	2
1	0.000	
2	-0.422	0.000

TUKEY HSD MULTIPLE COMPARISONS. MATRIX OF PAIRWISE COMPARISON PROBABILITIES:

	1	2
1	1.000	
2	0.448	1.000

ONE-WAY ANOVA: Comparison of Percent Moisture
by Borehole (shales only)

LEVELS ENCOUNTERED DURING PROCESSING ARE:
HOLE$
CNAR
CNV

ANALYSIS OF VARIANCE

SOURCE	SUM-OF-SQUARES	DF	MEAN-SQUARE	F-RATIO	P
HOLE$	0.018	1	0.018	3.499	0.082
ERROR	0.071	14	0.005		

CELL MEANS AND STANDARD DEVIATIONS.

		MEAN	SD	N
HOLE$	=CNAR	0.153	0.075	12
HOLE$	=CNV	0.230	0.057	4

COL/
ROW HOLE$
1 CNAR
2 CNV

USING LEAST SQUARES MEANS.

POST HOC TEST OF MOIST

USING MODEL MSE OF 0.005 WITH 14. DF. MATRIX OF PAIRWISE MEAN DIFFERENCES:

	1	2
1	0.000	
2	0.077	0.000

TUKEY HSD MULTIPLE COMPARISONS. MATRIX OF PAIRWISE COMPARISON PROBABILITIES:

	1	2
1	1.000	
2	0.083	1.000

Appendix 6: Explanation of Box and Whisker Plots (78)

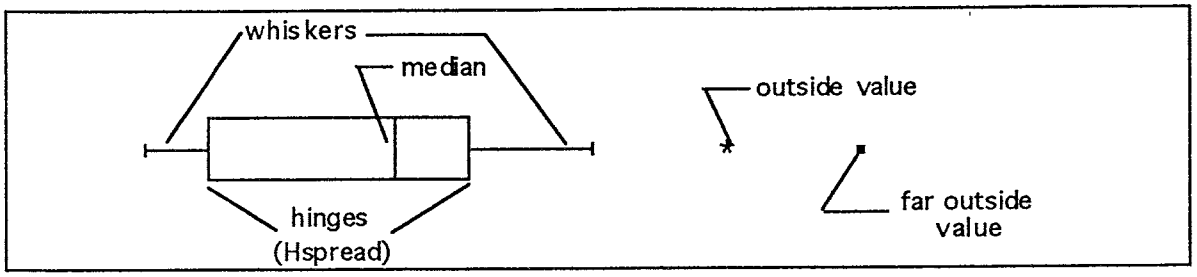

The median of the data set is indicated by the center line. When placed in order, the median splits the data set in half. The top and the bottom of the box are called hinges, and split the remaining halves of the data in half again. Thus the top and the bottom of the box represent the 75th and 25th percentiles, respectively. The bottom whisker marks the 5th percentile; the top whisker marks the 95th.

Two other demarcations, the inner and the outer fences, are not actually drawn. The inner and outer fences are calculated using the *Hspread,* which is defined as the absolute value of the differences between the values of the two hinges.

inner fences:
lower fence = lower hinge - (1.5 * Hspread)
upper fence = lower hinge + (1.5 * Hspread)

outer fences:
lower fence = lower hinge - (3.0 * Hspread)
upper fence = lower hinge + (3.0 * Hspread)

Any values that lie outside the inner fences are plotted with asterisks. Those values that lie outside the outer fences are plotted with dots.

Appendix 7: Calculaton of Peclet numbers

The peclet number is calculated using the following equation (20):

$$P = \frac{v_x d}{D_d}$$

where:

v_x = average linear velocity
d = average grain diameter
D_d = coefficient of molecular diffusion ((20); 1 x 10^{-9} to 2 x 10^{-9} m^2 s^{-1})

Lithology	velocity [a] (cm/sec)	Grain size [b] (cm)	Coefficient of molecular diffusion [c] (cm2/sec)	Peclet number
Mancos shale	7.23E-6 (h) 4.19E-5 (v)	3.9E-4 to 6.25E-3	1E-7 to 2E-7	0.01 to 0.46 0.08 to 2.62
sandstone	4.76E-7 (h)	6.25E-3 to 2.5E-10	1E-7 to 2E-7	0.02 to 0.12

a - from Pegram (55)
b - from Chamley (11)
c - from Fetter (20)

Graph of dimensionless dispersion coefficients versus Peclet number (20):

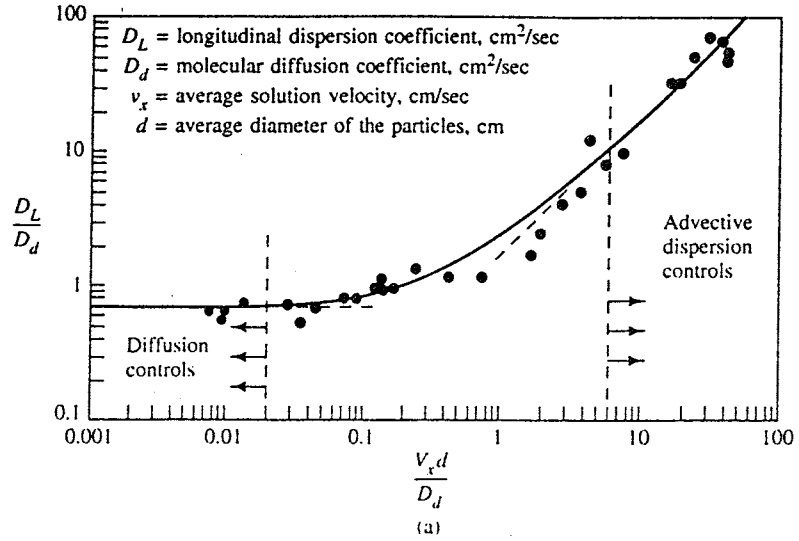

(a)

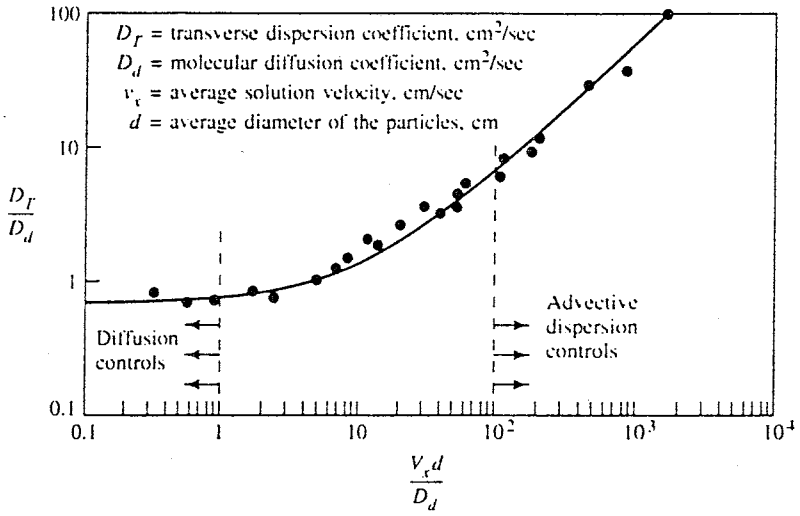

This thesis is accepted on behalf of the faculty
of the Institute by the following committee:

F. M. Phillips

Advisor

Thomas Engler

Robert A. Bowman

16 Jan 96

Date

I release this document to the New Mexico Institute of Mining and Technology.

Catherine S. Deibsey

Student's Signature

1/16/96

Date